



THE ACCURACY OF MINIATURE BEAD THERMISTORS IN
THE MEASUREMENT OF UPPER AIR TEMPERATURE

by

DONALD C. THOMPSON

B.Sc., University of New Zealand
(1955)

M.Sc., University of New Zealand
(1958)

SUBMITTED IN PARTIAL FULFILLMENT OF THE REQUIREMENTS
FOR THE DEGREE OF DOCTOR OF SCIENCE

at the

MASSACHUSETTS INSTITUTE OF TECHNOLOGY

October, 1966.

(January 1967)

Signature of Author
Department of Meteorology, October 1966

Certified by. *[Signature]*
Thesis Supervisor

Accepted by
Chairman, Departmental Committee on
Graduate Students.



Room 14-0551
77 Massachusetts Avenue
Cambridge, MA 02139
Ph: 617.253.5668 Fax: 617.253.1690
Email: docs@mit.edu
<http://libraries.mit.edu/docs>

DISCLAIMER OF QUALITY

Due to the condition of the original material, there are unavoidable flaws in this reproduction. We have made every effort possible to provide you with the best copy available. If you are dissatisfied with this product and find it unusable, please contact Document Services as soon as possible.

Thank you.

Due to the poor quality of the original document, there is some spotting or background shading in this document.

Pages 118 and 187 ARE NOT MISSING but are simply pagination errors on the author's part.

THE ACCURACY OF MINIATURE BEAD THERMISTORS IN
THE MEASUREMENT OF UPPER AIR TEMPERATURE

by

Donald C. Thompson

Submitted to the Department of Meteorology on 3 October 1966
in partial fulfillment of the requirements for the degree of
Doctor of Philosophy

ABSTRACT

A laboratory study was made of the errors of miniature bead thermistors of 5, 10, and 15 mils nominal diameter when used for the measurement of atmospheric temperature. Although the study was primarily concerned with the errors of the thermistors when used in Meteorological rocket soundings between about 70 km and 30 km altitude the results are also valid for other applications of these thermistors at all altitudes down to sea level.

Several distinct sources of error are present, and these have each been discussed and estimates of their magnitude made from laboratory tests. In general, all errors increase rapidly above about 50 km.

Certain items which had not been fully considered in previous discussions of this problem have been shown to be highly significant. In particular it is found that the lead wires play an important part in determining thermistor response, particularly at high altitude, and that the temperature rise of the thermistor due to solar radiation is strongly dependent on the radiation absorbed by the lead wires as well as by the bead proper.

Thesis Supervisor: D.P. Keily
Title: Associate Professor of Meteorology

ACKNOWLEDGEMENTS

The author would like to express his sincere thanks to Professor D.P. Keily for his practical advice and encouragement during the course of this work. Thanks are also due to Mr.P.J. Harney for his many discussions of the practical problems involved in rocket soundings. The author is especially indebted to Mr.E. Beane who constructed much of the apparatus, and to his wife for her careful typing of the manuscript.

This work was made possible by the financial support of the Air Force Cambridge Research Laboratory under contract number AF 19(623)-4165. During the course of this study the author also received financial support from the New Zealand Meteorological Service.

TABLE OF CONTENTS

1	INTRODUCTION	
1.1	Background to the Problem	1
1.2	Errors of Immersion Thermometers	5
1.3	Environmental Conditions	9
1.4	Outline of This Work	11
2	CALIBRATION AND PHYSICAL CHARACTERISTICS OF THERMISTORS	
2.1	Thermistors	13
2.2	Physical Characteristics	14
2.3	Electrical Characteristics	16
2.4	Calibration of Thermistors	17
2.5	Stability of Calibration	22
2.6	Utilization of Thermistor Calibrations in this Work	23
3	SOLAR RADIATION ERRORS	
3.1	Theoretical Temperature Rise of an Irradiated Thermistor	28
3.2	Outline of Experimental Tests	38
3.3	Description of Apparatus	
	(a) Measuring Circuit	43
	(b) Vacuum System	46
	(c) Radiation Source	51
	(d) Thermistor Mounting, and Other Accessories	56
3.4	Procedure	64
3.5	Calibration of the Radiation Source	72
3.6	Results	
	(a) Physical Characteristics	74
	(b) Temperature Rise as a Function of Pressure	76
	(c) Reflectivities	88
	(d) Heat Transfer Coefficients	105
	(e) Dependence of Temperature Rise on Orientation of the Lead Wires	113
4	THE ERRORS DUE TO THE MEASURING CURRENT	
4.1	Introduction	117
4.2	An Instability Criterion	120
4.3	Method of Measurement	122
4.4	Results	123

5	CONDUCTION OF HEAT FROM THE SUPPORTS	
5.1	Introduction	127
5.2	Theoretical Expression for the Conduction Error	128
5.3	Experimental Methods	133
5.4	Results	134
6	ERRORS DUE TO LONG-WAVE RADIATION	
6.1	Introduction	137
6.2	Theoretical Expression for Temperature Error	139
6.3	Experimental Methods	140
6.4	Calculation of the Emissivities	145
6.5	Results	146
7	DYNAMIC RESPONSE OF THERMISTORS	
7.1	Introduction	150
7.2	Laboratory Measurements of the Time Constant	153
7.3	Experimental Method	154
7.4	Results	157
8	THE EFFECTS OF MOTION THROUGH THE AIR	
8.1	Introduction	165
8.2	Discussion of the Experimental Technique	166
8.3	Description of Apparatus and Procedure	
	(a) General Requirements	169
	(b) Construction of Rotating Arm Unit	169
	(c) Measurement of Rotation Speed	174
	(d) Allowance for "Drive" of the Air	174
	(e) Test Procedure	177
8.4	Results	177
9	AERODYNAMIC HEATING ERRORS	
9.1	Introduction	185
9.2	Experimental Method	188
9.3	Results	
	(a) Rise of Reference Temperature	191
	(b) Recovery Factors	192
	(c) Centrifugal Forces	196
10	THE INFLUENCE OF THE AMBIENT TEMPERATURE ON THE HEAT TRANSFER	
10.1	Introduction	197
10.2	Theoretical and Empirical Considerations	197
10.3	Experimental Verification	200

11	THE ERRORS OF THERMISTORS IN ACTUAL SOUNDINGS	
11.1	Introduction	202
11.2	Solar Radiation Error	
	(a) Effect of Lead Wire Orientation	202
	(b) Reflected and Scattered Radiation from Below the Thermistor	204
	(c) Computations of the Radiation Error	204
11.3	Measuring Current Error	209
11.4	Conduction Error	209
11.5	Long-wave Radiation Error	213
11.6	Aerodynamic Heating	216
11.7	Lag Error	219
11.8	Sample Computations of Combined Temperature Errors	221
12	CONCLUSIONS	
12.1	Discussion of Results	225
12.2	Thermal Boundary Layer Effects	228
12.3	Recommendations for Future Work	230

LIST OF FIGURES

1.	Heat Transfer Modes Affecting Thermistor Bead Temperature	7
2.	Photomicrographs of Bead Thermistors	15
3.	Calibration Curves, $\log R_T$ vs $1/T$	20
4.	Expanded Calibration Curve, G-2	25
5.	Temperature Change per K-ohm Resistance Change	26
6.	Heat Balance of Section of Thermistor Lead	29
7.	Temperature Distribution along Lead Wires of Irradiated Thermistors at Different Altitudes	34
8.	Temperature Rise of Irradiated Thermistors	37
9.	Measuring Circuit	45
10.	General View of Equipment	52
11.	Reflectance of Freshly Deposited Aluminum Film	54
12.	Schematic Diagram of Radiation Source	54
13a.	Mounted 5 mil Thermistor	58
13b.	Exploded View of Thermistor Mount	58
14.	Thermistor Enclosure and Baffle	60
15.	Enclosure Mounted on Pump Plate	60
16.	Showing Window, Enclosure and Baffles	62
17.	Underside of Pump Plate Showing Heat Shields, Radiation Source, and Chopper Disk.	63
18.	Recorder Chart Showing Response of Thermistor to Radiation	69
19.	Change in Lamp Output with Operating Time	73
20.	Measured Response of Thermistor to Radiation	77
21.	Measured Response of Thermistors to Radiation	80
22.	Measured Response of Thermistors to Radiation	82
23.	Measured Response of 10 mil Rod Thermistor to Radiation	84
24.	Measured Response of Thinistor to Radiation	86
25-29	Photomicrographs of Thermistor Bead Surfaces	97-101
30-32	Photomicrographs of Thermistor Lead Wire Surfaces	102-104
33.	The Quantity ϵ_2K for G-5	107
34.	Heat Transfer Coefficients for Thermistor Beads and Lead Wires (Still Air)	110
35.	Heat Transfer Coefficients of Thermistors Deduced from K	112
36.	Response of Thermistor to Radiation at an Oblique Angle	115
37.	Temperature Rise of X2047 Thermistor vs Power Dissipation	124
38.	Measured Dissipation Rates of Thermistors	126
39.	Conduction Error for Thermistors using 1 mil Platinum-Iridium Leads	130

40.	Conduction Error for Thermistors using 0.7 mil Platinum-Iridium Leads	132
41.	Measured and Computed Dissipation Rate for Different Lead Lengths	135
42.	Device for Long-Wave Radiation Tests	142
43.	Apparatus for Testing Response of Thermistors to Long-Wave Radiation	143
44.	Response of Thermistors in L/W Radiation Tests	147
45.	Heating Unit for Time Constant Tests	156
46.	Correction to τ for Nonlinearity of R-T Curve	156
47.	Recorder Chart Showing Response of 5 mil Thermistor in Time Constant Tests	158
48.	Semi-log Plot of Curve in Fig.47	159
49.	Measured Time Constants of Thermistors	160
50.	Measured Time Constants with Different Lead Lengths	162
51.	Rotating Arm	170
52.	Rotating Arm	171
53.	Drive of Air in Bell Jar, MSL Pressure	175
54.	Speed Controller Calibration	176
55.	Time Constant and Dissipation Rate of 5 mil Thermistor	178
56.	Time Constant and Dissipation Rate of 10 mil Thermistor	179
57.	Time Constant and Dissipation Rate of 15 mil Thermistor	180
58.	Time Constant and Dissipation Rate of Thinistor	181
59.	Effect of Airspeed on Dissipation Rate	183
60.	Two-Channel Measuring Circuit	189
61.	Temperature Rise of Thermistor vs Airspeed	193
62.	Measured Recovery Factors of Thermistors	194
63.	Solar Radiation Error of Thermistors	206
64.	Effect of Albedo on Solar Radiation Error	208
65a.	Arcasonde Power Dissipation	210
65b.	Self-Heating Error, Arcasonde: 10 mil Thermistor	210
66.	Conduction Error	212
67.	Long-Wave Radiation Error of a Thermistor	214
68.	Aerodynamic Heating, Arcasonde	218
69.	Lag Errors of Thermistors	220

LIST OF SYMBOLS

a_w	Cross-sectional area of lead wire
A_T	Surface area of thermistor bead
A'_T	Projected area of thermistor bead
d	length of one lead wire
h_T, h_w	Convective heat transfer coefficients for thermistor bead and lead wires respectively
h'	Heat transfer coefficient expressing the exchange of long-wave radiation for small temperature differences
J	Intensity of direct radiation falling on thermistor
k	Thermal conductivity of lead wire material
k_a	Thermal conductivity of air
K	Dissipation rate of a thermistor
Ma	Mach number
Nu	Nusselt number
p	Representing the quantity $\sqrt{\frac{2h}{kr}}$
p'	Representing the quantity $\sqrt{\frac{2h'}{kr}}$
Pr	Prandtl number
q	Representing the quantity $\frac{2 e_{sw} J}{\pi rk}$
Q_e	Electrical heat dissipated in thermistor bead
r	Radius of lead wire

Re	Reynolds number
R_T	Electrical resistance of thermistor
T	Absolute temperature
$\epsilon_{ST}, \epsilon_{SW}$	Absorptivities of thermistor bead and lead wires for solar radiation
$\epsilon_{LT}, \epsilon_{LW}$	Absorptivities of thermistor bead and lead wires for long-wave radiation
θ_1	Temperature difference between support post and air
θ_2	Temperature difference between thermistor bead and air
θ_{20}	Temperature difference between thermistor bead and air in absence of radiation.

CHAPTER 1

INTRODUCTION

1.1 Background to the Problem

The last 25-30 years have seen a continued expansion of our observations of the upper atmosphere. This expansion has been characterized by a series of upward and outward steps in which techniques developed for soundings to a particular altitude range at a limited number of stations have been further developed to enable "synoptic" soundings at more frequent intervals of time and space to be performed. These latter developments have to a considerable extent been influenced by requirements of economy and convenience. Thus the techniques used in a synoptic system do not necessarily represent the most sophisticated methods for carrying out the measurements concerned.

The development of high altitude sounding rockets since World War II has enabled much information to be obtained about the atmosphere above the level attainable with balloons. Because of cost, soundings were at first limited to rather infrequent firings, but recently more economical rockets have been developed which allow study of synoptic scale phenomena. In 1959 the Meteorological

Rocket Network (MRN) was established. This network, described by Webb et al (1961,1962), is a cooperative arrangement of various independent groups which operate rocket ranges (mostly in North America), under which data and information is exchanged and firings coordinated in time. The aim of this network is to obtain data on winds and temperatures up to an altitude of 60-70 km on a time and space scale suitable for at least preliminary studies of synoptic scale phenomena above radiosonde level. A considerable amount of information has been obtained by the network since its inauguration. The rockets most used have been the Arcus and the Loki ; details of these rockets and their characteristics have been freely published elsewhere. (See for example, Ballard (1965)).

Perhaps because of economy considerations, the telemetry package for the temperature measurements was made to be compatible with the GMD-1 ground equipment, and the primary temperature sensor chosen was a 10 mil bead thermistor. It was found, however, that temperatures obtained with this sensor above about 50 km were too high when compared with other results, such as the sound-grenade experiments. Subsequently, various workers have attempted to analyze the errors of these rocketsonde measurements, with a view to obtaining correction equations

by means of which the validity of the measurements could be extended to higher levels. The chief contributions in this respect were those of Barr (1961) and of N.K. Wagner (1961,1964). The computations of these authors relied rather heavily on theoretical and/or assumed values for the various heat-transfer coefficients involved in the analysis, because of a lack of published experimental data on the characteristics of the thermistors. However they did confirm that the errors amounted to some tens of degrees near the upper part of the soundings.

As is the case with many instrumentation problems, much of the literature concerning the errors of these small thermistors when used for air temperature measurements is of a fragmentary nature, being perhaps part of various unpublished reports which are not easy to find. There does not appear to be any really thorough treatment of the subject which takes into account all the pertinent factors. Further, it is evident from a critical review of this literature that there are prevalent a number of serious misconceptions. These are due to a lack of understanding of the physical processes involved, and to the neglect of certain items which in fact turn out to be of major importance.

The present study is intended to be a laboratory investigation of the various types of errors to which the

small thermistors used in the rocketsondes are subject. These thermistors are also being used for other types of atmospheric temperature measurements, for example on high altitude floating balloons, and although the emphasis in this work will be on rocket soundings it is hoped that the results will be of much wider application. In addition to the bead thermistors, some data will be given on the characteristics of miniature rod thermistors and on the recently developed "thinistors" which have flat-plate geometry.

It is unfortunate that a more thorough study of bead thermistor errors was not made in the earlier stages of development of the rocketsondes for the MRN, for it turns out that the altitude to which meaningful corrections can be applied to existing data is limited, while relatively minor changes in the mounting and utilization of the sensors would have very greatly improved the measurements. It is only very recently that improved types of mountings have been developed which reduce one of the major sources of error - conduction of heat from the rocketsonde body through the lead wires to the thermistor bead. This new mount has not yet been adopted by all contributing ranges of the MRN, but it is obvious from comparisons with other methods that the results are greatly superior to the previous ones

above 50 km. (See Ballard (1966)). Even so, it is not clear to exactly what extent they are improved, nor is it clear what the remaining errors may be. There is therefore still a considerable amount of data being produced whose accuracy in the upper levels is not known.

It is hoped that the present work will throw some light on this question, and also provide quantitative data leading to an improvement in sensor design.

1.2 Errors of Immersion Thermometers

There are many methods available for measuring atmospheric temperature, but the most common method is "immersion thermometry". In this, the active part of the sensor is exposed to the air and is supposed to attain the same temperature as the air. The temperature of this part of the sensor is monitored in some way. It is not proposed in this work to carry out any comparisons with the other methods of temperature measurement. As has been noted in 1.1 above, cost and convenience considerations play a large part in the choice of sensors for a particular purpose. The inherent simplicity of immersion thermometry makes it an obvious contender for a synoptic meteorological sounding network, because there is the prospect of low or moderate cost, minimum restrictions on vehicle design, and relatively short

time required to carry out a measurement at a given point. It is not surprising therefore that immersion thermometry was chosen for the rocketsonde network. The active part of the sensor in this case is of course the bead of the thermistor. Temperature is deduced from the resistance of the bead (C/F Chapter 2).

It is well known, however, that immersion thermometers are subject to errors. This is because of the fact that in addition to the exchange of heat directly with the surrounding air there are other modes of heat transfer which cause the equilibrium sensor temperature to be different from the air temperature. Some of these factors will be listed below. In general the errors increase with altitude because the convection which causes the sensor element to approach the air temperature decreases while the other terms usually do not. If we have some knowledge of these terms it is possible to deduce the true air temperature from the sensor temperature by applying an appropriate correction. It is the uncertainty of this correction rather than its actual magnitude which determines the usefulness of a given sensor in a given situation. Good design of the sensor will minimize this uncertainty. Normally, but not necessarily, this is accompanied by a reduction in magnitude of the error.

Fig.1 illustrates schematically the main heat exchange mechanisms as they apply to a rocketsonde thermistor. Thus, we have convective heat exchange with the air both direct to the bead, 1, and to the lead wires, 2, whence some of this heat reaches the bead by conduction. There is conduction of heat from the instrument package via the support posts, 3, long wave radiation exchange between the sensor and the earth, clouds and atmosphere below the bead, 4, and between the sensor and the atmosphere above the bead, 5.

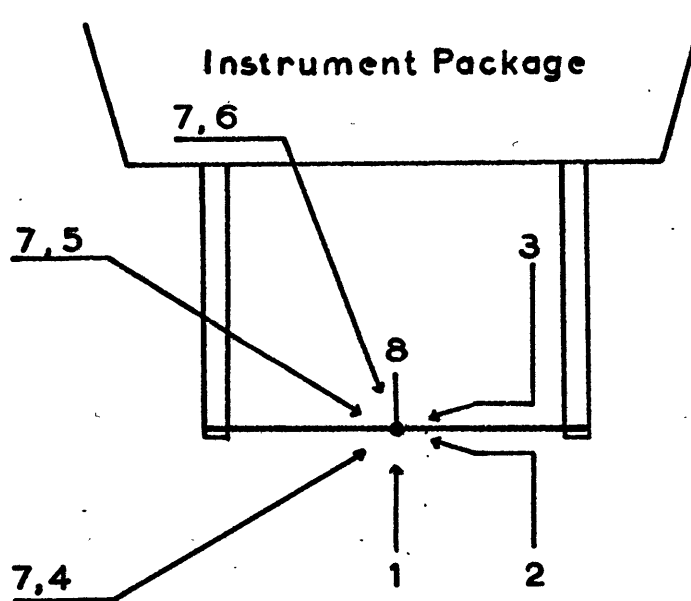


FIG.1. Heat Transfer Modes Affecting Thermistor Bead Temperature.

Long wave radiation exchange between the instrument package and the sensor, 6, must also be considered, and short wave radiation, 7, from the direct solar beam as well as that scattered by the earth, air, and clouds, and by the instrument package. Other effects arise from the self-heating of the bead by the measuring current, 8. Of these items, only 1 and 2 act beneficially in causing the temperature of the bead to approach that of the air, the others may be considered sources of error. One must also be sure that the temperature of the air around the thermistor is not influenced by the instrument package.

Other errors ensue as a result of the motion of the dropsonde through the air. Thus, depending on the lapse rate, the environment is in general changing and the sensor may not be able to follow these changes with sufficient rapidity. More important, at the top of the flight the sensor is ejected with a considerably different temperature than that of the air and it may fall through a considerable distance before it attains the air temperature. Since the density at the top of the sounding is very small the fall velocity of the dropsonde even when the parachute is fully deployed may be very high. There are therefore appreciable errors due to aerodynamic heating.

1.3 Environmental Conditions

It is worthwhile at this stage to briefly review the typical environmental conditions encountered by the sensor in falling from say 80 km. These are given in Table 1, which is abstracted from the U.S. Standard Atmosphere, 1962.

TABLE 1. Properties From the U.S. Standard Atmosphere, 1962.

Geom. Alt. km	Pressure mm Hg	Temp. °C	Molecules/cc	Mean Free Path cm
80	7.8×10^{-3}	-92.5	4.2×10^{14}	4.1×10^{-1}
70	4.1×10^{-2}	-53.4	1.8×10^{15}	9.3×10^{-2}
60	1.7×10^{-1}	-17.4	6.4×10^{15}	2.7×10^{-2}
50	6.0×10^{-1}	-2.5	2.1×10^{16}	7.9×10^{-3}
40	2.15	-22.8	8.3×10^{16}	2.0×10^{-3}
30	8.98	-46.6	3.8×10^{17}	4.4×10^{-4}
20	41.5	-56.5	1.8×10^{18}	9.1×10^{-5}
10	198.8	-49.9	8.6×10^{18}	2.0×10^{-5}
0	760.0	+15.0	2.5×10^{19}	6.6×10^{-6}

The first point to notice is that there is a range of 10^5 in pressure and about half this in the number of molecules per cc. Secondly we note that for a 10 mil bead thermistor of nominal diameter 2.54×10^{-2} cm the mean free path is equal to the thermistor diameter near 60 km. Therefore, for a large part of the altitude range of interest, the

flow of air around the thermistor cannot be treated as a continuous flow. On the other hand, the region where the conditions can be considered to be those of free molecule flow is essentially above the range of the rocket soundings in question. We are therefore dealing with a transition region which is very difficult to treat theoretically from the standpoint of the computation of the heat transfer. It will be seen later that it is at that altitude where the mean free path is not small compared to the thermistor that the rate of heat transfer between the air and thermistor begins to fall off rapidly, with consequent increase in the temperature errors. Thus it is very desirable to carry out laboratory measurements on the thermistors themselves rather than to attempt to use published heat transfer data for similar bodies which may not have been taken under exactly the same conditions.

Finally, we note that up to the maximum altitude of 70-80 km to be considered there is no diffusive separation of the constituent molecules. Therefore the kinetic and molecular scale temperatures are equal and there is no problem in defining atmospheric temperature. If there were no errors, an immersion thermometer would indeed indicate the desired air temperature.

1.4 Outline of This Work

It is clear that it is virtually impossible to simultaneously duplicate in the laboratory all the environmental conditions of a sounding; various aspects of the problem must be investigated separately. Because in general the different sources of error are not independent, we must have a mathematical model by means of which the interplay of these processes in an actual sounding can be predicted. This is possible with a simple system, for example one in which the thermistor is suspended in the atmosphere by its lead wires from relatively heavy support posts, well clear of the instrument package. This is the type of mounting used on the majority of rocketsondes, and in high altitude balloon work. Some of the more recent mountings being tried on the rocketsondes, however, would not lend themselves to this type of analysis (see Appendix), and the extent to which laboratory tests made on these could be applied to the atmosphere is questionable.

This work will be mostly concerned with thermistors mounted in the simple "post" manner described above. Not only has this the widest application, but the results are readily interpreted in terms of the characteristics of the thermistors themselves rather than the specific mounting conditions.

Chapter 2 will describe the calibration and the electrical and physical characteristics of the thermistors. Chapters 3-10 will consider the laboratory tests made to investigate the major sources of error. The relevant theory required for interpretation and application of these results will be developed and the results or deductions from the results will be compared with published data where this is available.

In Chapter 11 the combined results of Chapters 3-10 will be used to discuss the errors of the thermistors when they are used in the atmosphere, as in a balloon or rocketsonde sounding. It is only at this stage that conditions actually prevailing in the atmosphere will be introduced explicitly, although often these will have been considered in the design of the laboratory tests.

CHAPTER 2

CALIBRATION AND PHYSICAL CHARACTERISTICS OF THERMISTORS

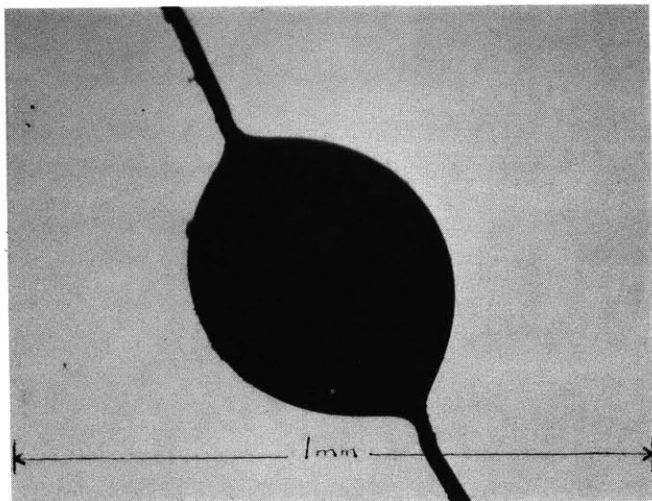
2.1 Thermistors

Thermistors are semiconductor devices whose electrical resistance is a marked function of temperature. They are available in a very large range of shapes sizes and electrical characteristics, and have very many uses besides temperature measurement. The most familiar examples to the meteorologist are the rod thermistors used on the standard radiosondes.

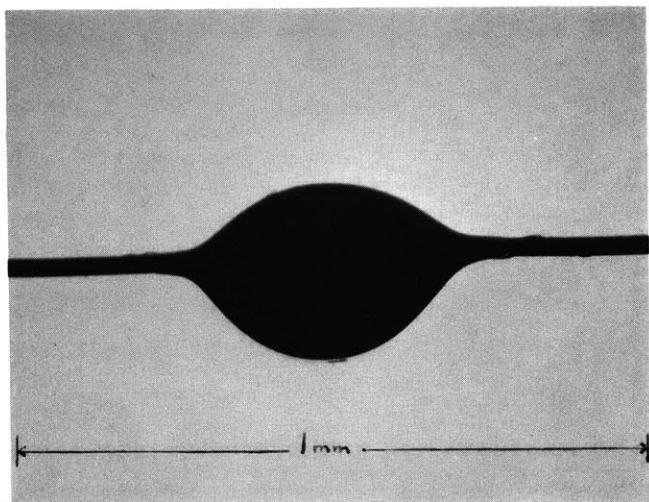
An important feature of thermistors with respect to their use in remote or telemetered temperature devices is their high sensitivity. Thus in a typical case a thermistor of resistance 50,000 ohms at 25°C might undergo a resistance change of 2000 ohms or 4% for a 1°C change in temperature. This can be compared to 0.36% change per °C for a platinum resistance thermometer. Since a wide range of "basic" resistances are available it is relatively easy for an engineer to design such a device with maximum simplicity and reliability.

2.2 Physical Characteristics

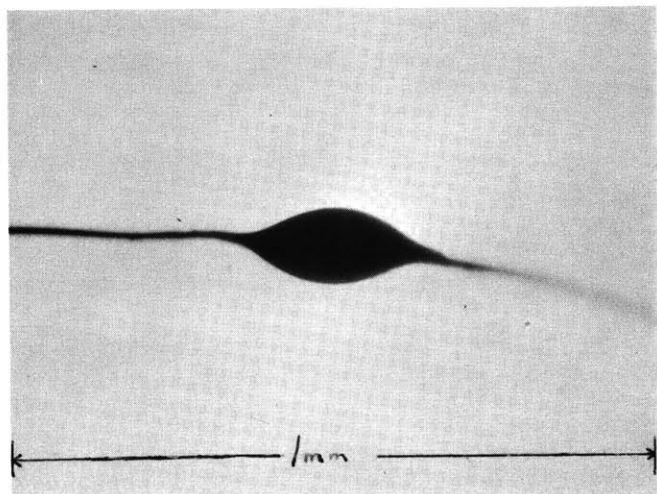
The thermistors studied in this work were mostly bead thermistors. The beads are more or less football shaped, with lead wires for the electrical connections extending from the ends. Some photographs of typical beads are given in Fig.2. The size of bead thermistors is normally expressed by the manufacturer as the diameter in mils, where 1 mil = 0.001 inch. This diameter refers always to the smallest diameter of the bead, but it is also only a nominal figure. These two facts are important, because some authors have published estimates of thermistor characteristics based on the assumption of a spherical bead having the nominal diameter. As an illustration of what can happen due to the departure from sphericity VB-2 shown in Fig.2 was estimated to have a volume of $1.5 \times 10^{-5} \text{ cm}^3$ and a surface area of $3.0 \times 10^{-3} \text{ cm}^2$. The minor diameter was $2.6 \times 10^{-2} \text{ cm}$ which is essentially the nominal diameter of 10 mils. Yet the volume of a true 10 mil sphere is $0.86 \times 10^{-5} \text{ cm}^3$ and its surface area is $2 \times 10^{-3} \text{ cm}^2$. Similar variations can arise through variations in the nominal diameters. Of 10 beads of 15 mils nominal diameter measured from one manufacturer, the mean diameter (of the smallest section) was 14.5 mils and the range of variation from 11.8 mils to 18.3 mils. The corresponding volumes



(a) 15 mil bead



(b) 10 mil bead



(c) 5 mil bead

FIG.2. Photomicrographs of Bead Thermistors.

were $1.55 \times 10^{-5} \text{ cm}^3$ and $6.0 \times 10^{-5} \text{ cm}^3$, a range of nearly 4 to 1.

The bead thermistors studied had nominal diameters of 5, 10 and 15 mils. In general the smaller sizes showed the largest departures from sphericity. The 10 and 15 mil bead thermistors had lead wires of 1 mil diameter platinum-iridium alloy, and the 5 mil beads had leads of the same material but 0.7 mil diameter.

The semiconductor material of the thermistors is sheathed in glass. In many of the beads tested there was a thin outer coating of vacuum deposited aluminum, the purpose of which is to reduce radiation errors.

2.3 Electrical Characteristics

The resistance-temperature characteristic of thermistors is approximately logarithmic, of the form

$$\log_{10} R_T = A - BT.$$

An empirical relation which is valid over larger temperature ranges is

$$\log_{10} R_T = \frac{a}{T} + b \quad (2.3.1)$$

where T is the absolute temperature. For the thermistors

studied, α is positive and therefore the resistance decreases with increasing temperature. Thermistor specifications usually include the nominal resistance at 25°C , together with tolerance limits for the spread of the actual resistance at 25°C about this.

2.4 Calibration of Thermistors

The calibration of thermistors was carried out in air at sea level pressure in a commercial environment chamber. The reason for using air rather than a liquid bath was to avoid contamination which may have altered the electrical resistance of the thermistors. At a temperature of -50°C the resistance of typical thermistors is several megohms and this could be greatly upset by the presence of electrical leakage. In many cases the beads were coated with aluminum. The gap in this coating necessary to break the electrical continuity across the leads is then very small and quite subject to contamination and resulting electrical leakage.

Some precautions were needed when calibrating in air because in a large environmental chamber of the type used the temperature is not uniform. Also there are turbulent fluctuations inside the chamber and the temperature at a given point is unsteady. These effects were avoided by

enclosing the thermistors inside a small copper cylinder, 2 inches in diameter and $2\frac{1}{2}$ inches long with closed ends. This cylinder was suspended by strings in the central part of the chamber. The high thermal conductivity of the cylinder ensured uniform temperature of the air within, and its relatively large mass kept the temperature steady.

The temperature of the copper cylinder was measured with a copper-constantin thermocouple. One junction was soldered to the inside of the cylinder wall and the other kept in an ice bath and the output measured with a Leeds and Northrup potentiometer. As a secondary check, an alcohol in glass thermometer was taped to the outside of the cylinder. This was almost always within 0.2°C of the thermocouple.

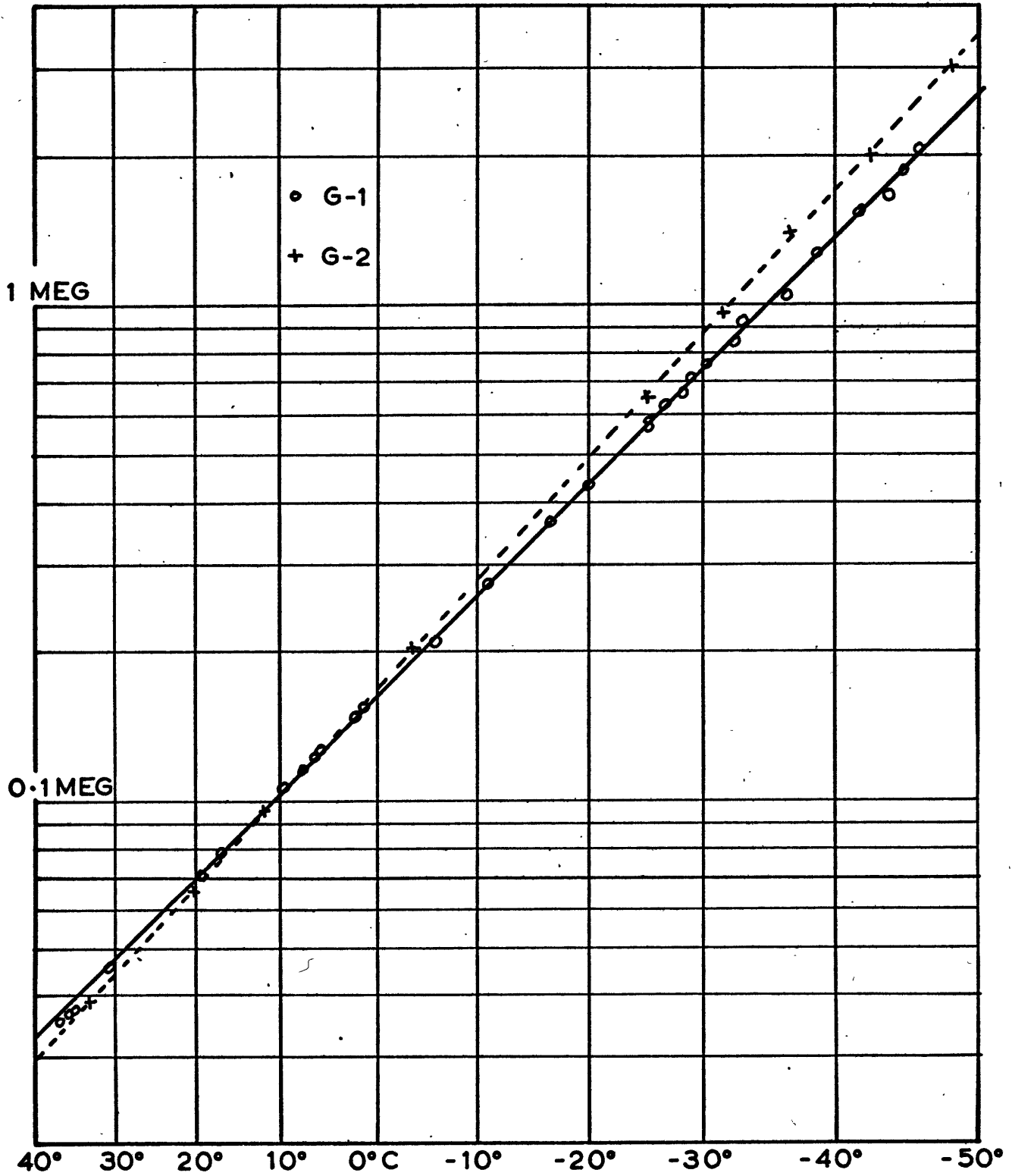
By operating the refrigerator or heater of the chamber the temperature was varied from about -50°C to $+40^{\circ}\text{C}$. It was found that satisfactory readings were only obtained if the chamber temperature was varied in steps, with plenty of time allowed at each step for the temperature to become steady. The resistance of the thermistor was measured using a bridge and recording circuit to be described in Chapter 3. The measuring current was kept small enough to avoid electrical heating of the thermistor bead, which can easily occur especially at low temperatures where

the resistance is high.

Fig.3 shows plots of the calibration of two Gulton type X2047 thermistors, G-1 and G-2 using $\log_{10} R_T$ vs $\frac{1}{T}$ coordinates. For these two 15 mil bead thermistors the relation is seen to hold quite well, but there is some difference in the slopes.

When purchased in quantity, these small thermistors show a significant spread of their actual resistances at 25°C about the manufacturer's nominal resistance, $\pm 20\%$ is typical. The manufacturers can provide matched thermistors whose resistances at a particular temperature are within a specified tolerance, but of course the smaller this tolerance is the greater the cost. Assuming that a universal calibration is not practicable, the next best would have been to have a standard calibration curve which could be adjusted to each thermistor by making a single calibration check at say room temperature. This is the procedure used with the standard radiosonde rod thermistors. For example, if in the relation (2.3.1) the value of a did not vary between thermistors of a given type one could merely adjust b by a single observation and obtain a calibration valid at all temperatures.

Since a defines the slopes of the curves in Fig.3,

FIG 3. CALIBRATION CURVES, LOG R_T VS $1/T$.

it is seen that this procedure cannot be applied with suitable accuracy. Thus, if a curve having the same slope as G-1 in Fig.3 is matched to the calibration of G-2 at 25°C, the calibration would be in error by about 4°C at -50°C and presumably greater at the temperatures of -70°C or so expected in the rocket soundings.

To avoid this type of error it is necessary for individual thermistors to be calibrated at more than one point. This entails significantly increased cost as well as some loss of convenience in the reduction of data. It is probable that in the future the thermistors can be made in quantity with the slope, a , constant. At present one can obtain at considerable extra cost matched sets of a small number of thermistors which accurately track the same temperature-resistance curve over a specified range, but these are probably selected by trial from a batch of standard thermistors. The Bendix-Friez company have developed a small 10 mil diameter rod thermistor for upper atmospheric work which they claim can be made to have much more closely controlled calibration characteristics than the small beads. Some characteristics of these rods will be discussed later.

Similar calibration plots to those given in Fig.3 have been made for other types of thermistors. For some

the $\log_{10} R_T = \frac{a}{T} + b$ relation did not hold over the full range of $+40^{\circ}\text{C}$ to -50°C , there being a slight increase in slope at temperatures below about -25°C . For these types, calibrations at several points over the range would be necessary. As expected, different thermistor types exhibited different slopes.

2.5 Stability of Calibration

In the early days of development, some thermistors suffered from the serious disadvantage that their resistance-temperature calibrations tended to drift or jump appreciably. This was often associated with mechanical or thermal shocks. More recent thermistors appear to be somewhat improved. In a test of the stability of thermistors for low temperature measurement, Sachse (1962) subjected small glass encapsulated thermistors to repeated thermal cycling between 90°K and 300°K . He reported calibration drifts of up to a few tenths of 1°C after the first 500-1000 cycles and much smaller drifts thereafter. On the other hand Droms (1962) observed drifts of from 0.3°C to over 5°C in small (14 mil) glass coated bead thermistors over a period of 90 days when stored at temperatures of 100°C and 200°C . The drift of 43 mil glass coated bead thermistors over the same time was less than

0.06°C when stored at 100°C.

The author has not carried out a detailed study of this problem, but one of the 15 mil bead thermistors was checked at room temperature against a thermocouple 4 or 5 times over a period of 4 months and there was no change in calibration within the accuracy of the tests (about 0.3°C). No calibration jumps were noticed with any of the many other thermistors used in the course of this investigation, although they were not specifically looked for. It is probable that thermistors stored at room temperature are relatively stable - nevertheless a pre-flight calibration check as in standard radiosonde practice would seem desirable.

2.6 Utilization of Thermistor Calibrations in this Work

In the major part of the work to be described, the important item was a temperature change rather than the actual value. Also, the majority of the tests were carried out at room temperature. The temperature changes ranged from tens of degrees down to tenths so there was a problem in having a single calibration curve plotted on a large enough scale to accurately cover this range.

The procedure adopted was to plot the calibration

points on a $\log R_T$ vs $\frac{1}{T}$ scale on large (20" x 18") sheets of prepared graph paper. A straight line was fitted by eye to the calibration points between about -10°C and $+40^\circ\text{C}$, and two points on this line used to determine the constants a and b . From these, R_T, T pairs were computed at 10°C intervals from 0°C to $+50^\circ\text{C}$ and these were replotted to obtain a series of calibration curves for each 10°C interval as illustrated in Fig.4 for the thermistor G-2. For evaluation of very small temperature differences it was more convenient to use the function $\frac{dT}{dR_T}$. This was very simply calculated from

$$\frac{dT}{dR_T} = \frac{-T^2}{2.303 a R_T} \quad (2.6.1)$$

Then $\Delta T \doteq \left(\frac{dT}{dR_T} \right)_{\text{mean}} \cdot \Delta R$

The curve corresponding to G-2 is given in Fig.5.

Calibration curves for all the thermistors tested were constructed in this way, except that in a few cases where two or three thermistors of the same type were to be tested only one was actually calibrated in the chamber and the quantity b was adjusted to match the calibrations of the remainder at room temperature. For temperature differences, the error involved in assuming the

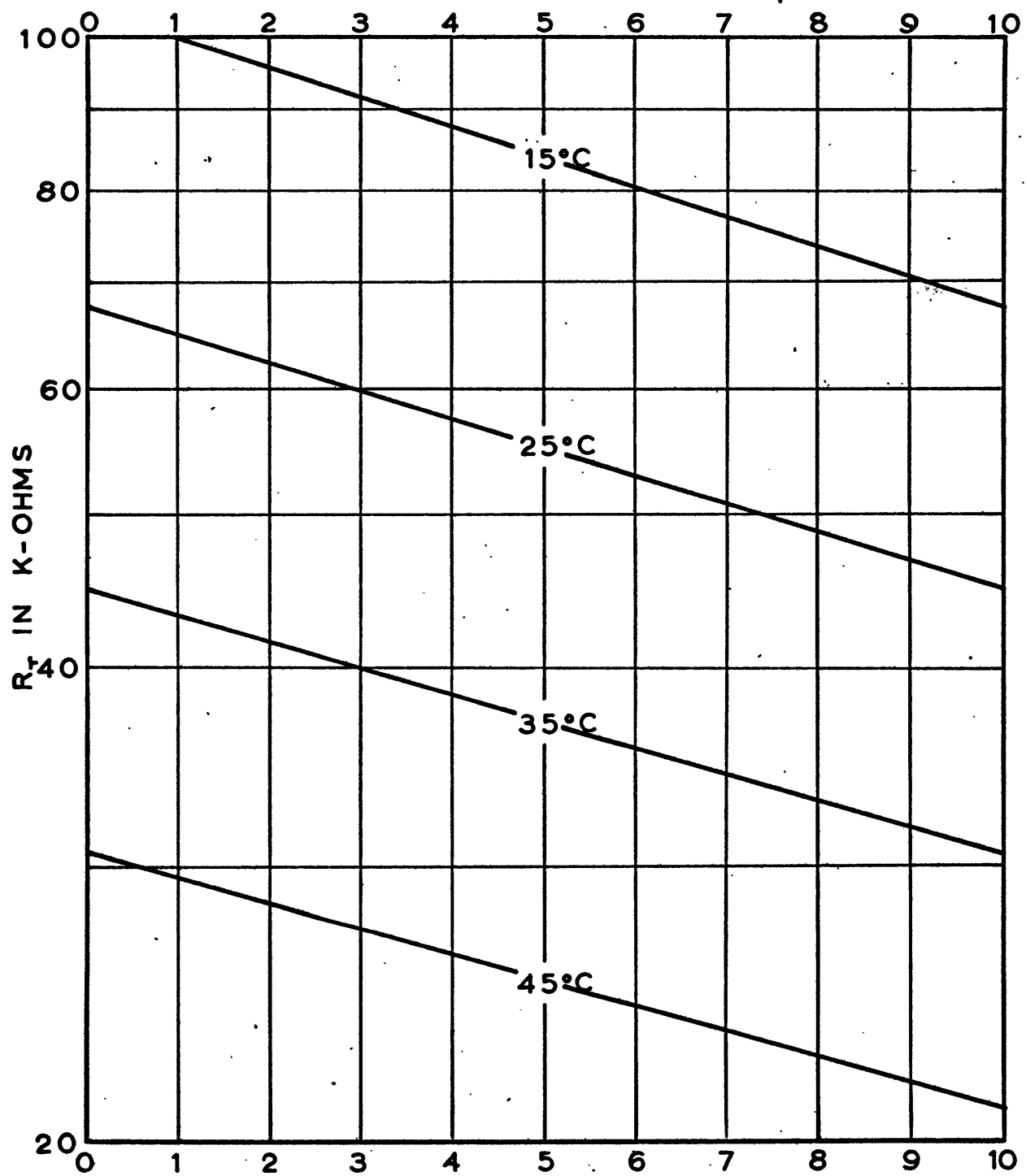


FIG 4. EXPANDED CALIBRATION CURVE, G-2.

G-2

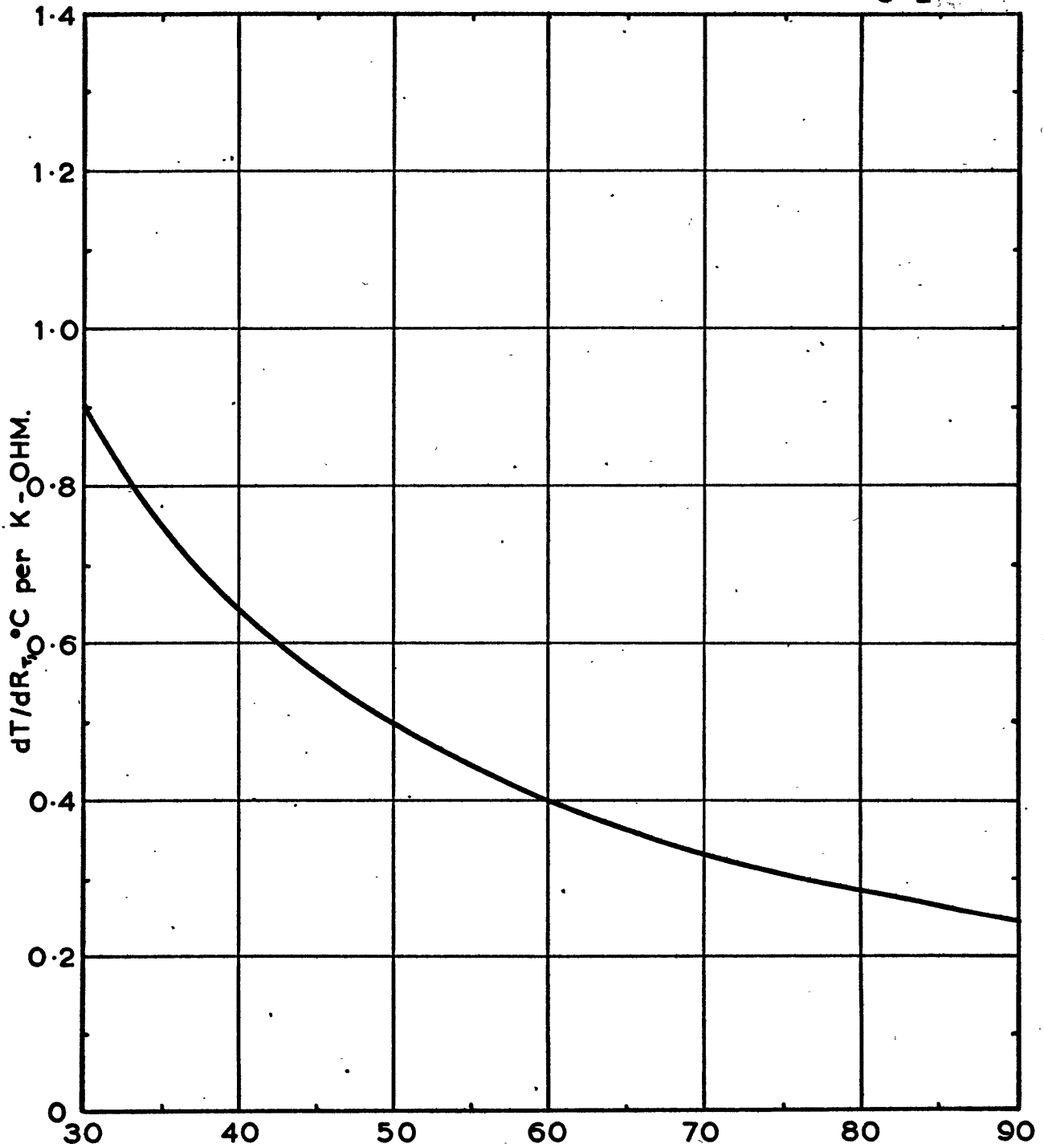


FIG. 5 TEMPERATURE CHANGE PER K-OHM RESISTANCE CHANGE.

same slope is at most a few percent.

Since they are of no intrinsic interest, the other calibration curves are not included in this work.

CHAPTER 3

SOLAR RADIATION ERRORS

3.1 Theoretical Temperature Rise of an Irradiated Thermistor

The error produced in an immersion temperature sensor by the heating effect of the sun's radiation is one of the most important. In the majority of applications of the small thermistors studied in this work no radiation shields are employed, for a number of reasons. Instead, attempts are made to minimize the error by the application of reflective coatings to the thermistor bead. Before describing the various laboratory tests used in investigating this problem it is convenient to derive an expression for the temperature rise of a thermistor when subjected to a uniform parallel beam of radiation, in terms of physical properties of the thermistor.

Consider radiation in the form of a uniform beam of intensity J watts cm^{-2} impinging normally on a thermistor bead and its leads, as shown in Fig.6. We shall first compute the equilibrium temperature distribution along the leads when the convection terms are held constant.

The heat balance for the element dx of this lead wire

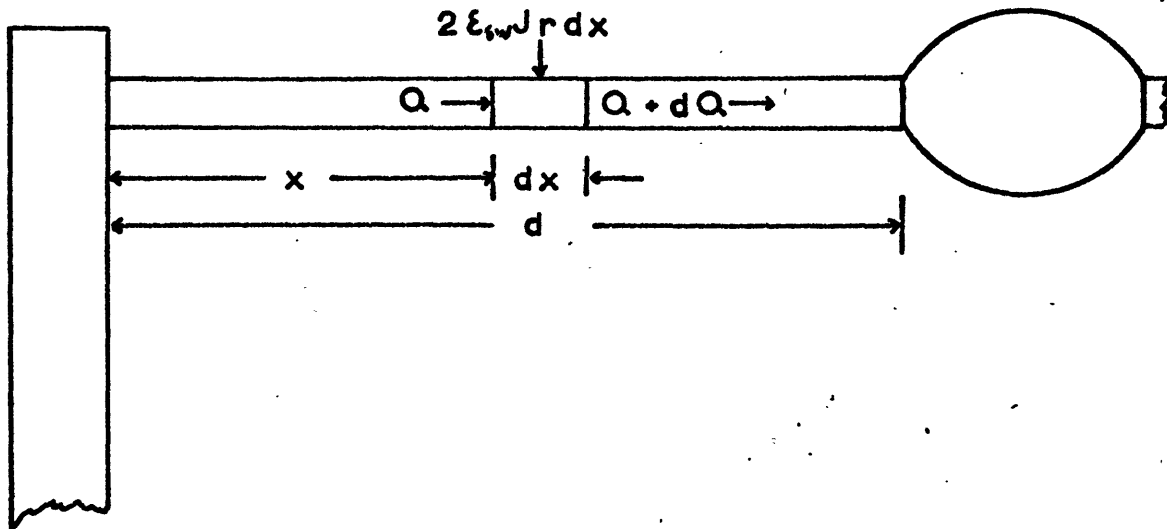


FIG.6 Heat Balance of Section of Thermistor Lead.

can be written

$$dQ = -2\pi r h_w (T_w - T) dx + 2 \epsilon_{sw} J r dx \quad (3.1.1)$$

where r is the wire radius, h_w the convective heat-transfer coefficient for the wire, T_w and T the temperatures of the wire and air, and ϵ_{sw} the fraction of the intercepted radiation absorbed by the wire.

The heat flow in the wire, Q , is related to the thermal conductivity k and the wire's cross-section

area a_w by

$$Q = -ka_w \frac{dT_w}{dx} \quad (3.1.2)$$

After differentiating (3.1.2) w.r.t. x and substituting the result in (3.1.1), the differential equation

$$\frac{d^2\theta}{dx^2} - p^2\theta + q = 0 \quad (3.1.3)$$

results in which $p = (2h_w/kr)^{\frac{1}{2}}$, $q = 2 \epsilon_{sw} J/\pi rk$, and we have written $\theta \equiv T_w - T$.

Since they are so heavy by comparison with the thermistor, the support posts will respond very much more slowly to the radiation than the thermistor and in general will differ in temperature from the air. Let θ_1 be the temperature excess at the support post, $x = 0$, and θ_2 that at the bead, $x = d$. Then the temperature distribution along the lead wires is given by

$$\xi = \operatorname{cosech} pd (\xi_2 - \xi_1 \cosh pd) \sinh px + \xi_1 \cosh px \quad (3.1.4)$$

Here, $\xi \equiv \theta - \frac{q}{p^2} = T_w - T - \frac{q}{p^2}$

Turning our attention to the heat balance of the bead, which is assumed to have uniform temperature, we

note that the heat loss is given by

$$2ka_w \left(\frac{d\xi}{dx} \right)_{x=d} + h_T A_T \theta_2$$

where h_T , A_T are the heat transfer coefficient and the total area of the bead respectively. Neglecting heating due to the measuring current, the heat balance condition for the bead is given by

$$2ka_w \left(\frac{d\xi}{dx} \right)_{x=d} + h_T A_T \theta_2 = J \epsilon_{ST} A'_T. \quad (3.1.5)$$

Here, ϵ_{ST} is the fraction of the radiation absorbed by the cross-section area A'_T of the thermistor bead.

Note that both ϵ_{sw} and ϵ_{ST} refer to average reflectivities, i.e. they include any variation of reflectivity with angle of incidence and with wavelength.

From (3.1.4),

$$\left(\frac{d\xi}{dx} \right)_{x=d} = p \xi_1 \sinh pd + p \coth pd (\xi_2 - \xi_1 \cosh pd) \quad (3.1.6)$$

To obtain the temperature rise due to the radiation we first find the equilibrium bead temperature θ_{20} in the absence of radiation. This is done by setting $q = 0$ and $J = 0$, combining equations (3.1.5) and (3.1.6), and solving for θ_2 .

Thus,

$$\theta_{20} = \frac{2k_a p \operatorname{cosech} pd}{A_T h_T + 2k_a p \coth pd} \cdot \theta_1 \quad (3.1.7)$$

The desired expression is then obtained by substituting for $\left(\frac{d\theta}{dx}\right)_{x=d}$ in (3.1.5) from (3.1.6) and making use of (3.1.7). The result is

$$\theta_2 - \theta_{20} = \frac{(2k_a q/p)(\coth pd - \operatorname{cosech} pd) + J \epsilon_{ST} A_T'}{A_T h_T + 2k_a p \coth pd} \quad (3.1.8)$$

It is seen that the temperature rise of the thermistor bead under radiation depends on a number of factors, each of which must be considered when conducting laboratory investigations.

If we were to put in typical values for the various quantities in (3.1.8) we would find that the contribution to the temperature rise due to the radiation falling on the lead wires is of the same order as that due to the radiation intercepted by the bead. This is clearly demonstrated in the experimental results given below, the effect being greater at higher altitudes than at sea level. This fact appears to have been overlooked or treated rather lightly in previous discussions of the problem.

It is instructive at this stage to note briefly the form of the temperature distribution along the lead wires. This is readily obtained from (3.1.4) after using (3.1.8). Fig.7 shows the results computed for a typical bead thermistor having 1 mil diameter platinum-iridium lead wires each 1 cm long. The three curves have been plotted for heat-transfer coefficients which correspond approximately to conditions at sea level, 60 km and 85 km, and the radiation intensity has been normalized to give a 1°C temperature rise in each case. The supports are taken to be at the air temperature. At lower levels the bulk of the wire assumes an intermediate temperature and the thermistor temperature rise is not affected significantly by the length of the leads, provided this is greater than some minimum length. As the air density decreases, more and more of the lead length becomes involved and eventually direct conduction of heat to the supports through the leads dominates the system.

Examination of (3.1.8), with typical values substituted, shows that if the lead length d is sufficiently great, the radiation error $\theta_2 - \theta_{20}$ is practically independent of the actual lead length and of the support post temperature. Thus, letting $pd \rightarrow \infty$ we obtain

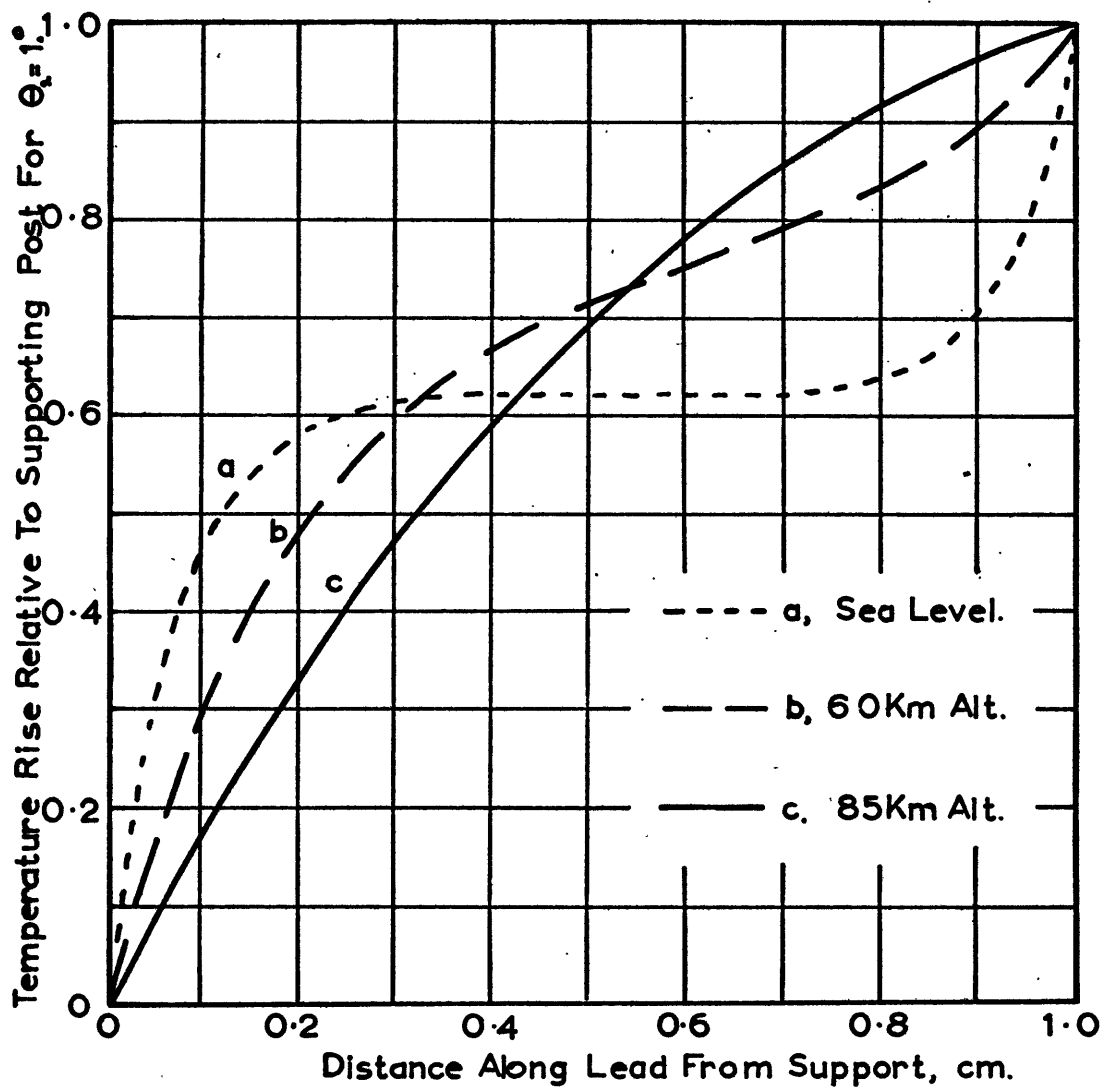


FIG 7. TEMPERATURE DISTRIBUTION ALONG LEAD WIRES OF IRRADIATED THERMISTORS AT DIFFERENT ALTITUDES.

$$\theta_{20} = 0$$

$$\theta_2 = \frac{2ka_w q/p + J \epsilon_{ST} A'_T}{A_T h_T + 2ka_w p} \quad (3.1.9)$$

Recalling that $p = (2h_w/kr)^{\frac{1}{2}}$, $q = 2 \epsilon_{sw} J/\pi rk$
and $a_w = \pi r^2$ this can be written as

$$\theta_2 = J \cdot \frac{2\sqrt{2} \epsilon_{sw} r^{\frac{3}{2}} k^{\frac{1}{2}} h_w^{-\frac{1}{2}} + \epsilon_{ST} A'_T}{2\sqrt{2} \pi k^{\frac{1}{2}} r^{\frac{3}{2}} h_w^{\frac{1}{2}} + h_T A_T} \quad (3.1.9a)$$

However for most purposes it will be more convenient to work with the variables of (3.1.9). These equations give the true radiation error of the thermistor when the lead length has been made sufficiently long to remove the effect of the support post temperature. If the lead length d is small, the temperature rise is smaller than that given by the above equation, but this is not an improvement, for it merely reflects the fact that the temperature of the bead is being influenced by the supports. This "conduction error" will be discussed further in Chapter 5. Here we shall merely point out that the minimum lead length necessary to sufficiently isolate the bead temperature from the support temperature increases with altitude.

The behaviour of (3.1.8) when the convective heat transfer terms approach zero is also of interest. The limiting case, when $h_w = 0$ and $h_T = 0$ is readily derived

by an independent analysis, or it may be obtained from (3.1.8) by the use of two successive applications of de L'Hospital's rule.

Thus,

$$T_{\text{bead}} - T_{\text{supports}} = \frac{qd + J \epsilon_{sT} A'_T}{2ka_w/d} \quad (3.1.10)$$

Fig.8 shows the results of computations of this quantity for various lead wire lengths and various thermistor effective diameters. The latter are defined so that $A'_T = \pi r_T^2$ (C/F section 2.2), the lead wire material is 1 mil platinum-iridium wire, and a reflective coating is assumed on the thermistor such that $\epsilon_{sT} = \epsilon_{sw} = 0.1$.

It is seen that although the temperature rise is significantly dependent on the bead size, this dependence is not as marked as the dependence on the lead length. The latter enters as d^2 . These observations are of interest in the interpretation of the experimental tests to be described below, where we have reduced the air pressure to vanishingly small amounts. However the exact conditions described by these equations can never be realized because in them no account was taken of heat losses by infra-red radiation. The modifications, described below, show significant departures from this simple theory for lead

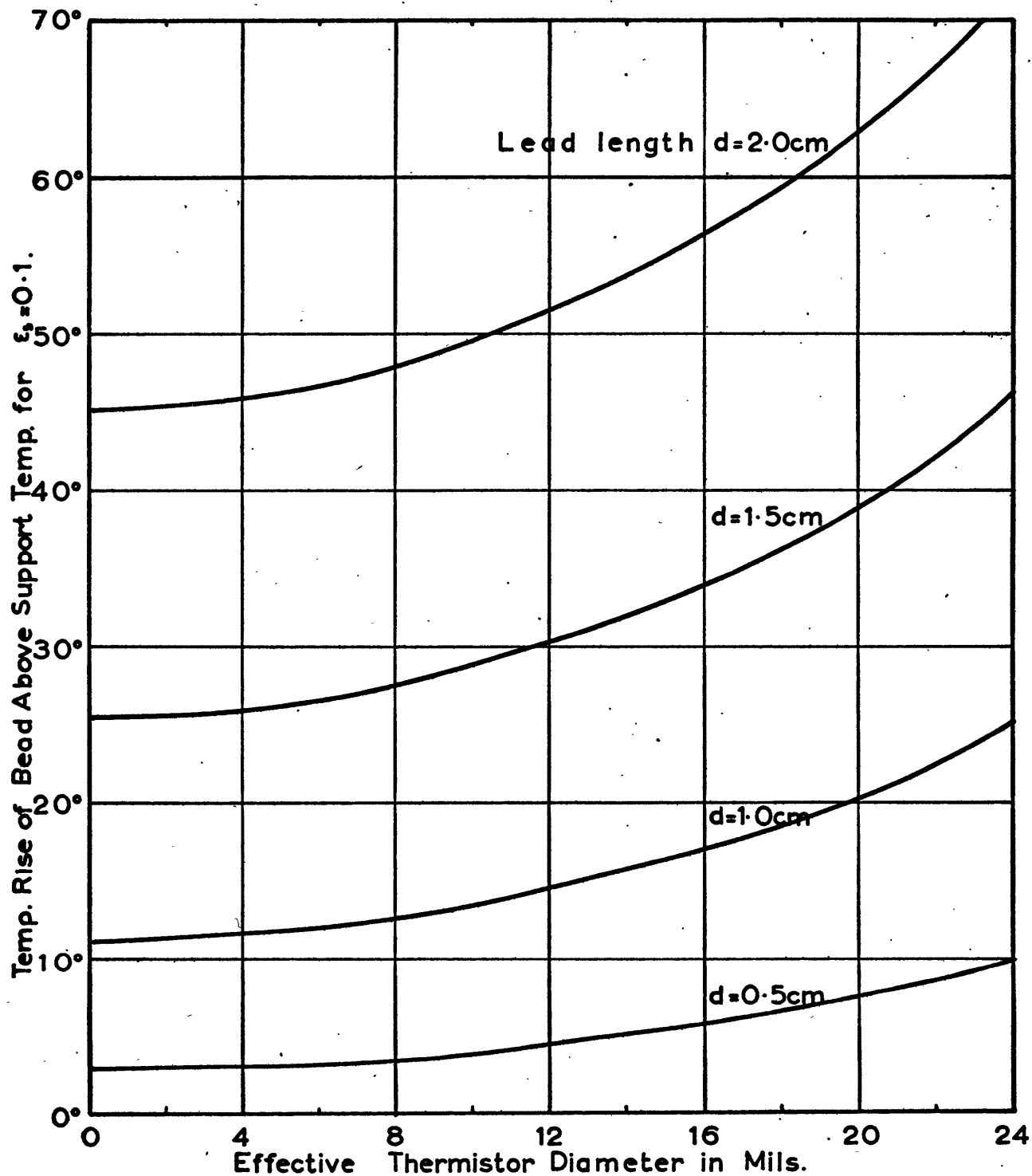


FIG 8. TEMPERATURE RISE OF IRRADIATED THERMISTORS

(In Vacuum. $J = 2.0 \text{ cal/cm}^2/\text{min}$. L/W Radiation Neglected)

lengths greater than about 0.7 cm in a typical case, but the general behaviour is similar to (3.1.10).

3.2 Outline of Experimental Tests

As shown in equation (3.1.8), the radiation error depends on a number of factors. To predict the performance of a given thermistor in an actual temperature sounding we need to know all of these factors, for in general mounting, exposure and environmental conditions will differ somewhat from those used in any laboratory tests. Also, we want to be able to estimate the effect of varying some of the parameters.

Many of the parameters are geometrical, (for example the cross-sectional area A_T' of the bead), and can be measured directly. The remaining ones are h_w , h_T , ϵ_{sw} , ϵ_{st} , and k . k is available in handbooks, although it can also be deduced from simple measurements as shown in Chapter 5. Values of the Nusselt number for cylinders, from which h_w may be obtained, are available in the literature on heat transfer for a wide range of conditions, although not necessarily the exact ones in which we are interested. Nusselt numbers for spheres are also available, but to a more limited extent. However, the wide

departures from sphericity of many thermistor beads, and the fact that both of these Nusselt numbers depend to some extent on surface conditions in the pressure range of interest make it preferable to deduce the heat transfer coefficients from measurements on the thermistors themselves if possible. ϵ_{sw} and ϵ_{st} depend on the nature of the reflective coatings (if any), applied to the thermistors and are therefore of basic interest to this study.

The basic test was to expose the thermistors to a beam of radiation of known intensity, under controlled conditions so that the support post temperature and the long-wave radiation environment (see below) were known. The pressure was varied to simulate different altitudes and the temperature rises due to the radiation observed as a function of pressure. No provisions were made to simultaneously simulate the temperature appropriate to a given pressure altitude, nor to simulate the motion of the thermistor through the air, as in a rocketsonde descent. The temperature effect, which is discussed in Chapter 10, is minor compared to that of the pressure variation. The effect of the motion has been studied separately and is discussed in Chapter 8. We will note here that this is negligible above a pressure altitude of about 50km for these small thermistors, but is considerable at sea level.

This test was broken up into two parts, to enable the separate contributions due to radiation falling on the bead and the lead wires to be studied. In the first part the radiation was allowed to fall uniformly on both the bead and the whole of the thermistor leads. In the second part, the radiation was confined to the bead and only a very short section of the lead wires adjacent to it. Ideally, of course, the radiation would have been confined to the bead alone, but this was not practicable with beads of such small size. An equation to describe the temperature rise of the thermistor bead under the conditions of the second part may be derived in an analogous manner to equation (3.1.8), by making use of the fact that the temperature and heat flow in the wire must both be continuous at the boundary of the irradiated section. The result is

$$\theta_2 - \theta_{20} = \frac{2ka_w q/p \left(\frac{1 - \operatorname{sech} p\Delta + \tanh pd_1 \tanh p\Delta}{\tanh pd_1 + \tanh p\Delta} \right) + J \epsilon_{ST} A_T'}{h_T A_T + 2ka_w p \coth pd} \quad (3.2.1)$$

where d_1 is the length of the shaded part of each lead wire and Δ the irradiated length of each lead, adjacent to the bead. (3.1.8) is, of course, a special case of (3.2.1).

The long-wave radiation environment was controlled by surrounding the thermistors with a blackened enclosure of known, uniform, wall temperature. This wall temperature determined the air temperature. The mounting of the thermistors was arranged so that the temperature of the supports was also kept equal to the enclosure wall temperature. Under these particular conditions the contribution of the long-wave radiation to the heat balance was significant only at very low pressures, and appeared as an additive term to the heat transfer with the air. The latter is shown as follows.

The long-wave radiant heat loss from any element dA of the thermistor surface is given by

$$\epsilon_s \sigma (T^4 - T_a^4) dA$$

where T_a is the common temperature of the air and the enclosure walls, ϵ_s the emissivity and T the temperature of the surface element. For small temperature excursions this can be closely approximated by

$$4 \epsilon_s \sigma \bar{T}^3 (T - T_a) dA$$

where \bar{T} is an appropriate mean temperature.

Hence the net heat flow per unit area for unit temperature difference due to long-wave radiation is $4 \epsilon_s \sigma \bar{T}^3$.

One can therefore define net heat transfer coefficients incorporating both radiation and convection as

$$\begin{aligned} h_w^* &= h_w + h'_w \\ h_T^* &= h_T + h'_T \end{aligned} \quad (3.2.2)$$

where

$$\begin{aligned} h'_w &= 4 \epsilon_{\mathcal{L}w} \sigma T^3 \\ h'_T &= 4 \epsilon_{\mathcal{L}T} \sigma T^3 \end{aligned} \quad (3.2.3)$$

In the experiments using the enclosure, the quantities h_w and h_T appearing in the equations (3.1.8) and (3.2.1) are to be replaced by h_w^* and h_T^* .

By carrying out the two radiation tests under high vacuum it was possible to deduce the short-wave reflectivities ϵ_{sw} and ϵ_{sT} . To do this, a knowledge of $\epsilon_{\mathcal{L}w}$ and $\epsilon_{\mathcal{L}T}$ was required. These were available in some instances from independent tests to be described in Chapter 6, in other cases assumed values were used. The quantity

$$h_T A_T + 2ka_w p \coth pd$$

which appears as the denominator of the right hand sides of (3.1.8) and (3.2.1) is a physically significant quantity called the dissipation rate, K . K is readily measured independently as a function of pressure, as described in Chapter 4. If the measured value of K , rather than the

computed value is used in equations (3.1.8) and (3.1.2) when solving for ϵ_{sw} and ϵ_{st} , the results are much less dependent on the assumed values of many of the parameters, including ϵ_{lw} , ϵ_{lt} , k , and a_w . In all cases this latter procedure was used.

Having obtained ϵ_{sw} and ϵ_{st} , the heat transfer coefficients h_w and h_t were deduced for some of the thermistors as a function of pressure, by making use of equation (3.1.8) and the measured values of K . These quantities were only obtainable by this method over the pressure range of about 10 mm mercury to 0.02 mm mercury, but this was the main region of interest in this study.

3.3 Description of Apparatus

(a) Measuring Circuit

The measurement of thermistor bead temperature is equivalent to the measurement of its resistance. In choosing a suitable bridge circuit to do this certain requirements had to be kept in mind. Firstly, it was desired to make recordings of the thermistor response to certain tests on a strip chart recorder. Secondly, the current through the thermistor had to be controllable and substantially constant during a measurement. Thirdly, provision had to be made for recording both very small

temperature changes, and changes of several tens of degrees - the latter producing changes approaching an order of magnitude in resistance. Forthly, provision had to be made to accommodate thermistor resistances ranging from about 7000 ohms to 250,000 ohms.

The circuit used is shown in Fig.9. It was basically a series circuit in which the current was kept substantially constant by using a suitably large resistor in series with the thermistor. The voltage developed across the thermistor was then proportional to the resistance. A variable bias voltage source was provided which allowed the difference between it and the thermistor voltage to be presented to the recorder, rather than the total voltage. In this way, small temperature changes could be made to cover the whole of the recorder chart, the degree of amplification being adjusted to suit the particular need. A decade resistance box was built in, covering 0 to 1.11 megohms in 1000 ohm steps. This could be switched into the circuit instead of the thermistor, to provide calibration marks on the recorder chart. Current was monitored on the second channel of the recorder by recording the voltage across a standard resistance in series with the thermistor. In addition, the value of the current could be measured precisely by

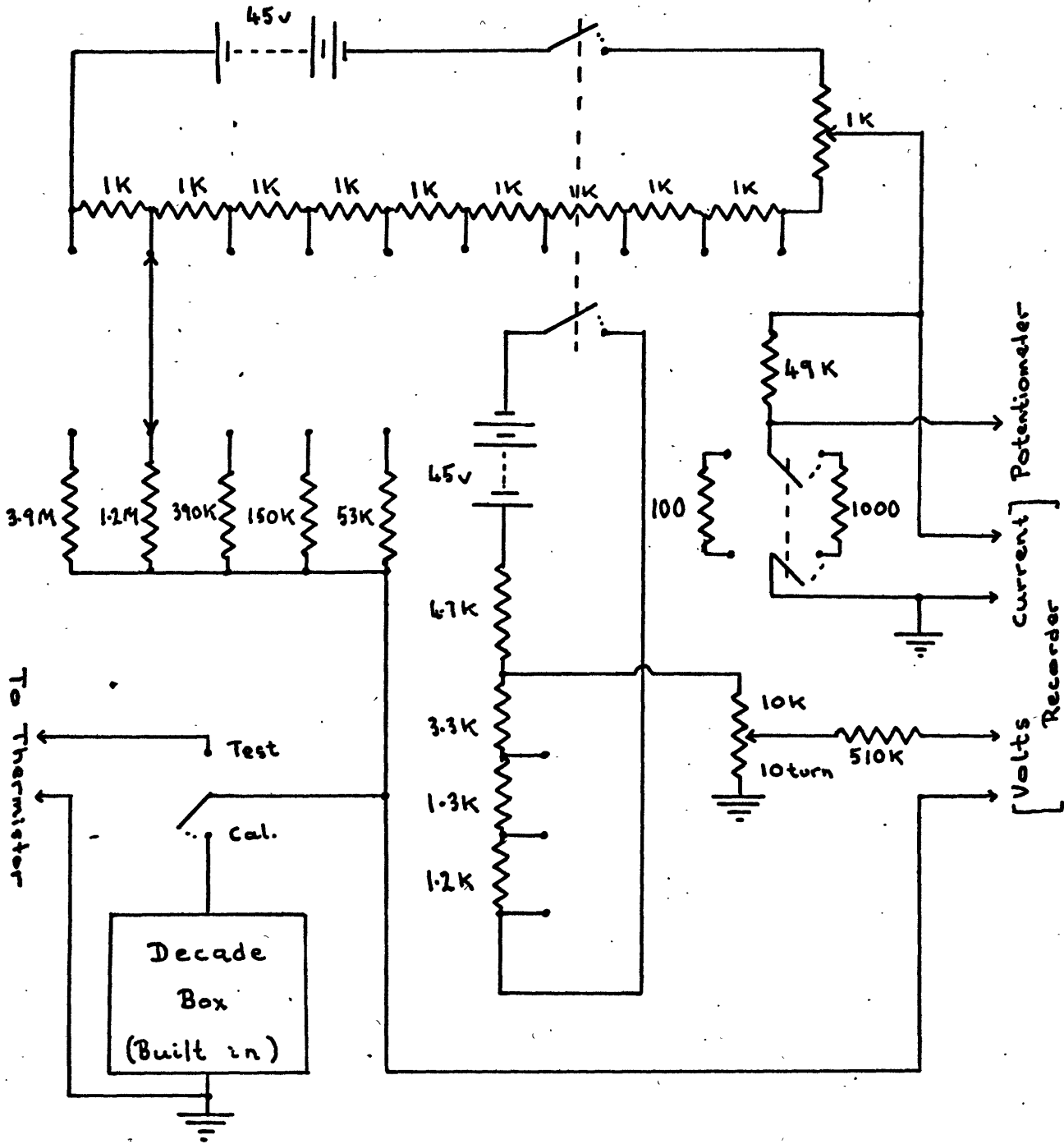


FIG 9. MEASURING CIRCUIT.

measuring the voltage across a second precision resistor with a Leeds and Northrup potentiometer. This circuit was preferred over a standard Wheatstone Bridge because the current could be more readily regulated under varying load conditions.

The recorder used was a Sanborne "Twin-Viso" strip chart recorder, having a maximum sensitivity of 5 milliwatts per cm deflection. A range of speeds from 0.5 mm/sec to 10 cm/sec was available and this, together with a rise time of less than 13 millisecc enabled adequate recordings to be made of the response of all the thermistors tested.

Because of relatively high thermistor impedance and the need for high amplification in some cases, adequate shielding against 60 cycle hum pickup had to be provided for all parts of the measuring circuit and connecting cables.

(b) Vacuum System

As shown in Table 1, Chapter 1, a range in atmospheric pressure of from 760 mm mercury down to less than 10^{-2} mm mercury is encountered between sea level and an altitude of 80 km, and this range of pressure

had to be available for the laboratory tests. In addition, a vacuum of at least 10^{-4} mm mercury had to be achieved for the measurement of the reflectivities, and also for the work to be described in Chapter 6. This did not involve any particular problems provided that the basic principles of good vacuum practice were observed. Several general reference books were consulted on this subject, perhaps the most useful was that by Guthrie and Wakerling (1949).

The system was built around a Cenco 17 inch pump plate. This plate had a $3\frac{1}{2}$ inch hole in the centre designed for the possible installation of a large diffusion pump. A bolt-on flange having an inlet pipe for a mechanical pump was provided to cover this hole. The latter was not used, instead one of the accessory holes near the perimeter was drilled out and tapped with a 1 inch pipe thread into which the plumbing for connection of the mechanical pump and the vacuum gauge was screwed. This allowed the central part of the pump plate to be used for the mounting of a window to admit radiation into the system from below. The vacuum pump was a Cenco Hyvac 14 two stage oil-filled mechanical pump. It was connected via a short length of 1 inch I.D. rubber vacuum tubing to a bellows seal high vacuum angle valve, and thence to the

pump plate via short lengths of 1 inch copper tubing and 1 inch wrought copper solder fittings. When used with a Cenco 15 inch aluminum bell jar, this pump was able to achieve a vacuum of 2 to 3×10^{-3} mm mercury. By sealing off the bell jar from the vacuum pump with the angle valve, and admitting air to the system through a release valve situated in the pump plate, intermediate pressures up to MSL could be obtained.

A Cenco "Supervac OD-25" oil diffusion pump was used for tests requiring pressures sufficiently low that the effect of the air on the thermistors could be neglected. This pump was also mounted near the perimeter of the pump plate rather than in the usual position at the centre. Another of the accessory holes was drilled out to $1\frac{1}{4}$ inches and a special flange was made up which allowed the diffusion pump to be bolted to the pump plate directly underneath this. Vacuum seal was achieved by incorporating an "O-ring" seal in the flange. An aluminum baffle was made to fit over the outlet hole to the diffusion pump. Its main purpose was to condense any oil vapour which might otherwise have found its way into the bell jar.

When the diffusion pump was being operated, the mechanical pump was used as the backing pump, and was therefore

connected to the vacuum system through the former rather than directly. The change-over was facilitated by the use of Cenco vacuum couplings and a short length of rubber tubing. A pressure of less than 2×10^{-5} mm mercury was obtainable without difficulty. This was reached within about $\frac{1}{2}$ hour of switching on the diffusion pump heater, except that somewhat longer was required if the vacuum system had been opened to atmospheric pressure for a prolonged period. With this set-up there was no provision for varying the pressure, so the majority of tests were carried out using only the mechanical pump, connected through the angle valve as described above. In the latter case, the unused diffusion pump remained in the system, but its outlet was sealed off with a plug.

A certain amount of research had to be conducted into the question of obtaining the most suitable vacuum gauge, because the common types did not adequately cover the whole pressure range between atmospheric and 10^{-4} mm mercury. A McLeod gauge was tried for a brief time but it was found to be highly inconvenient when it was desired to vary the pressure in steps. Also the range of accurate pressure readings was limited. The gauge finally adopted was an Alpatron type 530, manufactured by the National Research Corporation. This gauge had 7 linear ranges, in decade

steps from 0 - 1000 mm mercury down to 0 - 10^{-3} mm mercury. The gauge head was installed via a T junction at the same point that the connection to the mechanical pump entered the pump plate. A vacuum angle valve was installed between the gauge and the vacuum chamber, because it was desirable to keep the gauge head sealed under vacuum when the rest of the system was to be opened to the atmosphere for any length of time. The combined length of 1 inch copper tubing and fittings between the gauge head and the vacuum chamber was 14 inches, which should have been short enough to allow representative pressure readings even at the lowest pressures.

Some initial trouble was experienced with this gauge, for the system would not pump down to much less than 10^{-2} mm mercury. The trouble was found to be outgassing of a faulty part in the gauge head. It should be noted that unless a gauge will pump down to considerably less than the lowest pressure desired to be measured there is no guarantee that its readings will be accurate. This is because the presence of leaks, outgassing, or faulty design of the connecting tubes can result in quite different pressures between the gauge head and the bell jar. After the faulty part had been replaced by the manufacturer no more trouble was experienced, and the system could be pumped down to

a gauge reading of less than 2×10^{-5} mm mercury with the diffusion pump. A calibration check was carried out by the manufacturer at the time of this repair, so that pressure measurements made during the course of this study should have been accurate to the rated tolerance of 2% of full scale on each range.

The entire vacuum system was mounted on a rigid structure made from plywood and "Dexion" slotted angle. This greatly simplified the installation and adjustment of the radiation source and other equipment to be described below. A general view of the equipment is shown in Fig.10.

(c) Radiation Source

The ideal radiation source would have produced a parallel beam of radiation whose intensity and spectral content accurately matched that of the sun at the altitude concerned. In recent years elaborate solar simulation systems have been constructed in connection with the development of space vehicles. See, for example, Mann and Benning, (1963). In many of these applications, close spectral duplication of solar radiation is necessary for such studies as the effect of the radiation on the durability of certain materials, and/or the exact duplication of the degree of parallelism of the radiation

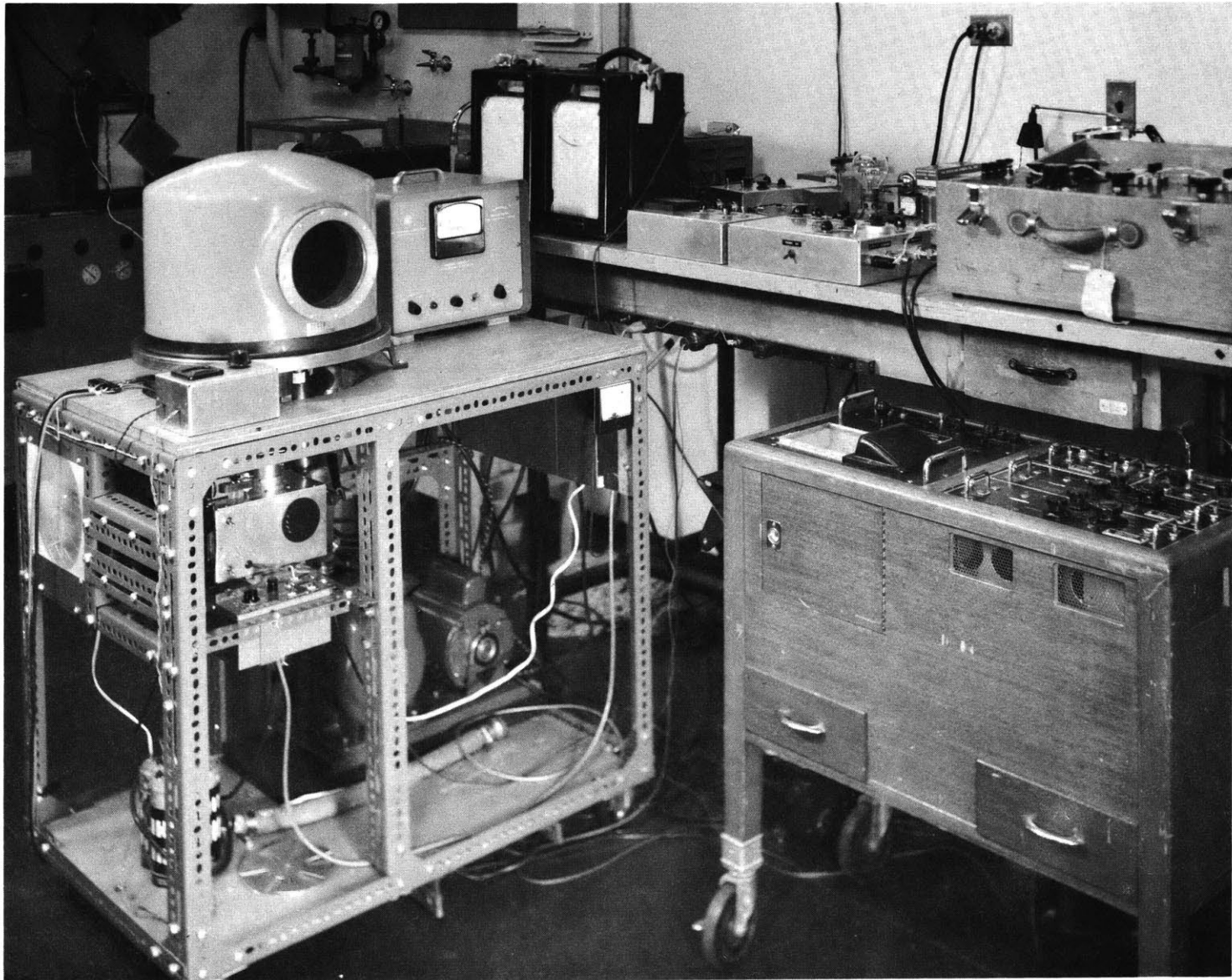


FIG.10. General View of Equipment.

is necessary in order to study the thermal gradients induced at the edge of shadows. Almost without exception these systems are elaborate and costly. In the present study it was decided that somewhat more modest requirements would be sufficient. The heat absorbed by the thermistor is an integrated function combining the absorption at each wavelength interval and the spectral intensity of the radiation over the same intervals. Provided the absorption does not change much over the wavelength of the radiation there will not be much difference in the heat absorbed for two beams of differing spectral composition but equal integrated intensity. The surfaces of the thermistors to be tested were either black, or relatively bright metals, such as aluminum and platinum. Fig. 11, taken from Turner (1962), shows that over the wavelength range of solar radiation, 0.3μ to 2.5μ , the reflectivity of freshly deposited aluminum films varies only a few percent. The same is true of polished platinum, so one would not expect the response of a thermistor to depend too critically on the spectral composition of the radiation.

With these considerations in mind, a tungsten filament lamp was chosen as the radiation source. It was a Sylvania type DEF 21.5 volt, 150 watt projection lamp, primarily intended for 8 mm movie equipment. This lamp

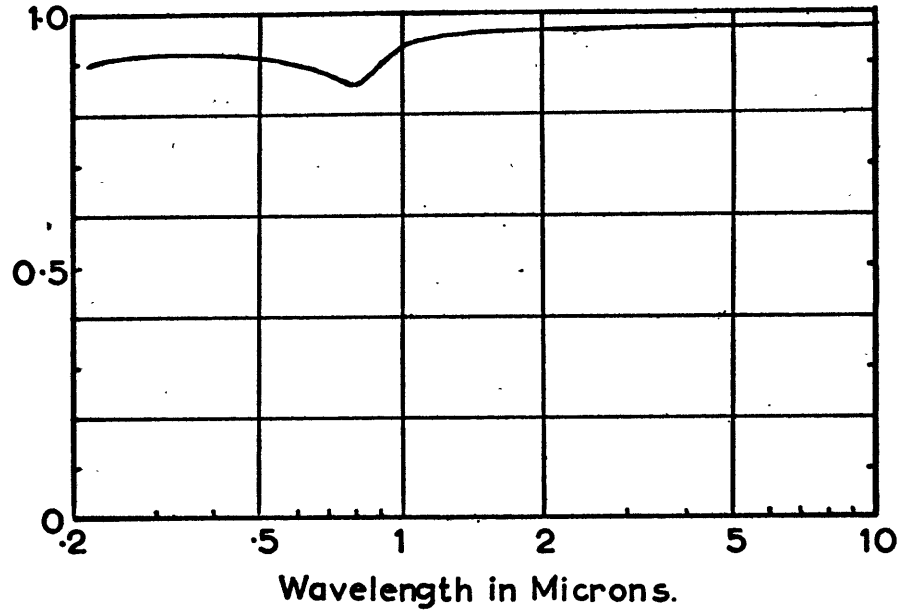


FIG 11. REFLECTANCE OF FRESHLY DEPOSITED ALUMINUM FILM.

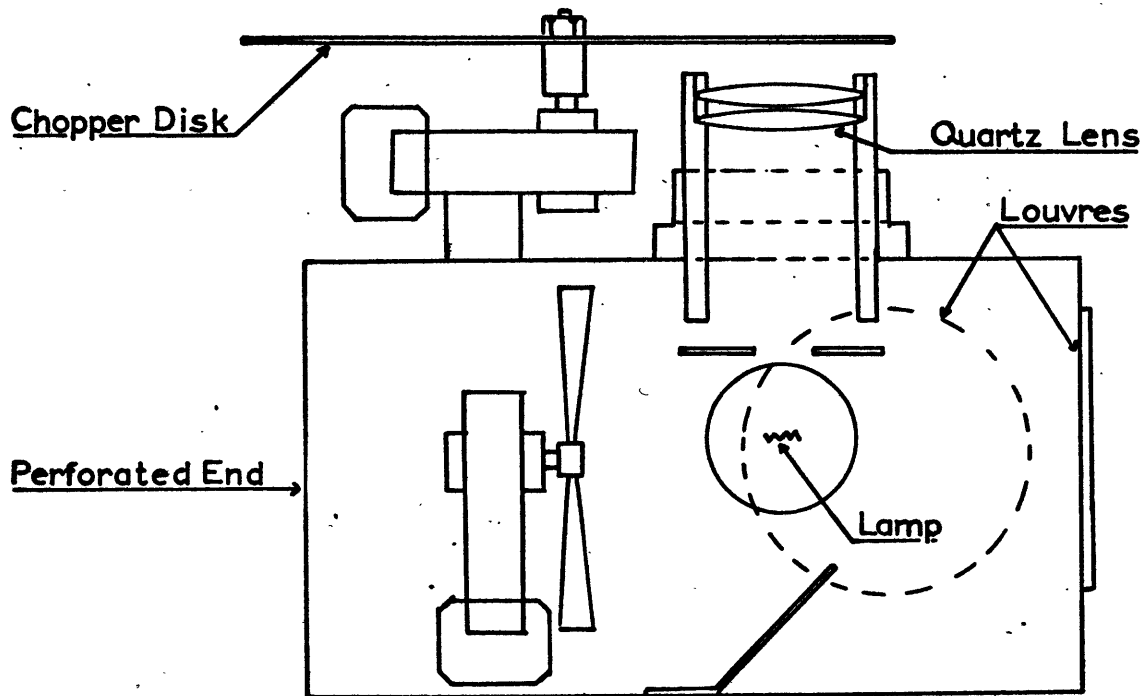


FIG 12. SCHEMATIC DIAGRAM OF RADIATION SOURCE.

type has a very compact, robust filament which operates at a somewhat higher colour temperature (about 3300°K) than higher voltage projection lamps. Even so, the spectral distribution varies significantly from that of the sun (colour temperature $\sim 6000^{\circ}\text{K}$).

To form a parallel beam of radiation of sufficient intensity a simple lens system was used. This consisted of two $1\frac{1}{2}$ inch diameter double convex quartz elements in a simple mount which facilitated focussing. Quartz was chosen rather than regular optical glass to prevent any further distortion of the spectral content beyond that caused by the lamp envelope.

This type of projection lamp has a built-in reflector, which was not used in the optical system. A plate with a $7/16$ inch aperture was installed very close to the lamp, on the lens axis, to cut off the majority of the radiation from this reflector. Any remaining radiation from this source was highly divergent after passing through the lens, and consequently of negligible intensity in the plane of the thermistor.

The lamp was installed in an aluminum housing including a small blower for cooling and a transformer for the 21.5 volt supply. Because of the finite size of the fil-

ament a strictly parallel beam was not possible. The best results, including evenness of illumination over a $1\frac{1}{2}$ inch circle in the intended plane of the thermistor, were obtained when the image of the lamp filament was in focus on a screen at a distance of about 12 feet. In this condition the intensity of the radiation was about $4 \text{ cal cm}^{-2} \text{ min}^{-1}$ at the thermistor. To provide a means of reducing this intensity without altering the filament temperature a small motor was installed, to which was attached one of a set of chopper disks. These choppers had six blades, with angular widths such that when they were rotated at 3000 rpm in the radiation beam the latter was reduced to $\frac{1}{2}$, $\frac{1}{4}$, or $\frac{1}{8}$ intensity, depending on the disk used. For the majority of the tests, the $\frac{1}{8}$ disk was used so that the intensity of radiation falling on the thermistor was approximately that of the solar constant.

A schematic diagram of the radiation source is included in Fig.12.

(d) Thermistor Mounting, and Other Accessories

As noted above, the thermistors were mounted inside a copper sub-enclosure during the radiation tests. This enclosure had several functions. (i) The enclosure walls determined a stable, steady air temperature, free from fluctuations

due to convection. (ii) It provided a heat sink for radiation not intercepted by the thermistor. (iii) Its blackened inner walls provided a uniform long-wave radiation environment of known black-body intensity during the tests.

The enclosure was similar to the one used in the calibration tests, except that ventilation holes were provided for evacuation, and a small viewing port was provided to facilitate final alignment of the radiation beam on the thermistor. The two ends of the enclosure were removeable. The top end carried the thermistor, mounted between two copper support posts $3/64$ inch diameter and $1/2$ inch long. An exploded view of the thermistor mounting is shown in Fig.13. This arrangement was used to maximize the thermal conduction between the thermistor support posts and the enclosure walls, so that these two points were always at the same temperature. Each thermistor to be tested was mounted on its own individual end plate and mount, complete with shielded electrical connector. The thermistor beads were centered with respect to the end plates by holding the latter in a lathe chuck and bringing up tailstock centre. However a final adjustment was permitted by the use of oversize mounting holes in the end plates. The distance between the thermistor support

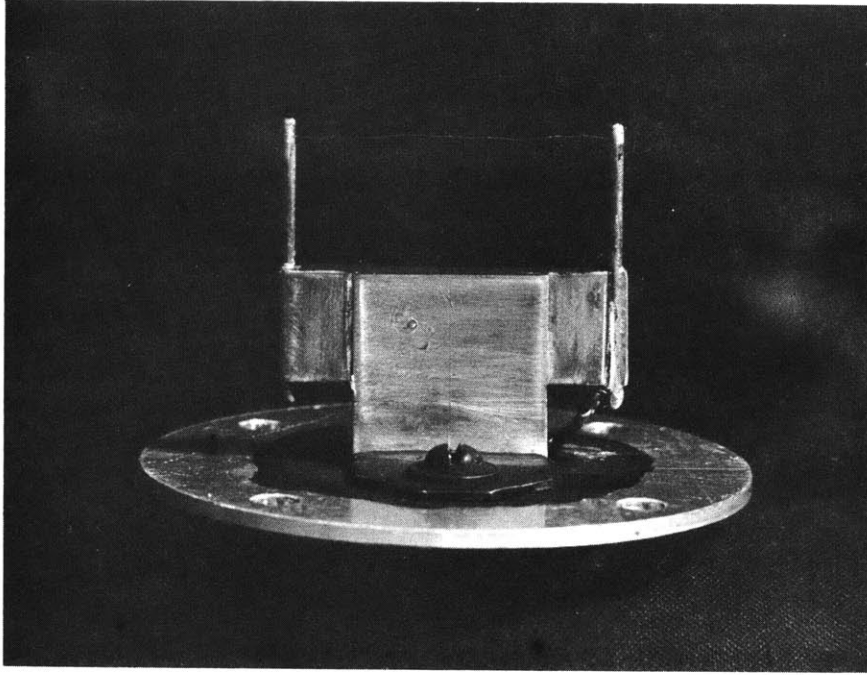


FIG.13a. Mounted 5 mil Thermistor.

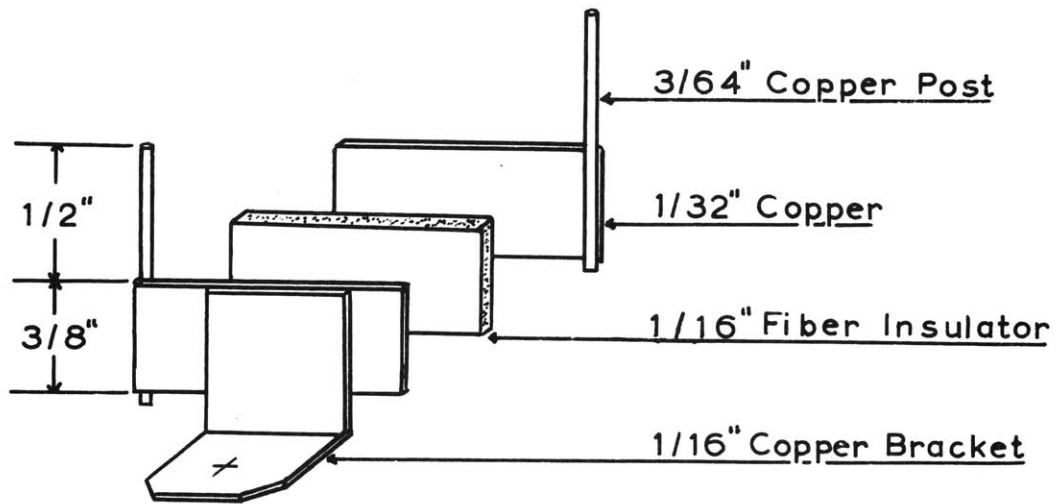


FIG.13b. EXPLODED VIEW OF THERMISTOR MOUNT.

posts depended on the lead lengths available, but was usually between 2 and 3 cm.

The lower end of the enclosure was a baffle containing either a hole or a $3/16$ inch wide slot, depending on the type of radiation test (see above). A second baffle plate was mounted on this so that when the whole unit was assembled, the latter was $\frac{1}{2}$ inch to $\frac{3}{8}$ inch from the thermistor. This second baffle had either a slot $3/32$ inch wide or a 2 mm diameter hole, and was intended to define the radiation falling on the thermistor. The slot could be changed in length and was generally made to be 1 mm shorter than the total length between the thermistor support posts. It thus allowed radiation to fall on the thermistor and substantially the whole of its leads, but not the support posts, while the baffle with the hole confined the radiation to the bead and only short lengths of lead wire adjacent to it. It was necessary to place these baffles close to the thermistor because the radiation beam was not perfectly parallel.

The lower surfaces of all these baffles were of highly polished aluminum. The upper surfaces (facing the thermistor) were blackened with flat black paint, as were the internal walls of the enclosure and the thermistor mounts. Fig.14 shows a photograph of the enclosure

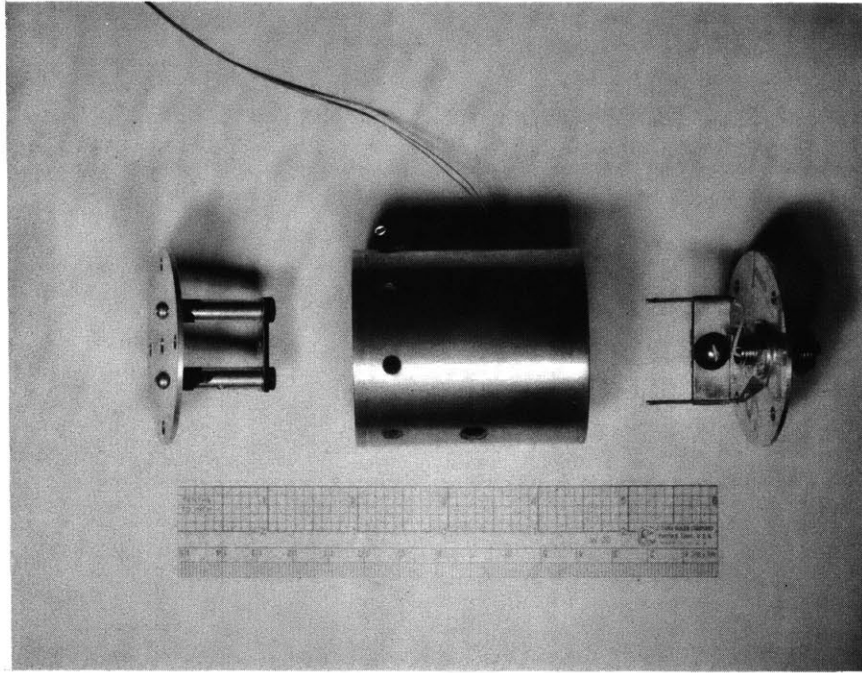


FIG.14. Thermistor Enclosure and Baffle.

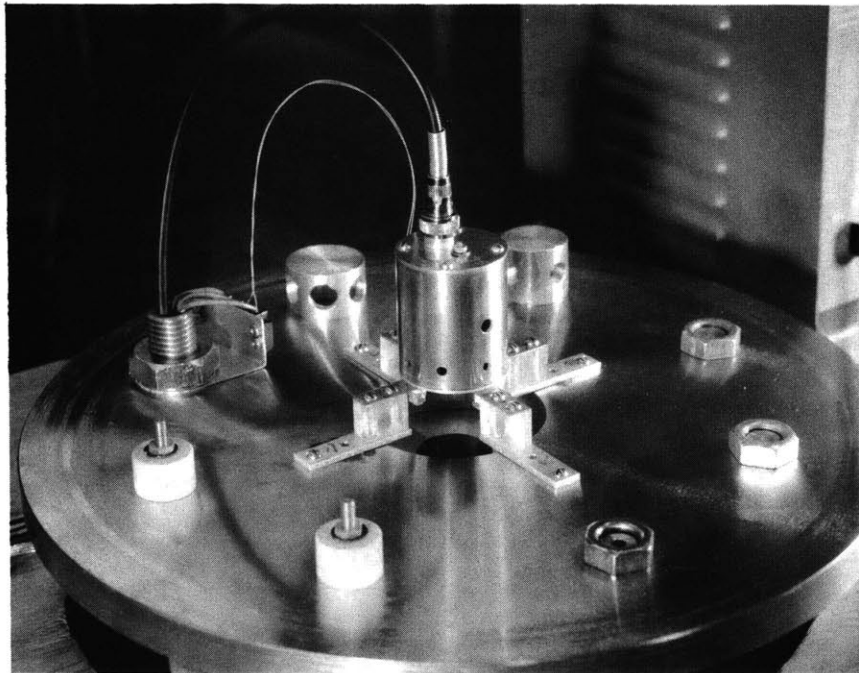


FIG.15. Enclosure Mounted on Pump Plate.

with the "hole" type baffle plates, and a mounted thermistor. Fig.15 shows the enclosure mounted on the pump plate.

Note that although the enclosure is small, it is very large compared to the thermistor diameters.

The flange supplied with the pump plate, and intended for connection of the vacuum pump, was modified to take a $1\frac{1}{2}$ inch diameter window of fused quartz, $\frac{1}{8}$ inch thick. Construction of the vacuum seal used for this window is shown in Fig.16. The lower O-ring was not a vacuum seal but served as a convenient means of clamping the window without having any metal to glass contact. A camera shutter was mounted below the window, and below that four circular baffles, which are also shown in Fig.16. These were intended to prevent stray radiation and heat from the source from reaching the pump plate and causing unsteadiness of the ambient temperature. Since the shutter aperture was only 2 cm it could not be used for tests requiring more than 2 cm of lead wire to be irradiated. In these cases it was removed, and a hand operated metal slide used. The assembly underneath the pump plate can be seen in Fig.17.

A high-vacuum electrical feed through was installed in the pump plate. In addition to 3 ordinary shielded wires

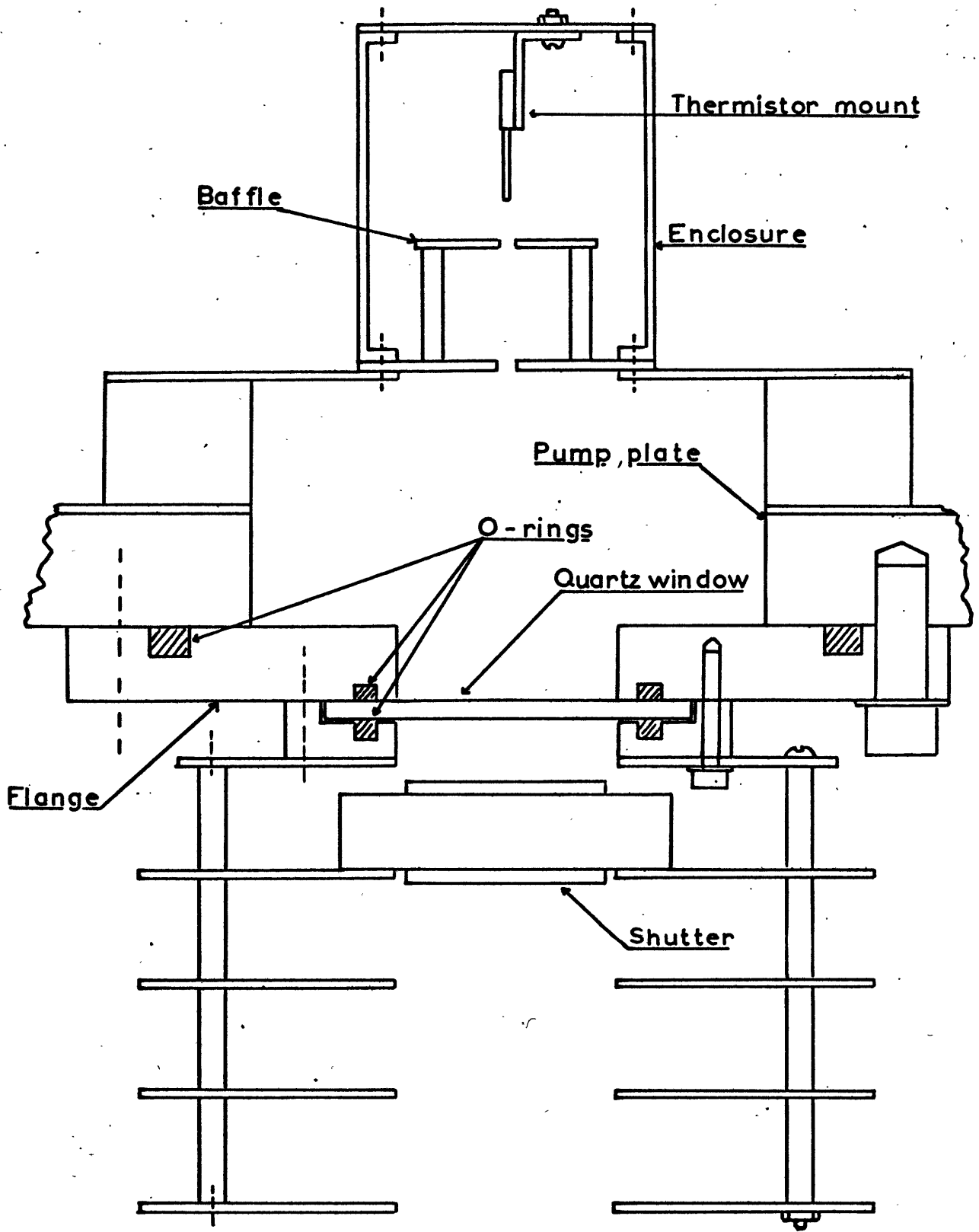


FIG 16. SHOWING WINDOW, ENCLOSURE & BAFFLES.

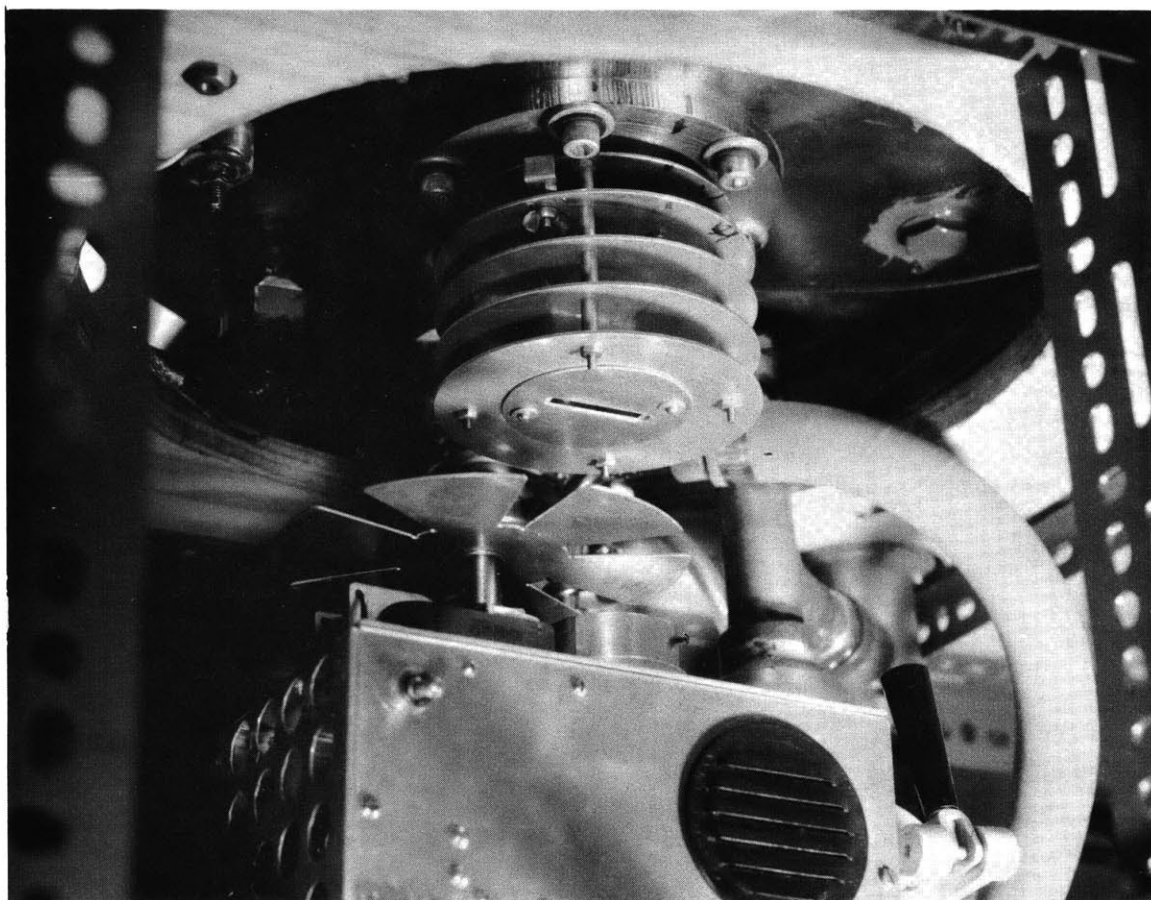


FIG.17. Underside of Pump Plate Showing Heat Shields,
Radiation Source, and Chopper Disk.

for thermistor circuits etc. 4 channels were used for two thermocouple circuits. The copper and constantin leads of these thermocouples passed continuously through tubes in the feed-through so that no errors could be introduced by temperature differences between the inside and outside of the vacuum chamber.

One of the thermocouples was used to monitor the temperature of the enclosure walls. It was soldered to the latter on a level with the thermistor. A Weston Inductance Amplifier and a Esterline Angus 0-1 milliamp recorder were used to display the output. An ice bath was used for the reference junction.

3.4 Procedure

Once the apparatus had been built and set up the carrying out of the radiation tests was very straightforward, although time consuming. A good deal of trouble had been taken in the design and construction of the equipment to assure representative, reproduceable results, and this trouble proved to be well worthwhile. In general all thermistors were subjected to the same procedures, except that some variation in lead lengths was allowed.

The first step was to photograph the thermistor bead

with a Spencer photomicroscope. The regular sub-stage illuminator was used to produce a silhouette of the bead. Some examples of these photomicrographs were given in Fig.2, Chapter 2. A 0-1 mm scale was photographed using the same magnification to give a calibration. The silhouette was then traced on to mm graph paper and the outline divided into strips 0.4 mm wide. The lengths of the strips were summed, and from this and the calibration the cross-sectional area of the bead was found. The total area, and volume were then estimated on the assumption that the beads were prolate spheroids. Thus, the semi-minor axis b was measured from the photomicrograph, and the effective semi-major axis a deduced from the cross-sectional area A_T' and the relation

$$A_T' = \pi ab.$$

a was usually 5-10% shorter than the actual measured semi-major axis as a result of distortions where the lead wires joined the bead. The total area A_T was then computed from the formula

$$A_T = 2\pi b^2 + 2\pi \frac{ab}{e} \sin^{-1} e$$

where $e = \sqrt{1 - \frac{b^2}{a^2}}$.

The volume was computed from the formula

$$V = \frac{4}{3} \pi ab^2.$$

As far as could be judged, the cross sections perpendicular to the major axes were reasonably circular. It is felt that the areas and volumes estimated in the above manner were correct to 5-10%.

The thermistors were next mounted between the ends of the support posts on the mounts described above. Because of their very small dimensions this required considerable patience and care. One difficulty was the need to have the thermistor bead reasonably well centered between the posts.

Another was the fact that many of the thermistors as supplied had lead lengths only fractionally longer than the distance between the support posts. It was also considered imperative not to handle the thermistor or its leads with the fingers, for this would almost certainly have resulted in deterioration of any reflective coatings.

The above work was greatly assisted by the use of an 8 inch by 5 inch glazed porcelain plate as a working surface. This provided a good visual background, and could also be kept perfectly clean to prevent contamination of the thermistors by dust and grease. Illumination was provided by a Tensor model 5975 high-intensity lamp.

Manipulation of the thermistors was carried out by using various dental type probes. The eye of a sewing needle was also found very useful. A low-power magnifier, and a variety of jeweler's loupes, were also useful aids. The leads were soft-soldered to the support posts, using a small soldering iron. Soldering was possible but difficult with rosin or paste flux, but very simple with stainless steel flux. In the latter case, however, great care had to be taken to avoid any possibility of the flux contaminating the bead or the lead wires, with ruinous effects on any surface coatings. After soldering, the joints but not the beads were washed in clean water to remove all traces of flux.

After centering the thermistor bead with respect to the enclosure end plate (see 3.4(d)) and making electrical connections, optically flat black paint was applied to any surfaces of the end plate or mount likely to reflect radiation. When thoroughly dry, the mount was installed in the enclosure. Final centering with respect to the baffles was accomplished by eye, looking through the baffles while the thermistor was illuminated from the side through a small hole in the enclosure wall. The enclosure was then mounted in the vacuum chamber and the system evacuated with the mechanical pump.

After the system had been evacuated for some time the tests were commenced. A measuring current small enough to cause only a very small self-heating temperature rise in the thermistor was applied and the measuring circuit balanced. Resistance calibration marks were applied to the recorder chart by use of the built-in resistance box, the thermistor switched in again, and radiation applied by opening the shutter. After the thermistor was steady again at the new temperature the shutter was closed. A typical response is shown in Fig.18.

The pressure was then increased to the next desired point by closing off the angle valve to the pump, and admitting a little air through a release valve in the pump plate. As the pressure was increased, the gain of the recorder had to be increased from time to time to maintain a suitably large deflection. It was convenient to apply fresh calibration marks to the record for each test rather than only after each gain change.

To conserve lamp life, the radiation source was switched off between tests. About 3 min prior to the next radiation test the lamp was switched on at reduced voltage (by using a variac), and brought up to full voltage about 1 min prior to the test. In this way lamp life

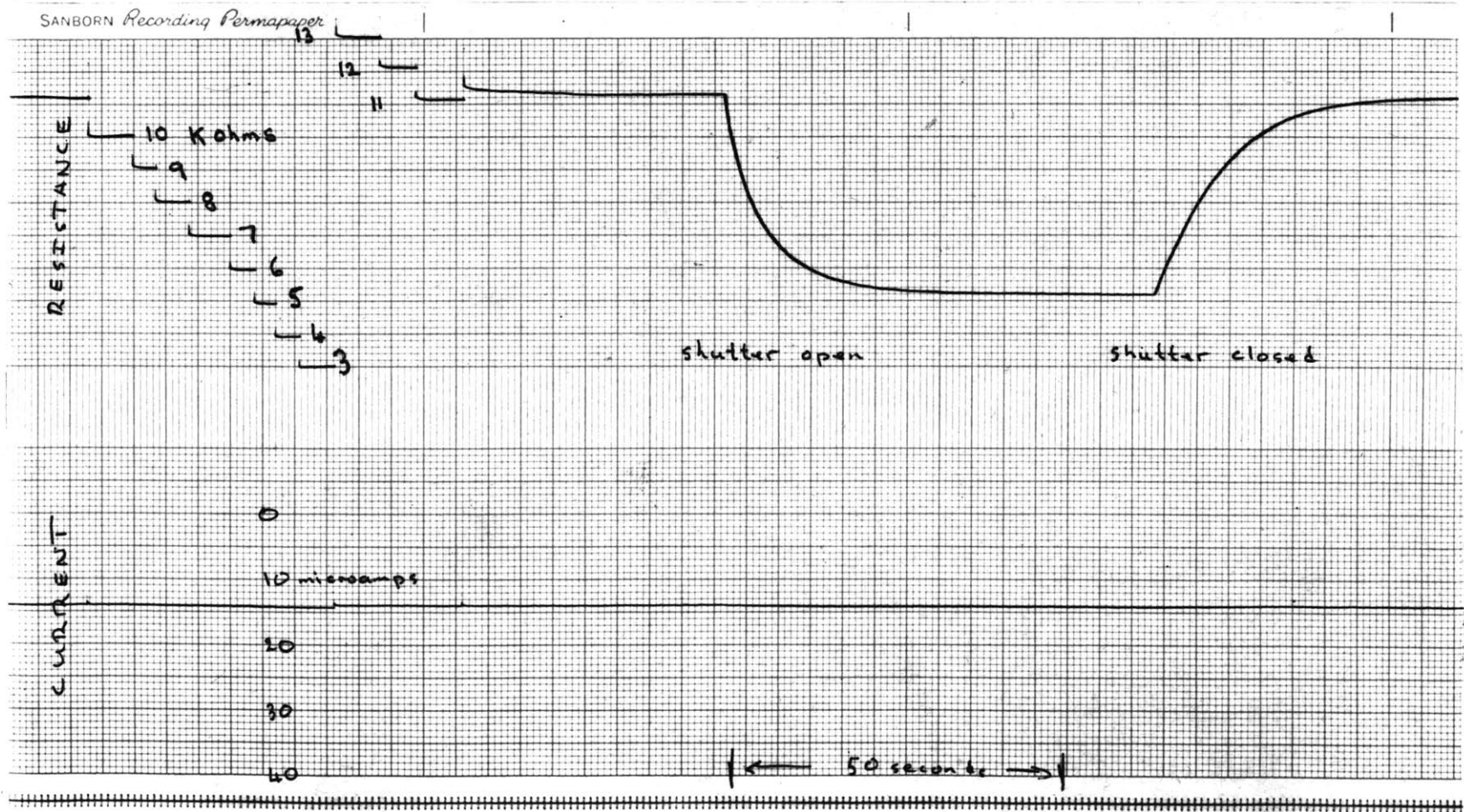


Fig 18. Recorder Chart Showing Response of Thermistor to Radiation

was prolonged, and errors due to a small change in output as the lamp heated up were avoided. A Sola constant-voltage transformer was used ahead of the variac to ensure that the variac settings represented the same voltage independently of supply fluctuations.

In all cases, the first run was the "bead only" type of test, using the baffles with circular holes. When the last test, at atmospheric pressure, was completed the diffusion pump was coupled into the system and the test repeated at the highest possible vacuum. Atmospheric pressure was then let in and the baffles changed over for the "whole leads" tests. This was carried out under the high vacuum, again using the diffusion pump. Finally the diffusion pump was removed from the pumping system and the mechanical pump used to complete the tests at the desired pressure intervals.

At high pressures the temperature rise under the radiation was only a few tenths of a degree. When performing the "whole of leads irradiated" tests, especially at pressures above 10 mm mercury, the temperature of the thermistor did not completely level off, but continued to rise slowly so long as the radiation was on. This was due to heating of the thermistor enclosure and the supports by the radiation passing through the baffles

and not absorbed by the thermistor. The rate of temperature rise due to this effect was always very small compared to the thermistor's rate of response to the radiation. The procedure was adopted of measuring the temperature rise approximately five time constants after the onset of radiation. At that time the thermistor would have been within less than 1% of its equilibrium value, yet the contribution to the temperature rise due to the heating of the enclosure was still negligible. The same effect was noticeable in the thermocouple records of the enclosure temperature when tests were being carried out at lower pressures, but it was so small compared to the thermistor temperature change that it was not discernable in the output of the latter.

In general, other tests were carried out at the same time as the radiation tests. For example the time constant (Chapter 7) was measured along with the "bead only" tests, and the dissipation rate (Chapter 4) was measured on the same runs as the "whole leads" tests. In some cases, when only the reflectivities were of interest, only the tests at high vacuum with the diffusion pump were performed.

3.5 Calibration of the Radiation Source

To obtain quantitative measurements, the intensity of the radiation falling on the thermistor was required. This was measured by suspending an Eppley Pyrheliometer inverted over the window in the pump plate. The thermistor enclosure was removed and the sensitive element of the Pyrheliometer carefully centered on the window at the position normally occupied by the thermistor. The shutter was removed for this test, as its maximum aperture was less than the area of the Pyrheliometer. The output of the Pyrheliometer was measured with a potentiometer and converted to $\text{cal cm}^{-2}\text{min}^{-1}$ using the calibration furnished with the instrument.

This procedure gave the mean intensity over the area of the 1 inch diameter Pyrheliometer disk, and although the intensity of the illumination appeared even to the eye when viewed on a white paper screen there was some concern about whether this value applied at the actual position of the thermistor bead. However an independent check was available in the observations of the response of black thermistors, including a thinistor, described below. The fact that the recorded temperature rises were consistent with those expected of black bodies under the assumed radiation intensity confirms the assumption that the radiation was in fact uniform.

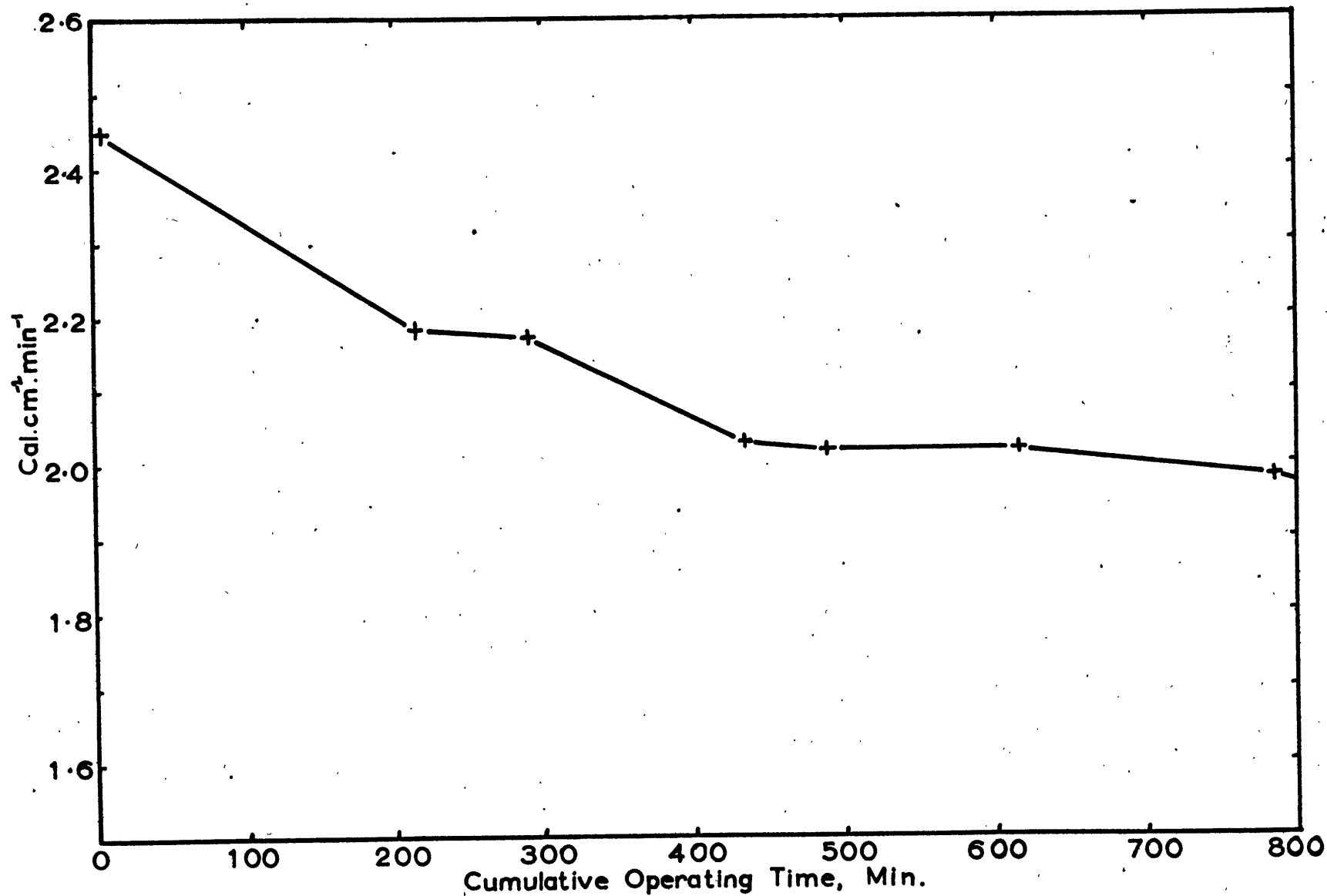


FIG 19. CHANGE IN LAMP OUTPUT WITH OPERATING TIME.

Since it was well known that a tungsten filament lamp gradually declines in output throughout its life, the output of the radiation source was checked in the above manner with the Eppley Pyrheliometer from time to time during the course of the experiments. By keeping an approximate log of the minutes of operation of the lamp at full voltage it was possible to plot the lamp output vs cumulative operating time. Fig.19 shows an example for one of the lamps. From this graph the actual output at the time of a given experiment could be readily interpolated. Where a chopper disk was employed, the calibration was performed with the disk in operation. The lamps were changed after about 15 hours use to avoid the possibility of failure in the middle of a run.

3.6 Results

(a) Physical Characteristics

Table 2 shows the results of the estimation of the dimensions, areas, and volumes of the bead thermistors used in the radiation tests, as described in section 3.4 above. These quantities will be needed in later discussions.

TABLE 2. Physical Characteristics of Thermistors

Number	Type	Nom. Diam. mils	Minor Diam. mils	a 10^{-2} cm	b 10^{-2} cm	A'_T 10^{-3} cm ²	A_T 10^{-3} cm ²	Vol. 10^{-5} cm ³
G-2	X2047	15	18.3	2.64	2.33	1.94	7.45	6.00
G-3	"	"	14.8	2.28	1.88	1.35	5.08	3.38
G-4	"	"	12.4	2.18	1.58	1.08	3.94	2.27
G-5	"	"	15.6	2.34	1.98	1.45	5.52	3.84
G-6	"	"	15.6	2.28	1.98	1.42	5.42	3.74
G-9	"	"	13.5	2.11	1.72	1.14	4.30	2.62
G-10	"	"	-	-	-	-	-	-
G-11	"	"	16.0	2.28	2.03	1.45	5.59	3.94
G-12	"	"	14.9	2.44	1.89	1.45	5.38	3.64
G-7	L500C	15	12.2	2.03	1.54	0.98	3.64	2.03
G-8	"	"	11.8	1.65	1.50	0.78	3.01	1.55
F-1	-	10	13.2	3.00	1.67	1.57	5.47	3.50
F-2	-	"	13.2	2.96	1.68	1.56	5.43	3.49
F-3	-	"	14.4	2.48	1.83	1.42	5.30	3.48
VB-1	41A5	10	10.1	2.19	1.29	0.88	3.11	1.53
VB-2	"	"	10.7	1.94	1.36	0.82	3.00	1.50
GB-2	45CD5	15	14.9	2.75	1.90	1.64	6.00	4.15
V5B1	TX1718	5	4.7	1.18	0.60	0.22	0.76	0.18
V5B2	"	"	4.6	1.16	0.59	0.21	0.73	0.17
R-1	-	10	10.1	-	-	35.1	116	-
T-1	FN1A5	-	-	-	-	76	152	15.5

(b) Temperature Rise as a Function of Pressure.

The results presented in this section are strictly the results of the experiments. Their implications for actual temperature measurements in the atmosphere will be discussed in Chapter 11.

Fig.20 shows the observed temperature rise of a Gulton X2047 15 mil (nominal) bead thermistor as a function of pressure. This thermistor had a vacuum deposited aluminum coating of relatively high quality (see below) on the bead and presumably over much of the lead wires. The temperature rise has been corrected to a radiation intensity of $2.0 \text{ cal cm}^{-2} \text{ }^{\circ}\text{C}^{-1}$. The temperature rise in still air is seen to be fairly constant from atmospheric pressure down to about 3 mm mercury. This reflects the constancy of the convective* heat transfer coefficients in the region. At pressures below 1 mm mercury the temperature rise increases quite rapidly with decreasing pressure. The levelling off below about 0.02 mm mercury is due to the combined effects

* Strictly speaking the term conduction should be used here instead of convection, but the latter will be retained to provide continuity with other parts of this work, and to avoid confusion with heat conduction in the lead wires.

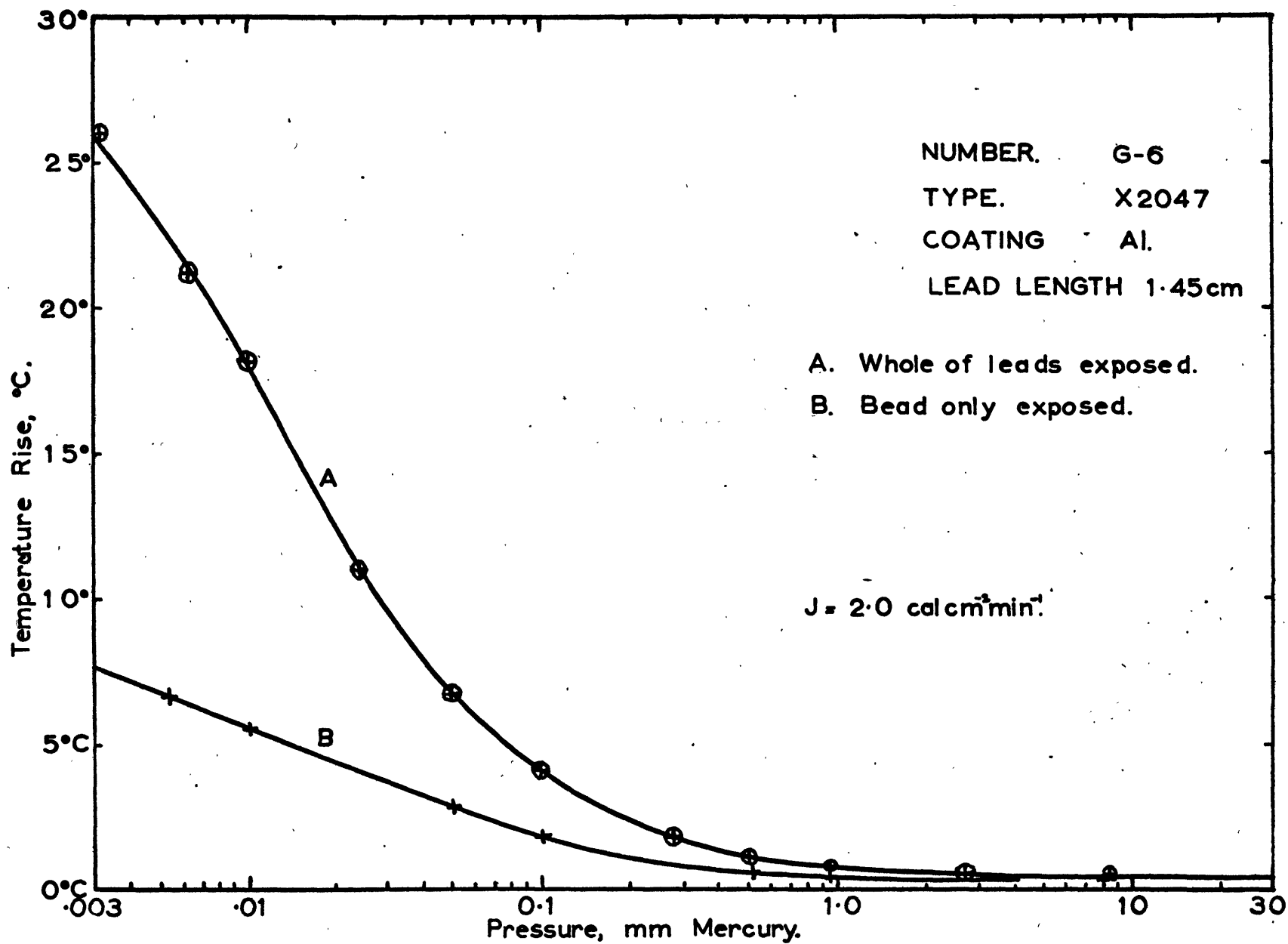


FIG 20. MEASURED RESPONSE OF THERMISTOR TO RADIATION.

of heat conduction in the lead wires and long-wave radiation exchange with the enclosure walls in dominating the heat balance of the thermistor, rather than convection. Under these circumstances the results are heavily dependent on the particular mounting conditions, including the lead lengths, used in the experiments.

It is immediately apparent from the difference between the two curves of Fig.20 that the temperature rise is strongly influenced by the radiation intercepted by the lead wires. Thus, without even taking into account the fact that a short length of lead wire is still included in the "bead only" tests one can see that the lead wires in this particular case contribute more than the temperature rise of the bead alone at 0.10 mm mercury and more than twice the temperature rise of the bead alone at 0.01 mm mercury.

The proportional contribution of the lead wires is less at higher pressures. In the above example the observed temperature rises at sea level pressure were 0.30°C with only the bead irradiated, and 0.42°C when the whole thermistor was irradiated.

As mentioned in section 3.1 the effect of the radiation on the lead wires of these small bead thermistors has not received much attention previously. There is much discussion

of the effectiveness of various bead coatings in reducing the radiation error but no consideration appears to have been given to the reflectivity of the lead wire surface. An example of what can happen is given in Fig.21 which shows the effect of radiation on two 15 mil (nominal) thermistors of the same manufacturer, but of differing type. The thermistor G-5 was a Gulton X2047 thermistor with a relatively good aluminum coating. G-8 was a Gulton type L500C thermistor in which the bead had been aluminized and then given a quartz coating, presumably to preserve the aluminum coating. The leads, however, had been tinned to facilitate soldering, and this tinning, which extended over the whole length, had not taken well and visually appeared very dull. The lead lengths and mountings used for the two thermistors were similar. Obviously the rather more elaborate treatment given the L500C thermistor bead was more than nullified by the dirty lead wires.

The response of an uncoated thermistor to radiation is also of interest. The uncoated beads are black, so that one would not normally want to use an unshielded thermistor of this type in the atmosphere, but they provide a kind of "limiting case" for the radiation errors. Also it is possible to compute from the observed response the errors which would result if a coating of given reflectivity

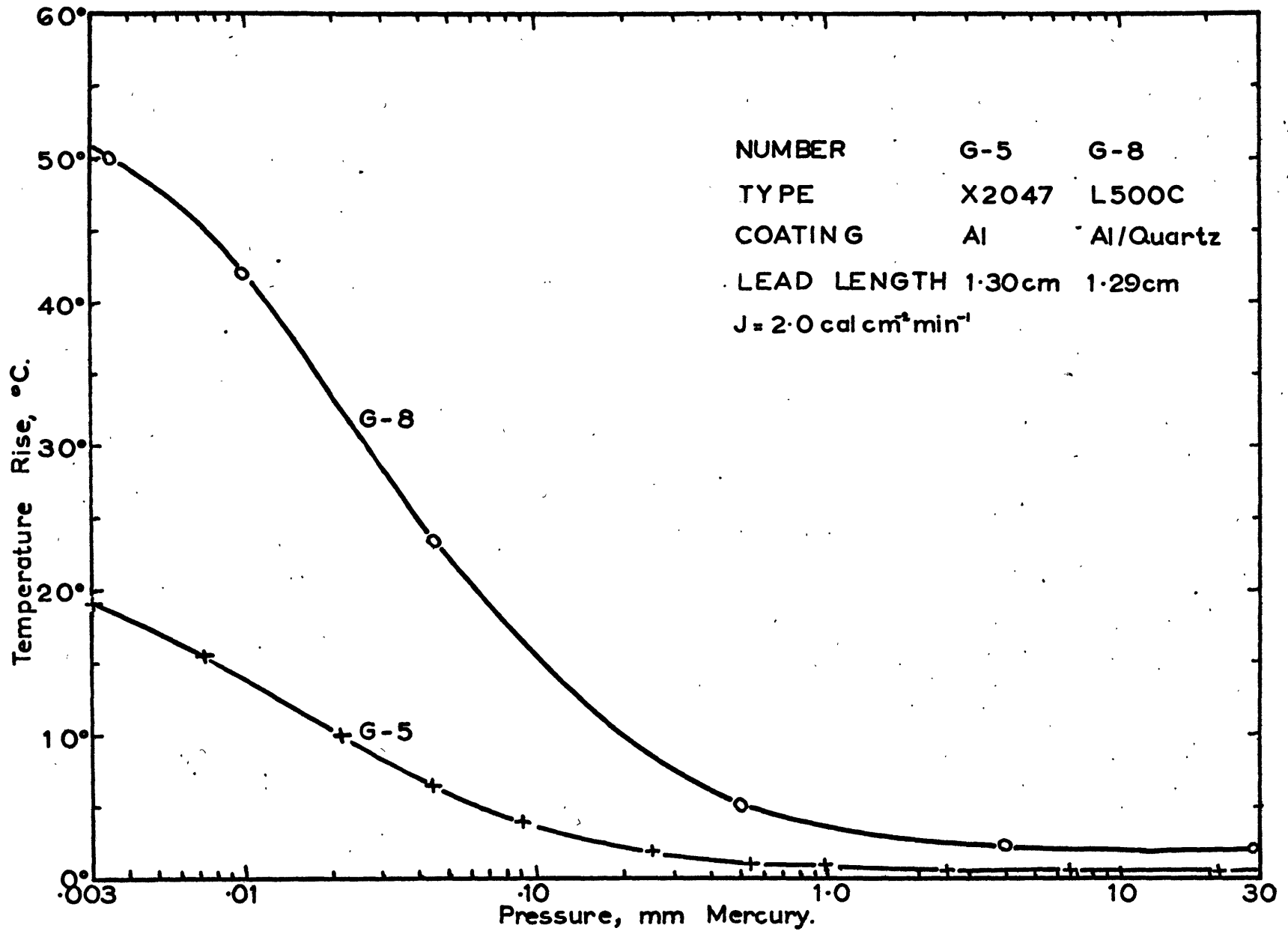


FIG 21. MEASURED RESPONSE OF THERMISTORS TO RADIATION.

was applied. For example, if the temperature rise observed in the "bead only" tests is considered to be the contribution of the black bead to the temperature rise for the complete thermistor, then a reflective coating of 90% reflectivity would reduce this to 10% of its former value. Similarly the contribution of the lead wires is given by the difference between the "whole leads" response and the "bead only" response and this too is proportional to $(1 - \text{reflectivity})$. Assuming that the reflectivity of the original lead wires has been calculated it is therefore possible to deduce the lead wire contribution for other reflectivities. Of course these estimates would have to be based on the assumption that the coating would not appreciably change the physical size or the heat-flow characteristics of the thermistors, so they would have to be treated with due caution.

Fig.22 shows the observed response of two uncoated thermistors. GB-2 is a Gulton 45CD5 15 mil type and V5B-1 a Veco TX1765 5 mil thermistor. Note that this time a logarithmic scale had been used. The rather high temperature rise of the smaller thermistor at very low pressures was due in part to the fact that this type of thermistor had 0.7 mil diameter lead wires compared to the 1 mil leads on the larger thermistors and so had a

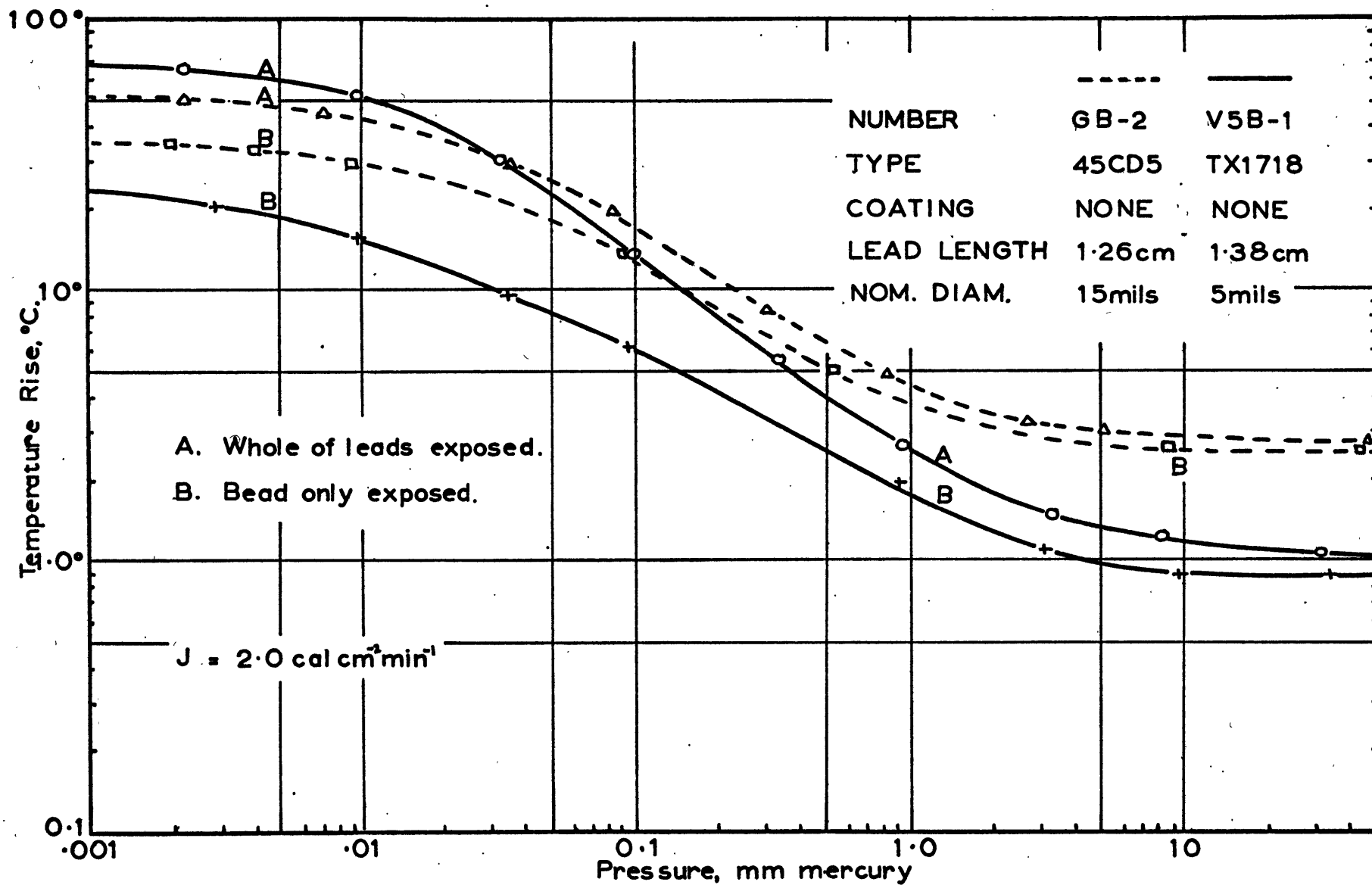


FIG 22. MEASURED RESPONSE OF THERMISTORS TO RADIATION.

smaller rate of heat loss by conduction.

It will be seen that the smaller thermistor has a smaller temperature rise at high pressures due to its superior convective heat transfer characteristics. This advantage is lost at lower pressures because the dimensions approach the mean free path of the air molecules at an earlier stage.

Another point of interest about these results is the fact that the relative contribution of the lead wires to the temperature rise of the 5 mil bead thermistor was very great at low pressures, despite the fact that the bead itself was black. This is due to the rather small cross-sectional area of the small bead compared to the area of the lead wires. As a result the reflectivity of the lead wires of the 5 mil thermistors would be considerably more important at high altitudes than the type of reflective coating used on the bead itself.

Fig.23 shows the temperature rises observed with an experimental 10 mil diameter aluminum coated rod thermistor, manufactured by the Bendix-Friez Company. This rod was approximately $\frac{3}{8}$ inch long and was furnished with 4 mil diameter leads of unknown material.

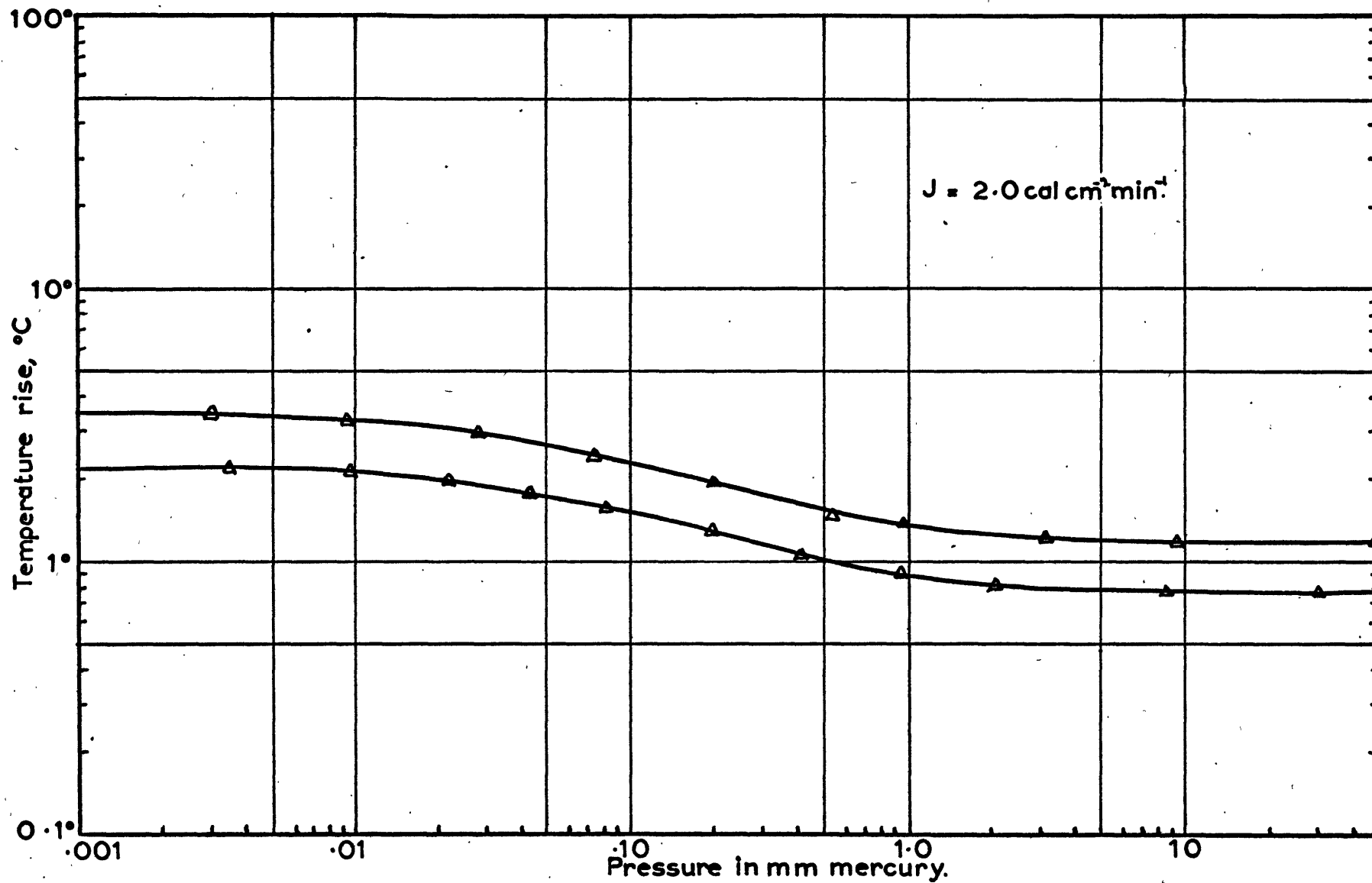


FIG 23. MEASURED RESPONSE OF 10mil ROD THERMISTOR TO RADIATION.

The rod was mounted for the tests in the same way as the bead thermistors, but using a modified baffle to achieve the "rod only" tests. The temperature rise at low pressures was much smaller than that observed for the bead thermistors. Subsequent tests have shown, however, that this is due to the fact that with the lead lengths used, conduction of heat through the lead wires to the supports was a dominant item even at moderately high pressures. The results therefore do not represent the true response of the rod to radiation because at all pressures the leads were too short and thick and of too high thermal conductivity for it to be a satisfactory air temperature sensor. The lead length used in the tests was 1.22 cm and it is interesting to note that this was considerably longer than that used in an experimental mount for these rods supplied by the manufacturer.

Fig.24 shows the response of a Veco FN1A5 "thinistor", T-1, to radiation. This is a type of thermistor having flat-plate geometry instead of a spherical bead, with consequent improvement to the surface area to volume ratio. The size of the flat plate was approximately $\frac{3}{32}$ inch square, and according to the manufacturer's specification 0.0008 inch thick. The upper side of the plate had a flat black finish. The thinistor was mounted so that the

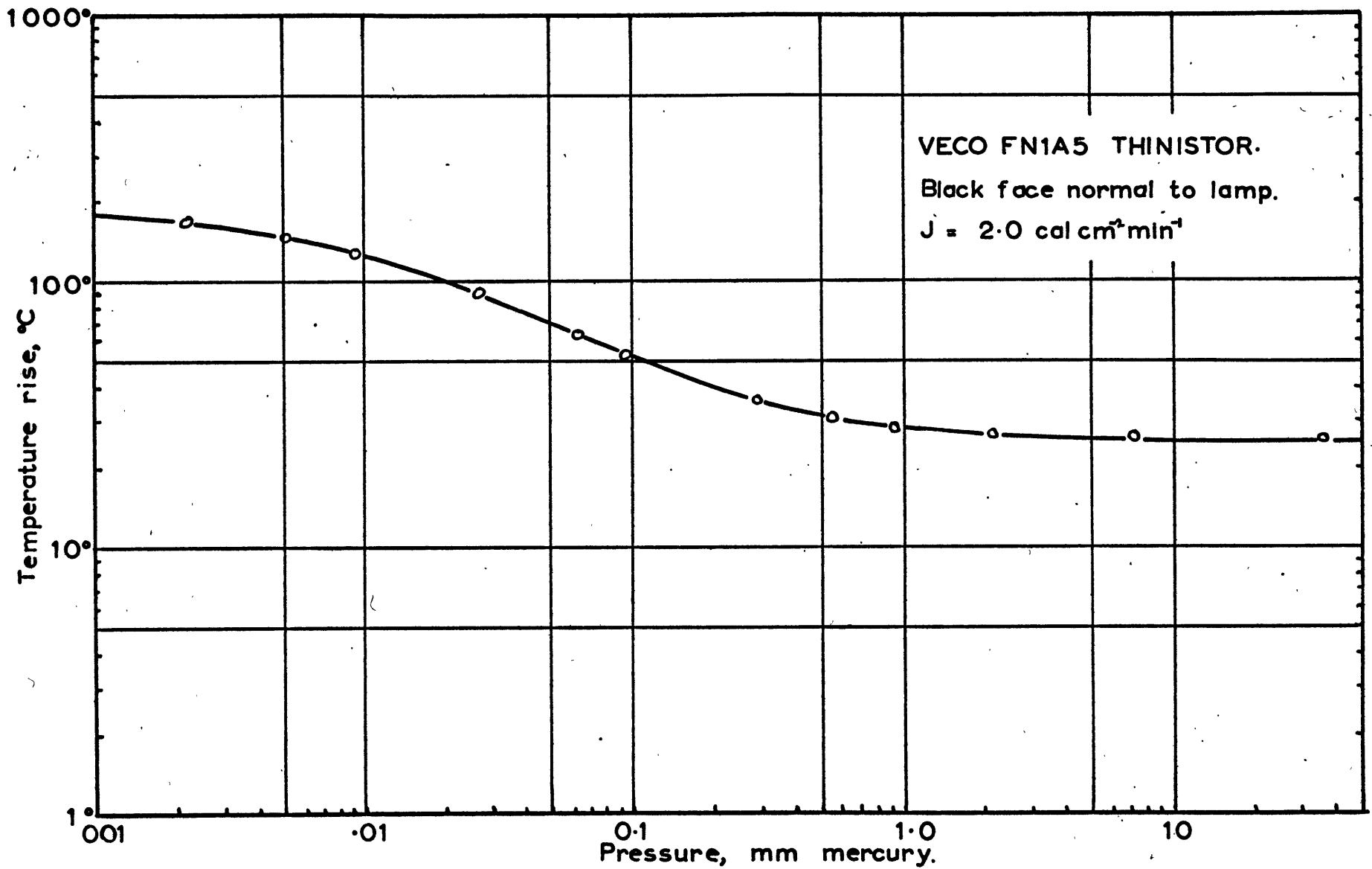


FIG 24. MEASURED RESPONSE OF THINISTOR TO RADIATION.

flat black surface was perpendicular to the radiation. The length of each 1 mil platinum-iridium lead wire of the mounted thinistor was 1.0 cm.

To avoid excessive temperature rises during the tests, the intensity of the radiation was reduced to about $\frac{1}{4}$ of the solar constant with one of the chopper disks. The appropriate calibration factor was then used to obtain the values given in Fig.24. In the case of the thinistor the contribution of the lead wires to the temperature rise was negligible, so only one curve is shown. The temperature rise is seen to be constant in still air down to rather lower pressures than was the case for the bead thermistors. If the thinistor had been given a coating of 90% reflectivity we should expect the still-air temperature rise at sea-level pressure to be $\frac{24^{\circ}\text{C}}{10} = 2.4^{\circ}\text{C}$ under the same radiation. This is still much greater than the temperature rises observed with coated bead thermistors, but because the rate of increase of the temperature rise with decreasing pressure is less, the advantage of the beads is diminished with altitude until at around 0.05 mm mercury (about 225,000 ft) the coated thinistor would show a comparable or smaller temperature rise.

The results of measurements of the type described in this section on a number of other thermistors will be found in Appendix I.

(c) Reflectivities

The reflectivities of the beads and the lead wires of a number of thermistors were computed from measurements of the dissipation rate and the "whole leads" and "bead only" temperature rises under high vacuum. Writing these as $K(0)$, $\theta_2(0)$ and $\theta'_2(0)$ respectively we see from (3.1.8) and (3.2.1) that

$$\theta_2(0) \cdot K(0) = \epsilon_{sw} \frac{4Jr}{p'} (\coth p'd - \operatorname{cosech} p'd) + J \epsilon_{ST} A'_T \quad (3.6.1)$$

$$\text{and } \theta'_2(0) \cdot K(0) = \epsilon_{sw} \frac{4Jr}{p'} \left(\frac{1 - \operatorname{sech} p'\Delta + \tanh p'd_1 \tanh p'\Delta}{\tanh p'd_1 + \tanh p'\Delta} \right) + J \epsilon_{ST} A'_T \quad (3.6.2)$$

Under the conditions of the experiments, $\theta_{20} = 0$

In the right-hand sides of these equations, r was taken as 1.27×10^{-3} cm for 1 mil lead wires and 0.89×10^{-3} cm for 0.7 mil wires. k was assumed to be $0.31 \text{ watt cm}^{-1} \text{ }^\circ\text{C}^{-1}$, a value obtained from "Handbook of Chemistry and Physics", Chemical Rubber Company, p 2254 for platinum-iridium (10%) alloy. This latter value has been verified independently, see Chapter 5. Measurements using a microscope fitted with a micrometer eyepiece have also verified the lead-wire

dimensions given.

The quantity $p' = \sqrt{\frac{2h'}{kr}}$ was obtained from (3.2.3) and an assumed value of ϵ_{lw} . A value between 0.05 and 0.2 was generally chosen for the latter, depending on the appearance of the wire surface. As pointed out in section 3.2 the values of ϵ_{sw} and ϵ_{st} are not very sensitive to the value of ϵ_{lw} for the range of lead lengths used.

With these assumptions, the coefficients of ϵ_{sw} on the right-hand sides of (3.6.1) and (3.6.2) are known, as are the left-hand sides, thus permitting solution for ϵ_{sw} and ϵ_{st} . Table 3 shows the results of these computations. Information concerning the physical characteristics of these thermistors has been given in Table 2.

The first 6 were aluminized 15 mil Gulon type X2047 bead thermistors. Like all the thermistors used in this study they were unused, having been taken from their original packing only immediately prior to mounting. Visually all of these thermistors appeared very bright, with no discernable flaws in the aluminum coatings. An exception was G-11, the lead wires of which did not appear as bright as those of the others.

The mean absorptivity (short-wave) of the 6 beads was 0.16, with a range of over 2:1 of 0.10 to 0.22. For

TABLE 3. Measured Absorptivities of Thermistors

Number	Nom. Diam.	Coating	ϵ_{ST}	ϵ_{SW}	Visual Condition	
					Bead	Leads
G-2	15 mil	Al	.15	.12	good	good
G-3	15 mil	Al	.22	.14	good	good
G-4	15 mil	Al	.17	.19	good	good
G-5	15 mil	Al	.13	.11	good	good
G-6	15 mil	Al	.10	.15	good	good
G-11	15 mil	Al	.21	.45	good	poor
G-7	15 mil	Al/Quartz	.86	.63	poor	bad
G-8	15 mil	Al/Quartz	.72	.61	poor	bad
F-1	10 mil	Al	.83	.39	bad	poor
F-2	10 mil	Al	.54	.45	poor	poor
F-3	10 mil	Al	.57	.45	poor	poor
VB-1	10 mil	None	.93	.27	black	fair
VB-2	10 mil	None	.95	.29	black	fair
GB-2	15 mil	None	.88	.31	black	poor
V5B-1	5 mil	None	1.07	.31	black	fair
V5B-2	5 mil	None	.95	.30	black	fair
T-1	-	-	.95	-	black	exc.
R-1	10 mil	Al	.08	.13	exc.	good

the lead wires, the mean was 0.19 with a range of 0.11 to 0.45. Neglecting the obviously poor leads of G-11 the mean was 0.14.

The values for the aluminized beads are considerably greater than those given in the literature for vacuum deposited aluminum films, which range from about 0.08 down to 0.04 for radiation in the solar wavelength range. (C/F Fig.11 and see also Armstrong (1965)). Evidently, coatings applied to these small objects do not approach the same degree of perfection obtainable under more ideal conditions. The range of variation is also of interest for this variation would ultimately be reflected in the variability of the radiation error.

Thermistors G-7 and G-8 were Gulon type L500C thermistors of nominal size 15 mils. The beads were aluminized, with a protective quartz coating on top of this. The lead wires had been tinned, but this tinning had not taken well, with the result that there were numerous small lumps of solder and other debris attached to them, and their overall visual appearance was quite dark. The aluminum coatings on both these thermistors looked poor under a low power magnifier, in particular the bead of G-7 appeared to have a black area where the aluminum was missing. The measured reflectivities confirm these observations. A good deal of

the apparently low reflectivity was no doubt a result of the effective increase in area caused by the foreign matter on the lead wires. In particular, there was a large piece of debris adjacent to the bead of G-8 which would have been illuminated together with the bead in the "bead only" part of the tests. Nevertheless the poor overall performance is inescapable. In the case of G-7 it so happened that the black area was towards the radiation during the tests. For other orientations the reflectivity of the bead may have been much higher but the poor lead wire reflectivity would still give rise to a large radiation error.

The thermistors F-1, F-2, and F-3 were bead thermistors of 10 mil nominal diameter but somewhat greater actual diameter, manufactured by Fenwall Electronics Inc. These thermistors had been aluminized under vacuum by an independent organization. Their overall visual appearance was poor, in particular one of the beads, that of F-1, was dull all over to the point of blackness, while F-2 and F-3 were quite bright on one side but dull on the other. As was the case with G-7 a large percentage of this dull area was turned towards the radiation in the tests. It was not possible when mounting the thermistors to arrange for a particular orientation so no particular effort was made to either avoid or favour these dull areas in the tests.

The results obtained for the uncoated (black) bead thermistors were very encouraging, because all of the measured absorptivities appeared to be very reasonable values. This indicates that the system was working correctly, in particular that the source intensity measured by the Eppley Pyrheliometer was representative of the intensity at the thermistor, for we might equally have assumed a value near 1 for ϵ_{ST} and used this to estimate J.

The test of the thinistor, T-1, was of particular interest because in many respects this resembled a conventional radiation detector. See for example Strong (1946). A baffle with a 3/16 inch hole allowed the radiation to fall on the flat black surface of the thinistor. Since there was no significant contribution from the lead wires it is possible to write simply

$$J \epsilon_{ST} A'_T = \theta_2(0) \cdot K(0)$$

where $\theta_2(0)$ is the temperature rise under vacuum for $J \epsilon_{ST} A'_T$ watts of radiant power, and $K(0)$ is the electrical power which must be supplied to the thinistor plate to produce 1°C temperature rise in the absence of the radiation. Ideally, $K(0)$ should have been obtained by using enough electrical power to produce the same temperature rise $\theta_2(0)$ as that produced by the radiation.

However in the present case this was not convenient and the temperature rise used for $K(0)$ was approximately 10°C as opposed to 55°C measured for $\theta_2(0)$. The heat loss of the thinistor plate is by thermal radiation and conduction. The latter was computed to be $\approx 3 \times 10^{-6}$ watts $^{\circ}\text{C}^{-1}$ for two 1 mil leads 1 cm long. Thus, the remainder of the measured $K(0)$ of 45×10^{-6} watts $^{\circ}\text{C}^{-1}$ was due to thermal radiation loss to the enclosure walls. Denoting this by $K_r(0)$, and noting Stefan's law, we see that

$$K_r(0) \propto \bar{T}^3$$

where \bar{T} is approximately the mean absolute temperature of the walls and the heated plate. Since \bar{T} in the measurement of $K(0)$ was 305°K and \bar{T} in the measurement of $\theta_2(0)$ was 324°K the appropriate corrected value of $K(0)$ to be used in the computation of ϵ_{sT} was taken as

$$\left(3 + 42 \cdot \left(\frac{324}{305}\right)^3\right) \times 10^{-6} = 53 \times 10^{-6} \text{ watt } ^{\circ}\text{C}^{-1}.$$

Using this value, and the appropriate calibration factor for the chopper disk employed, the value of 95% for ϵ_{sT} was obtained.

Similar measurements and computations were made for the aluminized rod thermistor R-1. It is noteworthy that this recorded the best reflectivity of any of the thermistors

tested, possibly indicating that superior coatings can be achieved on the larger bodies. Several other rods of this type were inspected (but not tested), and all exhibited a high degree of brightness and uniformity in their coatings.

In view of the generally disappointing reflectivities of the thermistors tested a number were subjected to close examination, both under low-power magnifiers and under the microscope. Under the magnifiers a number of the Gulton X2047 aluminized thermistors appeared to have black spots of the type noted with respect to G-7 above. Mostly these were of such small area compared with the total bead area that they were of no consequence, but out of about 20 beads of this type inspected two had quite large black areas. Of the four aluminized Fenwall 10 mil thermistors received, all had dull areas extending over more than $1/3$ of their surface area (including the ones tested above). These latter areas were of a different nature to the black spots noted above, for they were not so sharply defined.

Microscopic inspection of the bead surfaces was hampered for a time by lack of an adequate illuminator, but towards the end of the project a vertical illuminator became available. Even so, observation, and particularly photography of the beads was very difficult because of the extremely curved nature of the surfaces and the extremely

small depth of focus available when the desired amount of magnification was used. Some improvement was obtained by using a lower powered objective and enlarging from the negative but in general only a limited area of the curved bead surface could be focussed at one time. Some photographs of parts of thermistor beads are given in Figs.25-29, together with brief descriptions of the features shown.

A study was also made of some of the thermistor lead wires, since the reflectivity of these is just as important as that of the beads at high altitude. Under low magnification there were noticeable variations in the apparent brightness of the lead wires of different thermistors, and even between different parts of the same lead wire. Under the microscope the wires were often found to have numerous irregularities. Some photographs of lead wires are given in Figs.30-32.

No study was made of the possible effects of prolonged exposure to the air on the reflectivity of the aluminum coatings. Some workers, for example W.C. Wagner (1965), have advised storage of the thermistors in an inert gas until immediately prior to use. This is probably a worthwhile precaution especially if they may otherwise be exposed to tropical conditions or even industrial atmospheres. The Gulton X2047 thermistors tested above showed no notice-

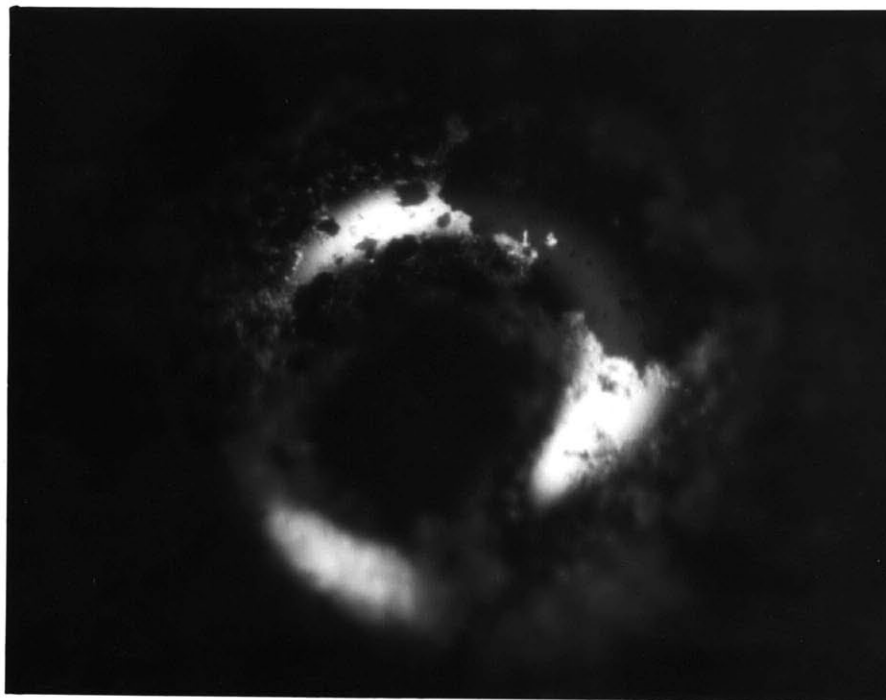


FIG. 25

Thermistor Type: Gulton X2047, Aluminum coating.

Approx. Magnification: 200X

Remarks: Major flaw, probably in glass coating, in centre of photograph. Elsewhere are areas where aluminum coating is missing or irregular.

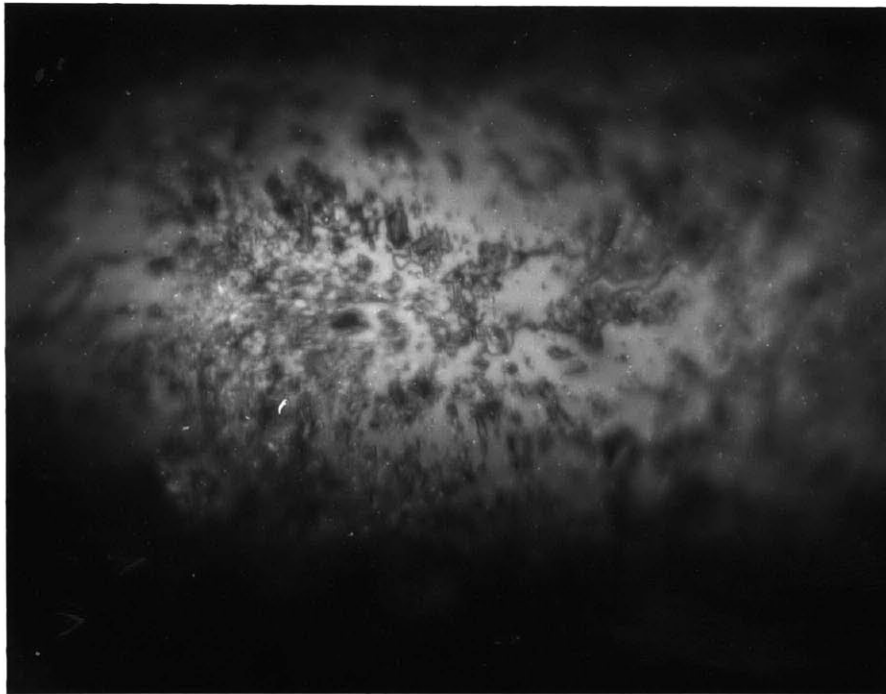


FIG. 26

Thermistor Type: Fenwall GB41110, Aluminum coating.

Approx. Magnification: 200X

Remarks: Photograph shows visually dull area of coating,
with small dark areas showing through.

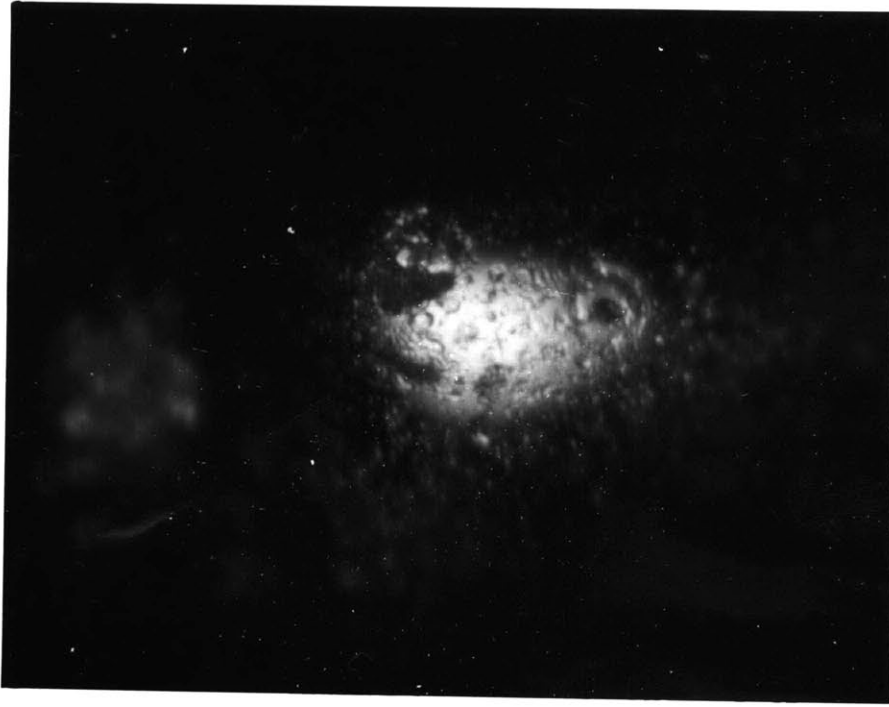


FIG. 27

Thermistor Type: Fenwall GB41L10, Aluminum coating

Approx. Magnification: 200X

Remarks: "Bright" side of same thermistor shown in Fig.26.

Notice small "dimples" in coating which were observed on all aluminized beads to a greater or lesser extent.

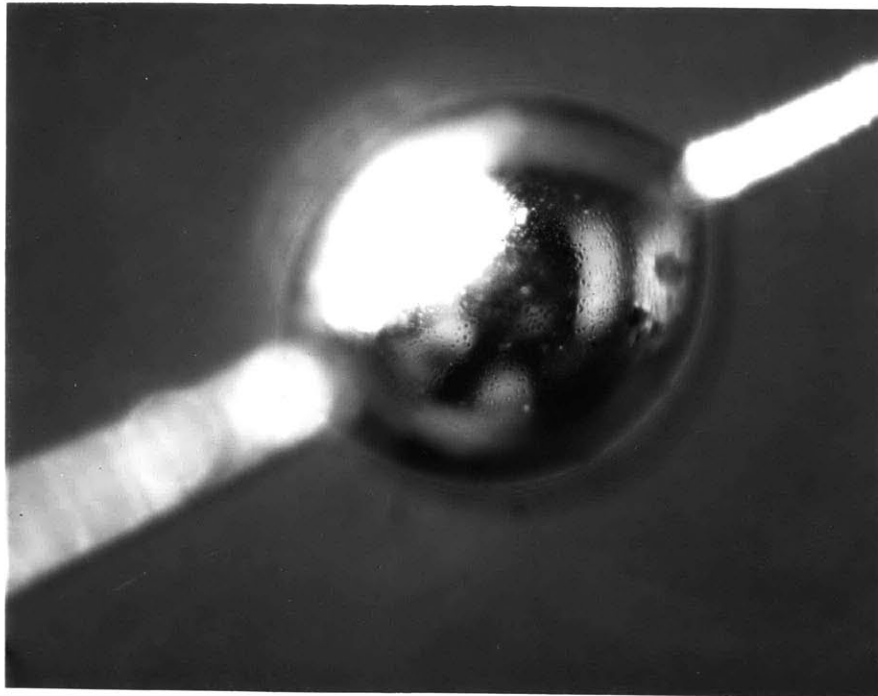


FIG. 28

Thermistor Type: Gulton X2047, Aluminum coating

Approx. Magnification: 100X

Remarks: Coating on this bead was visually as near perfect as any that were examined.

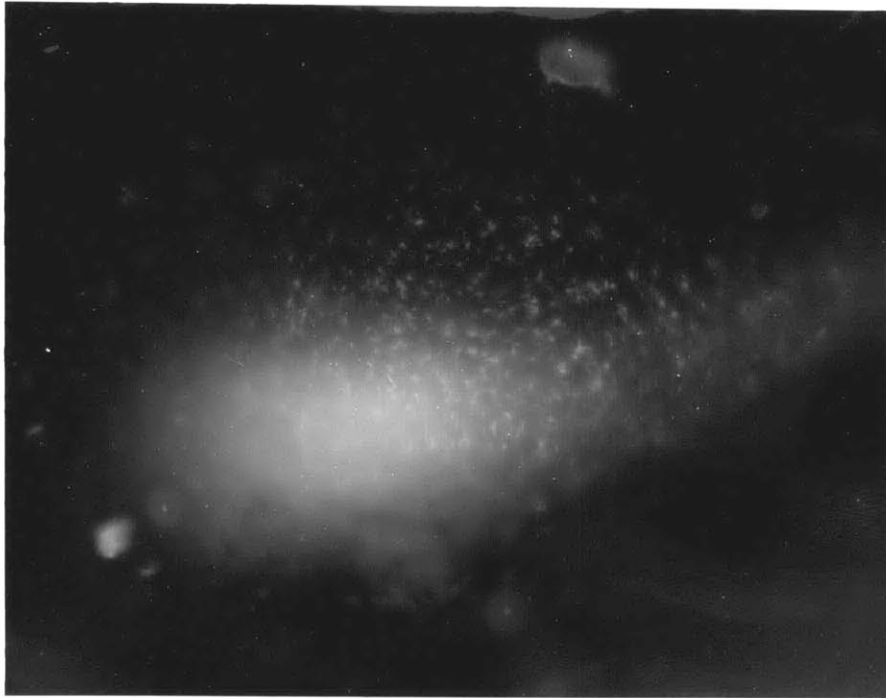


FIG. 29

Thermistor Type: Veco 41A5, Uncoated

Approx. Magnification: 400X

Remarks: Notice numerous small imperfections, resembling pits in the glass surface.

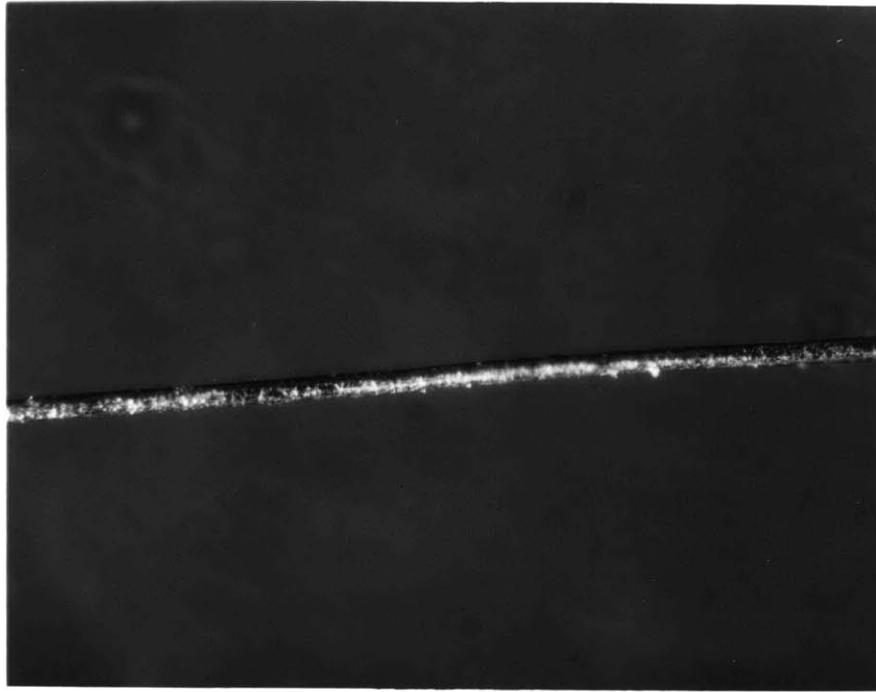


FIG. 30

Thermistor Type: Culton L500C, Aluminum/Quartz coating

Approx. Magnification: 200X

Remarks: Photograph shows part of "tinned" lead wire of thermistor number G-3 referred to in text, but does not include any of the larger pieces of debris mentioned in connection with this thermistor.



FIG. 31

Thermistor Type: Fenwall GB41L10, Aluminum coating

Approx. Magnification: 200X

Remarks: Lead wire of thermistor number F-2, fairly close to bead, showing irregular globs of aluminum coating.

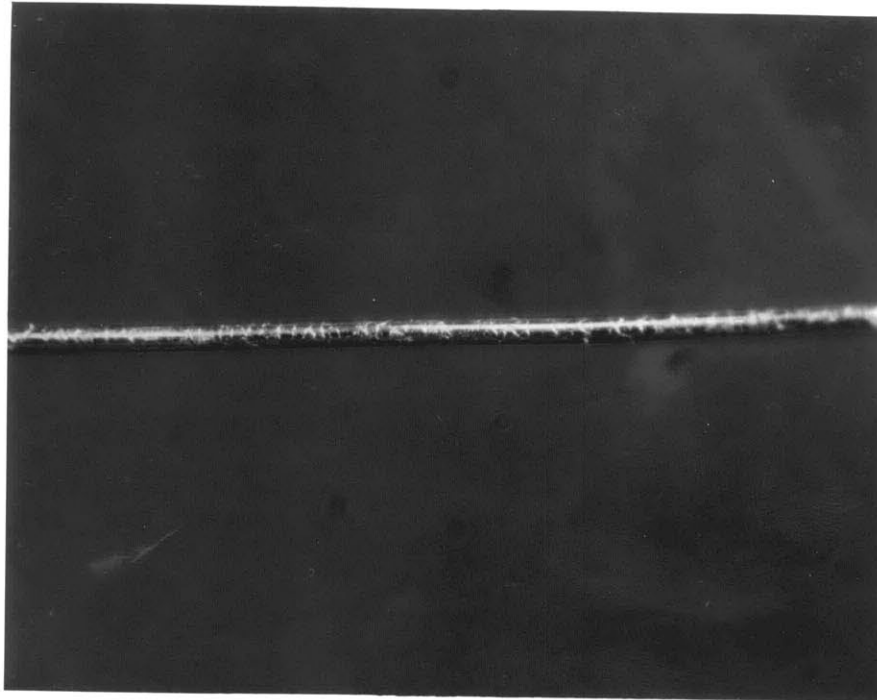


FIG. 32

Thermistor Type: Veco 41A5, Uncoated

Approx. Magnification: 200X

Remarks: Lead wire of uncoated thermistor. Visually smoother than those shown in Figs. 30 and 31, but still has some irregularities of a type frequently observed.

able signs of having deteriorated when removed from their regular packing boxes prior to testing. However some which subsequent to testing were exposed to the open air in the laboratory for a few months were significantly less bright in appearance than the ones stored in their boxes.

(d) Heat Transfer Coefficients

Having determined ϵ_{sw} , ϵ_{sT} , A'_T , and A_T it was possible, from measurements of θ_2 and K to deduce the heat transfer coefficients h_w and h_T as functions of pressure in still air conditions. Thus from (3.1.8)

$$\theta_2 K - J \epsilon_{sT} A'_T = \frac{4 \epsilon_{sw} J r}{p^*} (\coth p^* d - \operatorname{cosech} p^* d) \quad (3.6.3)$$

and
$$K = 2ka_w p^* \coth p^* d + A_T h_T^* \quad (3.6.4)$$

where we have written

$$p^* = \sqrt{\frac{2h_w^*}{kr}} = \sqrt{\frac{2(h_w + h'_w)}{kr}}$$

and
$$h_T^* = h_T + h'_T$$

The left-hand side of (3.6.3) was known, and from it, p^* was determined. Then h_w was deduced by subtracting from h_w^* the contribution of the long-wave radiation, $h'_w = 4 \epsilon_{lw} \sigma \bar{T}^3$

By inserting p^* in (3.6.4), h_T^* and consequently h_T were determined.

The accuracy of this method at the lowest pressures was limited by the fact that only estimated values were in general available for $\epsilon_{\lambda W}$ and $\epsilon_{\lambda T}$, so that h'_W and h'_T were not well known. In a typical case $\bar{T} = 310^\circ\text{K}$ and if $\epsilon_{\lambda} = 0.1$, $h' = 0.7 \times 10^{-4}$. This was comparable with h'_W or h'_T at a pressure of about 5×10^{-3} mm mercury. By 2×10^{-2} mm mercury h was about four times larger and the possibility of error was reduced. For an uncoated bead we could assume $\epsilon_{\lambda T} = 1$ with some confidence, but the possibility of error was still great because the heat lost by radiation exceeded that by convection for pressures below about 5×10^{-2} mm mercury.

At high pressures the observed temperature rises were very small and in addition the terms $\theta_2 K$ and $J \epsilon_{ST} A'_T$ were nearly equal, so again the accuracy of the method became poor. This was especially so with the uncoated beads.

For the above reasons, computations were only made for aluminized bead thermistors, and at pressures between 2×10^{-2} mm mercury and 10 mm mercury. A typical graph of the function $\theta_2 K$ vs pressure is shown in Fig.33, together with the power absorbed by the bead, $J \epsilon_{ST} A'_T$.

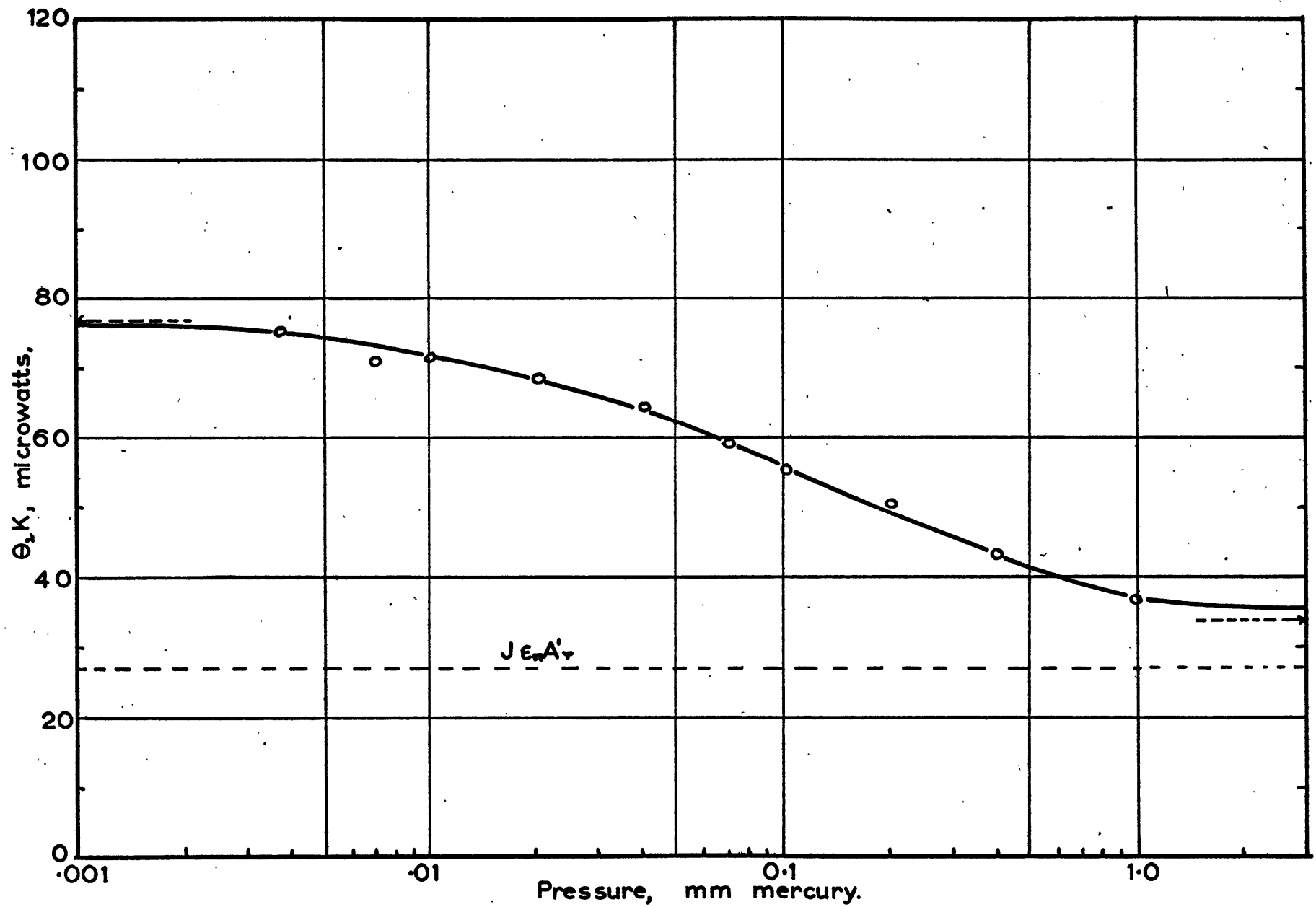


FIG 33. THE QUANTITY $\Theta_2 K$ FOR G-5.

Values for the computations were read off at suitable pressure intervals. Table 4 shows the results for five of the 15 mil aluminized Gulton type X2047 thermistors.

TABLE 4. Measured Heat Transfer Coefficients of Thermistors

(a) h_w in units of 10^{-4} watt $\text{cm}^{-2} \text{ } ^\circ\text{C}^{-1}$

Pressure, mm Hg	.01	.02	.04	.10	.20	.40	1.0	2.0	4.0	10.0
G-2	-	2.4	6.6	11	21	53	99	131	-	-
G-3	-	1.8	4.9	15	32	52	100	160	240	330
G-4	-	3.3	7.6	16	28	47	89	124	150	170
G-5	-	3.1	5.5	12	25	47	120	160	190	200
G-6	1.4	3.5	7.4	16	29	60	140	160	190	220

(b) h_T in units of 10^{-4} watt $\text{cm}^{-2} \text{ } ^\circ\text{C}^{-1}$

Pressure, mm Hg	.01	.02	.04	.10	.20	.40	1.0	2.0	4.0	10.0
G-2	1.4	-	5.0	13	21	28	50	-	54	56
G-3	-	5.4	8.3	13	20	34	57	73	76	74
G-4	-	2.8	4.6	13	29	47	75	98	111	123
G-5	-	3.3	6.2	12	20	33	50	68	82	90
G-6	1.0	2.3	3.7	10	19	29	52	66	74	85

There was considerable variation between the thermistors, especially outside the pressure range 0.04 to 2.0 mm

mercury. Most of this variation was probably due to the inaccuracies of the method at very high and very low pressures as discussed above, but some may have been caused by real variations in thermistor shape and surface conditions.

Fig.34 shows the mean heat transfer values for the thermistors of Table 4. The results for the 1 mil lead wires agree very well with heat transfer coefficients given in the literature for fine wires. See for example McAdams (1954), Collis and Williams (1959) or Ney (1963).

At very low pressures, the slope of the curves in Fig.34 approaches unity, i.e. the heat transfer coefficients become proportional to pressure as expected in a "free-molecule" regime. At higher pressures, above about 10 mm mercury, there is a levelling off. Near atmospheric pressure, in still air, the process is predominantly one of molecular conduction rather than free convection. This is because of the small magnitude of the Grashof number for these small bodies. Thus $Gr = \frac{gd^3}{\nu^2 T} \Delta T$ where ν is the kinematic viscosity. For a 15 mil thermistor bead with $\Delta T = 10^\circ\text{C}$, $Gr \approx 10^{-1}$ at atmospheric pressure. The theoretical expression for conduction of heat from a sphere into an infinite medium of conductivity k is well known. Thus

$$Q = 4\pi kr(T_s - T_\infty)$$

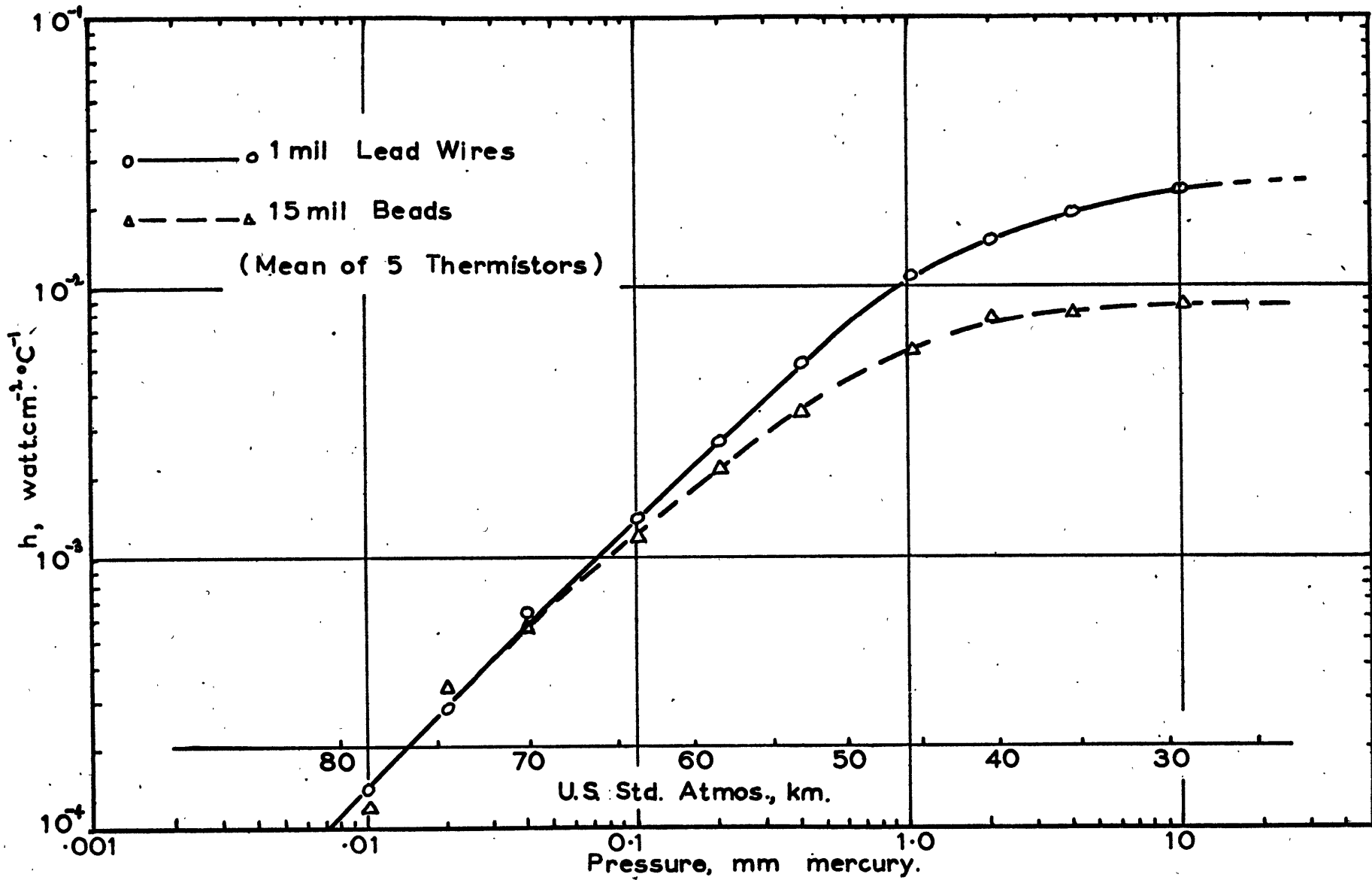


FIG 34. HEAT TRANSFER COEFFICIENTS FOR THERMISTOR BEADS AND LEAD WIRES
 (STILL AIR)

whence

$$h = \frac{Q}{4\pi r^2(T_s - T_\infty)} = \frac{k}{r}$$

For a 15 mil diameter sphere at atmospheric pressure,
 $h = 1.3 \times 10^{-2}$ watt $\text{cm}^{-2} \text{ } ^\circ\text{C}^{-1}$. This value seems consistent with the experimental results when it is remembered that the actual thermistor beads were larger than 15 mil spheres.

Heat transfer coefficients for some of the uncoated thermistors were computed from the measured dissipation rates by assuming that the mean heat transfer coefficient for 1 mil wires given by Fig.34 was applicable to their lead wires. The results are shown in Fig.35 for Veco 5 and 10 mil beads, and a Veco FN1A5 thinistor. This procedure is not completely satisfactory for the bead thermistors because the heat transfer coefficients of the lead wires depend to some extent on their particular surface conditions. It will be seen by comparison with Fig.34 that the heat transfer coefficients of the smaller beads are greater than those of the larger 15 mil coated beads. This is to be expected at higher pressures, but the fact that the values continue to be higher at lower pressures may be in part due to the use of too low values for the lead wires in the computations.

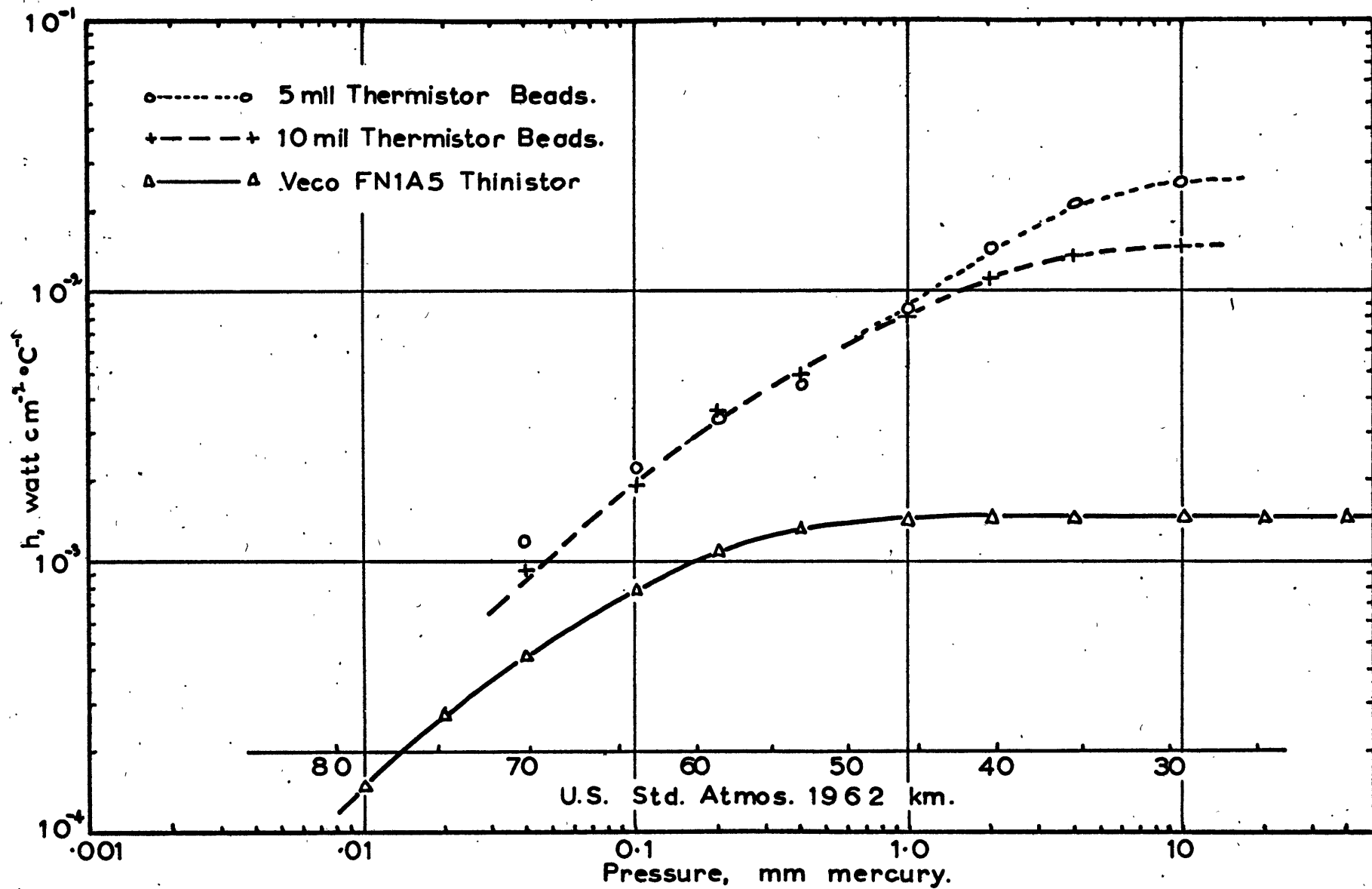


FIG 35. HEAT TRANSFER COEFFICIENTS OF THERMISTORS DEDUCED FROM K.

In the case of the thinistor the contribution of the lead wires to K was only 5-10% so the above problem was not present. A correction for long-wave radiation was applied to the above results, based on the assumptions $\epsilon_{LT} = 1.0$ for the uncoated beads, $\epsilon_{LT} = \frac{1}{2}(1.0 + 0.1)$ for the thinistor (1 black, 1 metallic side), and $\epsilon_{LW} = 0.1$.

(e) Dependence of Temperature Rise on Orientation of the Lead Wires

The radiation tests described in this chapter were all carried out with the lead wires normal to the radiation beam, intercepting a maximum amount of radiation. For other orientations equation (3.1.8) can readily be modified by writing $\epsilon_{sw} J \sin \alpha$ in place of $\epsilon_{sw} J$, where α is the angle between the leads and the radiation, and using an appropriately modified A'_T if the departure of the bead from spherical is great.

To obtain an experimental check on this procedure tests were run in the vacuum chamber with $\alpha = 90^\circ$ and $\alpha = 30^\circ$ on the same thermistor. The latter was mounted on one of the standard mounts which was suspended on a bracket over the window in the pump plate, at the same height as the thermistors in the previous tests, but without the enclosure. The support posts were horizontal and the thermistor mount could

be rotated about a horizontal axis to change the orientation of the thermistor with respect to the radiation. Aluminum foil was arranged to prevent excessive heating of the thermistor mount by the radiation, and some black material was applied to the inside top of the aluminum bell jar to minimize reflection of radiation back to the thermistor.

Fig.36 shows the results of these measurements, which were taken with the aluminized thermistor G-5. The lower curve was computed from the upper one and the previously measured dissipation rate as follows:

1. Calling the observed temperature rise for $\alpha = 90^\circ$ $\theta_2(90^\circ)$, the quantity

$$\left(\theta_2(90^\circ) - \frac{J \epsilon_{ST} A'_T}{K} \right) \sin 30^\circ$$

was computed at suitable pressures, $J \epsilon_{ST} A'_T$ being known from previous results.

2. The computed temperature rise for $\alpha = 30^\circ$ was then

$$\theta_2(30^\circ) = \left(\theta_2(90^\circ) - \frac{J \epsilon_{ST} A'_T}{K} \right) \sin 30^\circ + \frac{J \epsilon_{ST} A'_T}{K}$$

This is essentially the procedure discussed above but with a spherical bead assumed. The bracketed quantity on the RHS is the part of the temperature rise due to the lead wires.

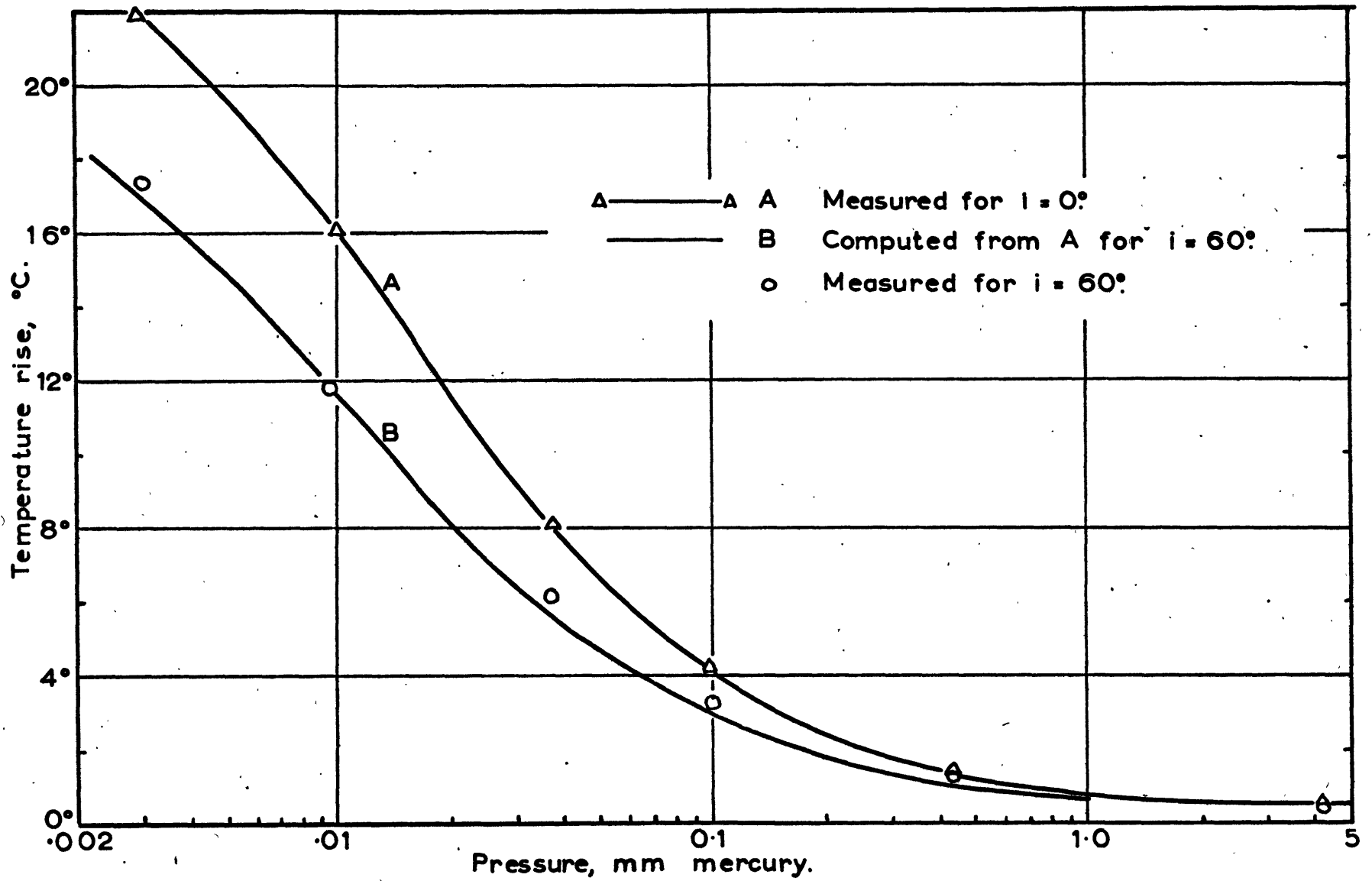


FIG 36, RESPONSE OF THERMISTOR TO RADIATION AT AN OBLIQUE ANGLE.

There was reasonable agreement between measured and computed values. The values of $\theta_2(90^\circ)$ measured in this test were all about 10% higher than those measured previously for the same thermistor using the enclosure. This was probably due to stray radiation which was not so well controlled in the latter tests. No adjustment was made for this fact.

CHAPTER 4

THE ERRORS DUE TO THE MEASURING CURRENT

4.1 Introduction

A small electrical current must be used in order to measure the resistance/temperature of a thermistor. Because of their large electrical resistance and small physical size this current produces a certain amount of heating in the thermistor bead which affects the temperature reading. The temperature rise of the thermistor above ambient air temperature is usually characterized by the "Dissipation Rate". This is defined as the amount of electrical power needed to produce a temperature rise of 1°C .

An expression for the dissipation rate is readily derived by modifying (3.1.5) to include the electrical power Q_e . Thus

$$2ka_w \left(\frac{d\theta}{dx} \right)_{x=d} + h_T A_T \theta_2 = J \epsilon_{sT} A_T' + Q_e \quad (4.1.1)$$

The new expression for (3.1.7) becomes

$$\theta_{20} = \frac{2ka_w p \operatorname{cosech} pd \cdot \theta_1 + Q_e}{2ka_w p \operatorname{coth} pd + h_T A_T} \quad (4.1.2)$$

The part of the temperature rise due to Q_e is obviously

$$\theta_{2e} = \frac{Q_e}{2ka_w p \coth pd + h_T A_T}$$

Hence the dissipation rate K is given by

$$K = 2ka_w p \coth pd + h_T A_T \quad (4.1.3)$$

For sufficiently long lead wires $\coth pd \rightarrow 1$ up to a given altitude and K reduces to

$$K = 2ka_w p + h_T A_T = 2\sqrt{2} \pi k^{\frac{1}{2}} r^{\frac{3}{2}} h_w^{\frac{1}{2}} + h_T A_T \quad (4.1.4)$$

If the appropriate heat transfer coefficients for the miniature bead thermistors are inserted in (4.1.3) it will be found that the contribution of the lead wires to K is comparable with the heat transfer from the bead itself at all pressures, and in many cases exceeds it. This is illustrated in Table 5 which shows these two terms, $2ka_w p \coth pd$ and $h_T A_T$ for the 15 mil Gulton thermistor G-5. The coefficients were taken from Table 4.

TABLE 5. Relative Contributions of Leads and Bead to G-5
Dissipation Rate. (microwatt $^{\circ}\text{C}^{-1}$)

Pressure mm Hg	.04	0.1	0.2	0.4	1.0	2.0	4.0	10
$2ka_w p \coth pd$	6	8	11	16	25	28	31	32
$h_T A_T$	4	7	12	19	28	38	46	50
K	10	15	23	35	53	66	77	82

As pointed out in Chapter 3, K appears as a fundamental quantity in the expressions for the radiation error. It is also important in determining the response speed of the thermistors (see Chapter 7). For these reasons, measurements of K as a function of pressure have been made for a relatively large number of thermistors.

In the earlier rocket soundings the electrical circuits were such that a considerable amount of electrical power was dissipated in the thermistor. According to graphs given by N.K. Wagner (1963) for example, a measuring power of about 45×10^{-6} watts was used at temperatures encountered near 65 km.- At this altitude a typical value of K for a 10 mil bead thermistor is 15×10^{-6} watts so an error of 3°C would have resulted. More recent telemetry circuits produce rather less heating in the thermistor, and according to Ballard (1966) this heating need no longer be a significant source of error. Pearson (1964) describes how the error may be reduced without reducing sensitivity by using a pulsed circuit.

4.2 An Instability Criterion

In extreme cases it is possible to get an unstable condition with certain types of measuring circuit. As an illustration, suppose the circuit supplies a constant voltage,

so that the power is given by $\frac{V^2}{R_T}$ where V is constant. If θ is the temperature rise due to the heating current, a small change $\delta\theta$ in θ would be accompanied by a change $\frac{dR_T}{dT} \cdot \delta\theta$ in R_T . But with this change in R_T the power would change by

$$\delta Q_e = - \frac{V^2}{R_T^2} \cdot \frac{dR_T}{dT} \cdot \delta\theta$$

A change δQ_e in power, however, would result in a change $\delta\theta'$ of $\frac{\delta Q_e}{K}$, i.e.

$$\delta\theta' = - \frac{V^2}{R_T^2} \cdot \frac{dR_T}{dT} \cdot \frac{\delta\theta}{K}$$

The displacement $\delta\theta$ is unstable if $\delta\theta' > \delta\theta$ i.e. if

$$- \frac{V^2}{R_T^2} \cdot \frac{dR_T}{dT} \cdot \frac{1}{K} > 1$$

Making use of (2.6.1) to substitute for $\frac{dR_T}{dT}$ the condition for instability becomes

$$\frac{V^2}{KR_T} \cdot \frac{2.303 a}{T^2} > 1 \quad (4.2.1)$$

An important case occurs at or just before ejection of the nose-cone, when the thermistor temperature might be rather high, yet the altitude so great that K is very small. For an example, consider a typical thermistor

ejected at 65 km where $K \approx 15 \times 10^{-6}$ watt $^{\circ}\text{C}^{-1}$ with T equal to a conservative 300°K . A typical value of R_T might then be 5×10^4 ohms, with $a = 1600$. With $V = 6$ volts the left-hand side of (4.1.5) is 1.9 so in this example an instability would have resulted. Rocket soundings which appeared to have instabilities of this type have been described to the author by Mr. P.J. Harney, of the Aerospace Instrumentation Laboratory, A.F.C.R.L.

4.3 Method of Measurement

The dissipation rate was measured by observing the resistance of the thermistor when each of two different measuring currents were used. The bridge and recording circuit described in 3.3(a) were used, the currents being measured with a Leeds and Northrup potentiometer.

Let the two measuring currents be I_1 and I_2 , and R_1 and R_2 the corresponding resistances after allowing sufficient times for the temperatures to stabilize. Then R_1 and R_2 enable the temperature difference ΔT to be evaluated, while the difference in electrical heating powers is given by

$$\Delta Q_e = I_2^2 R_2 - I_1^2 R_1$$

Then
$$K = \frac{\Delta Q_e}{\Delta T} .$$

The measurements were carried out with the thermistors mounted in the small enclosure as for the radiation tests (3.3(d)). This provided the same advantages as described in that connection. Generally I_1 was chosen so that the associated temperature rise was very small ($Q_e \approx 1$ microwatt typically) while I_2 was made sufficient to give a temperature rise of 3 - 10 °C. The two measurements concerned were carried out as closely as possible together to avoid changes in ambient temperature between tests. In many cases the test with the smaller current I_1 was repeated immediately after the second test and the mean temperature used, but in almost all instances the rate of drift was so small that this precaution was superfluous. For use in the calculation of the reflectivities, (3.6(c)), a special measurement of K was made under high vacuum using a heating current which gave a temperature rise of the same order (perhaps 20-30 °C) as that obtained with the radiation.

4.4 Results

Fig.37 shows plots of temperature rise vs electrical heating power for a Gulton X2047 thermistor at three different pressures. The relation is seen to be linear as implied by the above discussions, the slopes corresponding to $\frac{1}{K}$. This result is of some importance as it justifies the assump-

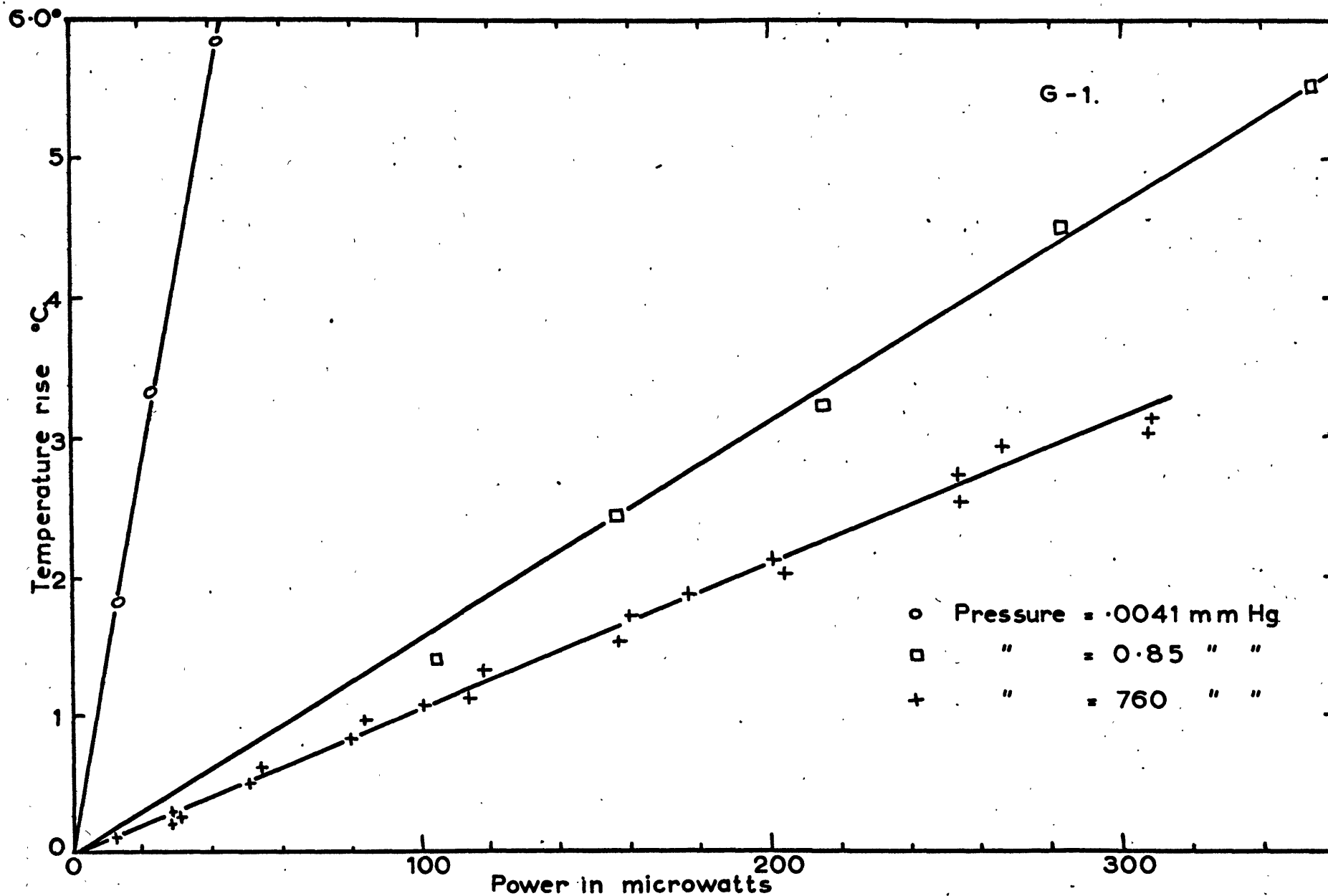


FIG 37. TEMPERATURE RISE OF X2047 THERMISTOR VS POWER DISSIPATION.

tion of a linear relation between temperature difference and heat transfer used throughout this work. Subsequent measurements of K required determination of only two points as described above.

Fig.38 shows plots of the measured dissipation rate as a function of pressure in still air for four thermistors. As was the case with the radiation temperature rise, K is fairly constant from sea level pressure down to a few millimeters of mercury, with the smaller thermistors starting to change at higher pressure. The curves at very low pressures level out to values dependent on the particular lead length and long-wave radiation conditions used in the tests.

Results for other thermistors are given graphically in Appendix 2.

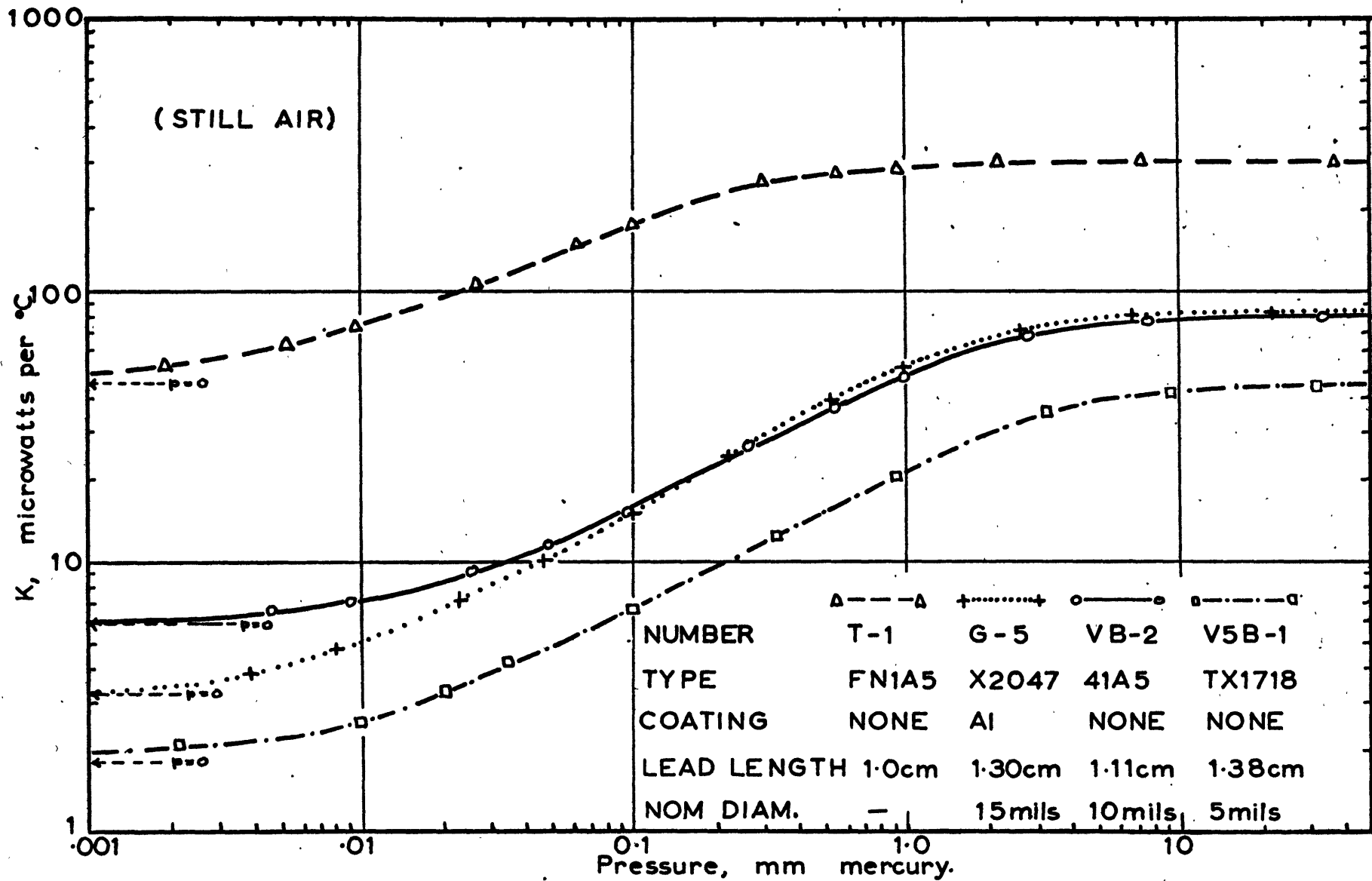


FIG 38. MEASURED DISSIPATION RATES OF THERMISTORS.

CHAPTER 5

CONDUCTION OF HEAT FROM THE SUPPORTS

5.1 Introduction

In general the supporting posts to which the thermistor is attached do not have the same temperature as that of the surrounding air. This may be due to their large thermal mass, heat conduction from the instrument package and/or absorption of heat from solar radiation. A certain amount of this temperature difference is passed on to the thermistor bead, the amount depending on the length of lead wire used.

In high altitude balloon soundings this temperature difference may be only a few degrees centigrade, but in rocket soundings it may be very much more especially at the highest altitudes. This is because the rocket attains its maximum altitude so rapidly that the rocketsonde is still near its launch temperature when the nose cone is ejected. In many cases, aerodynamic heating during the ascent results in even higher temperatures. Walker (1965) quotes temperatures near 100 °C for skin temperatures of the instrumented "Dart" system when using ablative coatings. For the Arcas system Ballard (1966) has mentioned a thermistor

temperature of 80°C immediately prior to nose cone ejection. This author has however stated that by experimenting with thermal shielding of the sensor unit within the nose cone he had been able to reduce this figure very considerably.

In a very large number of rocket soundings the measured temperatures have been too high because the method of mounting allowed these high temperatures, which persist in the instrument package and mounts for a considerable time because of their slow response, to excessively influence the bead temperature during descent.

5.2 Theoretical Expression for the Conduction Error

We shall consider only the steady-state (equilibrium) case in which the air temperature is assumed to be constant. This is applicable however, even when the air temperature is changing provided the change is slow compared to the response speed of the sensor (Chapter 7).

Consider a thermistor mounted as in Fig.6, and let θ_1 be the difference between the support post temperature and the air temperature. Then the equilibrium temperature of the thermistor bead, θ_{20} is given by equation (3.1.7), i.e.

$$\theta_{20} = \frac{2ka_w p \operatorname{cosech} pd}{A_T h_T + 2ka_w p \operatorname{coth} pd} \cdot \theta_1$$

It is often convenient to speak of the conduction error in terms of the fraction

$$\frac{\theta_{20}}{\theta_1} = \frac{2ka_w p \operatorname{cosech} pd}{A_T h_T + 2ka_w p \operatorname{coth} pd} = \frac{2ka_w p \operatorname{cosech} pd}{K} \quad (5.2.1)$$

To determine the conduction error, θ_1 must be known as well as the R.H.S. of (5.2.1) as a function of altitude. Usually this is not possible, and instead an estimate of θ_1 must be used. This approach was taken, for example, by N.K. Wagner (1964) in considering this problem, but in that case no account was taken of the effects of convection on the lead wires. The variability of the correction to be applied for lead wire conduction depends primarily on the ratio $\frac{\theta_{20}}{\theta_1}$ given by (5.2.1). Thus if $\frac{\theta_{20}}{\theta_1} = 0.05$, then in order to know the correction to 1°C we should have to know θ_1 to $\pm 20^\circ\text{C}$.

Fig.39 shows (5.2.1) as a function of lead wire length and heat transfer coefficient h_w , for a 15 mil effective diameter thermistor bead having 1 mil platinum-iridium lead wires. The appropriate values of h_T for use with the assumed values of h_w were estimated from Fig.34. Also plotted on this figure are the curves for a "0 mil" bead using the same wire.

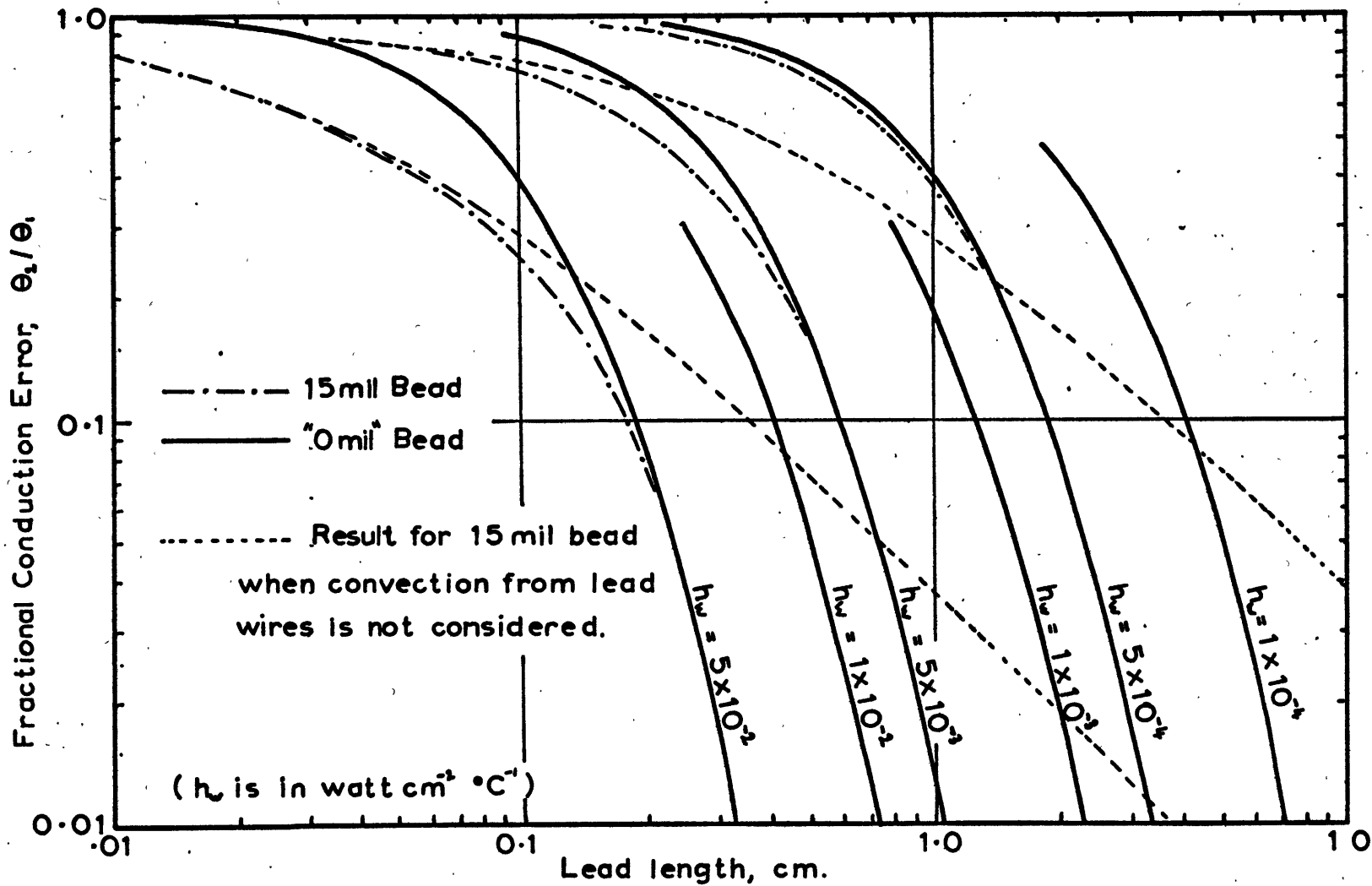


FIG 39. CONDUCTION ERROR FOR THERMISTORS USING 1mil Pt-IRIDIUM LEADS.

It is seen that for practical values of $\frac{\theta_{20}}{\theta_1}$ the effect of the thermistor bead is insignificant. With the aid of this figure one can determine the minimum lead length required to achieve a desired value of $\frac{\theta_{20}}{\theta_1}$ when h_w is given, or vice versa. Note that h_w is a function of pressure, ventilation speed etc. which can be evaluated under a given set of conditions from data given in this or other published works. The question of the conduction error in actual soundings will be taken up in Chapter 11.

The above computations differ considerably from those of authors who have not allowed for convection from the surface of the lead wires. The calculations corresponding to this erroneous assumption for a 15 mil bead thermistor are also illustrated in Fig.39. It will be seen that except for very small lead lengths and/or very small values of h_w the conduction error is greatly overestimated. In addition, the greatly increased benefits obtained by increasing the lead length are not correctly represented.

Fig.40 shows the same computations for 0.7 mil platinum-iridium lead wires as used on Veco 5 mil thermistors. This time the effect of the bead was neglected, so that (5.2.1) reduced to

$$\frac{\theta_{20}}{\theta_1} = \operatorname{sech} pd \quad (5.2.2)$$

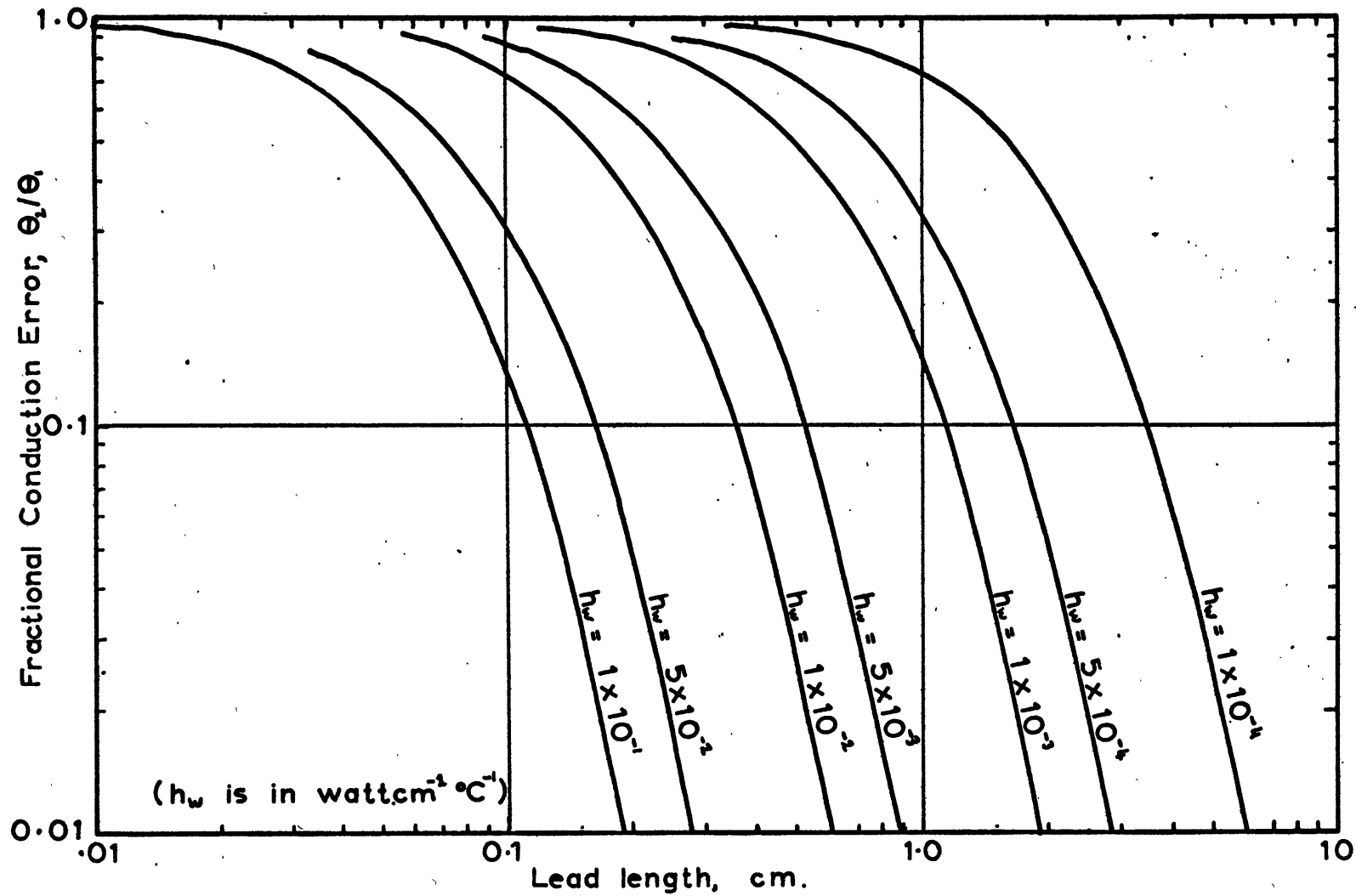


FIG 40. CONDUCTION ERROR FOR THERMISTORS USING 0.7mil Pt-IRIDIUM LEADS.

5.3 Experimental Methods

After some preliminary tests it was found that direct testing to determine the conduction error was not practical with the equipment available. Thus any attempt to artificially heat the thermistor supports above ambient temperature in still air resulted in a region of heated air collecting around the supports which to some extent enveloped the thermistor bead. In an actual sounding there would be a flow of undisturbed air around the thermistor and this would not happen. (Note that in measurements from floating balloons there is no ventilation and extra long lead wires might be necessary to avoid this effect). To properly carry out tests of this type a low density wind tunnel would be required.

To a considerable extent the measurement of the heat transfer coefficients carried out in Chapter 3 provides the necessary experimental data for estimation of the conduction error as a function of pressure, through (5.2.1). Since we could not experimentally check the validity of (5.2.1) we were at least able to check the validity of a relation based on the same type of assumptions - the expression for the dissipation rate

$$K = 2ka_w p \coth pd + h_T A_T \quad .$$

This was done by measuring K as a function of pressure on the same thermistor, but with three different lead lengths. The tests with the longest leads were made first after which the thermistor was re-mounted on a new mount having smaller post separation. Care was taken not to contaminate the bead or the lead wires during the mounting process.

5.4 Results

Fig.41 shows the results for a Gulston type X2047 aluminized thermistor. The lead lengths were $d_1 = 0.395$ cm, $d_2 = 0.725$ cm, and $d_3 = 1.46$ cm. Notice that the two longer lead lengths gave the same values for K down to a pressure of about 3×10^{-2} mm mercury. The values of K computed from the heat transfer coefficients given in Fig.34 are also given, and there is seen to be reasonably good agreement.

From the measurements at high vacuum it was possible to deduce the thermal conductivity k of the lead wires. Denoting the three values of K by K_1, K_2, K_3 corresponding to lead lengths d_1, d_2, d_3 we have

$$K_1 - K_2 = 2ka_w p (\coth pd_1 - \coth pd_2)$$

together with two similar relations. The value of h' required in p was estimated by putting $\epsilon_{lw} = 0.08$ although the result was not sensitive to this choice. The other

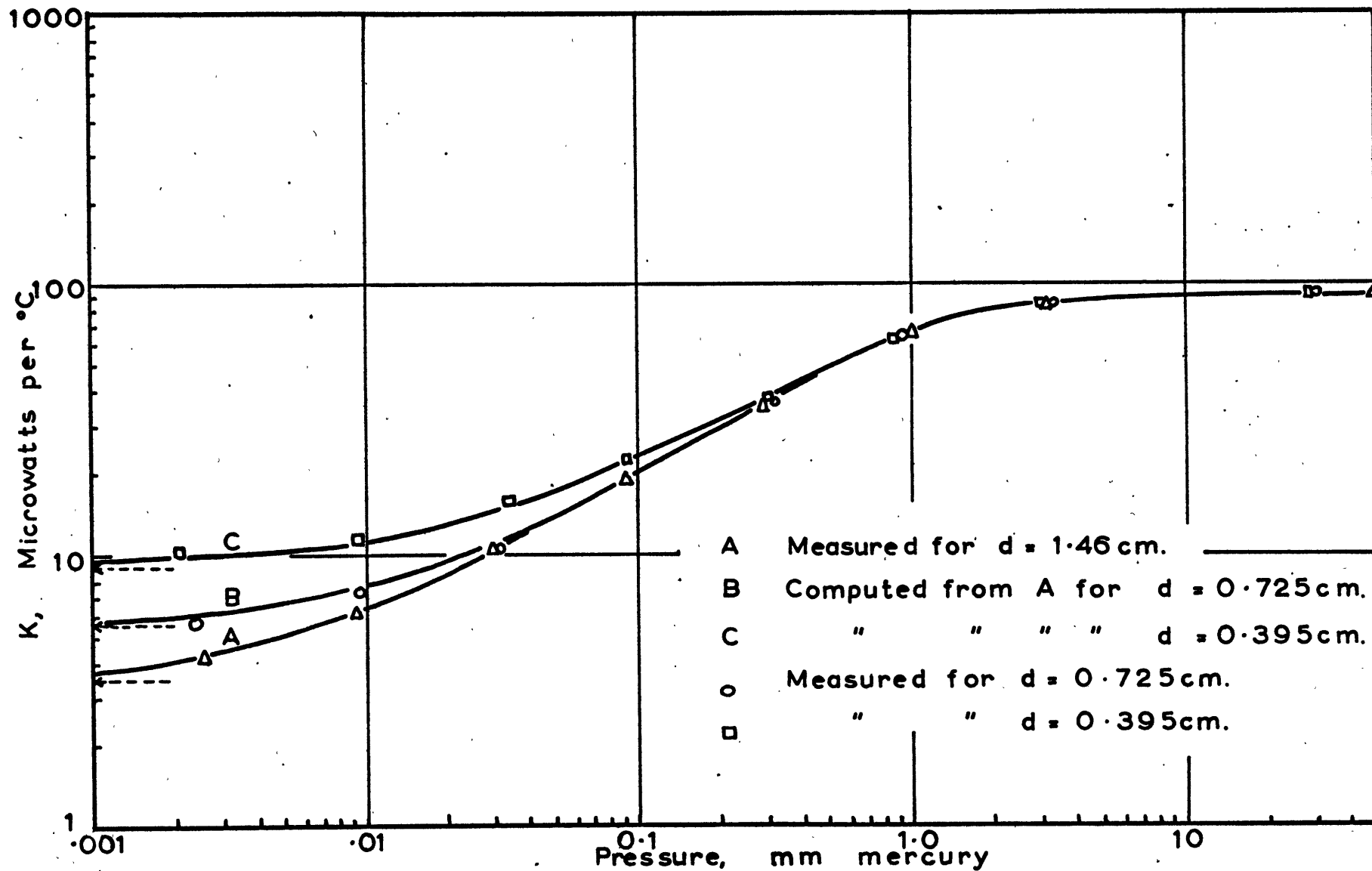


FIG 41, MEASURED AND COMPUTED DISSIPATION RATE FOR DIFFERENT LEAD LENGTHS.

quantities being known, graphical solution of these relations gave three values for K . The results were

K_1	K_2	K_3	
8.82×10^{-6}	5.64×10^{-6}	3.48×10^{-6}	watt $^{\circ}\text{C}^{-1}$.
$k(1,2)$	$k(2,3)$	$k(1,3)$	
0.28	0.34	0.30	watt $\text{cm}^{-1} \text{ } ^{\circ}\text{C}^{-1}$.

The mean value of k , $0.31 \text{ watt cm}^{-1} \text{ } ^{\circ}\text{C}^{-1}$ was the same as the published value for platinum-iridium alloy.

CHAPTER 6

ERRORS DUE TO LONG-WAVE RADIATION

6.1 Introduction

In addition to the radiation received directly and by reflection and scattering from the sun, which for the most part consists of relatively short wavelengths, the thermistor exchanges energy with its environment by means of long-wave (thermal) radiation characteristic of the temperatures involved. In the atmosphere this exchange of energy is extremely complex, for the radiation intensity and its spectral composition at any point is a function of the direction from which it is received, and also changes considerably with atmospheric conditions.

Since some of this radiation originates in the atmosphere itself, by emission from carbon dioxide and water vapour, the intensity in the spectral bands concerned is to some extent a measure of the atmospheric temperature. It is possible to devise a thermometer working on this principle. However Johnson (1953) shows that in the lower troposphere the effective sampling value of such an instrument in cloud-free air would be a sphere of $\frac{1}{8}$ to $1\frac{1}{2}$ miles radius, depending on the wavelength band chosen. Of course this

would be for an instrument which filtered out and measured only this wavelength band. In the upper atmosphere the amounts of carbon dioxide and water vapour present are vastly less, so the effective sampling volume would be enormous. In the case of a thermistor there is no selection of wavelength bands, so it is obvious that any long-wave radiation exchange must be considered a source of error rather than a possible beneficial influence on the measurement of air temperature.

Because of the complexity of the problem it is necessary to make gross simplifications in treating the errors produced in the thermistor. It is assumed that the upward component of the radiation flux can be considered due to a black body of temperature T_{eb} . Similarly the downward component, from the atmosphere above the thermistor is considered as a black body flux of temperature T_{ea} and the radiation from the instrument package that due to a black body of temperature T_p . The thermistor and its lead wires are assumed to be grey bodies.

The greatest possible exchange of thermal radiation would occur if $T_{eb} = T_{ea} = T_p = 0^\circ\text{K}$. Then the rate of heat loss per unit area of any part of the thermistor would be $\epsilon \sigma T^4$. Putting $T \approx 273^\circ\text{K}$, and $\sigma = 5.70 \times 10^{-12}$ watt $\text{cm}^{-2} \text{ }^\circ\text{K}^{-4}$ we see that this is of the order of

$$Q_L = \epsilon_L \times 3 \times 10^{-2} \text{ watt cm}^{-2}$$

This may be compared with the energy absorbed per unit cross-section area from the direct solar radiation,

$$Q_S = \epsilon_S J = \epsilon_S \times 1.39 \times 10^{-1} \text{ watt cm}^{-2} .$$

Since the area involved with Q_L is 3-4 times the area involved with Q_S , from geometrical considerations, we see that for comparable ϵ_S and ϵ_L the heat transfer rates are comparable. It is therefore just as important to have a thermistor coating with small emissivity in the infrared as it is to have high reflectivity in the solar radiation range. In general this is realized with metallic coatings, but not with reflective paints.

6.2 Theoretical Expression for Temperature Error

The expression for the temperature error may be derived in a similar manner to that used for the solar radiation error, equation (3.1.8), if we assume that the error is small (less than 15-20°C). The result is

$$(\theta_2 - \theta_{20}) = Q_L \cdot \frac{4\pi r \epsilon_L w}{p} \cdot \frac{(\coth pd - \operatorname{cosech} pd) + \epsilon_{LT} A_T}{h_T A_T + 2ka_w p \coth pd} \quad (6.2.1)$$

where

$$Q_L = \sigma \left(\frac{1}{2} T_{eb}^4 + \frac{1-2\gamma}{2} T_{ea}^4 + \gamma T_p^4 - T^4 \right)$$

γ depends on the angle subtended by the instrument package at the thermistor. In this expression, T is taken as the measured (bead) temperature, so that $T = T_{\text{air}} + \theta_2$.

(6.2.1) is therefore a quartic equation in T . However in most cases a satisfactory approximation will be obtained if T is taken as T_{air} .

It should be noted that for miniature bead thermistors the contribution of the lead wires to this radiation error is a significant item, just as it was in the case of the solar radiation error.

6.3 Experimental Methods

From the discussions in the above two sections it is evident that the primary quantities determining the long-wave radiation error of a thermistor are ϵ_{LW} and ϵ_{LT} . Since all other quantities appearing in (6.2.1) had already been studied the experiments were concerned only with the measurement of the emissivities.

To distinguish between ϵ_{LW} and ϵ_{LT} it would have been desirable to carry out a test in which radiant energy was supplied substantially to the bead alone, as was done in the case of solar radiation. This is much more difficult to do, however, because of the very small size of the beads

and the greater difficulty of ensuring closely controlled conditions. For this reason it was decided to attempt to measure only an "effective emissivity", combining $\epsilon_{\lambda w}$ and $\epsilon_{\lambda T}$. For metallic coatings on the beads we would expect $\epsilon_{\lambda w}$ and $\epsilon_{\lambda T}$ to be comparable, and in any case the results will give substantially the correct answer when applied to the evaluation of the error in the atmosphere.

The device used for the measurements is shown in Fig.42. The principle of the method was to subject the thermistor, including its lead wires, to black body radiation inside an evacuated enclosure of temperature T_2 , while holding the temperature of the thermistor support posts at a constant temperature T_1 . Under these conditions the thermistor bead assumed an intermediate equilibrium temperature T_T at a point where the net heat gained by radiation was equal to that lost by conduction through the lead wires.

The heated enclosure was a hollow brass cylinder $7/8$ inch long, $7/16$ inch outside diameter and $1/4$ inch inside diameter. A $3/32$ inch slot was cut down one side to facilitate the installation of the mounted thermistor. Once the thermistor had been installed this slot was closed off with a copper slide. The insides of the enclosure and slide were blackened with optically flat black paint.

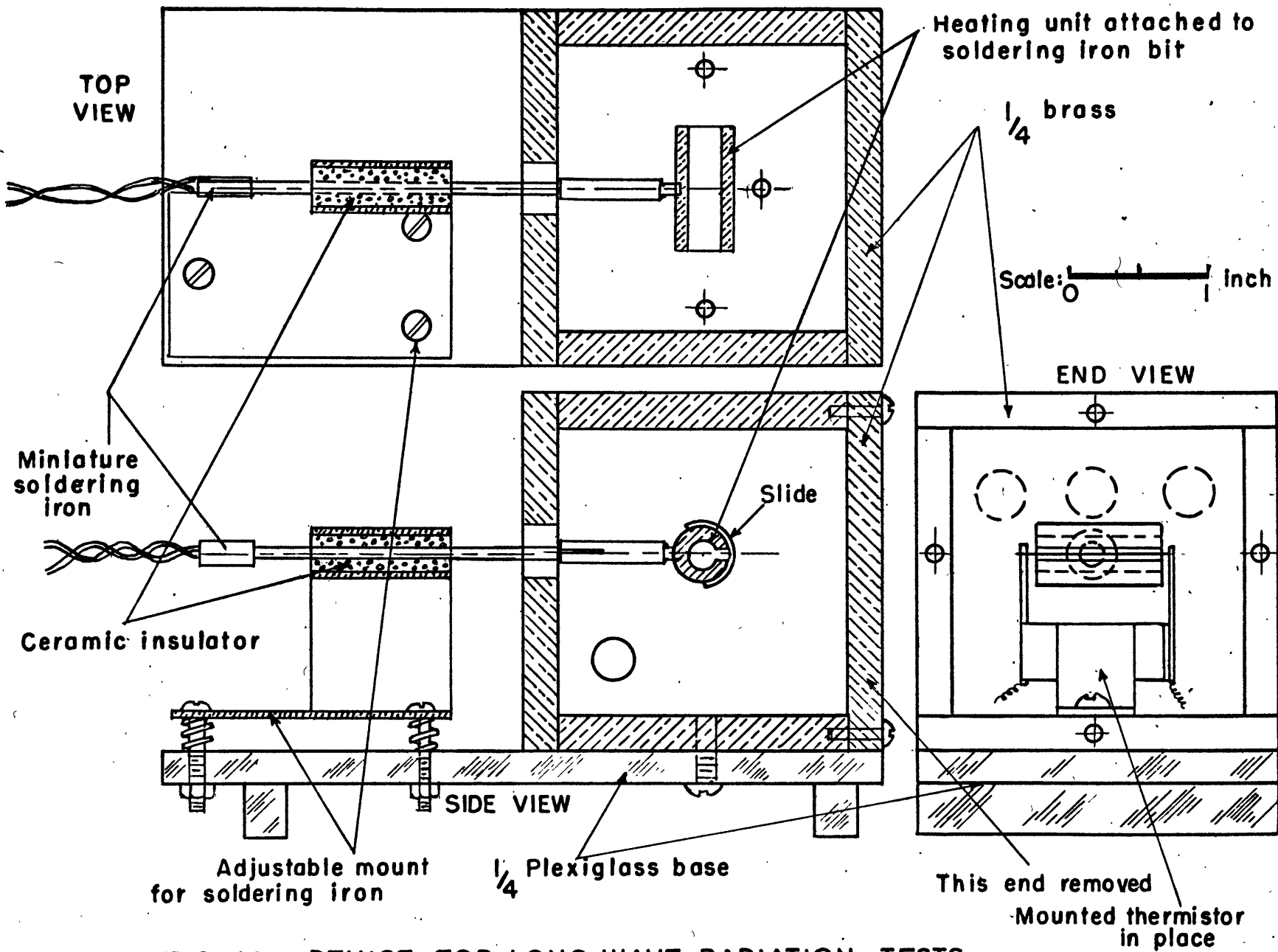


FIG 42 DEVICE FOR LONG-WAVE RADIATION TESTS.

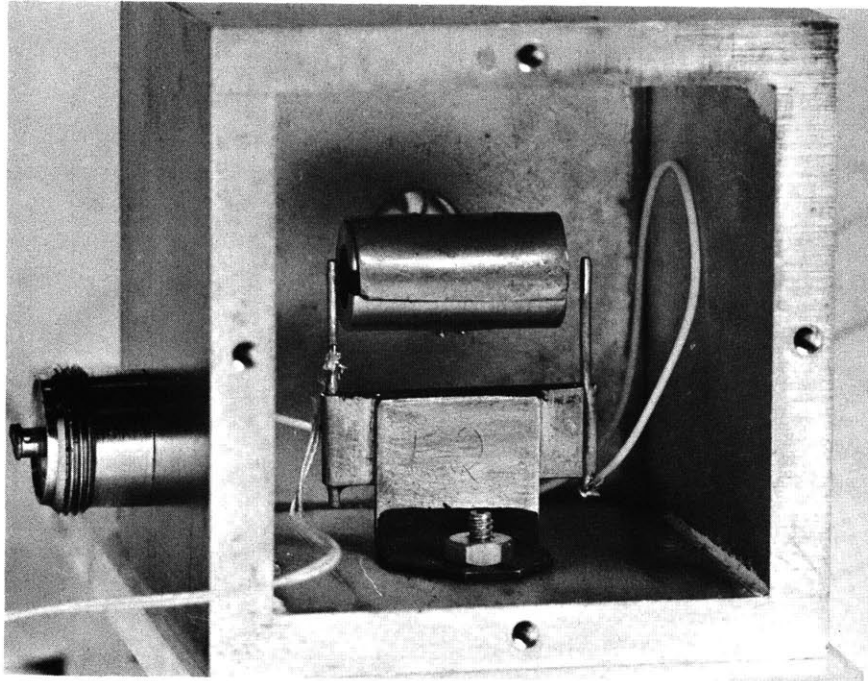
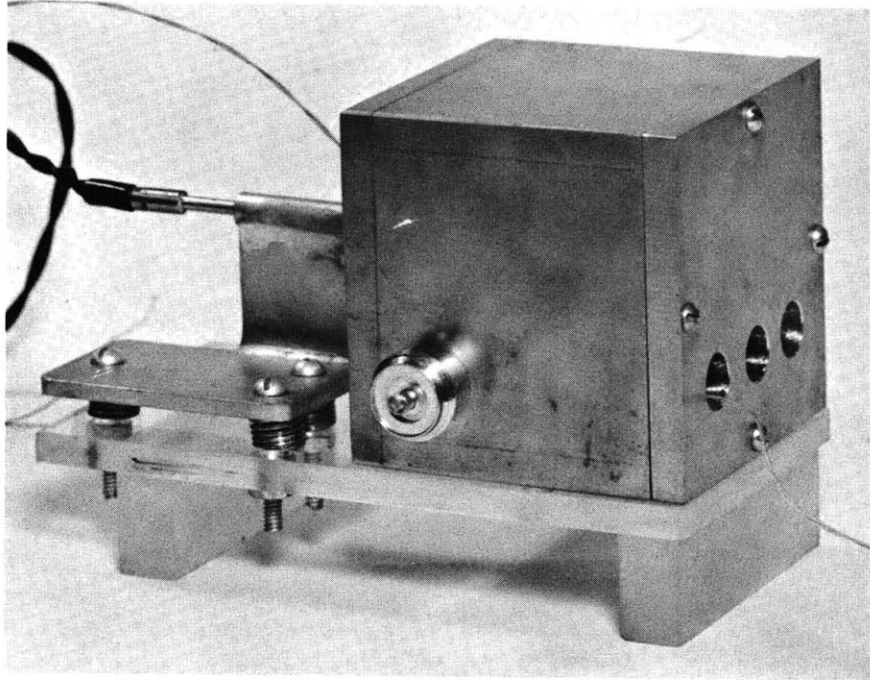


FIG.43. Apparatus for Testing Response of Thermistors
to Long-wave Radiation.

The thermistors were mounted on mounts of the type already described in section 3.3(d). These mounts were designed so that the thermal contact between thermistor support posts and the base-plate was a maximum. The whole was enclosed in a heavy-walled brass box of sufficient thermal capacity that it and the thermistor mount remained at a substantially steady temperature while the inner enclosure was being heated.

The heating unit was an "Oryx" miniature soldering iron which protruded into the brass box from the side. Power was supplied to this through insulated feed-throughs in the pump plate. Four number six dry cells provided the heating current, which was regulated by a rheostat and a small ammeter.

Copper-constantin thermocouples were soldered to one of the thermistor support posts, and to the heated cylindrical enclosure. The outputs of these were amplified by Weston Inductance Amplifiers and displayed on an Esterline-Angus recording milliammeter. An ice bath was used for the reference junctions.

The measurements were carried out under a vacuum of better than $2-4 \times 10^{-5}$ mm mercury obtained with the aid of the diffusion pump. After noting the thermocouple outputs

and the thermistor resistance (recorded on the Sanborne Recorder) a heating current of about 0.2 amps was applied for a short time, after which it was decreased to allow the various temperatures to become steady enough to take readings. The process was repeated to obtain further sets of readings up to a maximum heating of about 25°C above ambient. More readings were taken as the system cooled. The response time of the enclosure to heating or cooling was always much slower than the thermistor time constant so it was not necessary to wait for absolutely steady conditions before taking a set of readings. From one to two hours were required for the complete tests, during which time the support post temperature changed a maximum of 0.5°C.

6.4 Calculation of the Emissivities

Assuming that the radiation heat transfer can be linearized by introducing $h' = 4\epsilon\sigma\bar{T}^3$ as in section 3.2, it will be found that equation (3.1.7) applies. This equation can be written in a form more suitable for computations, i.e.

$$\frac{\theta_1}{\theta_{20}} = \cosh pd + \frac{h' A_T}{2ka_w} \cdot \frac{\sinh pd}{p} \quad (6.4.1)$$

In this equation,

$$\theta_1 = (T_{\text{enclosure}} - T_{\text{supports}})$$

$$\theta_{20} = (T_{\text{enclosure}} - T_{\text{bead}})$$

$$p = \sqrt{\frac{2h'}{kr}}$$

Note that we have assumed $h'_w = h'_T$.

The tests give θ_1 and θ_{20} , allowing the right-hand side to be solved (graphically in the present case) for h' . Since \bar{T} is known to sufficient accuracy, ϵ_λ can then be calculated. For example, if $\bar{T} = 310^\circ\text{K}$, $\epsilon_\lambda = \frac{h'}{6.9 \times 10^{-4}}$

The lead lengths used of ~ 1.3 cm allowed about 1 mm to project out of each end of the heating enclosure. No correction was applied for this. If δx is the small length of lead adjacent to the supports which is not influenced by the radiation it can be shown that the correction factor involves a term of the form $1 + \delta x^2$, which was not significant in this case.

6.5 Results

Fig.44 shows graphically some of the readings obtained with the above device. The lines have a slight curvature corresponding to the variation of \bar{T}^3 . For calculation of ϵ_λ , only one pair of points, that corresponding to $\theta = 20^\circ\text{C}$, was read off each curve.

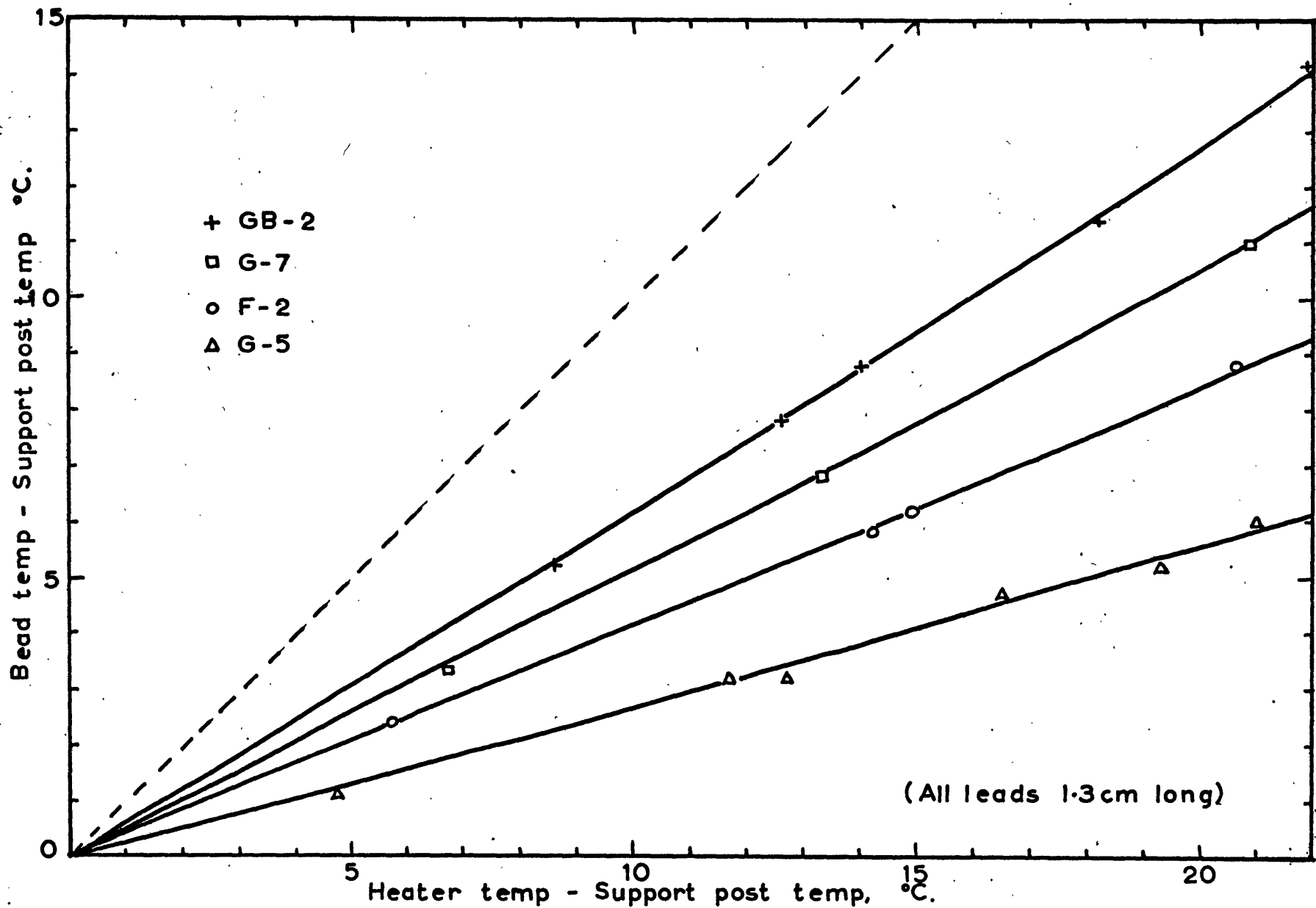


FIG 44 RESPONSE OF THERMISTORS IN L/W RADIATION TESTS.

The measured emissivities are given below in Table 6.

TABLE 6. Measured Emissivities of Thermistors.

Number	θ_1	θ_{20}	d	ϵ_λ	Visual Condition	
	$^{\circ}\text{C}$	$^{\circ}\text{C}$			Bead	Wire
G-5	20	14.5	1.30	.08	good	good
G-9	20	13.5	1.29	.11	good	good
G-11	20	11.1	1.26	.16	fair	poor
G-7	20	9.5	1.25	.24	poor	bad
F-2	20	11.6	1.25	.15	poor	poor
GB-2	20	7.2	1.30	.93 (of black bead)	-	fair

Except for G-9, which was an aluminized thermistor whose surfaces appeared in very good condition, all of these thermistors have been discussed in Chapter 3 in connection with their response to short-wave radiation.

In general the values of ϵ_λ are lower than the values of ϵ_s measured in Chapter 3, although they are still somewhat higher than those expected of polished metallic surfaces. There is considerable variation according to the state of the surfaces.

The emissivity of the black bead GB-2 was deduced as a test of the method, by assuming that $\epsilon_{\lambda w}$ was 0.10. The

agreement is satisfactory, for the overall accuracy of the method is probably about 10%.

To a limited extent the dissipation rate $K(0)$ measured as described in Chapter 4 under high vacuum can be used to estimate the emissivity. Thus

$$K(0) = 2ka_w \sqrt{\frac{2h'_w}{kr}} \coth \sqrt{\frac{2h'_w}{kr}} + h'_T A_T .$$

However, for lead lengths of 1 - 1.5 cm as used this quantity is actually rather insensitive to h' , except in the case of a black thermistor.

The spectral content of the radiation used was that of a black body at 310 to 320°K. In the atmosphere, the major source of error is loss of heat from the thermistor to the atmosphere above, so that it is the emission of black body radiation at the thermistor temperature which is important. This temperature ranges between about 200°K and 300°K. The wavelength of peak emission varies as only $\frac{1}{T}$ and the black body curves for these temperatures are rather broad, so the conditions under which the emissivities were measured above should have been an adequate simulation of the atmospheric conditions.

CHAPTER 7

DYNAMIC RESPONSE OF THERMISTORS

7.1 Introduction

The speed with which a thermometer approaches the ambient air temperature after exposure, and its ability to respond to rapid changes in air temperature, is usually expressed by the "time constant", τ . τ is defined as the time required for the sensor to record $1 - \frac{1}{e} = 63\%$ of a step change in ambient temperature.

For a simple system, the heat loss is proportional to the temperature difference θ existing between the thermometer and the air. Writing the heat loss as $\gamma\theta$ and letting C equal the thermal capacity, we have

$$\frac{d\theta}{dt} = -\frac{\gamma}{C} \theta \quad (7.1.1)$$

Therefore

$$\frac{\theta}{\theta_0} = e^{-\frac{\gamma t}{C}} \quad \text{when } \theta = \theta_0 \text{ at } t = 0. \quad (7.1.2)$$

The response is exponential and the reason for the definition of τ given above becomes clear. In this case, of course,

$$\tau = \frac{C}{\gamma}.$$

The response speed of a rocketsonde thermistor is particularly important because, as mentioned in section 5.1 above, the temperature of the thermistor and its mounting may be many tens of degrees warmer than the surrounding air when the sensor is first exposed. Since the rocketsonde fall rate is very large at the highest altitudes a good deal of the record may be lost if the thermistor does not respond rapidly.

In theory a correction can be applied on the basis of (7.1.1), for the error θ is given by

$$\theta = -\tau \frac{d\theta}{dt}$$

where $\frac{d\theta}{dt}$ is the rate of change of temperature as measured by the thermistor. In practice $\frac{d\theta}{dt}$ can only be obtained as an approximation and the correction determined in this way is subject to considerable uncertainty if τ is large.

An alternative approach has been used by N.K. Wagner (1964). In Wagner's work the correction was calculated for a sounding in a standard atmosphere using an assumed initial temperature, and it was proposed that this correction be applied to all actual soundings, since it would represent mean conditions.

Both methods require knowledge of τ . Since τ depends on the rate of heat exchange between the thermistor

and the air, it is a function of pressure, ventilation speed etc. and in general increases with altitude. Thus, the response of a rocketsonde thermistor is slowest at the point where a fast response is desired.

For a number of reasons there are difficulties in computing τ from the heat transfer rates and the heat capacity of the thermistor bead. Ney et al (1963) point out that for objects of very small size, the heat capacity of the heated air adjacent to the objects may be comparable with the heat capacity of the bodies themselves. According to Ney, failure to allow for this can result in an underestimation by a factor of 2-3 of the time constant of a 1 mil diameter wire thermometer. It is not clear to what extent this effect would be important in the response of small thermistors. It is not thought likely that the effective heat capacity of the beads would be significantly changed, but presumably the response of the lead wires would be influenced. A large part of the heat flow from a miniature thermistor bead is via the lead wires, so the response of a small thermistor to a change in air temperature depends significantly on the response of the lead wires and on the mounting used.

7.2 Laboratory Measurements of the Time Constant

The ideal method of measuring τ would be to observe the response to an actual step change in air temperature. This is not difficult to arrange at sea level pressures but problems are encountered at the low pressures of interest in this work. A simpler method of measuring the time constants of these small thermistors is to heat them above the temperature of the ambient air and then to observe their rate of cooling after sudden withdrawal of the source of heat. The time constant may also be derived from the rate of heating if the onset of heating is made sufficiently sudden. The source of heat may be a beam of radiation, or an electrical current passed through the thermistor bead. Measurements of this type have been described by Ballard (1961) and Hampel et al (1959)

This simpler method was the one used in this work. However it should be pointed out that the method is not exactly equivalent to the use of a step change in air temperature. This is because the initial and final temperature distributions in the lead wires are not the same in each case. It will be shown theoretically in Appendix 4 that for the simple "post" type of thermistor mount, which is the one with which this work is principally concerned, the error is small for the particular thermistors tested. On the other hand this method

may give quite erroneous results if used with thermistors mounted in a more complicated manner, for example the "foil" mounts now being used by some rocket network ranges.

7.3 Experimental Method

The time constants were measured with the thermistors mounted in the small sub-enclosure as for the radiation tests described in Chapter 3. When the source of heat was to be radiation this was controlled by a camera shutter situated under the window in the pump plate. For the electrical methods, the response to heating was observed by balancing the bridge circuit (section 3.3(a)) with a suitably high measuring current, switching off for a short time, and then recording the thermistor warm-up when the current was switched on. To observe the cooling part of the response, a separate heating unit was built, the circuit of which is shown in Fig.45. While the heating current was being applied to the thermistor a dummy resistance load was connected across the measuring circuit to keep the Sanborne recorder on scale. On throwing a DPDT switch the thermistor was disconnected from the heating circuit and substituted for the dummy load across the measuring circuit. A measuring current which was much smaller than the heating current, was used.

The response of the thermistor during these tests was recorded with the Sanborne recorder, using a suitable chart speed. Time marks placed automatically on the record at 1 sec intervals allowed calibration of the time-scale.

For the thermistors used it was soon found that all four variations of the method gave the same results within the limits of accuracy of about 5% obtainable. Since the latter variation described involved the simplest testing procedure the great majority of the measurements were made this way.

To evaluate the time constants from the recorder records the following procedure was adopted. A suitable time-scale division of the recorder chart as near as possible after the actual start of the cooling/heating curve was selected as $t = 0$. The ordinate of the curve, C_0 at $t = 0$ was noted, along with the ordinate C_∞ of the final steady value. The quantity $\frac{C_0 - C_\infty}{e}$ was computed and this either added or subtracted from C_∞ to find the ordinate corresponding to $t = \tau$. τ was then given by the time at which this ordinate was achieved on the cooling/heating curve (bearing in mind the calibration of the recorder time scale).

The recorder divisions were proportional to the thermistor resistance rather than to temperature, in terms of

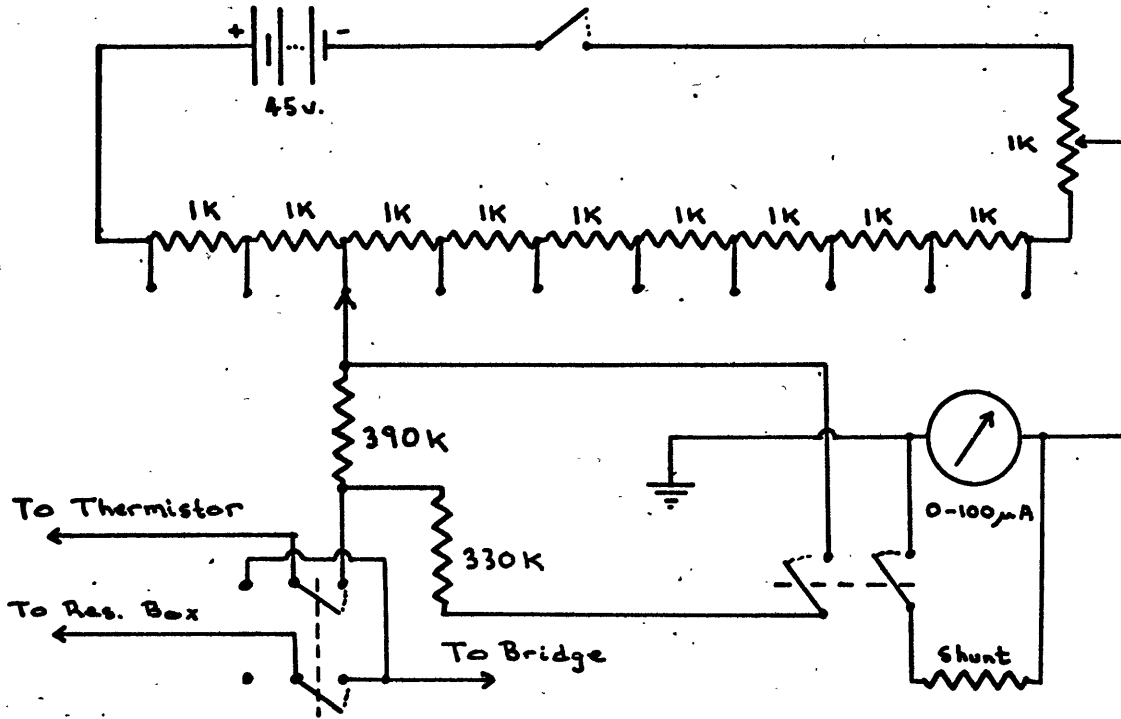


FIG 45. HEATING UNIT FOR TIME CONSTANT TESTS.

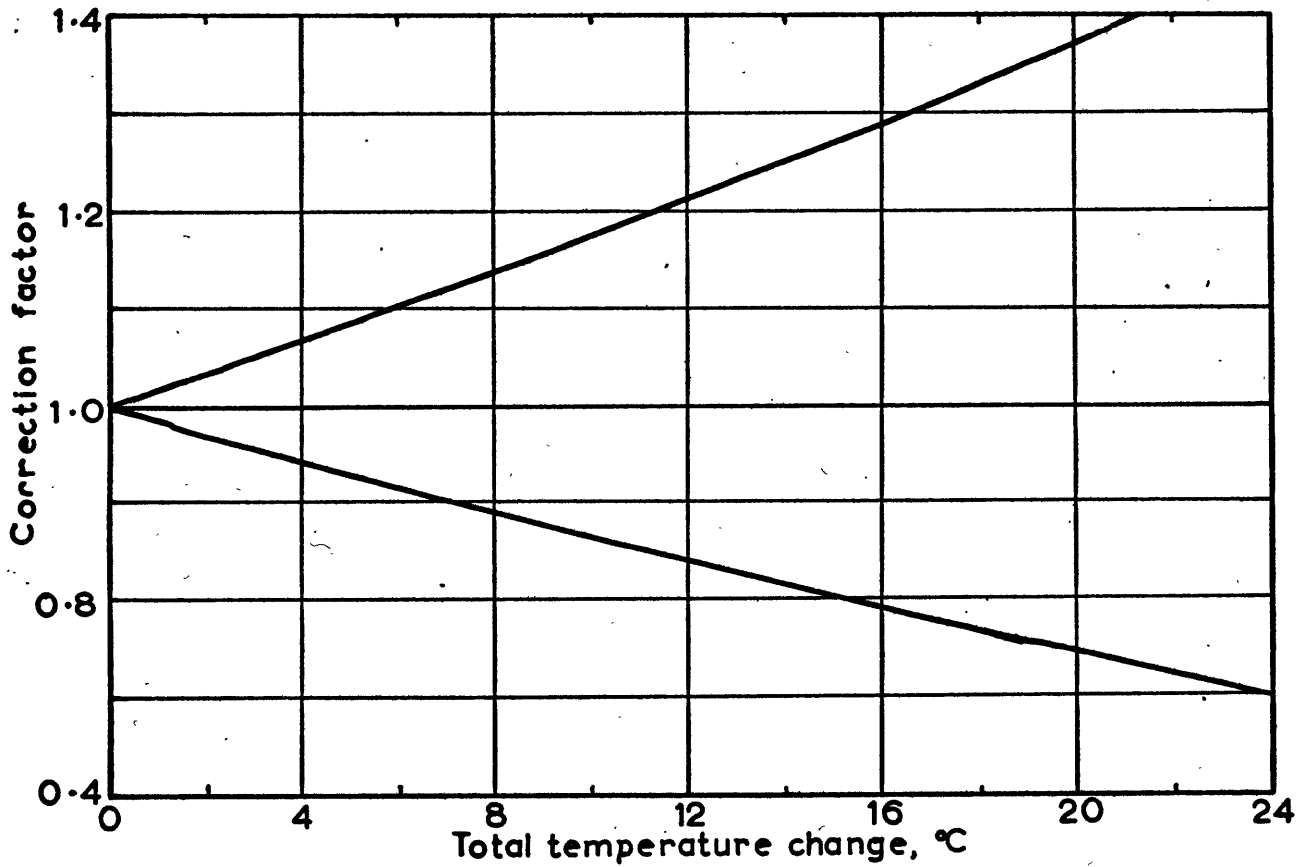


FIG 46, CORRECTION TO τ FOR NONLINEARITY OF R-T CURVE.

which τ is defined. Since the resistance/temperature characteristic of thermistors is highly non-linear the above procedure can lead to significant errors for temperature changes greater than one or two degrees. To take this into account a correction factor was computed as a function of the total temperature change which, when multiplied by the apparent time constant as determined above gave the correct value of τ appropriate to an exponential temperature response. Fig.46 shows this correction for typical thermistor material. Notice that the correction factor is greater than one for heating curves and less than one for cooling curves, and that the error is 5% for a temperature change of 3°C.

All results given below have been corrected in this manner. In the majority of cases the actual temperature change used in the tests was 3 - 5°C.

7.4 Results

Fig.47 is an example from a recorder chart showing a Veco 5 mil bead thermistor cooling after having been heated electrically. This same cooling curve is shown re-plotted on a semi-logarithmic scale in Fig.48.

Fig.49 shows the measured time constants of four

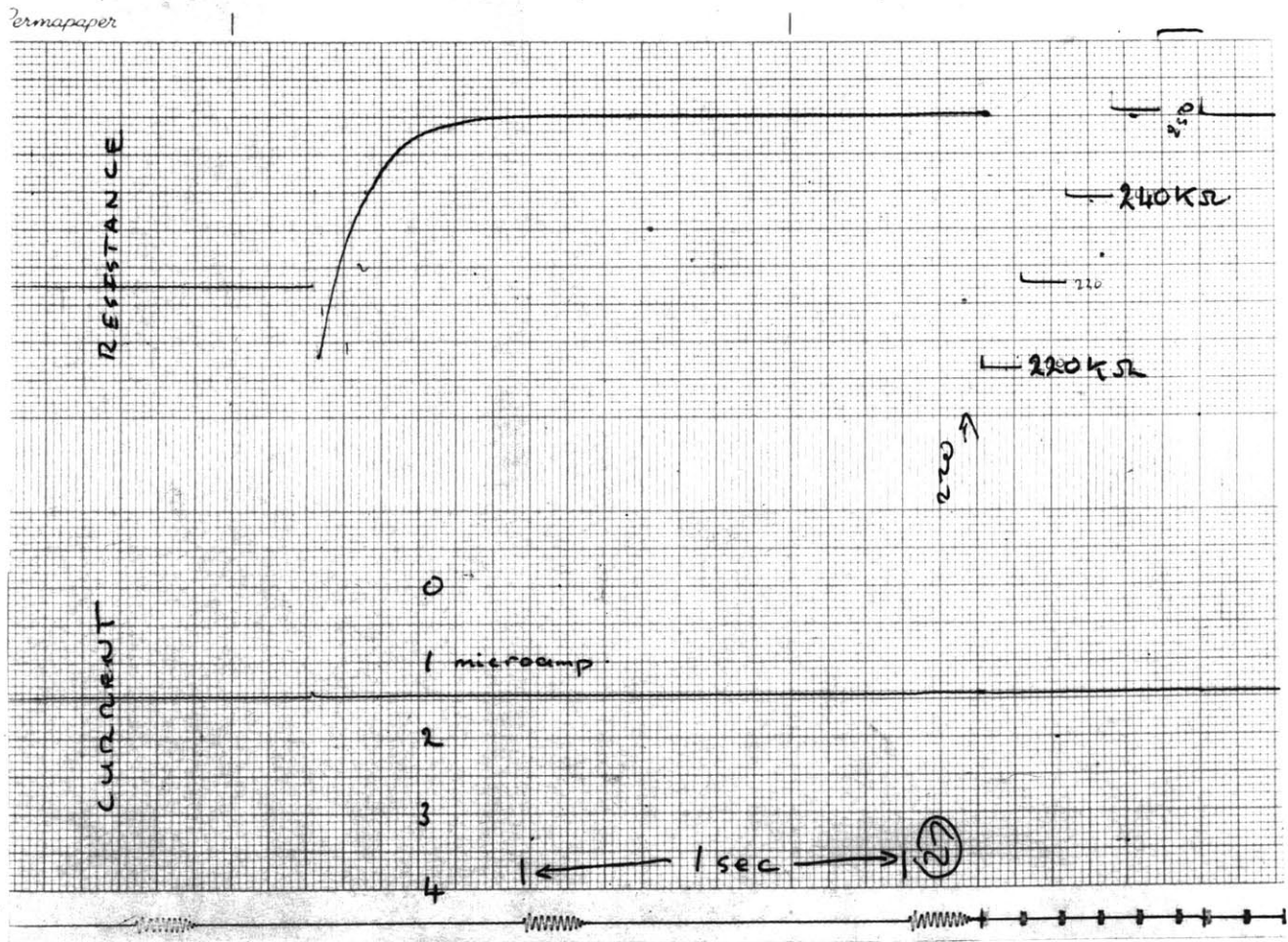


Fig 47. Recorder Chart Showing Response of 5 mil Thermistor in Time Constant Tests

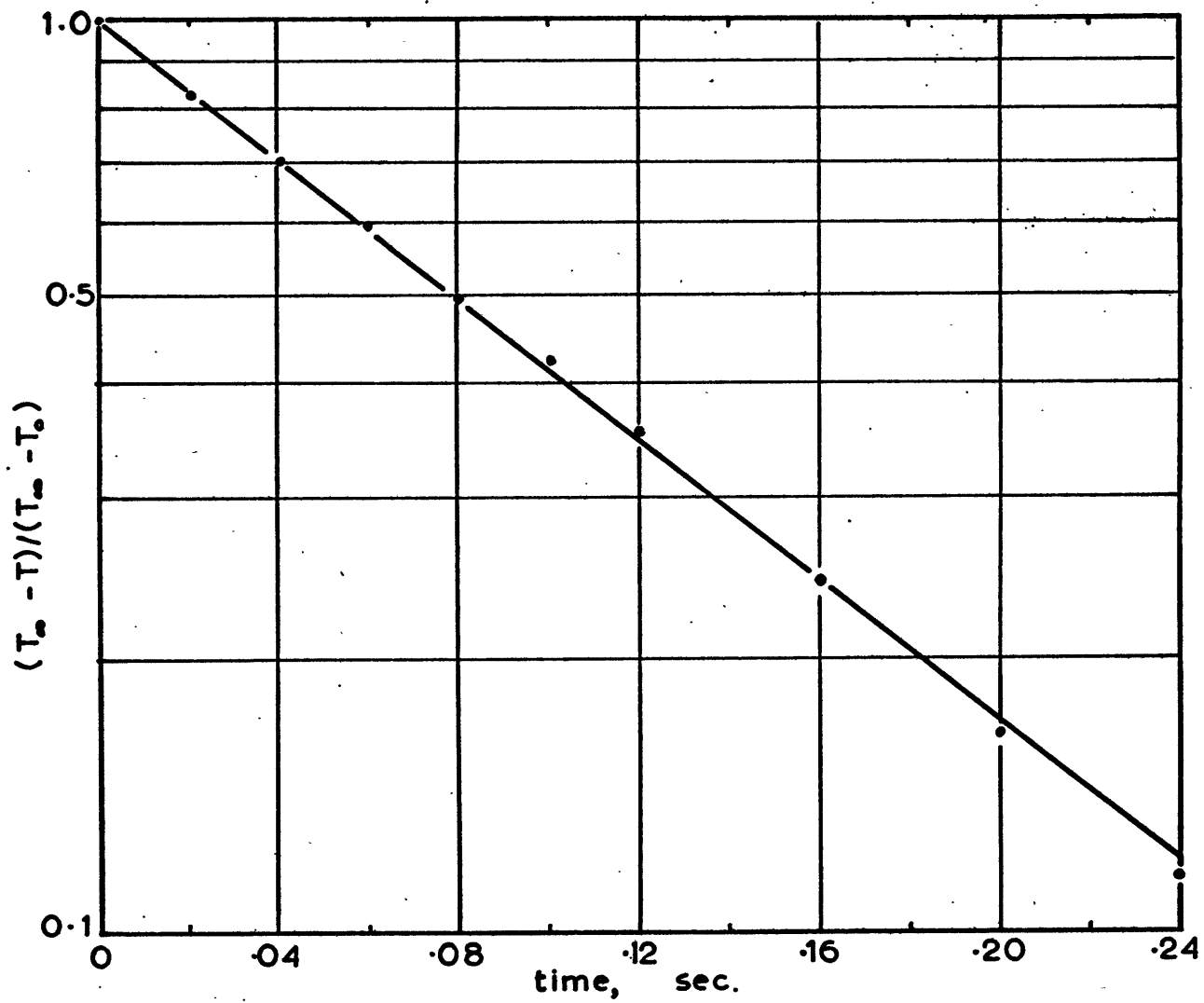


FIG 48. SEMI-LOG PLOT OF CURVE IN FIG 47.

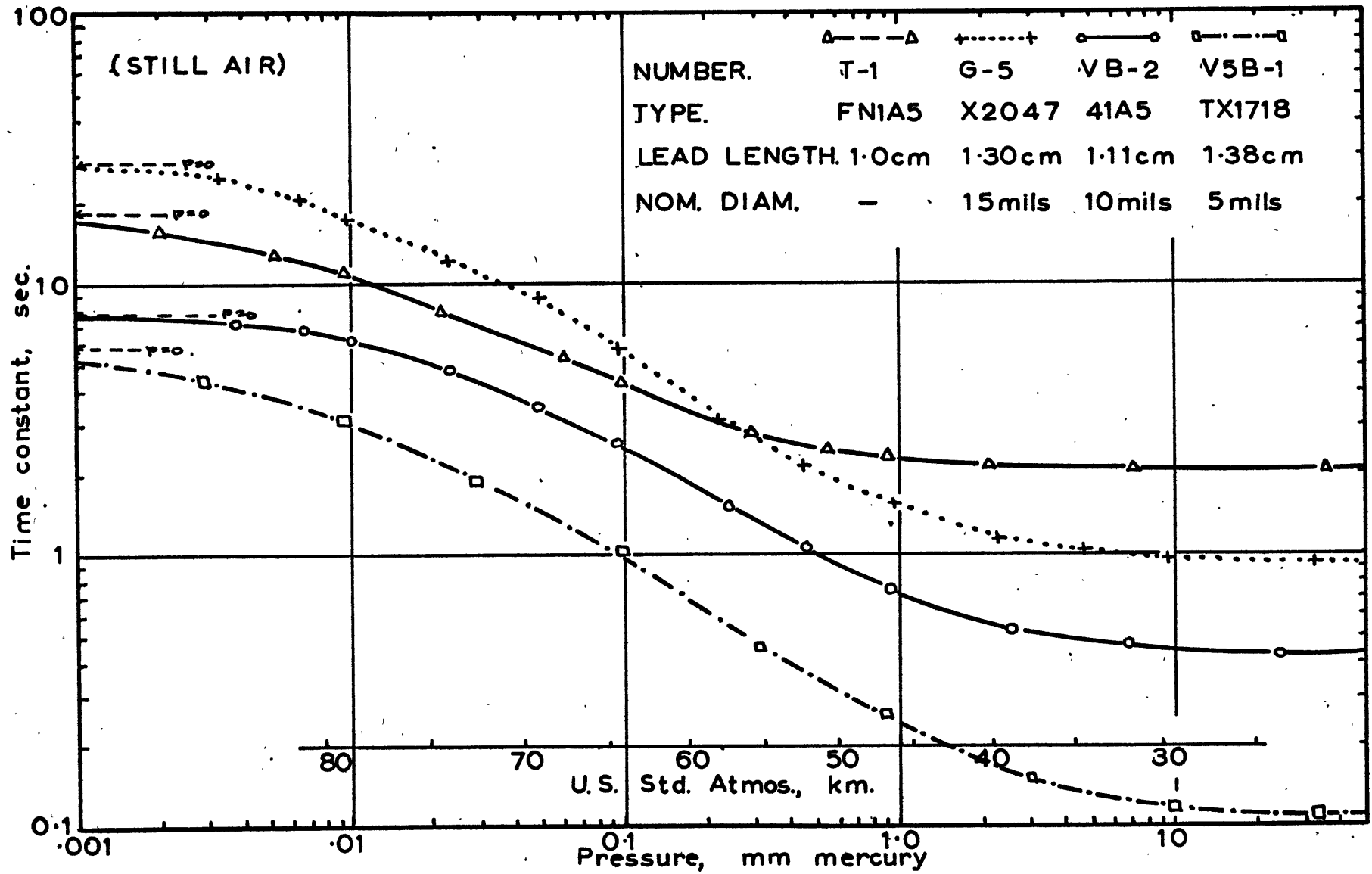


FIG 49, MEASURED TIME CONSTANTS OF THERMISTORS.

thermistors, including a thinistor, as a function of pressure. These values apply of course to still air (no ventilation) conditions. The effect of ventilation will be discussed in Chapter 8, but we shall remark here that it is large for pressures higher than 20 mm mercury and minor for pressures lower than about 2 mm mercury. The very much faster response of the small bead thermistors is clearly shown, although as in the case of the radiation error, the relative advantage decreases at lower pressures.

At very low pressures all of the thermistors show a levelling off, due to the predominance of heat conduction through the lead wires and long-wave radiation loss to the enclosure walls over the heat loss to the air. The pressure at which this levelling off takes place depends mostly on the length of the lead wires. If the latter are too short the time constant is decreased, but only at the expense of greatly increased conduction error (Chapter 5). As a general rule, if the time constant is influenced significantly by conduction to the supports then the conduction error will almost certainly be prohibitive. The effect of varying lead length is illustrated more clearly in Fig.50, which shows the time constant for the same Gulton X2047 thermistor when measurements were carried out with different lead lengths.

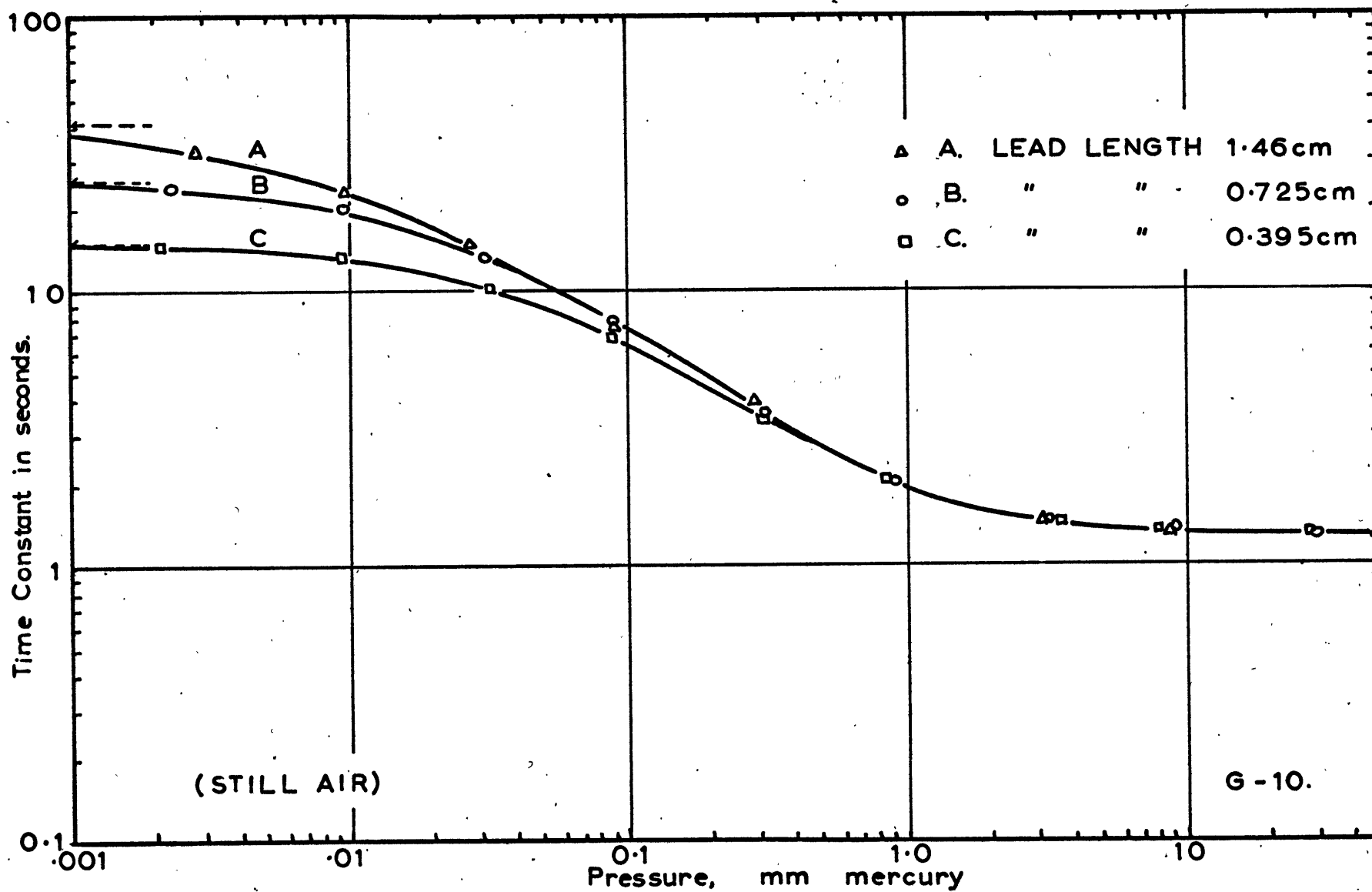


FIG 50, MEASURED TIME CONSTANTS WITH DIFFERENT LEAD LENGTHS.

For the simple system described by equation (7.1.1) we can identify γ with the dissipation rate K . It is seen that for such a system the product $K\tau$ should be constant and equal to the heat capacity C . That this is not the case with the miniature bead thermistors is readily verified by reference to Figs. 49 and 38. For example, at 760 mm mercury $K\tau$ for the 5 mil bead thermistor is 4.7×10^{-6} joule $^{\circ}\text{C}^{-1}$ and this value increases with decreasing pressure to a limiting value of 10.8×10^{-6} joule $^{\circ}\text{C}^{-1}$ under vacuum. This result would suggest that heat capacity of the lead wires plays an important part in determining the dynamic response. A similar trend is present in $K\tau$ with the larger thermistors, but not so marked. This is to be expected, for the heat capacity of the lead wires is then smaller compared to that of the beads.

It is of interest to compare the effective heat capacity of a typical bead thermistor computed from the product $K\tau$ with estimates of C from published data. At 1.0 mm mercury $K\tau$ for the 15 mil thermistor G-5 is 5.3×10^{-5} watt $^{\circ}\text{C}^{-1} \times 1.5$ sec = 8.0×10^{-5} joule $^{\circ}\text{C}^{-1}$. According to estimates given in the Wright Instrument Company report (1961), the mean specific heat of a thermistor bead is about 0.5 joule $\text{gm}^{-1} ^{\circ}\text{C}^{-1}$ and the mean

density 3.9 gm cm^{-3} . Taking the measured volume of G-5 as $3.8 \times 10^{-5} \text{ cm}^3$, the heat capacity estimated in this way is $7.4 \times 10^{-5} \text{ joule } ^\circ\text{C}^{-1}$. The agreement is very good especially when one considers the heterogeneous composition of a thermistor bead. For the 5 mil thermistor the heat capacity estimated from the Wright data is $3.4 \times 10^{-6} \text{ joule } ^\circ\text{C}^{-1}$. This agrees with $K\tau$ at sea level pressure, but at lower pressures the effect of the lead wires is evidently important.

Measured time constants as a function of pressure are given for further thermistors in Appendix 2. It will be noticed that there is considerable variability even between beads of the same nominal size. Table 7 shows the measured time constants of Gulton 15 mil thermistors in still air at MSL pressure. Since the time constants at other pressures are approximately proportional a similar variability would apply to all altitudes.

TABLE 7. Time Constants of Gulton 15 mil Thermistors at MSL.

Number	G-1	G-2	G-3	G-4	G-5	G-6	G-7	G-8	G-10	G-12
τ , sec	1.2	1.4	0.9	0.6	0.9	1.0	0.6	0.5	1.3	0.9
Vol, 10^{-5} cm^3	-	6.0	3.4	2.3	3.8	3.7	2.0	1.6	-	-

CHAPTER 8

THE EFFECTS OF MOTION THROUGH THE AIR

8.1 Introduction

In the majority of applications of thermistors to the measurement of atmospheric temperatures there is some relative motion of the air with respect to the thermistor. In the case of a rocketsonde this results from the dropsonde's fall through the atmosphere.

The tests described in the preceding chapters have all been carried out in still air. This was because the experimental techniques and the equipment required were very considerably simplified. We shall see also that apart from aerodynamic heating the effect of ventilation at ordinary speeds on the miniature thermistors is small at 100,000 ft and negligible above 150,000 ft altitude. Therefore the results of these tests are directly applicable in the upper part of rocket soundings where the errors are greatest. Provided the thermistors are properly exposed, the results are of course applicable to floating balloons at all altitudes.

Below 100,000 ft altitude the relative motion of the air has considerable effect on the convective heat transfer, such that in all cases the errors described above are less

than the values applicable to still air. Because the rocket sounding do extend down into this region, and because there are so many other applications of thermistors in which lower altitudes are of interest it was felt that the usefulness of this work would be greatly enhanced by a study of this topic.

8.2 Discussion of the Experimental Technique

The method used to simulate the motion of the thermistor through the air was to place the thermistor at the end of an arm which rotated inside the vacuum bell jar. Such a method has been used previously by Sion (1955) in the study of the time constants of radiosonde rod thermistors. Hampel et al (1959) also used the method to study the effect on the time constant of a 10 mil bead thermistor at pressures down to about 1 mm mercury, but their report does not show the variation explicitly, only at particular combinations of ventilation speed and pressure.

Devienne (1957,1958) has used the revolving arm technique in studies of heat transfer in rarified gases. His later report contains a discussion of the advantages of the technique over other methods, as well as some of the disadvantages. This paper was found very useful in the design of the apparatus.

One of the more obvious questions concerning the revolving arm method is whether the air in the bell jar is appreciably driven around by the arm. Devienne has carried out very careful measurements and concludes that there is no drive of the air at pressures of 2 mm mercury and lower. At atmospheric pressure there is some drive, but not much with a properly designed arm. Sion estimated less than 2.2% of the arm speed for his experiments. In the experiments to be described below, the drive was measured at 4% at sea level pressure.

For high arm speeds there is a certain amount of heating of the air near the arm, especially at high pressures. Devienne concludes that so long as any temperature changes are measured with respect to this higher ambient temperature, heat transfer measurements taken with the arm are valid at all pressures.

It was not of course possible to measure the response of the thermistors to radiation while they were being rotated. However it was possible to measure the dissipation rate K , and from this obtain a good estimate of the radiation error in terms of the still air measurements. We recall that the temperature rise under radiation is given by equation (3.1.9)

$$\theta_2 = \frac{\frac{4 \epsilon_{sw} Jr}{p} + J \epsilon_{st} A_T'}{K}$$

where $p = \sqrt{\frac{2h_w}{kr}}$ and $K = 2ka_w p + h_T A_T$.

For pressures sufficiently high so that the effect of ventilation is important, the term $\frac{4 \epsilon_{sw} Jr}{p}$ is 1/2 to 1/5 of $J \epsilon_{st} A_T'$ for typical small bead thermistors when $\epsilon_{sw} \approx \epsilon_{st}$. It follows that to a first approximation the radiation error is inversely proportional to K . Therefore

$$\theta_2(v) \doteq \theta_2(v=0) \times \frac{K(v=0)}{K(v)} \quad (8.2.1)$$

The relation (8.2.1) will in any case give an upper limit for the radiation error, because p increases with increasing ventilation velocity v .

Similar considerations apply for the long-wave radiation errors. The measuring current error is of course given directly by K . It is assumed that the lead lengths are sufficient to eliminate the conduction error, for at pressures above about 10 mm mercury where ventilation effects are important only a few millimeters of 1 mil platinum-iridium alloy wire are required even in still air.

8.3 Description of Apparatus and Procedure

(a) General Requirements

A schematic drawing of the rotating arm device is shown in Fig.51. The fall rate of a rocketsonde is very considerable at the highest altitudes because of the very low drag afforded the parachute. In a typical sounding speeds as high as 400 miles per hour may be reached, which result in considerable aerodynamic heating errors in the temperature measurement. For this reason it was desired to have the arm capable of achieving enough speed to allow measurement of the thermal recovery factors of the thermistors. (These measurements will be described in Chapter 9). In practice this meant a minimum simulated speed of about 120 mph and preferably 200 mph or faster. To achieve such speeds with an arm radius of 6 inches, as dictated by the 15 inch bell jar, a rotation rate of at least 3500 rpm and preferably 6000 rpm was required.

(b) Construction of Rotating Arm Unit

Since it was not desirable to have a variable speed electric motor within the vacuum chamber a rotary-motion vacuum seal was required. A feed-through capable of this speed was feasible, but being a special item, would have been costly.

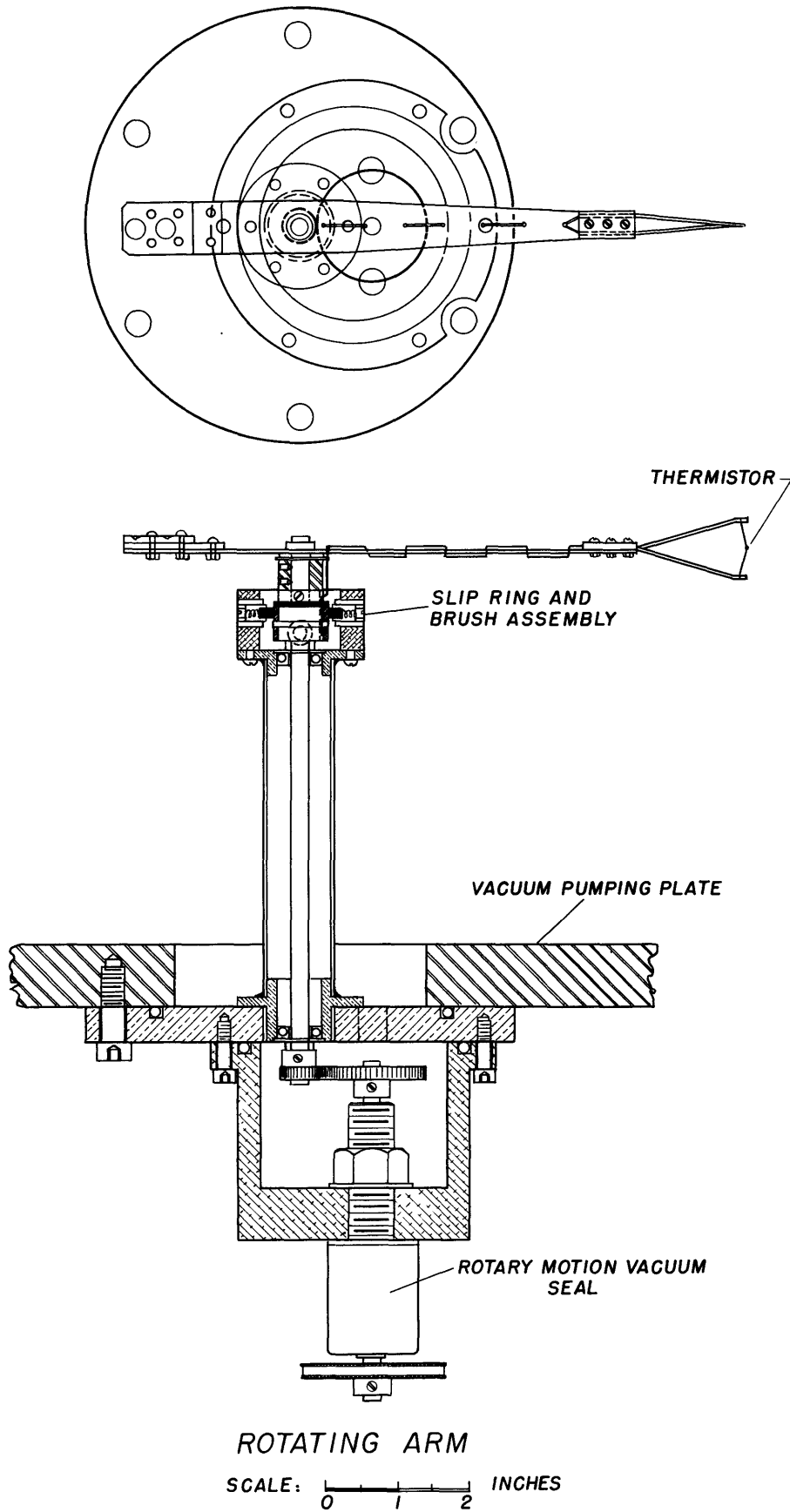


FIG.51.

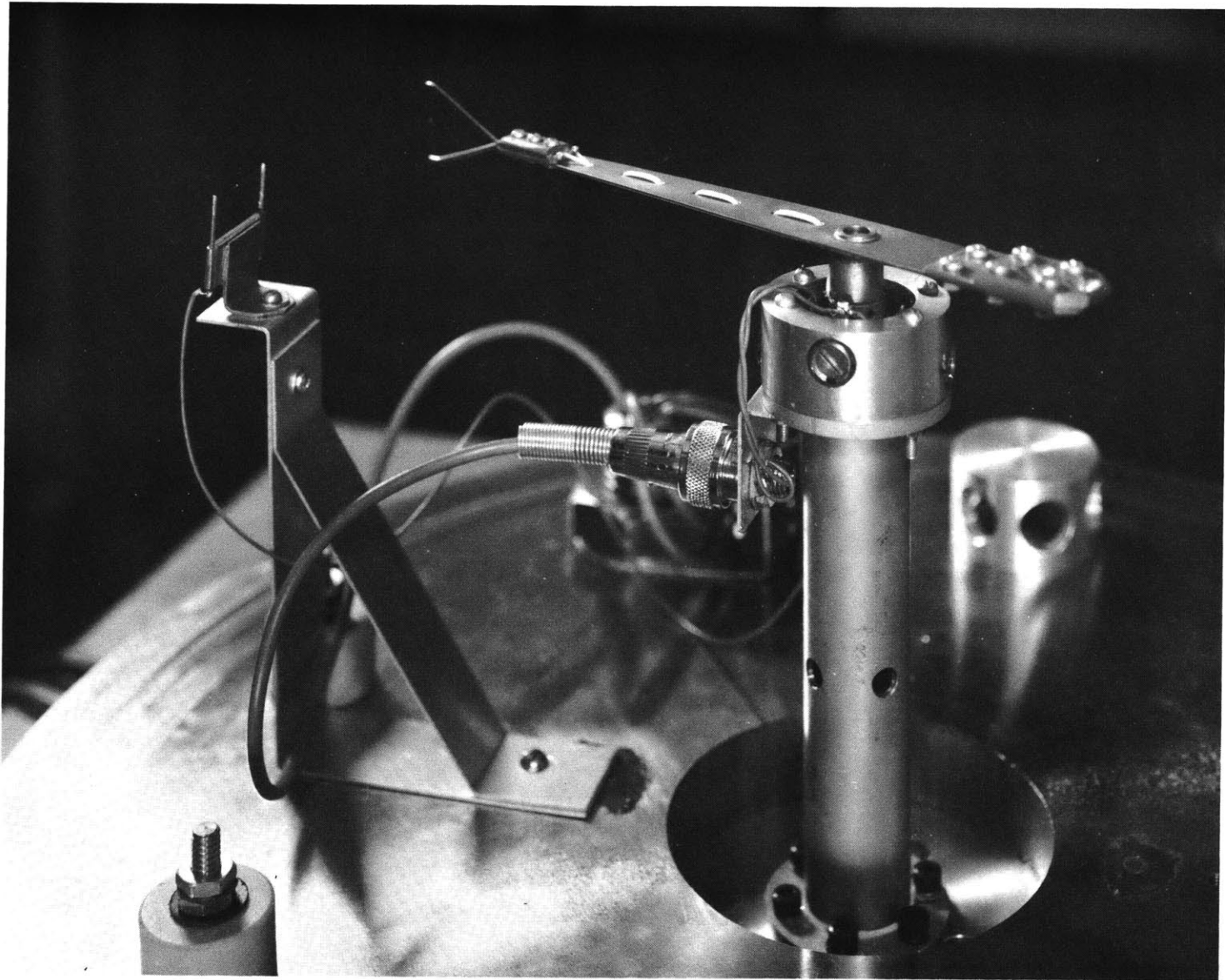


FIG.52. Rotating Arm.

A small ball-bearing rotary motion feed-through capable of speeds up to 3000rpm was available as a stock item from the National Research Corporation, so it was decided to use one of these in conjunction with a 3:1 step-up gear drive inside the vacuum system.

Some care had to be taken in the design and construction of the unit to obtain safe, smooth operation at the highest speeds desired. At speeds of 6000 rpm centrifugal accelerations approaching 10,000 G were developed at the end of the arm and the thermistor mount had to be able to stand this with a suitable safety margin. The arm was made of 0.036 inch stainless steel. The thermistor was mounted between two extending rods of 0.050 inch diameter stainless steel wire which were clamped to the main part of the arm with a grooved steel clamp. These rods passed through fiberglass sleeves at the position of the clamp to provide electrical insulation. Before tightening the clamp down, the sleeves were liberally soaked in epoxy bonding material.

The arm was attached to a length of $\frac{1}{4}$ inch precision steel shafting which ran in two high-speed precision ball-bearings. This shaft was driven from the rotary feed-through via two P.I.C. precision spur gears.

It was extremely important to have the arm perfectly

balanced. This was done by removing the arm from the unit and temporarily mounting it on a 3 inch length of shafting, which was then held horizontally on two precision ball-bearings of very low friction. Balancing within one or two milligrams was achieved by removing material from a small pocket of lead let into the brass counterweight on the arm. Because of their very small mass it was not necessary to make any adjustments when different thermistors were mounted on the arm.

Two copper slip-rings were mounted on the shaft just below the arm for the electrical connection to the thermistors. Contacts to these were made by carbon brushes, two to each slip-ring connected in parallel to minimize any possibility of erratic behaviour.

The entire unit was bolted on to the pump plate in the position previously occupied by the unit containing the window for the radiation tests. O-ring seals with the correct gland dimensions for high vacuum use were included between the aluminum gearbox and the mounting flange, and between the mounting flange and the pump plate.

Power was supplied by a $\frac{1}{8}$ H.P. "Bodine" shunt-wound D.C. motor operated by a "Heller" S-12 speed controller. The motor was bolted to one end of the Dexion trolley and

power was transmitted to the arm unit by means of a P.I.C. "no-slip" drive belt and P.I.C. toothed pulleys. A selection of the latter were available, allowing ratios of 1:1, 1:2 and 22:64 between the motor and the arm unit,

(c) Measurement of Rotation Speed

The rotation speed of the arm was calibrated against the speed controller dial setting for each of the three pulley combinations, by measuring the former with a General Radio "Strobotac". After an initial break-in period these calibrations (which were frequently checked) remained stable. It was found much more convenient to carry out subsequent tests at pre-determined controller settings rather than to actually measure the speed of rotation for each individual test. When the 1:1 pulley was used the calibration at the higher speeds depended noticeably on the pressure in the bell-jar, showing that the speed regulation provided by the controller was not perfect.

(d) Allowance for "Drive" of the Air

To determine the amount of "drive" of the air within the bell jar, the sensing unit of a Hastings air meter was temporarily mounted through one of the accessory holes in the pump plate, with the head as close as possible to the

path of the thermistor. The output of the air meter was determined as a function of the rotation speed of the arm. Fig.53 shows the results of this test, which was only possible at atmospheric pressure.

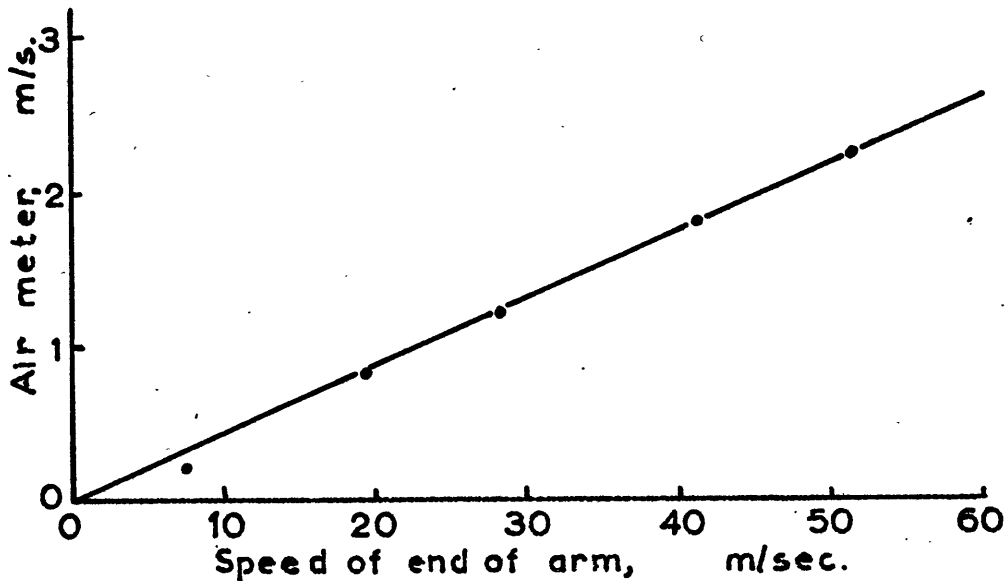


FIG.53. Drive of Air in Bell Jar, MSL Pressure

It is seen that the "drive" was 4% at sea level pressure. It was expected on the basis of Devienne's results that there would be no drive at very low pressures. Therefore, in constructing the final calibration curves of thermistor airspeed vs controller settings the "drive correction" of 4% at MSL pressure was arbitrarily decreased in direct proportion to the pressure. Fig.54 shows typical calibration curves for the three pulley ratios used.

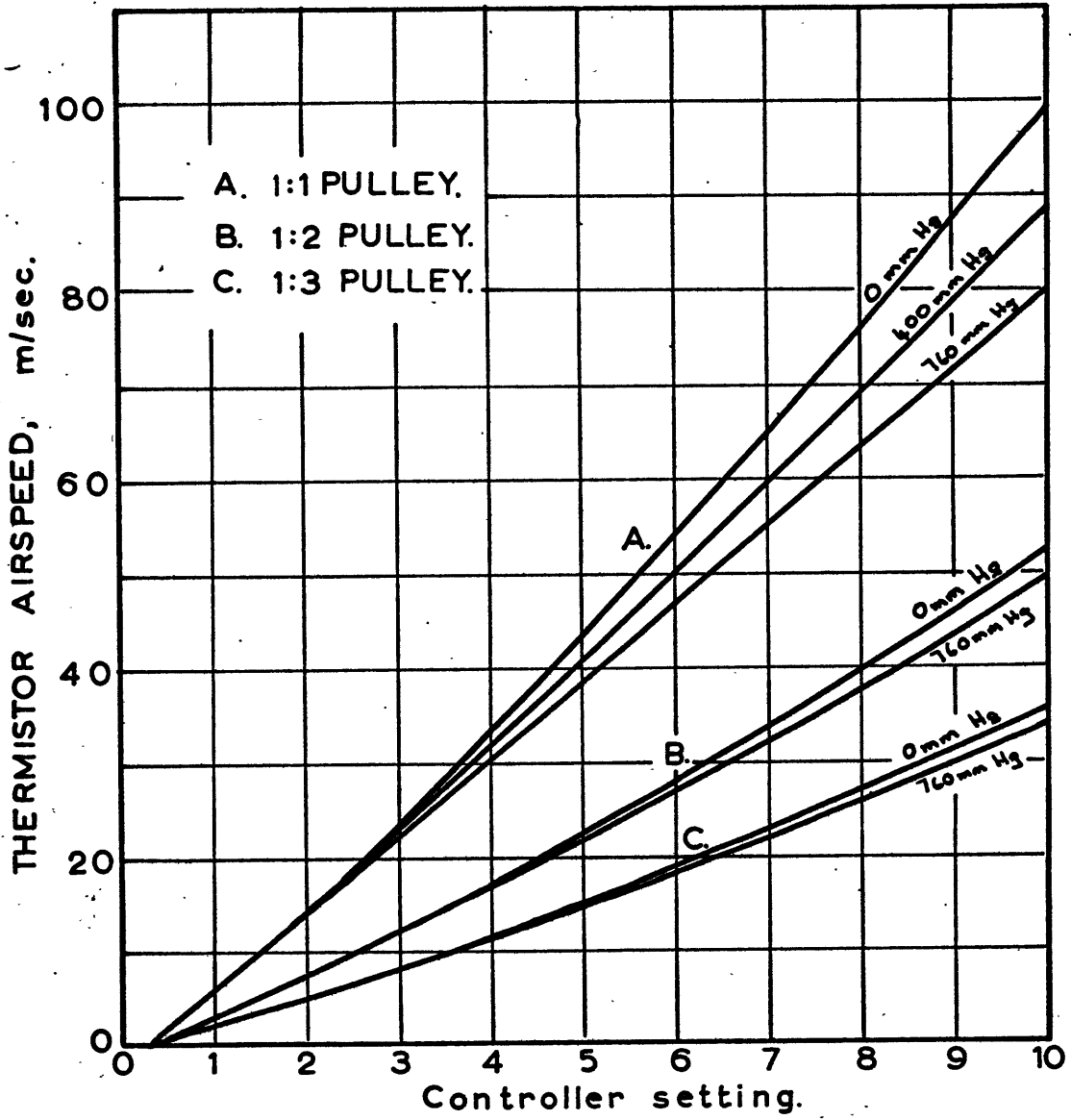


FIG 54, SPEED CONTROLLER CALIBRATION.

(e) Test Procedure

Two sets of measurements were made at various pressures and rotation speeds. These were the dissipation rate K and the time constant τ . The method of measurement of these quantities was exactly the same as that used for the still air tests already described, the electrical method being used for τ .

8.4 Results

Measurements of the time constant and the dissipation rate of 5, 10 and 15 mil (nominal) bead thermistors and a thinistor as a function of pressure and air speed are presented in Figs.55-58. The lead length used in all cases was 1.0 cm each lead wire.

The lack of dependence of these quantities on the ventilation speed at low pressures is clearly seen. Near sea level pressure, however, the ventilation speed had considerable influence.

Two sets of measurements were made with the thinistor, one with the plate perpendicular to the air flow and the other with the plate parallel to the flow. However centrifugal and aerodynamic forces caused deviations of up to about 20° from these orientations when the arm was rotating, and this

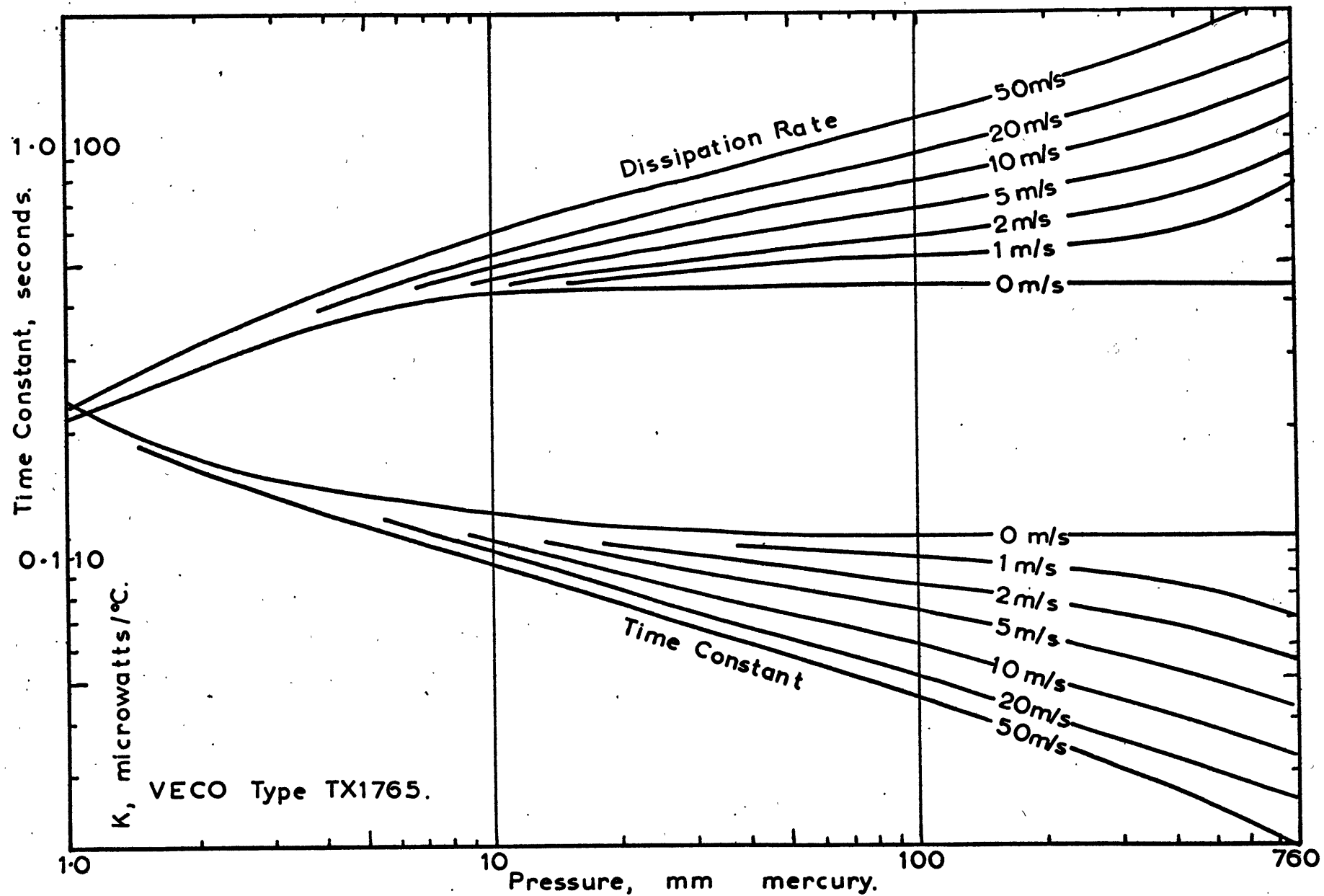


FIG 55, TIME CONSTANT AND DISSIPATION RATE, 5mil THERMISTOR.

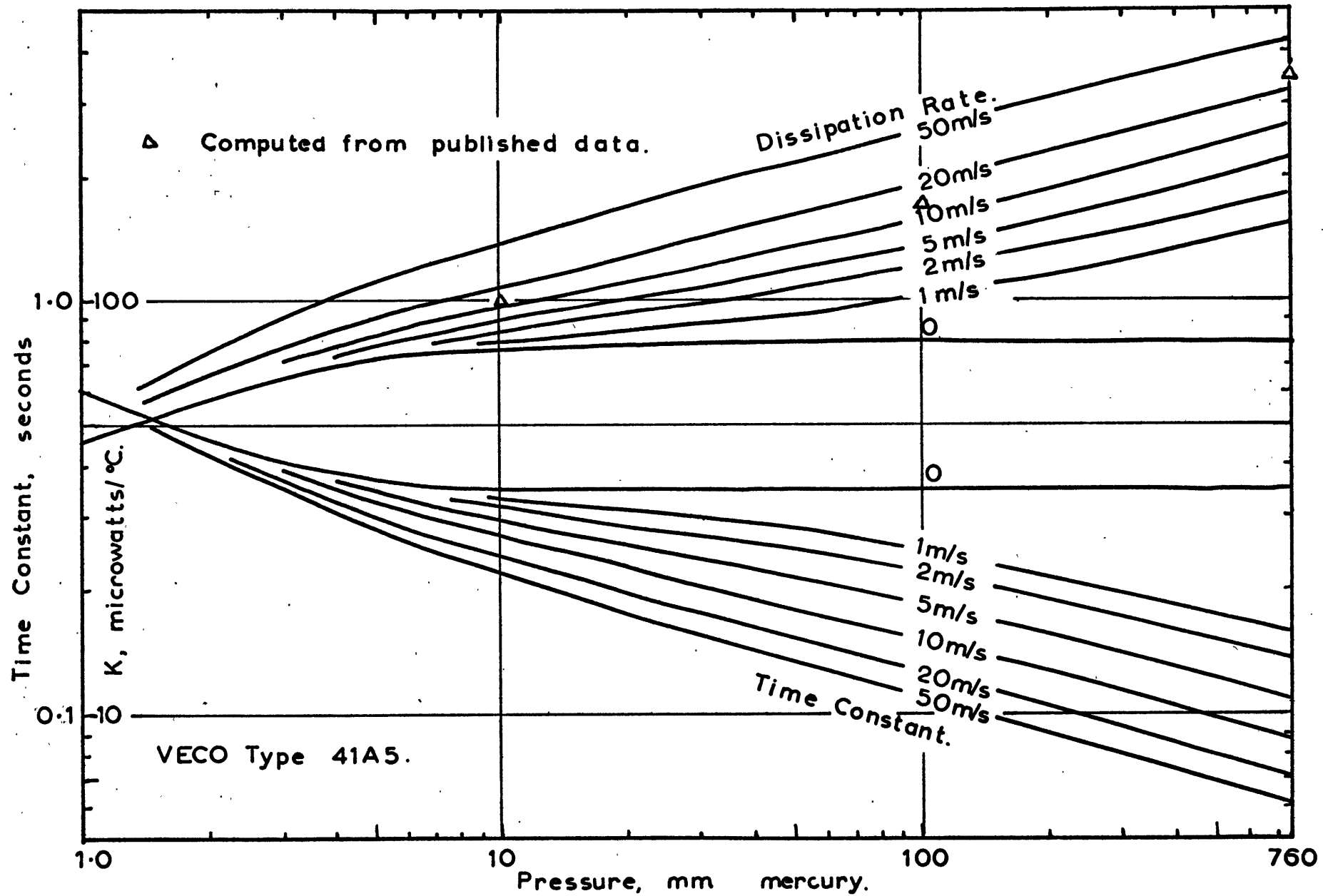


FIG. 56. TIME CONSTANT AND DISSIPATION RATE, 10mil THERMISTOR.

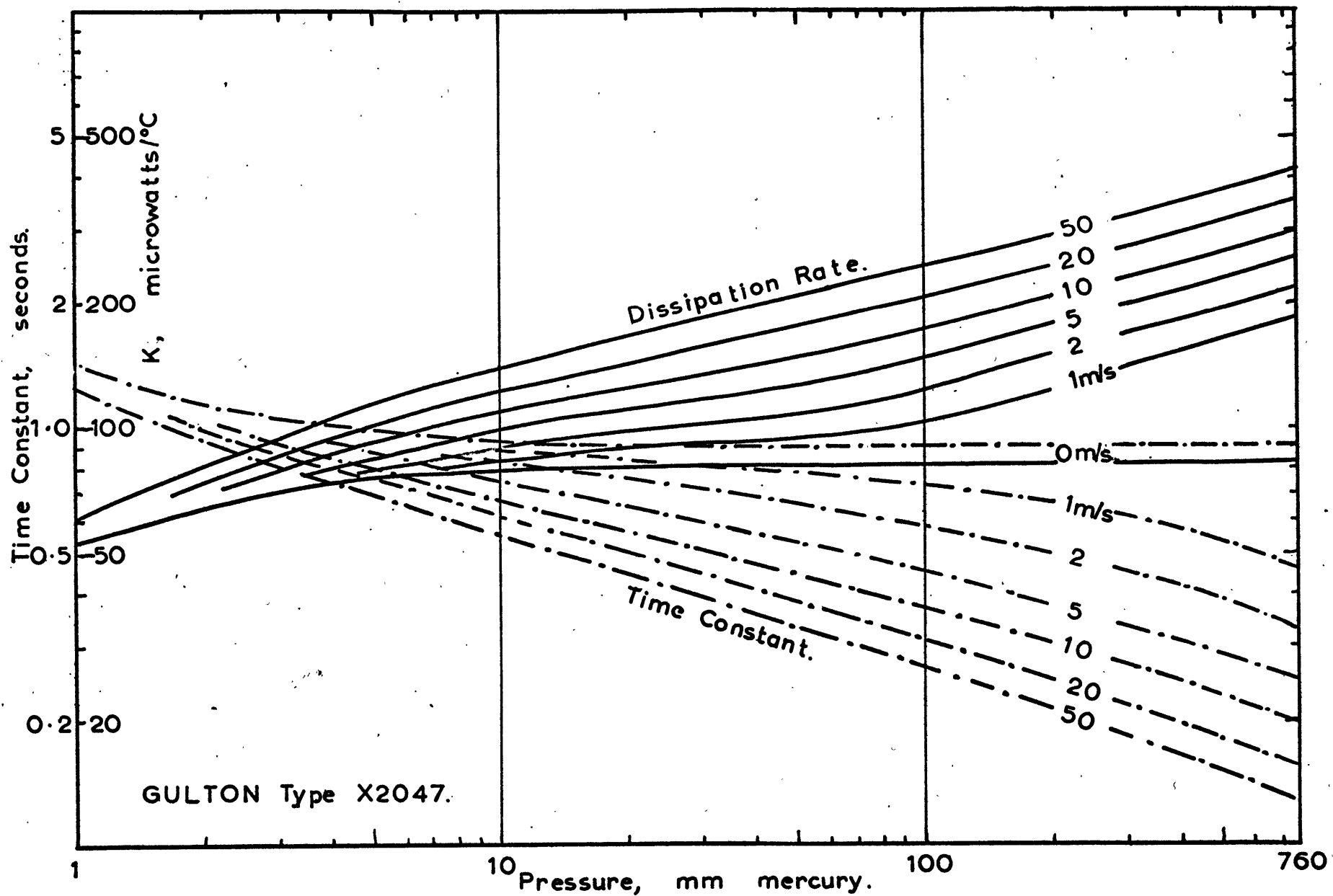


FIG. 57. TIME CONSTANT AND DISSIPATION RATE, 15mil THERMISTOR.

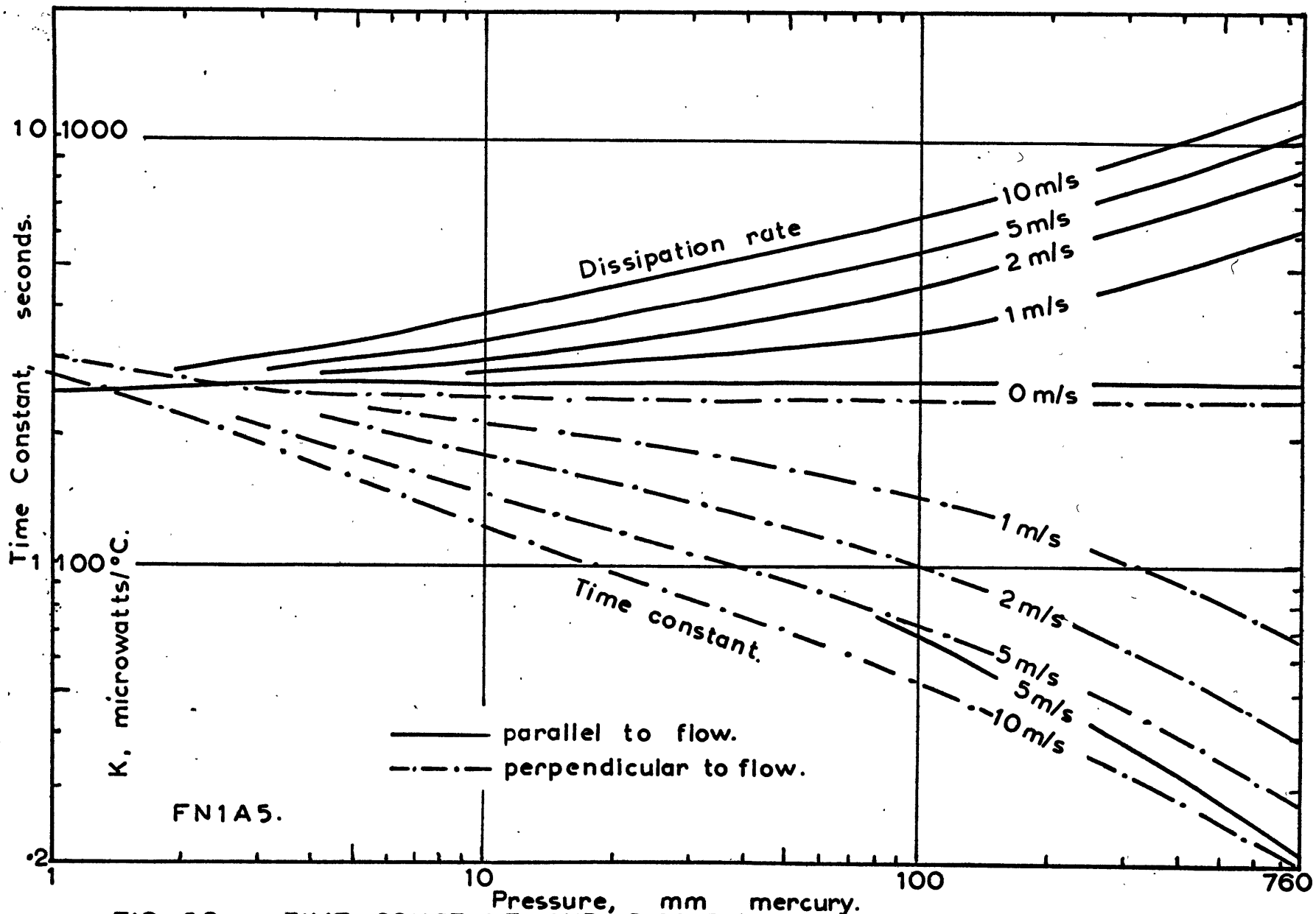


FIG 58, TIME CONSTANT AND DISSIPATION RATE OF THINISTOR.

may account to some extent for the fact that the results were not greatly different. This distortion of the orientation was readily observed with the "Strobotac".

The curves of K and τ vs pressure for still air conditions given in other parts of this work may be extended to take into account the effect of ventilation speed by using Figs.55-58 and the assumption that K or τ at a given speed and pressure are proportional to the corresponding values in still air. This assumption should give adequate results so long as the Figure appropriate to the nominal size of the thermistor in question is used.

Fig.59 shows the variation of K with airspeed at different pressures for the 10 mil bead thermistor. In this figure $K(v) - K(v=0)$ has been plotted against the airspeed using logarithmic scales, and it is seen that consistent with the accuracy of the data and the relatively small number of points at each pressure, relations of the form $K(v) - K(v=0) = Av^m$ hold, with $m \approx 0.4$ at sea level pressure. This is the type of relation found valid for heat transfer from fine wires as used in hot-wire anemometry. Thus, for example, Collis and Williams (1959) give a formula of the type

$$Nu = A + B.Re^m$$

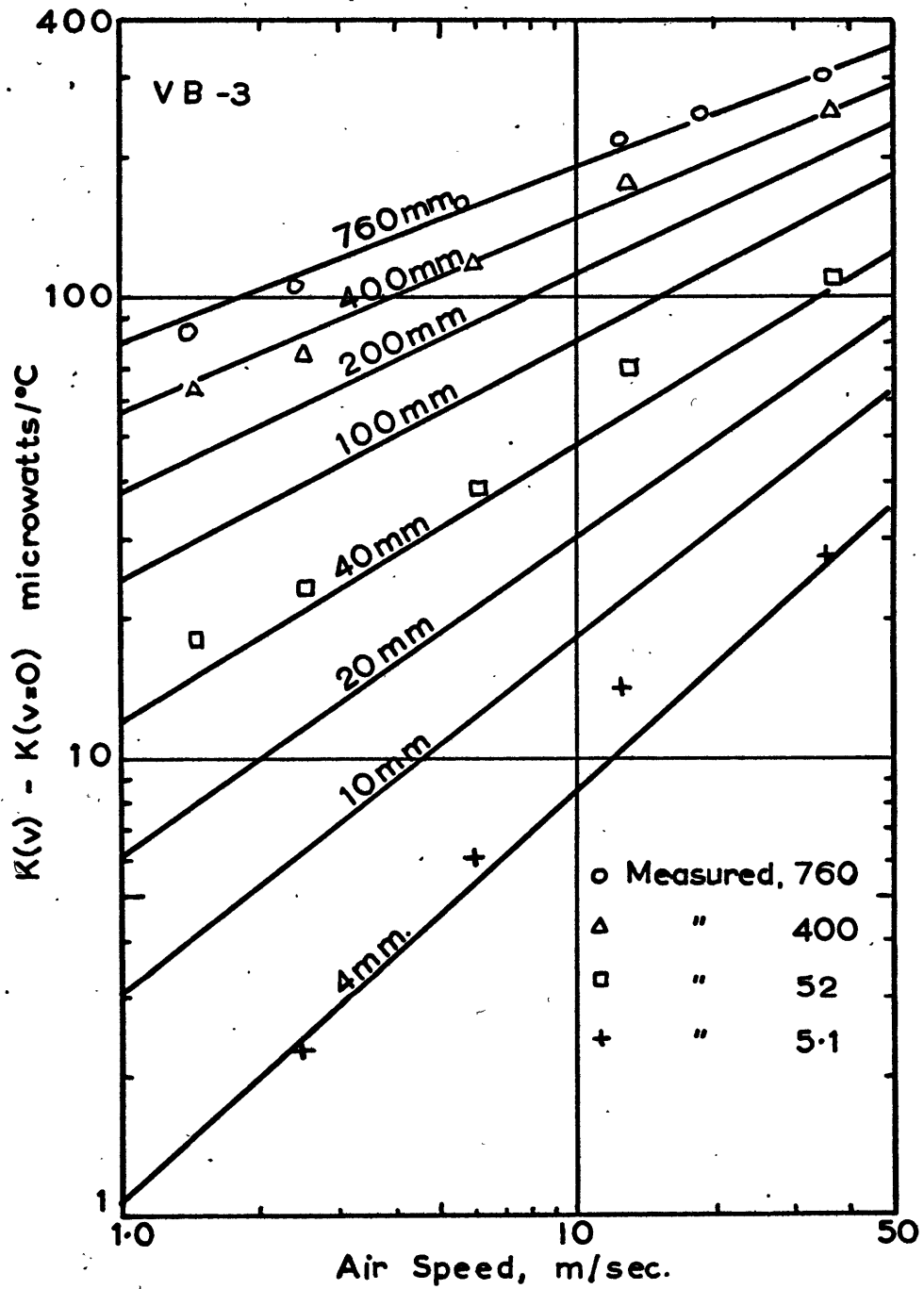


FIG 59. EFFECT OF AIRSPEED ON DISSIPATION RATE.

where in their case $m \approx 0.45$.

There are apparently no other published data of the type presented above for thermistors available for comparison. Some information was available, however, on the heat transfer from spheres and fine wires under these conditions and it was possible to reconstruct K from this. Fig.56 includes a few points computed in this way, using the results of Kavanaugh (1955) for spheres in computing the contribution $h_T A_T$ of the thermistor bead, and the results of Baldwin et al (1959) for the contribution $2ka_w p$ of the 1 mil lead wires. The thermistor bead was assumed to have the same area, $3.0 \times 10^{-3} \text{ cm}^2$, as VB-3, but the smallest diameter ($2.5 \times 10^{-2} \text{ cm}$) of the non-spherical bead was used in the expression for the Nusselt and Reynolds numbers which appeared in the computations.

The agreement between measured and computed results is only approximate but satisfactory considering the departure of the bead from sphericity and the possibility of local effects where the lead wires join the bead.

CHAPTER 9

AERODYNAMIC HEATING ERRORS

9.1 Introduction

As mentioned in the preceding chapter, the fall velocity experienced by a rocketsonde thermistor is very considerable in the upper part of a rocket sounding, due to the very small drag offered the parachute by the air. The actual speed depends considerably on many factors, including the altitude at apogee and the time at which the parachute becomes fully deployed, but typical fall rates for the "Arcas" system, for example, might be 220 m/sec at 70 km and 120 m/sec at 60 km. (Wagner (1964)). In addition to the fall velocity there may also be significant horizontal components before the parachute becomes fully "wind sensitive".

Due to a combination of adiabatic heating and viscous dissipation a thermometer exposed in a high-speed airstream will (neglecting all other sources of error) record a temperature higher than a thermometer moving along with the flow. The extent of this temperature rise for a particular thermometer is usually expressed in terms of the stagnation temperature rise $T_s - T_0$. T_s is the temperature which the moving gas would acquire if brought adiabatically to rest, and T_0 is the free-

stream temperature as recorded by the moving thermometer.

It is readily shown that

$$\frac{T_s}{T_0} = 1 + \frac{\gamma-1}{2} M^2 \quad (9.1.1)$$

where M is the Mach number. If T_r is the temperature recorded by the thermometer, the thermal-recovery factor r is defined by the relation

$$r = \frac{T_r - T_0}{T_s - T_0} \quad (9.1.2)$$

For thermometers operating in the lower atmosphere, r is a number less than 1, but for small thermometers operating in a rarefied gas, recovery factors greater than 1 are possible. This result has been shown theoretically by Oppenheim (1953) for free-molecule flow, where the rarefaction is so great that the size of the thermometer is small compared to the mean free path.

Oppenheim's results enable calculation of thermal recovery in terms of the Mach number and geometrical properties of the bodies concerned. However, for the small thermistors of the type studied in this work the requirements for free-molecule flow are fully met only above about 35 km altitude. In the region of interest in a rocket sounding the flow regime affecting the thermistor can be described

as either "transitional" or "slip-flow" depending on the value of the Knudsen number $Kn = \frac{\lambda}{D}$ where λ is the mean free path and D a characteristic dimension. Adequate theoretical treatment is not available for the calculations of recovery factors in either of these regimes.

The amount of published experimental data directly applicable to this question is also very limited. To the author's knowledge there are no published experimental results for actual bead thermistors taken under any conditions.

9.2 Experimental Method

The apparatus was the same as that used for the tests described in Chapter 8. A second thermistor was mounted so that its bead was less than 3/16 inch from the path of the test thermistor. This can be seen in Fig.52. Its purpose was to provide a reference temperature with respect to which the temperature rise of the test thermistor was measured, for, as predicted from the results of Devienne (1958), there was a small temperature rise in the air in the vicinity of the arm when the latter was in motion.

A special bridge circuit, shown in Fig.60, was built to provide simultaneous recordings of the outputs of the test and reference thermistors on the two channels of the

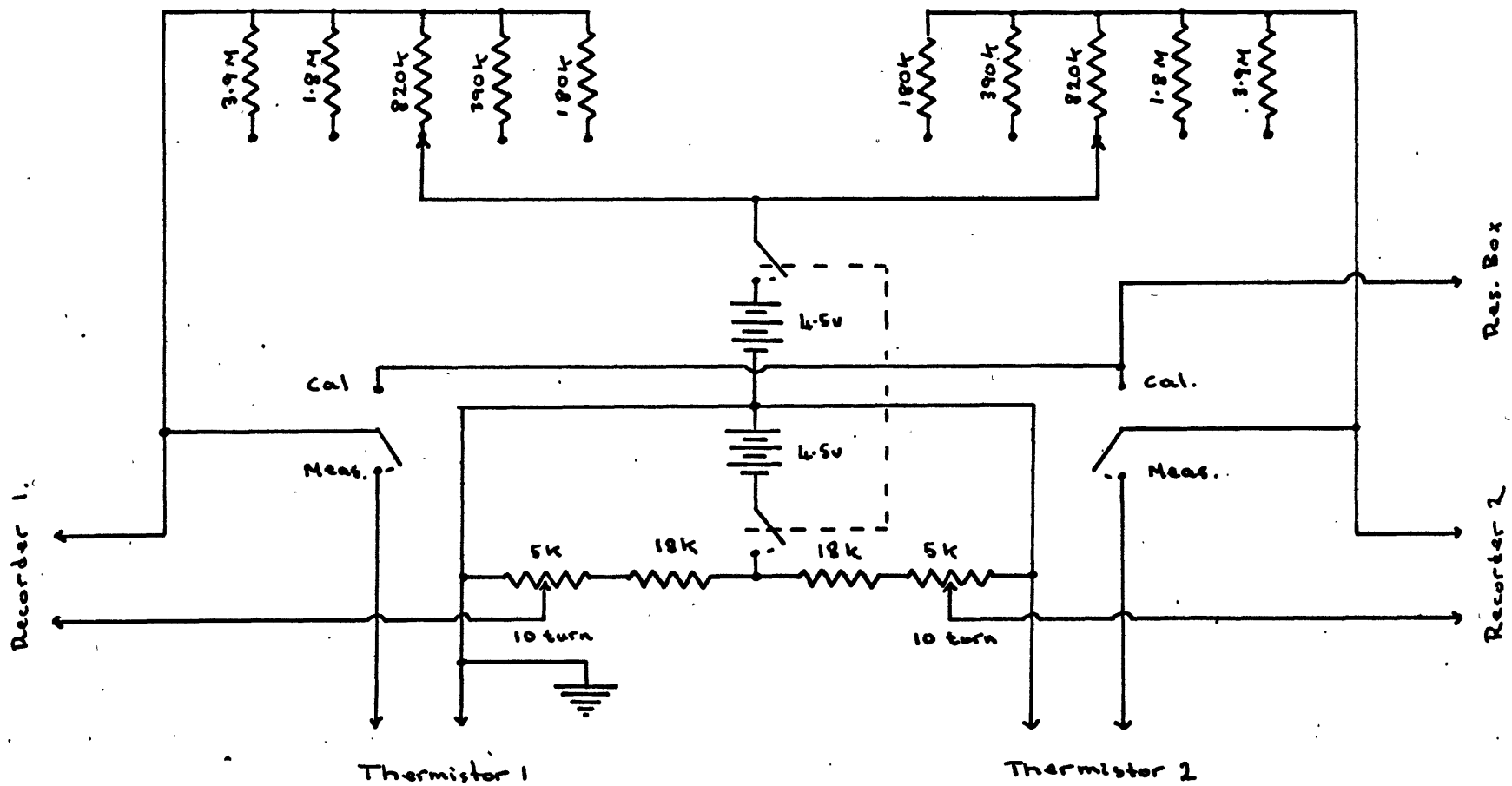


FIG. 60, TWO-CHANNEL MEASURING CIRCUIT.

Sanborne recorder. A measuring current which produced no significant self-heating in either thermistor at the lowest pressure of interest was used.

The procedure was very simple. After the desired pressure was set in the bell jar the arm was run at a low speed (about 6 m/sec) to define the free-stream temperature. The arm speed was then increased in steps up to the maximum desired, during which time the temperature rises of the two thermistors were recorded on the two channels of the recorder. The temperature rise for use in the calculation of the recovery factor was taken as the difference between that of the test thermistor and that of the reference thermistor. The arm speed was derived from the speed controller settings which in turn were calibrated at different pressures with a General Radio "Strobotac". The calibration of the latter was determined from the 60 cycle mains frequency by an internal calibration circuit. An allowance for "drive" of the air at high pressures was made in determining the effective airspeeds, as described in Chapter 8.

The recovery factor was calculated from the Mach number and the temperature rise by using equations (9.1.1) and (9.1.2).

9.3 Results

(a) Rise of Reference Temperature

When the arm was operated at high speed the air in its vicinity became heated. This was indicated by the reference thermistor. At very low pressures the rise was very small, for example at 4×10^{-2} mm mercury the reference temperature rise was about 3% of that of the test thermistor. At a pressure of about 0.25 mm mercury the heating increased quite sharply to 15-20% of the test thermistor's rise, and at higher pressures this percentage gradually increased so that at sea level pressure the reference temperature rise was 30-35% of the test thermistor's.

Although it was not difficult to deduce the net temperature rise with adequate accuracy from the recording of the two thermistors there was some uncertainty concerning the representativeness of the reference temperature, since observation was only at one point. In his 1958 report Devienne described detailed measurements of the temperature distribution near his rotating arm. These showed that at moderate and high pressures, when the heating was appreciable, temperature gradients near the arm were small. It would appear therefore that the reference temperature rise as measured should have been a reasonable estimate of the

mean conditions around the path of the moving thermistor.

(b) Recovery Factors

Fig.61 shows a typical plot of the net temperature rise vs airspeed using logarithmic scales, for a bead thermistor at several pressures. The points are seen to be reasonably well on straight lines with slope 2 as indicated by (9.1.1).

Fig.62 shows recovery factors as a function of pressure for a number of thermistors. These points were all computed from tests at Mach numbers between 0.18 and 0.29. At pressures greater than 10 mm mercury the measured values were fairly constant with pressure and lay between about 0.70 and 0.76. These results were somewhat lower than the values near 0.9 assumed for these pressures by some authors (eg. Barr (1961), Wagner (1963)) in evaluating the aerodynamic heating correction for rocketsonde thermistors. However reference to the original papers showed that the latter had based their estimates on measurements taken in supersonic flow, with Mach numbers between 2 and 4. Moffat (1962) has summarized results of measurements of the recovery factors of butt-welded cylindrical thermocouples of various diameters at sea level pressures and subsonic Mach numbers. When the wires were normal to the air flow the measured values of r were near 0.68 with about 10% variation.

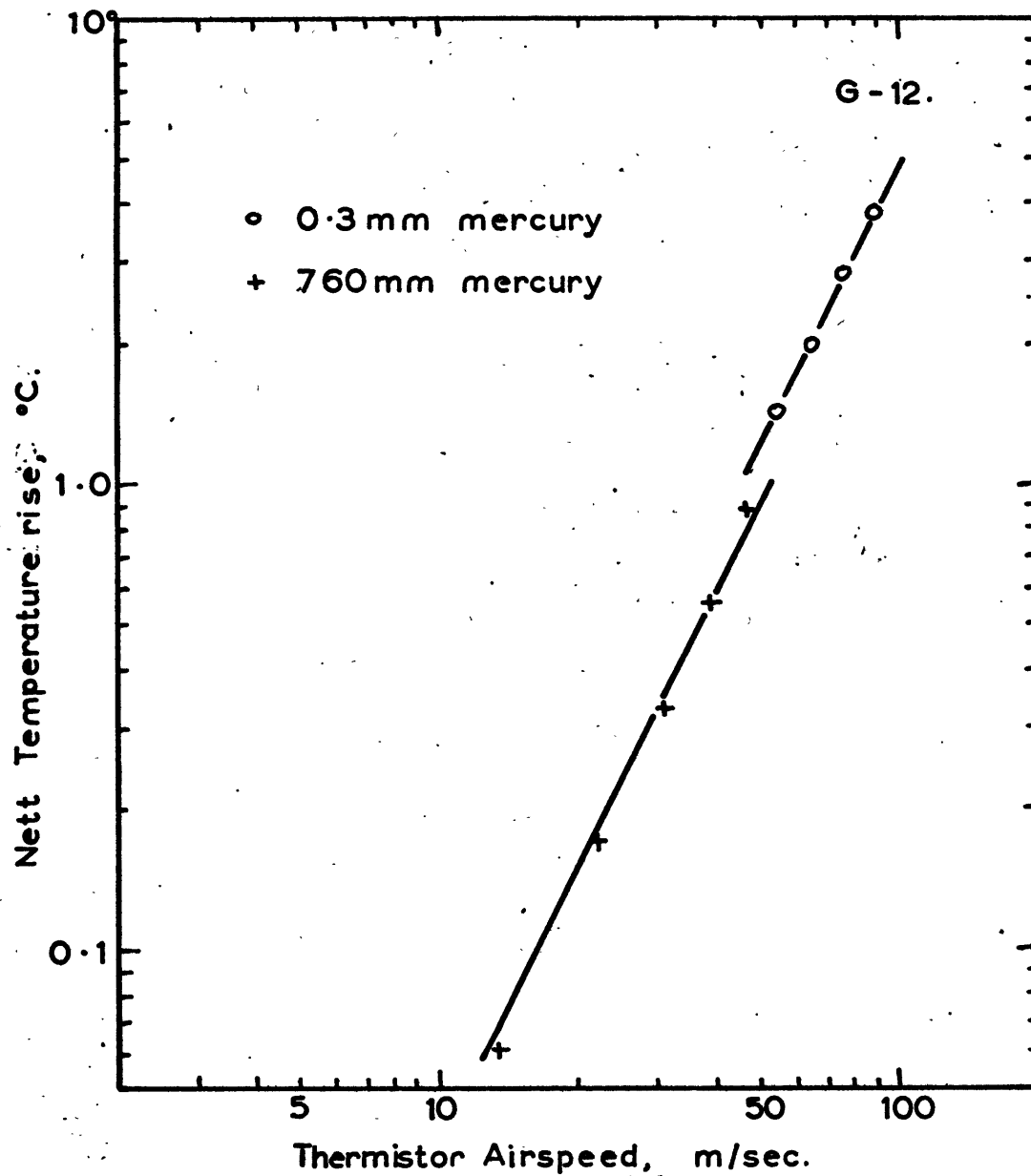


FIG 61, TEMPERATURE RISE OF THERMISTOR vs AIRSPEED.

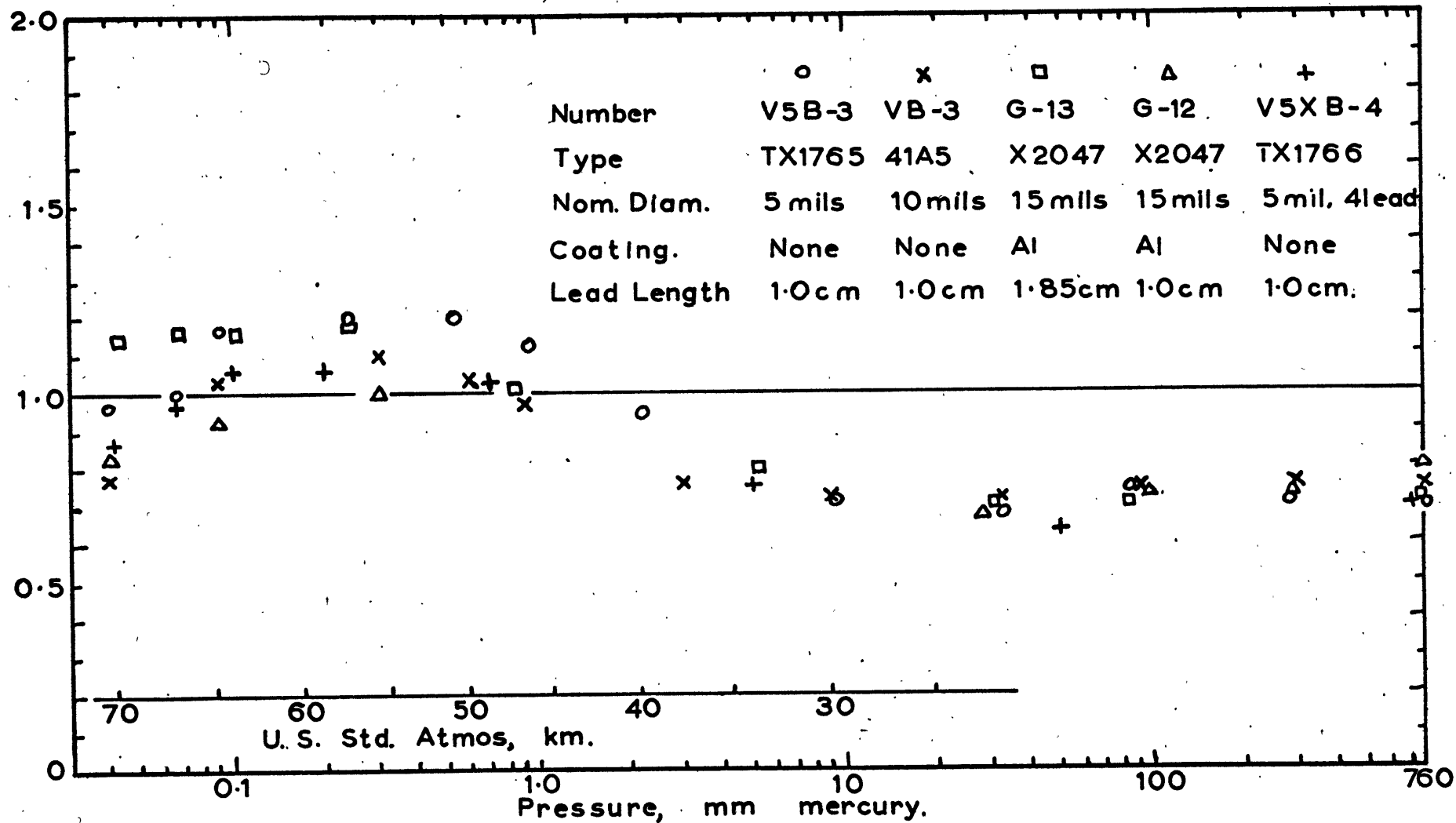


FIG 62. MEASURED RECOVERY FACTORS OF THERMISTORS.

For wires parallel to the flow $r = 0.86 \pm 0.09$. Hottel and Kalitinsky (1945) reported similar values for fine wire thermocouples. These authors also made tests on a thermocouple consisting of 0.010 inch diameter wires whose junction was encased in a 0.07 inch diameter solder ball. With the airstream parallel to the wire r was about 0.78 and for flow normal to the wire r was about 0.73.

At pressures below 7 mm mercury the measured recovery factors shown in Fig.62 increased with decreasing pressure and in most cases exceeded unity below 1 mm mercury. However all of the values fall short of the limiting values of 1.55 for spheres and 1.75 for cylinders normal to the flow as calculated by Oppenheim for free-molecule flow at low Mach numbers. Since at a pressure of 0.1 mm mercury the Knudsen number $\frac{\lambda}{D}$ is ≈ 2 for the thermistor beads and ≈ 20 for the lead wires one would have expected the latter results to be approached more closely at this pressure. One reason for the discrepancy was undoubtedly the effect of heat lost by radiation to the chamber walls at low pressures. For an uncoated bead the rate of heat lost by radiation per unit temperature difference equals that lost by convection at about 0.07 mm mercury, and a rough computation would indicate that a 10% error in r would result at about 0.3 mm mercury. For an aluminized thermistor the error would be 10% at about 0.09 mm mercury.

Since all the pertinent conditions were not known with sufficient accuracy it was not thought desirable to attempt to correct the results for radiation. Consequently care should be taken in using the results at pressures below about 0.3 mm mercury.

(c) Centrifugal Forces

It is perhaps appropriate here to mention the centrifugal accelerations which the thermistors withstood in the course of these tests.

Both the 10 mil and the 5 mil thermistors were run at speeds exceeding 100 m sec^{-1} for considerable periods without any failures. The corresponding acceleration is given by

$$v^2/r = 100^2/0.152 = 6.6 \times 10^4 \text{ m sec}^{-2}$$

$$= 6.7 \times 10^3 \text{ G.}$$

The 15 mil thermistors withstood this loading only for short periods and there were two failures at speeds corresponding to about $6 \times 10^3 \text{ G}$. No failures were suffered in prolonged periods of operation at speeds corresponding to 4-5000 G accelerations.

On the other hand, several failures occurred with thinistors when speeds producing accelerations greater than about 200 G were attempted.

CHAPTER 10

THE INFLUENCE OF THE AMBIENT TEMPERATURE ON THE
HEAT TRANSFER10.1 Introduction

All of the tests described in the previous chapters were carried out at room temperature - generally between 22°C and 25°C. In an actual sounding, temperatures as low as -80°C may be encountered and it is necessary to know what, if any, modifications must be made to the results to make them valid under these conditions.

These modifications may be directly related to the effect of the temperature on the heat transfer coefficients h_T and h_w . Fortunately the latter are not especially sensitive to temperature and this fact, together with the fact that we are only dealing with errors which do not require to be evaluated to a particularly high level of accuracy, allows us to use substantial simplifications.

10.2 Theoretical and Empirical Considerations

The heat transfer coefficients are usually expressed by theoretical or empirical relations of the form

$$Nu = f(Re, Pr, Ma)$$

where the Nusselt number $Nu = \frac{hD}{k_a}$. We shall make the assumption that

$$Nu \propto Re^a \cdot Pr^b \cdot Ma^c$$

where in turn $Re \propto T^p$, $Pr \propto T^q$, $Ma \propto T^r$.

Under this circumstance h can be expressed as

$$h = h_0 \left(\frac{T}{T_0} \right)^w$$

where h_0 is the value of h at room temperature T_0 . To obtain a suitable value for the exponent w we shall consider a number of examples for which theoretical or semi-empirical relations are available.

(a) Conduction from a sphere into a stagnant medium

$$Nu = 2$$

i.e.
$$h = \frac{2k_a}{D}$$

The kinetic-theory expression for k_a is

$$k_a = A \cdot \frac{T^{3/2}}{T + 245 \times 10^{-12}/T}$$

from which, approximately, $k_a \propto T^{1/2}$ and hence

$$h \propto T^{1/2}.$$

(b) Cylinder and sphere in free-molecule flow

Using a theoretical formula given by Stalder et al (1951) for long cylinders,

$$Nu = 0.03365 \alpha g(s)/Kn$$

where Kn is the Knudsen number, α the accommodation coefficient and $g(s)$ a function of the Mach number. Between $Ma = 0$ and $Ma = 0.5$, $g(s)$ varies only 8.5%, and on noting that $Kn = \left(\frac{\gamma\pi}{2}\right)^{\frac{1}{2}} \frac{Ma}{Re} = 1.48 \frac{Ma}{Re}$ we see that approximately $Nu \propto \frac{Re}{Ma}$. Now $Re = \rho \frac{vD}{\mu}$ and from kinetic theory $\mu = B.T^{\frac{3}{2}}(T + 110)^{-1}$. Thus to a first approximation we can write $Re \propto T^{-1} \cdot T^{-\frac{1}{2}} = T^{-\frac{3}{2}}$. Hence

$$Nu \propto T^{-\frac{3}{2}} \cdot T^{\frac{1}{2}} = T^{-1}$$

and $h \propto T^{-1} \cdot T^{\frac{1}{2}} = T^{-\frac{1}{2}}$.

A similar result holds for spheres.

(c) Cylinders in slip-flow

Collis and Williams (1959) quote an empirical formula of the type

$$Nu = A + B.Re^m \quad \text{where } m \approx 0.5 .$$

Then $h = \frac{A}{D} \cdot k_a + \frac{B}{D} \cdot k_a Re^m$

The first term on the RHS varies as $T^{\frac{1}{2}}$ and the second as $T^{-\frac{1}{4}}$.

In any particular instance the heat transfer from a rocketsonde thermistor in the upper atmosphere is somewhere between these idealized cases. It will be seen that there are compensating effects in action on the heat transfer and that the correct exponent w lies somewhere between $-\frac{1}{2}$ and $+\frac{1}{2}$. For the present purpose it will be adequate to take $w = 0$. The expected temperature range is approximately 200°K to 300°K , and it is therefore very unlikely that the error introduced by this assumption would exceed $1 - (\frac{2}{3})^{\frac{1}{2}}$ which equals 20%.

10.3 Experimental Verification

A commercial environmental chamber was available in the laboratory. This chamber was intended only for simulation of conditions encountered in conventional radiosonde soundings, but by using a larger vacuum pump, pressures as low as 1-2 mm mercury were obtainable.

Using this chamber, the still air time constant of a Gulton X2047 thermistor number G-1 was measured at different temperatures at atmospheric pressure and at 2.5 mm mercury. Measurements of the dissipation rate K would have perhaps been more appropriate, but it was not possible to keep the temperatures sufficiently steady to carry out these measurements to the desired accuracy. The time constant is,

however, very nearly inversely proportional to K .

The results are given below in Table 8. It is seen that there is no significant variation of τ with temperature at the two pressures.

TABLE 8. Measured Time Constant of G-1 at Different Temperatures.

Pressure	2.5 mm	Atmos.
-40°C	1.34 sec	1.22 sec
-13°C	1.40 sec	1.24 sec
+23°C	1.39 sec	1.23 sec

CHAPTER 11.

THE ERRORS OF THERMISTORS IN ACTUAL SOUNDINGS

11.1 Introduction

The tests described in the previous chapters were made under experimental conditions which only approximate those encountered in an actual sounding, and in general only one source of error was studied at a time. In this chapter these results will be extended and combined to illustrate the behaviour of thermistors under actual conditions.

With so many parameters involved there are an almost unlimited number of possibilities which could be described. For this reason only a few idealized cases will be selected, and these should principally be regarded as illustrative of the method of using the work in the previous chapters. At the same time it is hoped that the examples given will show the order of the errors involved in typical soundings, and their range of variability.

11.2 Solar Radiation Error(a) Effect of Lead Wire Orientation

It was shown in section (3.6(e)) that in evaluating the error due to direct solar radiation the contribution of the

lead wires may be taken proportional to $\sin\alpha$ where α is the angle between the lead wires and the solar beam. In a sounding, due to parachute swing, this angle will be constantly changing. An adequate mean value for $\sin\alpha$ may be obtained by assuming horizontal leads with a random azimuth angle ϕ with respect to the sun. Then

$$\cos\alpha = \cos\phi \cos h$$

where h is the solar elevation angle. Hence

$$\sin\alpha = \sqrt{1 - \cos^2\phi \cos^2 h}$$

and the mean value of $\sin\alpha$ is given by an elliptical integral of the second kind:

$$\overline{\sin\alpha} = \frac{2}{\pi} \int_0^{\pi/2} \sqrt{1 - \cos^2\phi \cos^2 h} \, d\phi \quad (11.2.1)$$

Table 9 gives values of $\overline{\sin\alpha}$ for various solar altitudes.

TABLE 9. $\overline{\sin\alpha}$ vs Solar Elevation Angle h .

h	0	15	30	45	60	75	90
$\overline{\sin\alpha}$.64	.68	.77	.86	.93	.98	1.0

Although the thermistor beads show appreciable departures from spherical any allowance for the variation of the

radiation intercepted with orientation would seem to be an unnecessary and unrealistic refinement.

(b) Reflected and Scattered Radiation from Below the Thermistor

In many cases the thermistors will be exposed above cloud layers or above highly reflecting terrain such as desert sands. If a is the mean albedo of the cloud cover or terrain, then, assuming diffuse reflection, the upward flux of radiation through a horizontal surface is given by $aJ \sin h$. Let A'_T be the cross-sectional area of the thermistor bead. Then the energy absorbed by the almost-spherical bead is, from geometrical considerations,

$$aJ \sin h \times 2 \epsilon_{ST} A'_T \quad (11.2.2)$$

Similarly the energy absorbed per unit length of cylindrical lead wire is given by

$$aJ \sin h \times \frac{\pi}{2} \times 2 \epsilon_{sw} r \quad (11.2.3)$$

These quantities will be substantially independent of the orientation of the lead wires.

(c) Computations of the Radiation Error

In this section the radiation error will be computed

on the assumption that all other sources of error have been eliminated. Specifically, the lead lengths will be assumed long enough to eliminate any modification due to conduction of heat from the support posts. In this case a modified form of equation (3.1.9) holds, in which allowance is made for the effects discussed in (a) and (b) above.

$$\theta_2 = \frac{4 \epsilon_{sw} J \frac{r}{p} (\overline{\sin \alpha} + \frac{\pi}{2} a \sinh h) + J \epsilon_{st} A'_T (1 + 2a \sinh h)}{A_T h_T + 2ka_w p} \quad (11.2.4)$$

Fig.63 shows the solar radiation error computed in this way for thermistors of 5, 10 and 15 mils nominal diameter. A solar elevation angle of 40° was assumed, and an albedo of 0.30. The solar absorptivities ϵ_{sw} and ϵ_{st} were each set equal to 0.15, which is very nearly the mean value measured for aluminized thermistors whose surfaces were in good visual condition (see section 3.6(c)). The areas of the thermistor beads were taken as the mean of the measured areas for the nominal size concerned, from Table 2. The heat-transfer coefficients were taken from the measured values shown in Figs.34 and 35.

In considering Fig.63 it should be kept in mind that a variability of $\pm 50\%$ was noted among ϵ_{sw} and ϵ_{st} even for apparently well-coated thermistors, and that some with

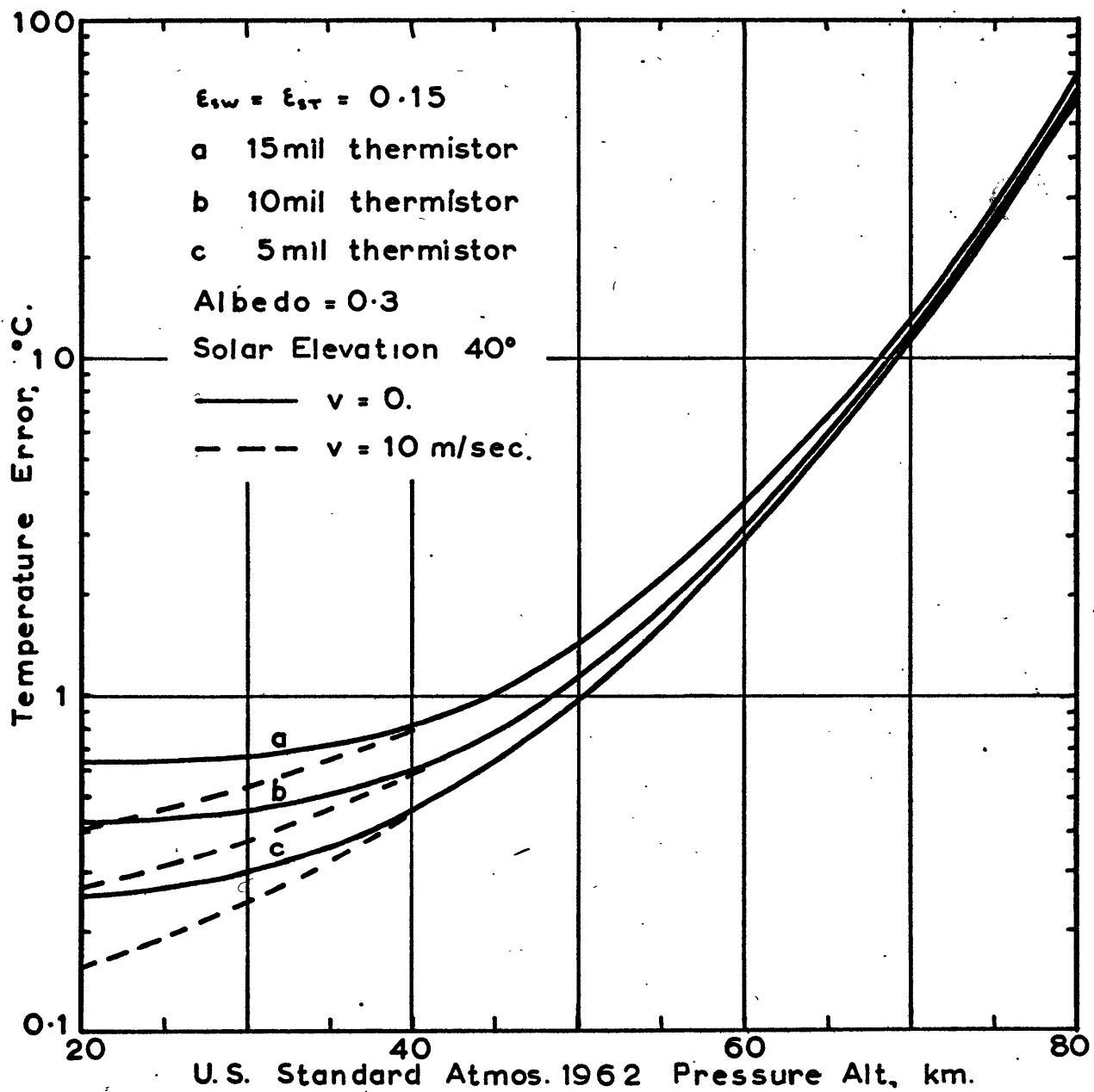


FIG 63. SOLAR RADIATION ERROR OF THERMISTORS.

faulty coatings recorded values four or five times greater than the ones assumed here.

Fig.64 shows the computation for the 10 mil coated thermistor repeated for albedos of 0, 0.5 and 1.0, other conditions being the same. The contribution of reflected radiation may be very substantial, particularly over cloud cover where albedos of 0.75 and greater have been frequently recorded (Conover, 1965).

In a rocket sounding there will be times when the thermistor is shaded by the swinging parachute. Oscillations in the temperature record due to this are common and it is sometimes suggested (Thiele, 1966) that the amplitude of these may be used to determine the radiation error. It is seen from the above, however, that there may still be a substantial steady contribution from reflected radiation.

It should be pointed out here that the experimental curves obtained in section (3.6(b)) are nearly proportional to the temperature error expected in the atmosphere under still-air conditions for altitudes up to about 65 km. It will be seen from the above discussions that the solar radiation error up to this altitude may be estimated by multiplying by a factor of $(1 + 1.8 a \sinh)$ to allow for reflected radiation.

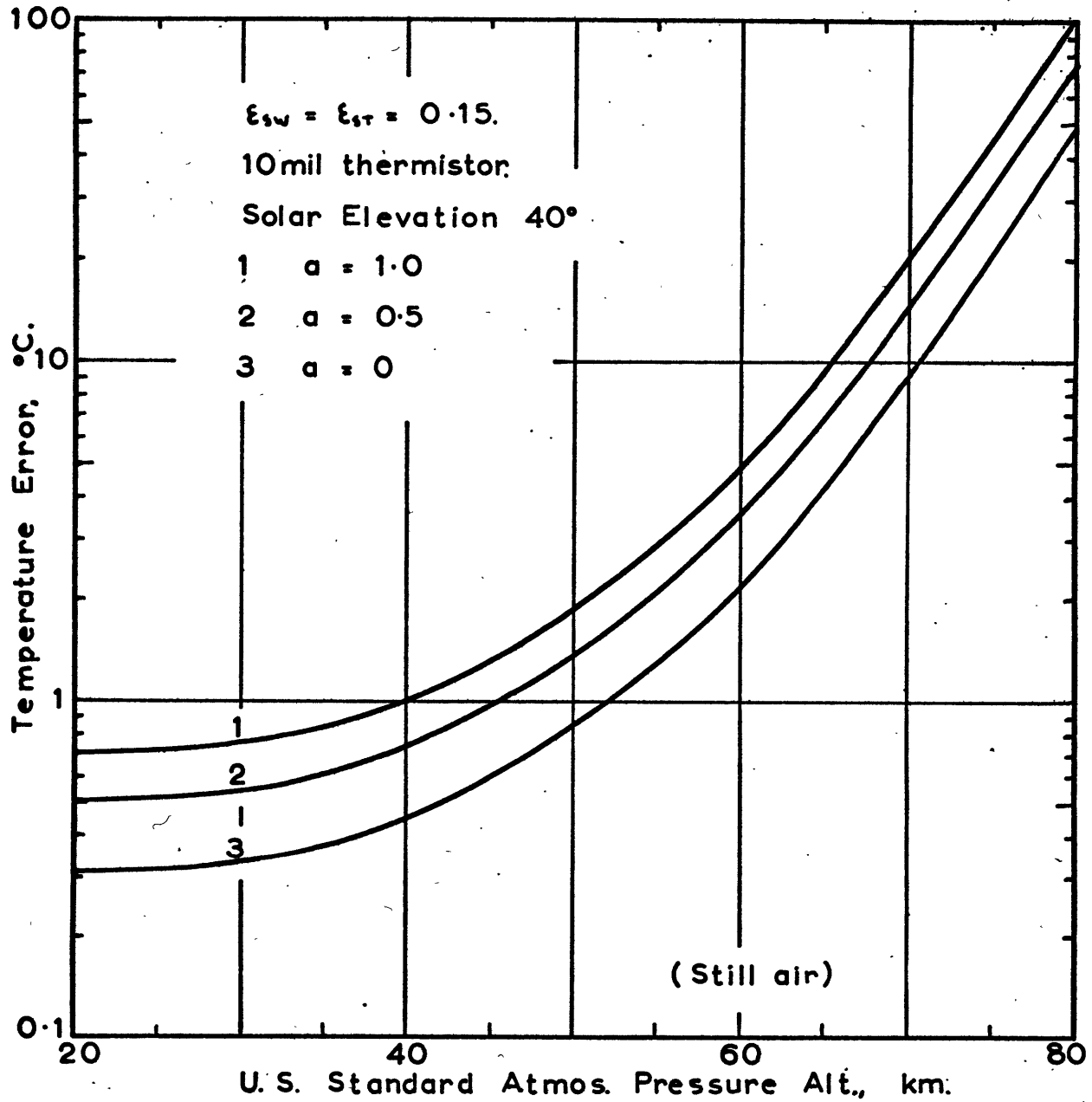


FIG 64. EFFECT OF ALBEDO ON SOLAR RADIATION ERROR.

11.3 Measuring Current Error

Fig.65(a) shows the power dissipated in the Arcasonde thermistor as a function of resistance. This curve was supplied to the author by Mr.P.J. Harney of the Aerospace Instrumentation Laboratory, AFRL. The resulting temperature error for 10 mil thermistors of 10,000 ohm and 50,000 ohm nominal resistance are shown in Fig.65(b). These were computed from the measured dissipation rate on the assumption that the thermistor temperature was near that of the U.S. Standard Atmosphere at each altitude level. The assumption may be quite erroneous near the top of the sounding, as mentioned in Chapter 4, nevertheless it is seen that with this particular instrumentation the errors in temperature must be very small. In earlier rocketsondes this was not the case.

11.4 Conduction Error

It is not possible to give an explicit value for the error due to conduction at a given altitude without knowing the temperature of the mounting posts. For this reason it is more convenient to discuss the ratio of this conduction error, θ_{20} , to the difference θ_1 between the mounting post and air temperatures. The term conduction error is in fact often applied to this ratio, rather than to the

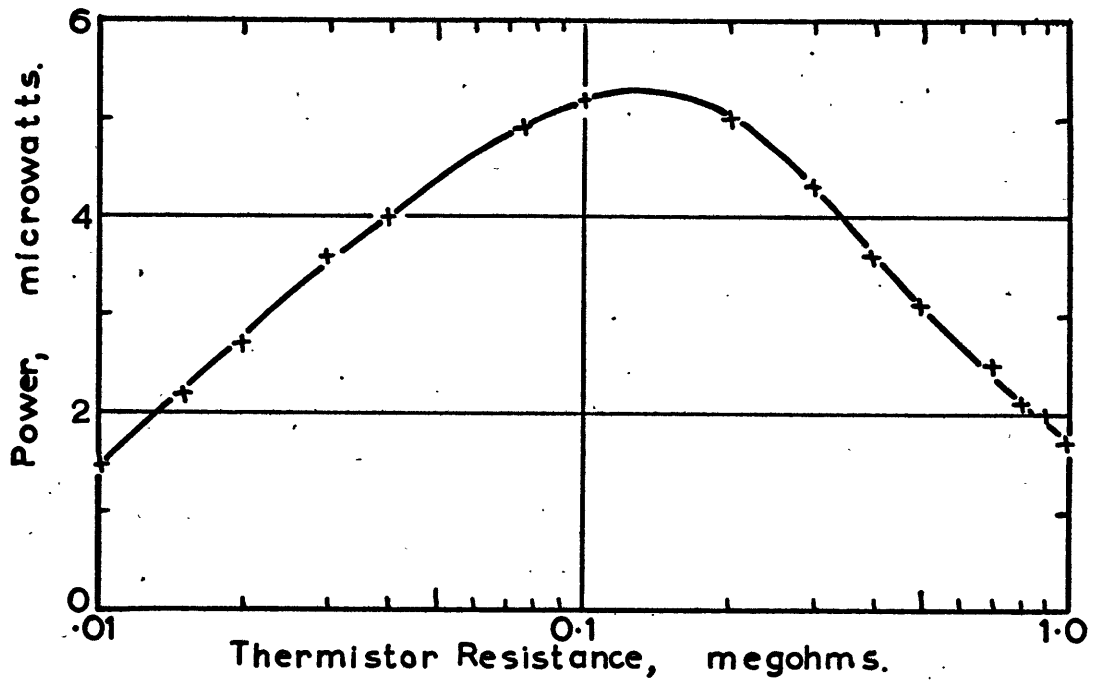


FIG 65a, ARCASONDE POWER DISSIPATION.

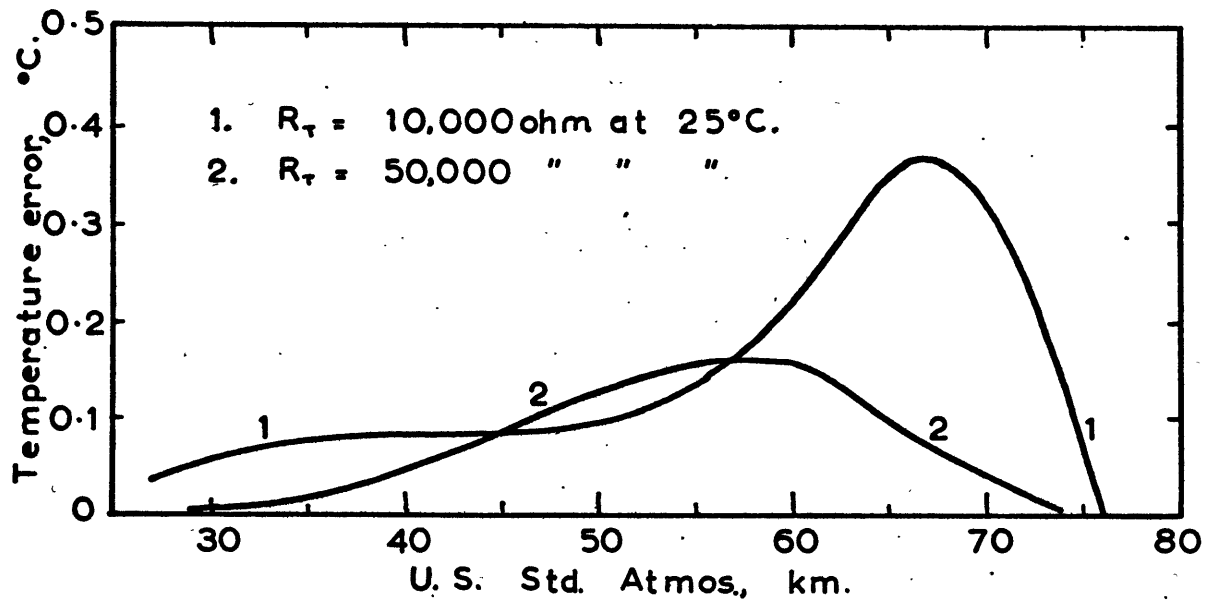


FIG 65b. SELF-HEATING ERROR, ARCASONDE: 10mil THERMISTOR.

actual temperature error. An expression for $\frac{\theta_{20}}{\theta_1}$ has been derived in section 5.2.

In a given type of sounding system it would normally be possible to know the value of θ_1 within certain limits (eg. $\pm 50^\circ\text{C}$), perhaps from the results of tests in which θ_1 was specifically measured, and from this estimate deduce an approximate value for θ_{20} .

Fig.66(a) shows the percentage conduction error as a function of altitude and lead length for small bead thermistors using 1.0 and 0.7 mil platinum-iridium leads. These curves were derived from the measured heat-transfer coefficients given in Fig.34, and from the computations given in Figs.39 and 40. Bearing in mind that a typical value of θ_1 might be 100°C we see for example that a 6°C error might be expected at 60 km, with 1 mil leads each 1 cm long. In this case, if θ_1 was known to the nearest 50°C the error would be known to 3°C . It is seen that greatly increased reduction of error is obtained by using longer lead wires and/or a smaller diameter.

Fig.66(b) shows the same material as Fig.66(a) presented in a way more convenient for design purposes. This figure shows that for useful values of the conduction error the lead length required becomes rather long above about 70 km

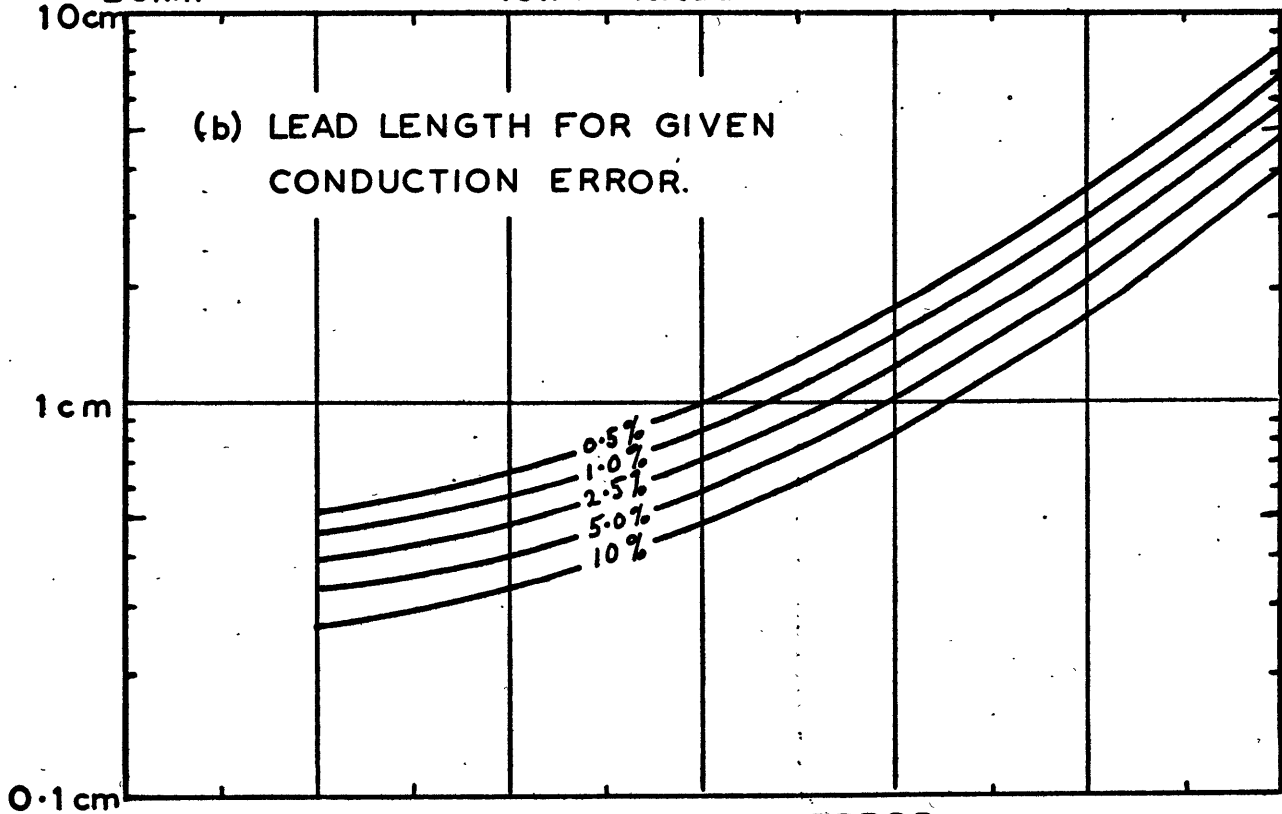
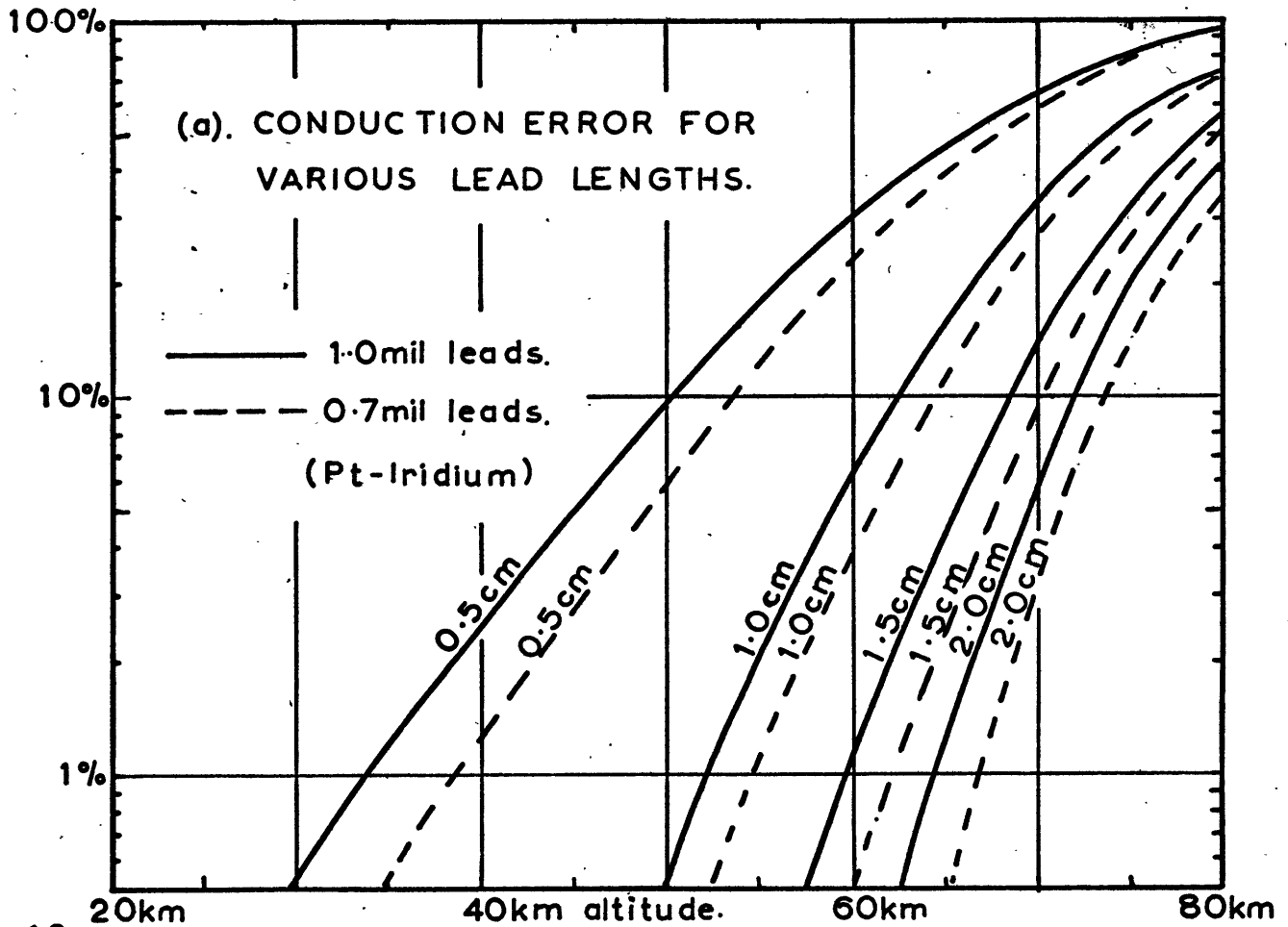


FIG. 66. CONDUCTION ERROR.

and an alternative approach such as the "foil" mount would seem desirable for use in this region.

11.5 Long-Wave Radiation Error

An expression for the long-wave radiation error was presented in section 6.2. We shall consider for illustration purposes the case where the lead length is long enough so that the error is not modified by conduction to the supports. Then the error can be written as

$$\theta_2 = Q_L \cdot \frac{4\pi r \epsilon_{\lambda_w}/p + \epsilon_{\lambda_T} A_T}{h_T A_T + 2ka_w p} \quad (11.5.1)$$

where as before,

$$Q_L = \sigma \left(\frac{1}{2} T_{eb}^4 + \frac{1-2\gamma}{2} T_{ea}^4 + \gamma T_p^4 - T^4 \right) .$$

The quantity γ is the ratio of solid angle subtended by the instrument package at the thermistor to 4π . If the front of the rocketsonde is circular we can write

$$\gamma = \frac{1}{2}(1 - \cos\alpha)$$

where α is the semi-angle subtended.

Fig.67 shows (11.5.1) evaluated as a function of altitude for a 10 mil bead thermistor. In this hypothetical

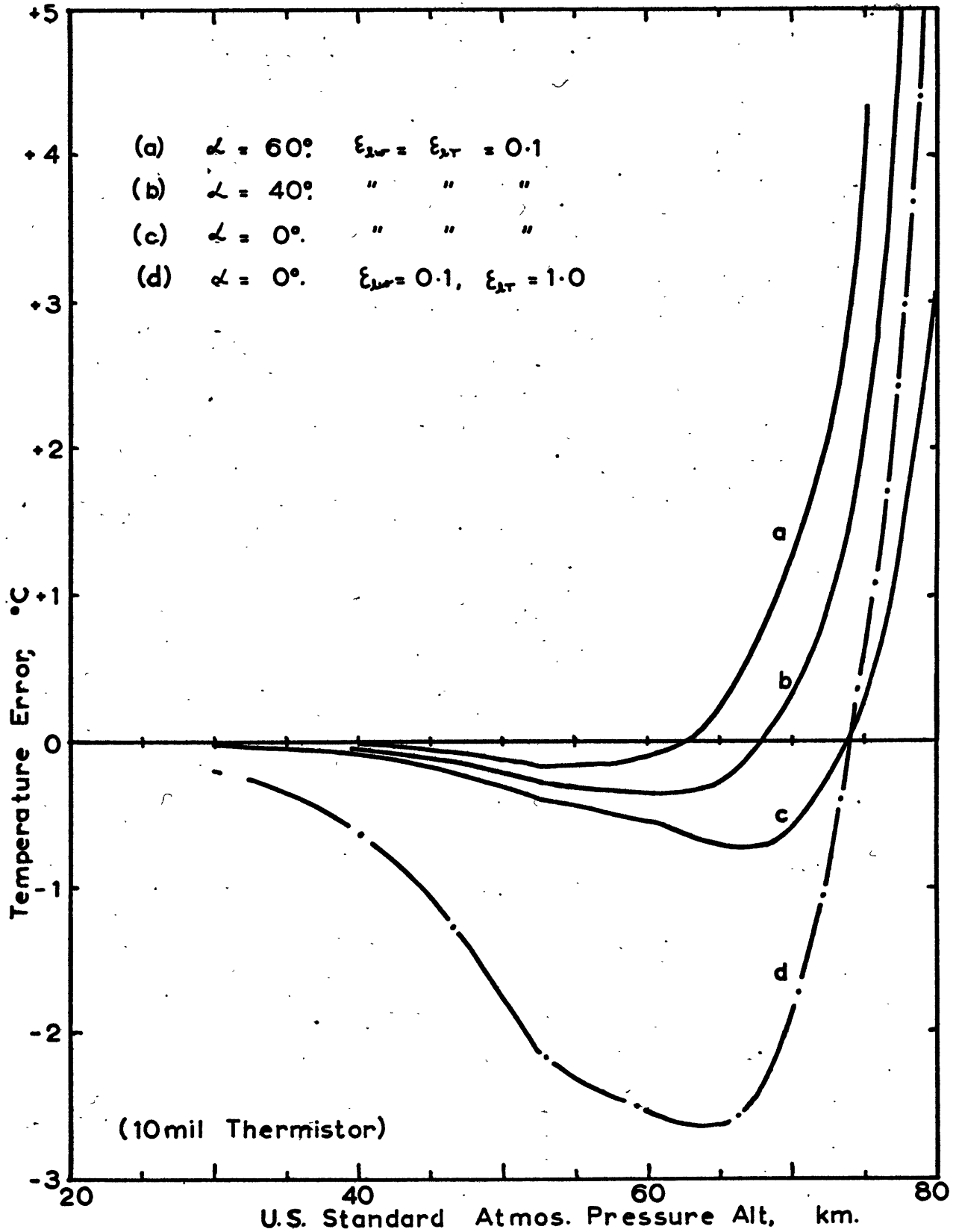


FIG 67. LONG-WAVE RADIATION ERROR OF A THERMISTOR.

example the air temperature was assumed to be that of the U.S. Standard Atmosphere, 1962, and the effective black-body temperature of the environment below the sensor was assumed to be 244°K . The contribution from T_{ea} can be neglected at the altitudes shown. The instrument package was assumed, for illustration, to have a constant temperature of 300°K and to radiate as a black-body. The value of ϵ_{λ} chosen was consistent with the measured results for aluminized thermistors whose surfaces were in good visual condition.

The computations show that with aluminized thermistors the temperature errors are quite small below 70 km. The results depend to some extent on the value of T_{eb} chosen, and variations would also be expected in an actual sounding due to departures of the air temperature from the standard atmosphere values. It is readily verified from (11.5.1), however, that the change in error for a departure of 20°C in either quantity from the reference conditions is less than 1°C at 70 km and considerably less at lower altitudes. The influence of the radiation received from the instrument package is significant above 65 km particularly for $\alpha > 40^{\circ}$. To a large extent the actual value of T_p is unknown, so it is best to minimize its influence by making α as small as possible.

The computations for the uncoated bead show that the

errors are considerably increased. If, in addition, the emissivity of the lead wires were greater than 0.1 the errors would be increased even more. In the limiting case $\epsilon_{LW} = \epsilon_{LT} = 1$ the error would be approximately ten times the ones shown in the computations for $\epsilon_L = 0.1$.

11.6 Aerodynamic Heating

The fall velocity of a rocketsonde at a given altitude depends on a large number of factors so that in general the aerodynamic heating error will vary considerably with type of equipment and techniques used for the sounding. To illustrate the typical errors involved in a sounding, computations have been made using the Arcasonde fall velocities given in Wagner's 1963 report. The recovery factors were taken from the mean results of Chapter 9 Fig.62, extrapolated above 63 km.

The errors are very large, particularly at high altitude. For example at 65 km the computed aerodynamic heating is 17.7°C , compared with 6°C for the solar radiation error of an aluminized 10 mil thermistor. A correction can, of course, be applied for this error. Because it depends on the square of the velocity it is highly desirable that this correction be based on the actual measured fall rate of the particular sounding rather than an assumed

mean rate.

At very high altitudes there may be a considerable horizontal component of the rocketsonde velocity, because the rockets are not normally launched exactly vertically, and it takes a certain amount of time before the parachute becomes fully wind-sensitive. The contribution of this component must also be taken into account when assessing the correction for aerodynamic heating. Ballard(1966) gives some measured values for the horizontal component of velocity on a typical Arcasonde flight. These indicate, for example, a horizontal component of 300 m/sec at 70 km although in a particular case there would be considerable variation with the angle of launch. Taking this component into account at 70 km would increase the correction in the above example from 32°C to 38°C.

To apply such a correction routinely one would need to make use of the relevant radar data. However a major obstacle arises in that winds at the altitude concerned may be very strong, speeds well in excess of 100 m/sec being common (Craig (1965) p.81). Since the speed required is that relative to the air, the uncertainty of the correction would be very great above altitudes where the parachute was known to be wind-sensitive.

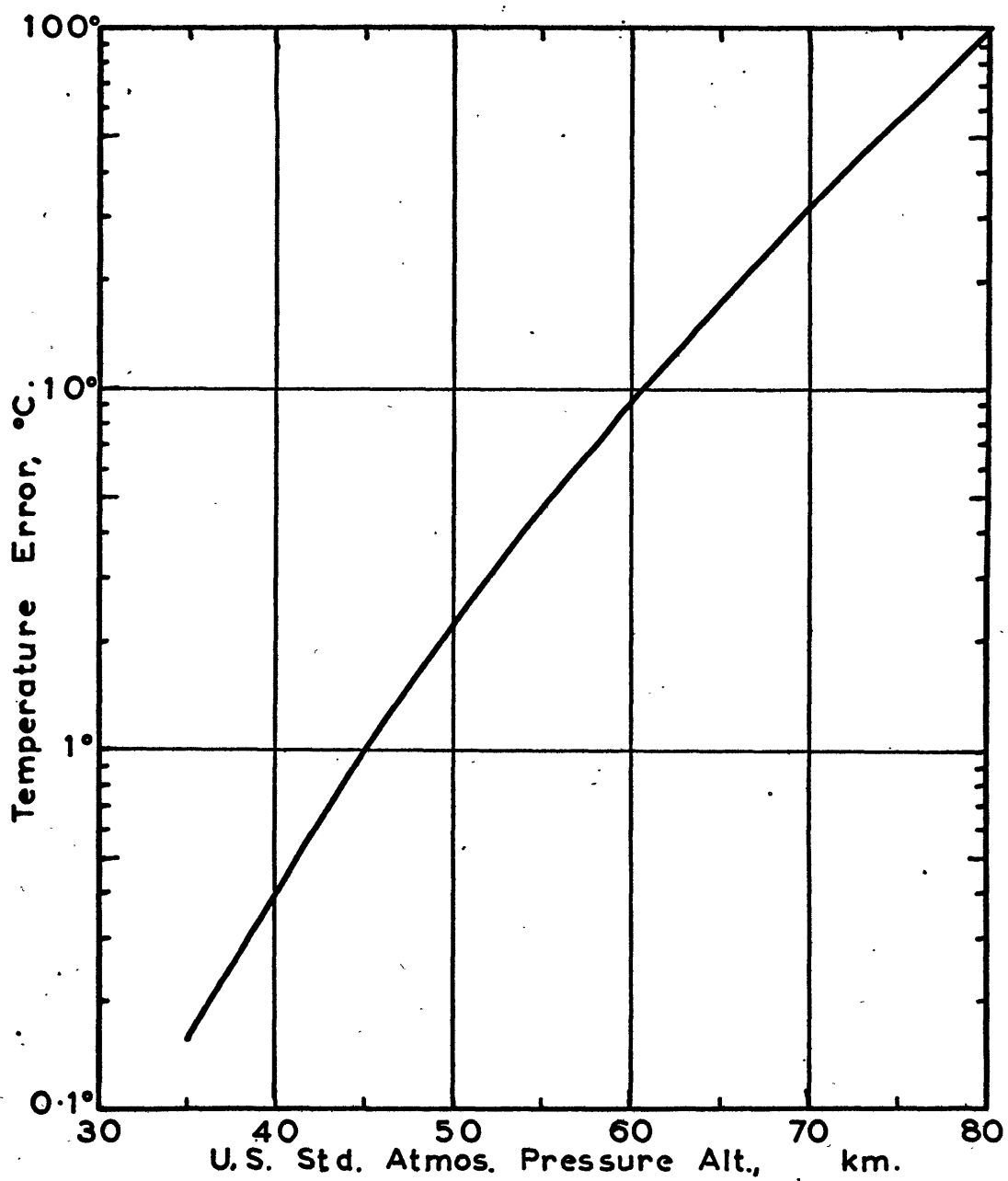


FIG 68. AERODYNAMIC HEATING, ARCASONDE.

11.7 Lag Error

The computed lag errors for hypothetical soundings in which the fall speed was that given for the Arcasonde by Wagner (1963) and in which the thermistor was assumed to be 100°C warmer than the ambient air at 70 km are shown in Fig.69. All other sources of error were neglected and the air temperature in this example was assumed to be that given by the U.S. Standard Atmosphere, 1962. The time constants used in the computations were the measured ones for three thermistors of 5, 10 and 15 mil nominal size.

As the rocketsonde falls, the initial temperature difference decreases quite rapidly and the thermistor temperature "rounds out" to a quasi-steady value which depends on the fall speed, lapse rate, and time constant at the altitude in question. From 70 km about 4.5 km altitude is lost by the 15 mil thermistor before "rounding out". The heights lost by the 10 and 5 mil thermistors under the same conditions are 3.5 km and 1.6 km respectively. The errors are small for all three thermistors below 55 km, although it must be remembered that these computations do not take into account any departures from the standard lapse rates which may occur in practice. Bearing this in mind it is seen that the 5 mil thermistor shows a worthwhile improvement over the larger types.

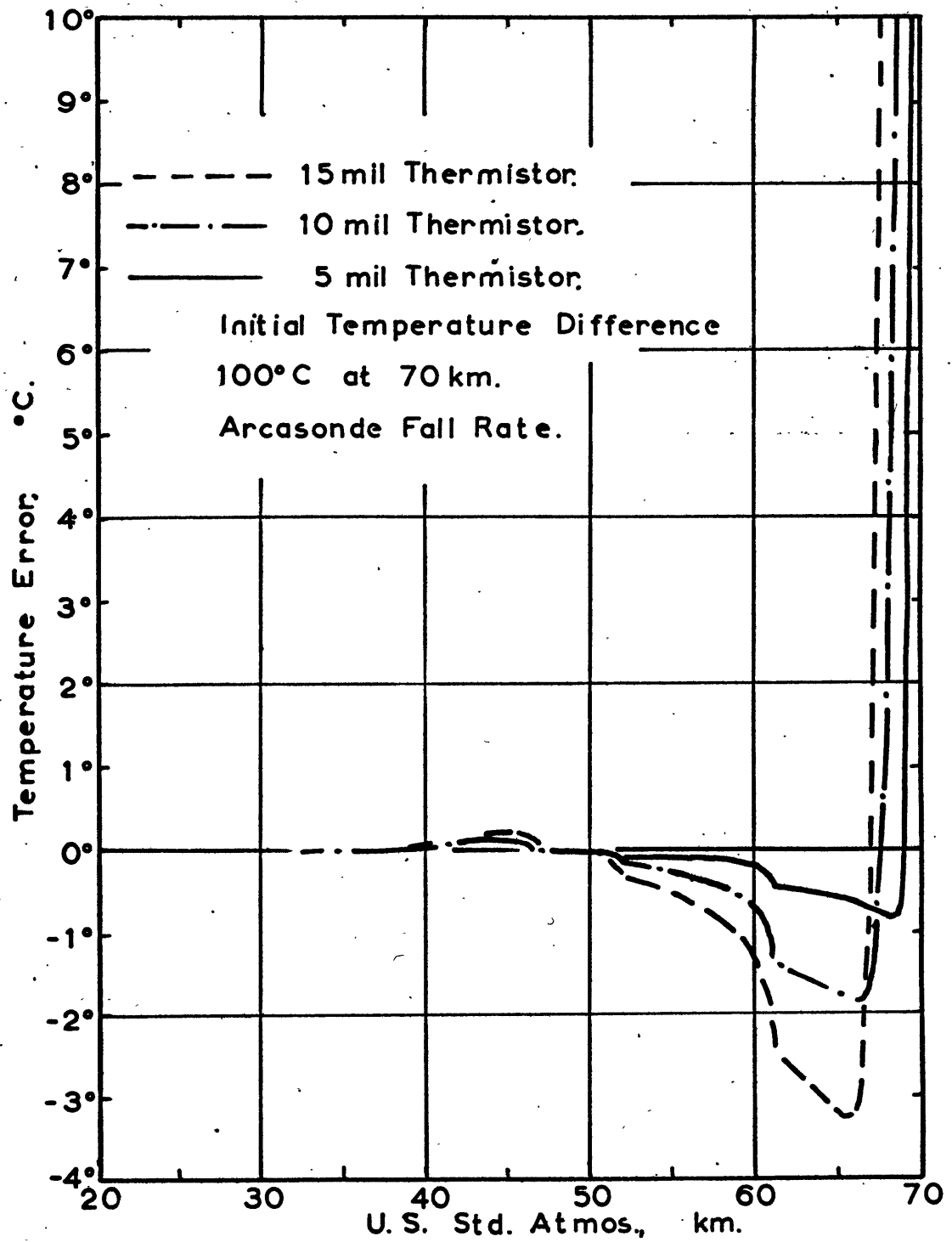


FIG 69. LAG ERRORS OF THERMISTORS.

11.8 Sample Computations of Combined Temperature Errors

As a final illustration of rocketsonde thermistor errors two examples are given below of the combined errors resulting from soundings under certain assumed conditions. It should be noted that because the heat transfer processes interact somewhat the errors are not merely the algebraic sum of the component errors discussed above. For example the presence of conduction error modifies the radiation, lag and measuring current errors.

In carrying out the computations the complete formulae, which take into account the lead wire length and support post temperature were used, with the ambient air temperature T in each case replaced by the appropriate recovery temperature $T_r = T + 0.2 r T M^2$.

The first example, given in Table 10, is essentially a recomputation of the temperature corrections given by Wagner (1963). This is of interest because these corrections have been applied in operational use, see Ballard (1965). The assumptions regarding support post temperature, initial altitude of 80 km, fall velocity, thermistor reflectivity and emissivity, ambient air temperature etc. remain the same as in Wagner's paper, but the formulae given in preceding chapters, which take into account the effects of radiat-

ion and convection on the lead wires have been used, together with the measured heat transfer coefficients, dissipation rates and time constants for 10 mil bead thermistors.

TABLE 10. Temperature Errors of 10 mil Krylon-coated Thermistor Using 0.6 cm Lead Length.

Alt km	Aero °C	Cond °C	L/W Rad °C	S/W Rad °C	Meas °C	Lag °C	Total °C	Wagner °C
65	17.7	14.8	-5.6	3.6	4.5	-1.4	33.6	33.5
60	8.7	5.9	-2.7	2.2	3.1	-0.6	16.6	19.0
55	4.7	1.7	-2.3	1.4	2.1	-0.2	7.4	7.5
50	2.2	0.5	-1.8	0.9	1.6	0	3.4	5.0
45	1.0	0.3	-1.1	0.6	1.4	+0.1	2.3	4.5
40	0.4	0.1	-0.6	0.5	1.0	0	1.4	3.5
35	0.2	0.1	-0.3	0.4	0.7	0	1.1	-

The results for the net error are very similar to those given by Wagner at the highest altitudes, although there is probably some redistribution of the component errors. The aerodynamic heating is practically the same, as the same fall velocity was assumed in each case. At 65 km the conduction error is nearly 40% with the very short lead lengths used, so that the temperature error is very dependent on the assumed support post temperature. In an actual sounding

this might differ from Wagner's assumption by as much as 50°C at this altitude, with a corresponding change of nearly 20°C in the net error.

At lower altitudes the conduction error is reduced considerably by convection of heat directly from the lead wires, and this probably accounts for the fact that the net errors are smaller than those given by Wagner.

The second example, given in Table 11, shows the same computations carried out for an aluminized 5 mil bead thermistor with 0.7 mil platinum-iridium lead wires each 1.5 cm long. It was assumed that $\epsilon_{sw} = \epsilon_{sT} = 0.15$, that $\epsilon_{lw} = \epsilon_{lT} = 0.1$, and that, (as in example 1), the albedo was 0.30 and the solar elevation angle 40° . A measuring circuit similar to that used in the later model Arcasonde was assumed (see section 11.3) which would produce a much smaller self-heating error in the thermistor than that assumed in the first example.

The total error is greatly reduced, mainly as a result of a very much smaller conduction error. An estimation of the probable variability of the total error has been included. This was based on a variability of $\pm 15\%$ for aerodynamic heating if derived from actual fall velocity, (this would be greatly exceeded above 65 km due to

the possibility of horizontal velocity components as discussed above), and a variability of $\pm 50^{\circ}\text{C}$ in support post temperature, $\pm 0.5^{\circ}\text{C}$ for the long-wave radiation error and $\pm 50\%$ for solar radiation and other errors.

TABLE 11. Temperature Errors of 5 mil Aluminized Thermistor Using 1.5 cm Lead Length.

Alt km	Aero $^{\circ}\text{C}$	Cond $^{\circ}\text{C}$	L/W Rad $^{\circ}\text{C}$	S/W Rad $^{\circ}\text{C}$	Meas $^{\circ}\text{C}$	Lag $^{\circ}\text{C}$	Total $^{\circ}\text{C}$
65	17.7	0.9	-0.7	5.4	0.5	-0.6	23.2 ± 4.0
60	8.7	0.2	-0.5	2.9	0.4	-0.2	11.5 ± 2.0
55	4.7	0	-0.4	1.6	0.4	-0.1	6.2 ± 1.1
50	2.2	0	-0.3	1.0	0.3	0	3.2 ± 0.6
45	1.0	0	-0.2	0.7	0.2	0	1.7 ± 0.5
40	0.4	0	-0.1	0.5	0.1	0	0.9 ± 0.3
35	0.2	0	-0.1	0.4	0	0	0.5 ± 0.2
30	0.1	0	0	0.3	0	0	0.4 ± 0.2
25	0	0	0	0.3	0	0	0.3 ± 0.1
20	0	0	0	0.2	0	0	0.2 ± 0.1

CHAPTER 12

CONCLUSIONS

12.1 Discussion of Results

The results presented in the preceding chapters provide a basis for the assessment of the errors of miniature bead thermistors under a rather wide range of applications. In discussing these errors we should bear in mind the meteorological requirements. In the majority of cases, because of the variability of the atmosphere, it is unrealistic to attempt to measure the air temperature at a given time to better than a certain degree of accuracy. On the other hand, for climatological and statistical studies it is very desirable that the errors average out in the mean of a large number of measurements. Thus there are two criteria for the allowable errors, one for the random component and the other for the systematic errors, with the latter in general more stringent. The errors discussed in this work have mostly been of the systematic type, and one of the main purposes of the study has been to provide experimental data for their assessment and correction.

One of the major sources of error is the temperature rise caused by direct and reflected solar radiation. This

is usually minimized by the use of reflective coatings on the thermistor beads. The results of this work show that at very high altitude the radiation absorbed by the lead wires is equally as important as that absorbed by the bead, and that at least as much attention should be paid to the reflectivity of the lead wire surface as to that of the bead itself. The reflectivity of thermistor lead wires and of reflective aluminum coatings on the beads has been shown to be lower in general than that usually associated with highly polished surfaces of the same metals prepared under ideal conditions, and this has been related to surface imperfections visible under a microscope. In many instances thermistors had large imperfections some of which would have resulted in temperature errors of up to five times those of the better types.

It will be noted from the results that in spite of these effects the radiation error of miniature aluminized thermistors is very small at low altitudes, especially if allowance is made for the effect of any ventilation speed. Because of its superior heat-transfer characteristics at low altitude the errors are appreciably smaller for the 5 mil thermistor than for the 10 and 15 mil thermistors, provided the reflectivities are comparable. However it has not been verified whether or not equally good reflect-

ivities can in fact be obtained on the smaller thermistors.

All of the thermistor errors studied increased rapidly above 55-60 km to the point where, above about 70 km, the uncertainty of any corrections would become quite unacceptable. It is felt that with certain precautions good results should be obtainable with rocketsonde thermistors up to about 65 km with the present equipment. These precautions would have to include proper mounting of the thermistors to minimize conduction errors, use of observed velocities in the calculation of the aerodynamic heating correction, and some form of quality control in the production of reflective coatings. In the past, not all of these requirements have been met.

Most of the discussion in this work has been with respect to thermistors mounted between mounting posts of relatively high thermal capacity. This mounting configuration has the advantage that the behaviour of the thermistor in an actual sounding can be confidently predicted from simple laboratory tests ; it is a simple system whose behaviour is readily represented mathematically and whose characteristics can now be considered to be fairly well known. Earlier users of this type of mounting have used rather short lead lengths with a resulting high conduction error, but by using longer leads the error can be made very small.

The "thin film" or "foil" mounts now being used for rocketsonde thermistors have probably eliminated the conduction error, at least up to 65 km, but only at the expense of increased complexity. It is more difficult to carry out laboratory tests, and difficult to relate the results to actual soundings. For example, the radiation error would depend on the orientation of the foil with respect to the direct and reflected radiation, and the aerodynamic heating would probably depend on the orientation of the foil with respect to the airflow. Oppenheim (1953) shows that in free molecule flow the recovery factor for a flat plate varies by a factor of nearly 2 between flow parallel to and flow normal to the plate. Due to parachute swing at high altitude the orientation would not be known at a given time.

In spite of the above difficulties it should be possible to use the results of this work to a considerable extent in studying the characteristics of the foil-mounted thermistors, for the correction equations derived above are valid if the temperature of the supports is interpreted as the temperature of the foil where the thermistor lead wires are joined on.

12.2 Thermal Boundary Layer Effects

In all of the results discussed above it has been assumed that the thermistor was exposed to air undisturbed by the

mountings or the instrument package itself. Much has been written on this subject for the case of temperature measurements from floating balloons (Ney 1961, W.C. Wagner 1965), but in the case of rocket soundings it is usually assumed that if the thermistor is situated at the forward (lower) end of the dropsonde, the relative motion through the air will ensure no errors from this source (C/F Pearson 1964).

In rarefied gas flow the boundary layers are very thick, as a result of the high value of the kinematic viscosity, and it is not clear exactly how far from the dropsonde the thermistor must be to be in undisturbed air at a given fall speed. In the Delta 1 temperature sonde used with the Arcas rockets the thermistor is less than an inch away from a $2\frac{1}{2}$ inch diameter base plate which would normally be at a much higher temperature than the air, and a question arises as to whether or not the clearance is really enough.

The thermal boundary layers of parts of the thermistor mount which may not be at air temperature must also be considered. Clark and McCoy (1962) have described temperature oscillations in the early Dartsonde found to be due to flow of air from the rather thick mounting posts over the thermistor at certain angles of parachute swing. This subject requires further investigation, but it is clear that unnecessarily thick mounting posts should be avoided.

12.3 Recommendations for Future Work

It would seem that there is some scope for the improvement of the reflective coatings applied to rocketsonde thermistors. The effort should to a large extent be directed towards the attainment of more uniform reflectivities among thermistors rather than the production of a more highly reflective type of coating, so that any corrections applied for the radiation error can be relied upon. There is a possibility that a marked increase in the reflectivity due to the achievement of a higher quality metallic coating may be nullified by a drop in the thermal accommodation coefficient and hence poorer heat transfer characteristics at very high altitudes. Hartnett (1961) and Devienne (1965) point out that the variation of the accommodation coefficient with the nature and cleanliness of the surface is greater than previously supposed, and that lower values generally accompany uncontaminated surfaces.

For further tests of the reflectivities of thermistors it is recommended that a radiation source having more nearly the spectral content of solar radiation be used. This would enable valid tests to be made on other than metallic coatings; for example white "Krylon" coated thermistors have been used extensively in rocketsonde work. As a stage one improvement a quartz-iodine lamp could be used, but ultimately a Mercury-

Xenon arc lamp would be preferred.

In view of the importance of aerodynamic heating errors, further study should be made of thermistor recovery factors. If the rotating arm method is used, more attention should be given to the measurement of the reference temperature distribution inside the bell jar, and to the radiation environment of the thermistors during the tests. By using coated thermistors exclusively and applying a radiation correction the results may be extended to lower pressures than were possible in the present work.

Except for the problem of reflective coatings, the behaviour of thermistors themselves is now probably sufficiently well understood. Further experimental work is necessary, however, for the study of the particular types of mounting systems now being used by members of the Meteorological Rocket Network, to see what modifying effects these have on thermistor response. Since the behaviour of post-mounted bead thermistors with suitably long lead lengths can be confidently predicted from the results of simple laboratory tests of the type described in this work, it would be very instructive to carry out comparative soundings between a well designed mount of this type and some of these other systems.

REFERENCES

- Armstrong, R. W., 1965: Improvement in Accuracy of the ML-419 Radiosonde Temperature Element for Heights above 50,000 ft and up to 150,000 ft. Technical Report Ecom - 2634 DA. Task No. 1V0-14501-B-53A-02.
- Baldwin, L. V., Sandborn, V. A., Laurence, J. C., 1959: Heat Transfer from Yawed Cylinders in Rarefied-Air Flows. ASME Paper No. 59-HT-5 presented at the ASME-AICHe Heat Transfer Conference, Storrs, Conn., Aug.
- Ballard, H. N., 1961: Response Time of and Effects of Radiation on the Veco Bead Thermistor. Report prepared for U.S. Army Signal Missile Support agency Contract D.A. 29-040-ORD-2410 Schellenger Res. Laboratories, Texas Western College, April 7.
- Ballard, H. N., 1965: Rocketsonde Techniques for the Measurement of Temperature and Wind in the Stratosphere. U.S. Army Research and Development Activity, White Sands Missile Range, New Mexico. Report ERDA-269 of Feb. D.A. Task 1V650212D127-03.
- Ballard, H. N., 1966: The Measurement of Temperature in the Stratosphere. AMS/AIAA Paper No. 66-385. Presented at AMS/AIAA Conference on Aerospace Meteorology, Los Angeles, March.
- Barr, W. C., 1961: Theoretical Considerations in the Design of Atmospheric Temperature-Sensing Elements. U.S. Signal Research and Development Lab., Ft. Monmouth, N.J. Tech. Report 2195 April.
- Clark, G. Q. & McCoy, J. G., 1962: Meteorological Rocket Thermometry. USASMSA Tech. Report MM-460 White Sands Missile Range, New Mexico, Aug.
- Clark, G. Q. & McCoy, J. G., 1965: Measurement of Stratospheric Temperature. J. Appl. Meteor. 4 pp. 365-370.
- Collis, D. C. & Williams, M. J., 1959: Two Dimensional Convection from Heated Wires at low Reynolds Number. J. Fluid Mech. 6 pp.357-386.

- Conover, J. H., 1965: Cloud and Terrestrial Albedo Determinations from TIROS Satellite Pictures. J. Applied Met. 4,3 pp.378-386.
- Craig, R. A., 1965: The Upper Atmosphere, Meteorology and Physics. Academic Press N.Y. p.81.
- Devienne, F. M., 1957: Experimental Study of the Stagnation Temperature in a Free Molecular Flow. J. Aeronautical Sci. 24 p.403.
- Devienne, F. M., 1958: The Revolving Arm Method and its Application to Rarefied Gas Dynamics and Aerothermodynamics. Report No. AFOSH TN-58-769, Contract AF 61-(514)1126. ASTIA AD-201866 Div.9.
- Devienne, F. M., 1965: Low Density Heat Transfer. Advances in Heat Transfer, Vol 2. J. P. Hartnett, ed. Academic Press N.Y. pp.271-356.
- Droms, C. R., 1962: Thermistors for Temperature Measurements. Temperature, its Meas. and Control in Science and Industry III pt 2. pp.339-346. Reinhold Pub. Corp. N.Y.
- Guthrie & Wakerling, 1949: Vacuum Equipment and Techniques. McGraw-Hill.
- Hampel, V. H., Jeffries, L. A., Sneed, R. J., Svinis, B., 1959: Final Report, Rocketsonde - Phase III. Contract AF 33-(616)3704, Physics Group Convair/Pomona Sept.
- Hartnett, J. P., 1961: A Survey of Thermal Accomodation Coefficients. "Rarefied Gas Dynamics". Academic Press N.Y. pp.1-29.
- Hottel, H. C. & Kalitinsky, A., 1945: Temperature Measurements in High Velocity Air Streams. Trans. ASME. 67. A-25.
- Johnson, J. C., 1953: A Radiation Thermometer for Meteorological Use. Final Report to the National Advisory Committee for Aeronautics under Contract NAW-6122.
- Kavanaugh, L. L., 1955: Heat Transfer from Spheres to a Rarefied Gas in Subsonic Flow. Trans. ASME 77;5.

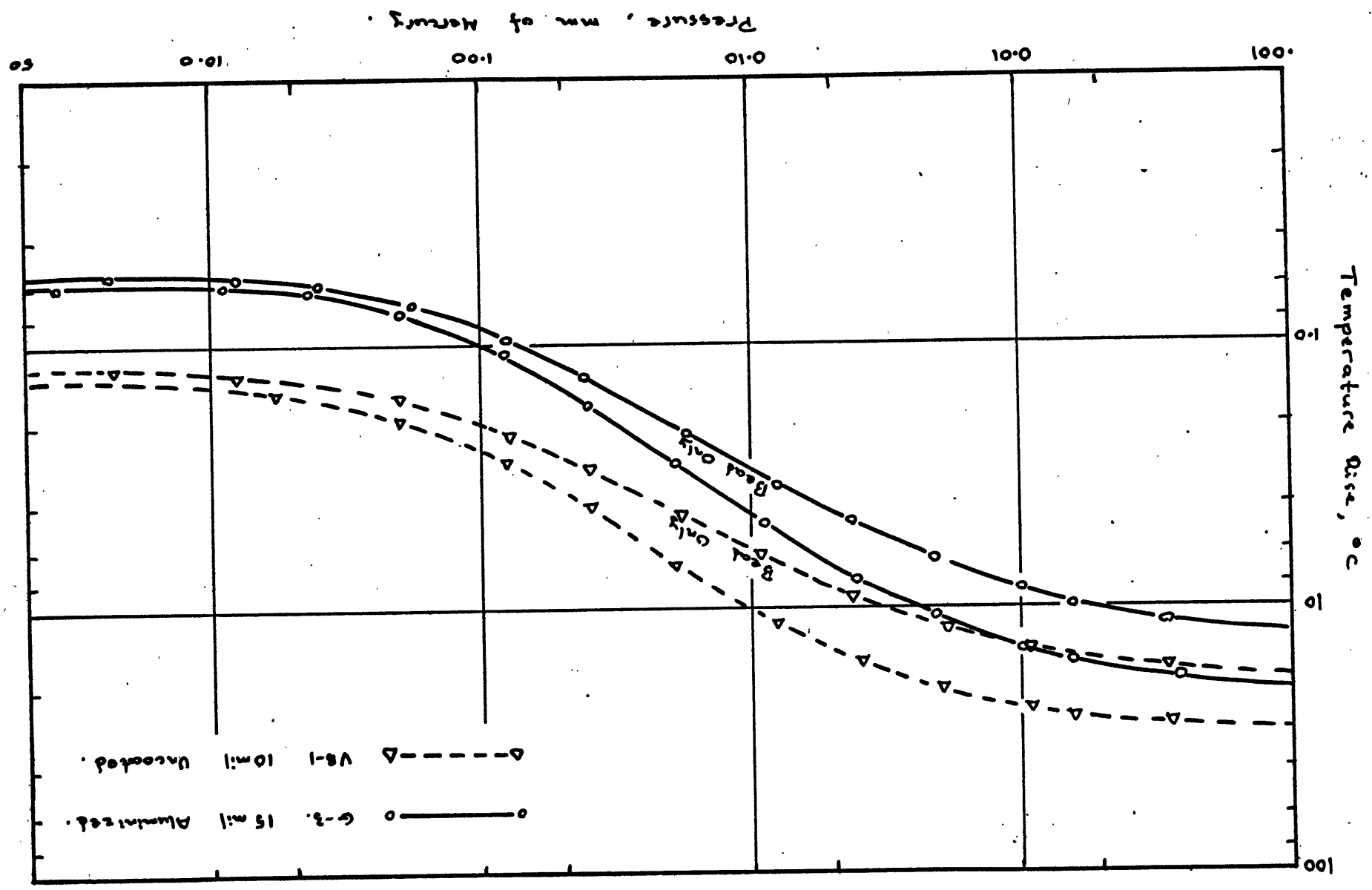
- Mann, A. E. & Benning, F. N., 1963: Reaching for the Sun. Environmental Quarterly. Sept. pp.16-31.
- McAdams, W. H., 1954: "Heat Transmission". McGraw Hill Book. N.Y. pp.267-259.
- Moffat, R. J., 1962: Gas Temperature Measurement. "Temperature; its Meas. and Control in Science and Industry" III pt 2. pp.553-571. C. M. Herzfeld, Ed. Reinhold Pub. Corp. N.Y.
- Ney, E. P., 1960: Immersion Thermometry at High Altitude. Summary Report, 1959 & 1960 Atmospheric Physics Program Nonr - 710(22). Univ. of Minnesota pp.9-27.
- Ney, E. P., 1961: The Measurement of Atmospheric Temperature. J. Meteorology 18. 60.
- Oppenheim, A. K., 1953: Generalized Theory of Convective Heat Transfer in a Free Molecule Flow. J. Aeronautical Sci. 20 No.1 pp.49-58.
- Pearson, P. H. O., 1964: An Investigation into the Response and Corrections to a Thermistor and a Platinum Wire Resistance Thermometer for Temperature Measurement in the Upper Atmosphere. Australian Defence Scientific Service Weapons Research establishment, Tech. Note PAD 83.
- Rockney, V. D., 1965: Recent Developments in High Altitude Meteorological Soundings in the U.S.A. Presented at Fourth Session, Commission for Instruments and Methods of Observation, W.M.O. Tokyo, October.
- Sachse, H. B., 1962: Measurement of Low Temperatures by Thermistors. "Temperature", its Measurement and Control in Science and Industry. Vol III Part 2. pp.347-353. C. M. Herzfeld Ed. Reinhold Pub. Corp. N.Y.
- Sion, E., 1955: Time Constants of Radiosonde Thermistors. Bull. Amer. Met. Soc. 36 16-21.
- Strong, J., 1946: "Procedures in Experimental Physics" Prentice-Hall New York.
- Thiele, O. W., 1966: Observed Diurnal Oscillations of Pressure and Density in the Upper Stratosphere and Lower Mesosphere. J. Atmos. Sci. Vol 23 No.4 pp.424-430. July.

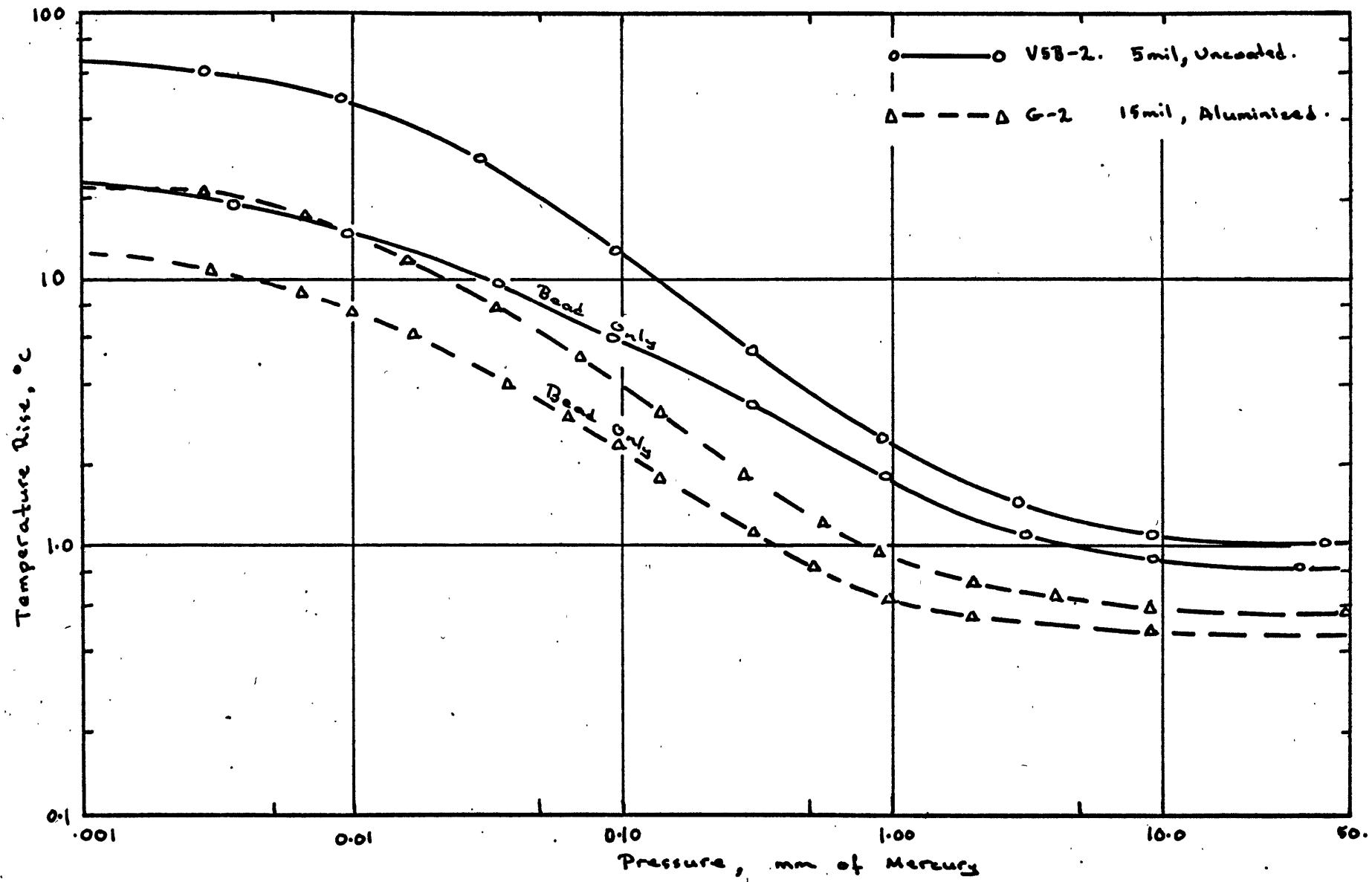
- Turner, A. F., 1962: Reflectance Properties of Thin Films and Multilayers. Radiative Transfer from Solid Materials, Henry Blau and Heinz Fischer, Eds. Macmillan.
- Wagner, N. K., 1961: Theoretical Time Constant and Radiation Error of a Rocketsonde Thermistor. J. Met. 18 p.606.
- Wagner, N. K., 1963: Theoretical Accuracy of the Meteorological Rocketsonde Thermistor. Report 7-23 Contract DA-23-072-ORD-1564 U.S. Army Electronics and Development Activity, White Sands Missile Range.
- Wagner, N. K., 1964: Theoretical Accuracy of a Rocketsonde Thermistor. J. Applied Met. 3. pp461-469.
- Wagner, W. C., 1964: Temperature Measurements from Floating Balloons. Proc. 1964 AFCRL Scientific Balloon Symposium Arthur O. Korn Ed. Air Force Surveys in Geophysics No.167 pp157-168.
- Walker, L., 1965: Design, Development and Flight Test Results of the Loki Instrumented Dart System. Final report, contract No. AF19(628)-4164. AFCRL-65-844 SDC TM-92.
- Webb, W. L., 1961: The First Meteorological Rocket Network. Bull. Amer. Met. Soc. 42 (7) 482-494.
- Wright Instruments Inc., 1961: A Survey for N.O.L. of High Altitude Atmospheric Temperature Sensors and Associated Problems. Final Report 1961. Performed under Navy Contract N-60921-6136 for the Naval Ordnance Laboratory.

APPENDIX 1

ADDITIONAL MEASUREMENTS OF THE RESPONSE
OF THERMISTORS TO RADIATION

The following are additional measurements of the type described in section 3.6(b). The results have in all cases been corrected to obtain the temperature rise expected for a radiation intensity of $2.0 \text{ cal cm}^{-2} \text{ min}^{-1}$. As pointed out in section 11.2(c) an estimate of the radiation error in an actual sounding may be obtained from these results by multiplying by a factor $(1 + 1.8a \sin h)$ to allow for reflected radiation. This procedure is valid down to pressures of about 0.08 mm mercury (65 km) beyond which point the particular mounting and environmental conditions used for the tests become important.

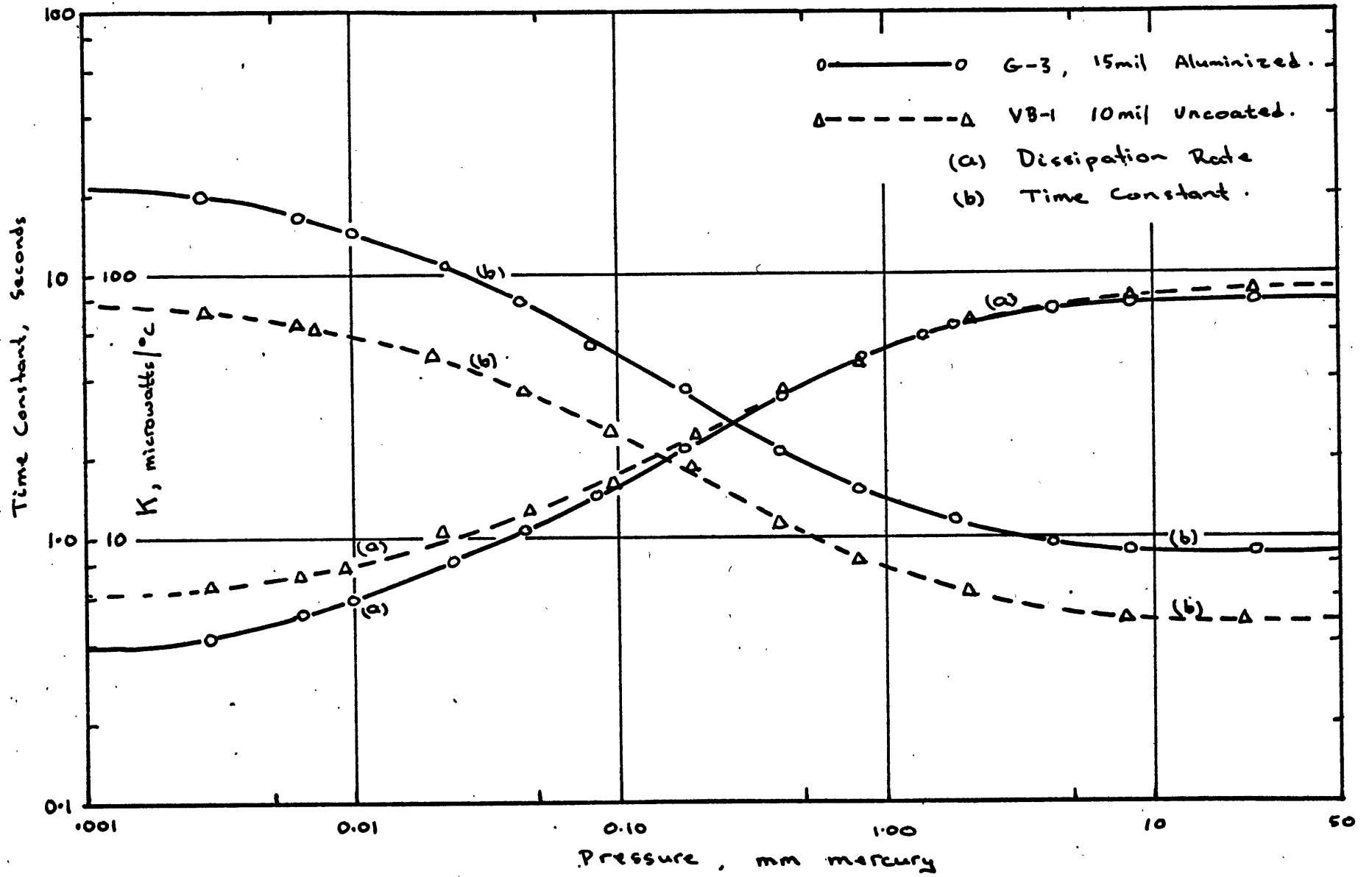


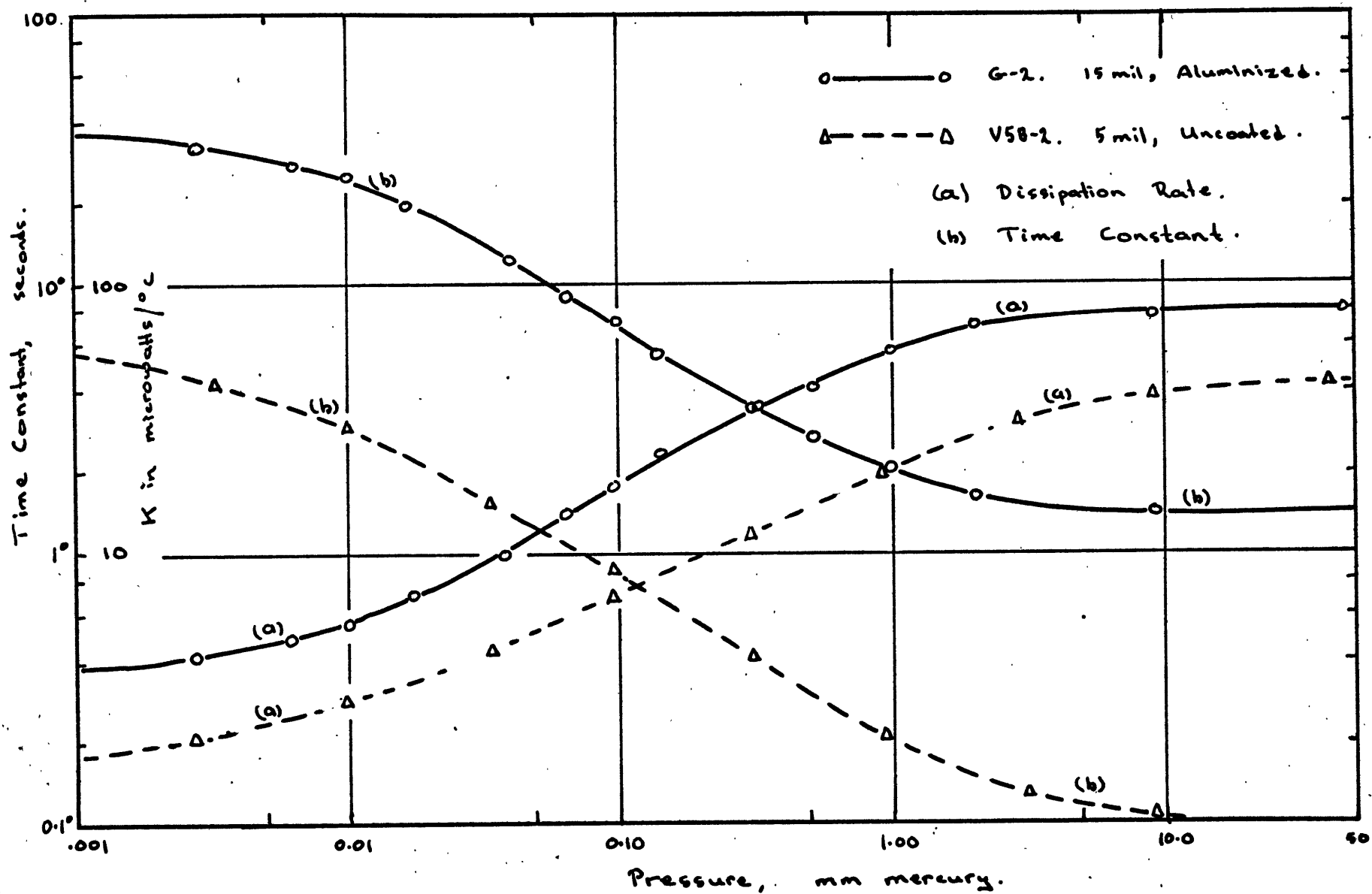


APPENDIX 2

ADDITIONAL MEASUREMENTS OF THE TIME CONSTANTS AND
DISSIPATION RATES OF THERMISTORS

The following are additional measurements of the time constant and dissipation rates of thermistors. The time constants were measured from observation of the cooling rate after removal of an electrical heating current, as described in Chapter 7, and the dissipation rates were measured as described in Chapter 4.





APPENDIX 3

TESTS ON ATLANTIC RESEARCH CORPORATION "THIN-FILM" MOUNT

Some tests were carried out on a "Thin-Film" mount supplied by Mr. P. Harney of AFCRL. This mount has been used extensively on Arcasonde systems and has been described by Rockney (1965). It consists essentially of two upright phenolic posts $1\frac{1}{2}$ inches long and $\frac{3}{4}$ inch apart between which is stretched a 1 mil thick mylar film. On opposite surfaces of the film are vacuum-deposited two U-shaped silver films with two legs exactly opposed on each side of the mylar. An aluminized 10 mil bead thermistor is soldered between the two opposing films at the bottom centre of the mount, using lead lengths of between 1 and 2 mm.

The device was mounted over the window in the pump plate in the position used for the tests on the other thermistors (Chapter 3), with the mylar film (a) at right angles, and (b) at an angle of 10° to the radiation beam. Measurements were made of the response to radiation, the dissipation rate and the time constant (using both the electrical heating method and the response to radiation). The copper enclosure used in the tests of Chapter 3 was of course omitted.

The results are shown in Figs.A3.1 and A3.2. It will

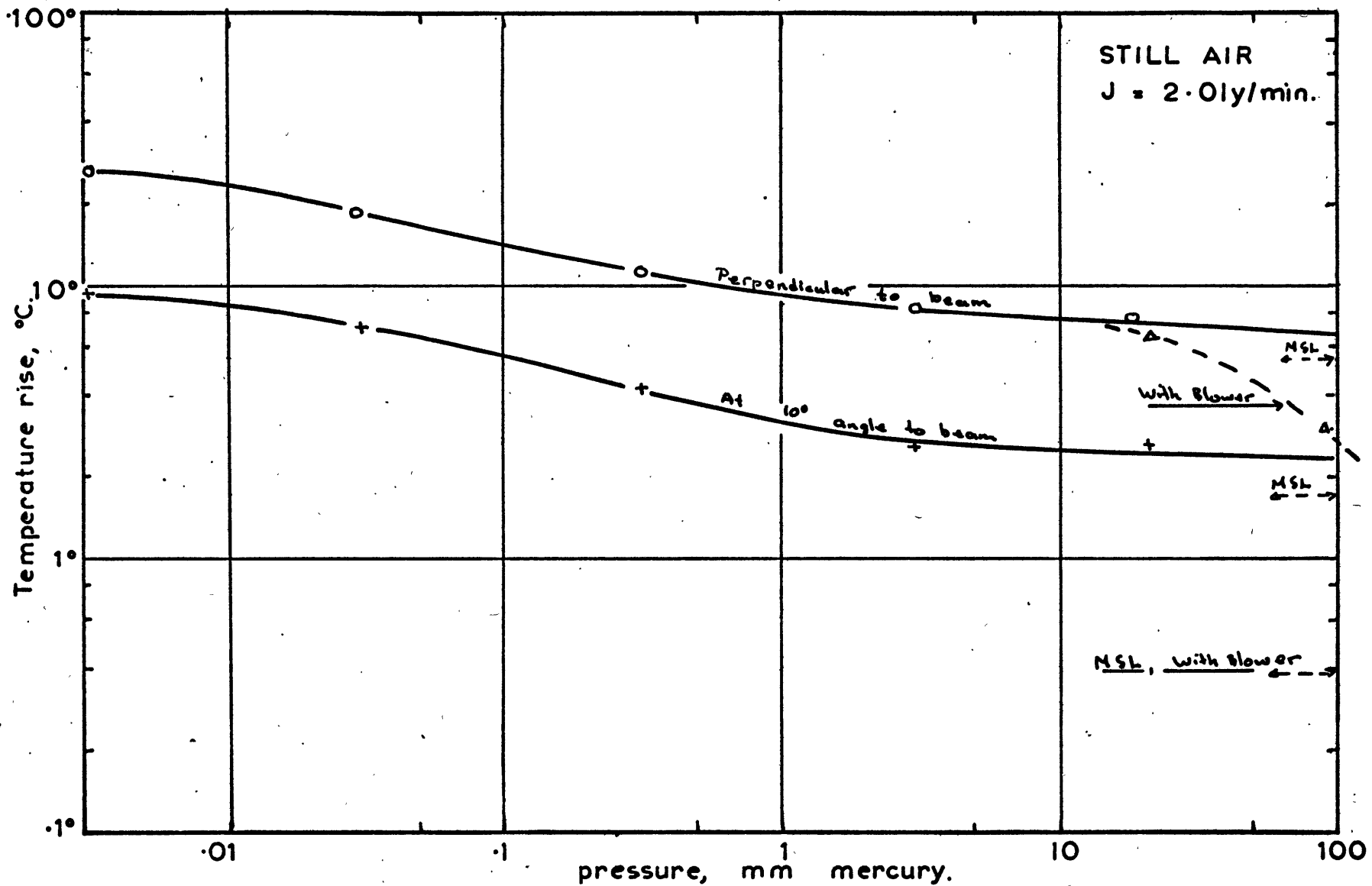


FIG. A3-1, RESPONSE OF THIN-FILM MOUNTED THERMISTOR TO RADIATION.

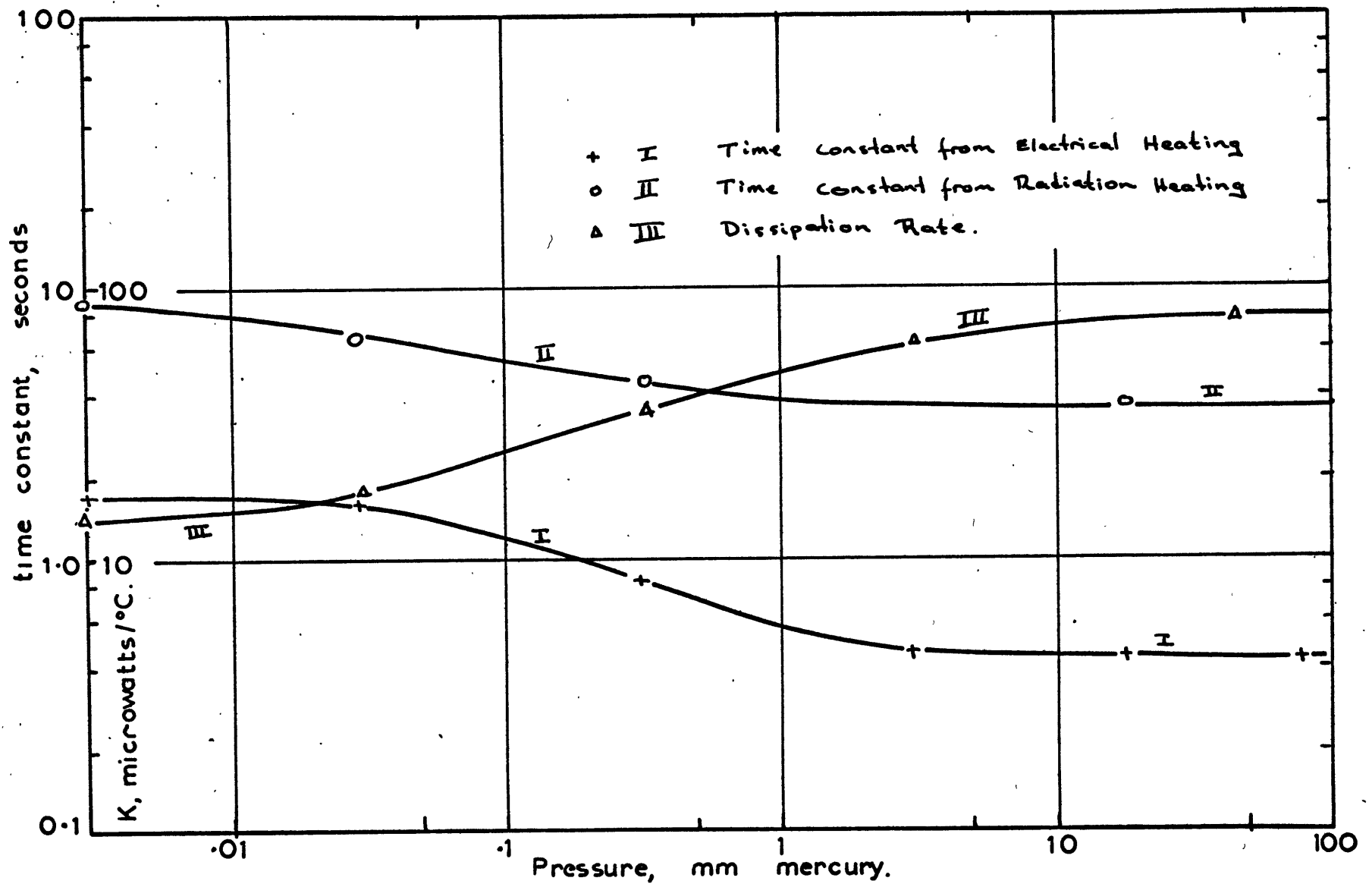


FIG A3-2. TIME CONSTANT & DISSIPATION RATE, THIN-FILM MOUNTED THERMISTOR.

be noted that the time constants measured by the two methods differ considerably. The electrical method does not supply sufficient power to influence the temperature of the mylar so only the thermistor response is observed. In practice, because of the very short lead lengths, the response of the thermistor would be heavily influenced by the response of the mylar foil which is evidently somewhat slower than that of the thermistor itself.

The measured radiation error of the device was quite high even at sea level pressure. There was evidence that in the tests, which were carried out in still air, a layer of thermally disturbed air was formed around the relatively large mylar film which also enveloped the thermistor bead. Thus, even at high pressures the response of the thermistor to radiation was governed by the response of the mylar. The response was expected to be considerably modified in the presence of ventilation and a small ventilating fan was installed in the chamber, directed towards the thermistor. At sea-level pressure the radiation error dropped to a value consistent with that of an aluminized thermistor, but this change was not observed at lower pressures probably as a result of the fan being ineffective. However it should be noted that at sufficiently low pressures the effect of conduction through the short lead wires would cause the bead to

sense the mylar rather than the air temperature regardless of ventilation.

APPENDIX 4

NUMERICAL STUDY OF THE DYNAMIC RESPONSE OF THERMISTORS

It was pointed out in section 7.2 that the response of a thermistor to a sudden change in electrical or radiational heating was not exactly equivalent to its response to a sudden change in air temperature. This is because conduction of heat into or out of the bead through the lead wires is a considerable item in the heat budget of the bead, and the initial and final temperature distributions in the lead wires are quite different in each case. To gain some quantitative idea of the errors involved in using the electrical methods of Chapter 7 to measure thermistor time constants rather than using actual step changes in air temperature some computations were made of the theoretical response of thermistors under the respective conditions.

Consider a section of lead wire of radius r conductivity k , and length δx . Then the heat flow into the section by conduction is

$$-\pi r^2 k \left(\frac{\partial T}{\partial x} \right)_x + \pi r^2 k \left(\frac{\partial T}{\partial x} \right)_{x+\delta x}$$

and the heat flow by convection is

$$2\pi r h_w \delta x (T_a - T_w)$$

where T_a and T_w are the air and wire temperatures respectively. Then if ρ_w , S_w are the density and specific heat of the lead wire it follows that

$$\frac{\partial T_w}{\partial t} = \frac{k}{\rho_w S_w} \left\{ \frac{\partial^2 T_w}{\partial x^2} + \frac{2h_w}{kr} (T_a - T_w) \right\} \quad (\text{A4.1})$$

Similarly, if the thermistor bead is situated at $x=0$ the heat gained by conduction is

$$2ka_w \left(\frac{\partial T_w}{\partial x} \right)_{x=0}$$

and that gained by convection is

$$h_T A_T (T_a - T_T) = h_T A_T (T_a - T_{w0})$$

where T_{w0} is the temperature of the lead wire at $x=0$, and the heat gained by the dissipation of electrical power is Q_e .

If the thermal capacity of the bead is C_T we have

$$\frac{\partial T_{w0}}{\partial t} = \frac{1}{C_T} \left[h_T A_T (T_a - T_{w0}) + 2\pi r^2 k \left(\frac{\partial T_w}{\partial x} \right)_{x=0} + Q_e \right]$$

(A4.2)

Numerical solutions for the two linked equations (A4.1) and (A4.2) were obtained for the following two sets of boundary conditions, corresponding to the two methods of measuring the time constant.

- Step (a) $T_a = 0, t \leq 0 ; T_a = 1, t > 0$
 (b) $Q_e = 0$ all t
 (c) At $t = 0, T_w = 0$ all x
 (d) At $x = 1.0, T_w = 0$ all t .

- Electric (a) $T_a = 0$ all t
 (b) $Q_e = 0, t \leq 0 ; Q_e = 10^{-4}, t > 0$
 (c) At $t = 0, T_w = 0$ all x
 (d) At $x = 1, T_w = 0$ all t .

The program was arranged so that after the bead temperature had approached sufficiently close to a steady value, T_a or Q_e were returned to zero, thus enabling the "cooling" part of the response to be observed.

The computations were carried out for three model thermistors - 5 and 10 mil beads having volumes and areas similar to actual 5 and 10 mil thermistors, and a hypothetical "2 mil" spherical thermistor whose volume was adjusted so that its basic time constant $\frac{C_T}{h_T A_T}$ was equal to that of the wire, $\frac{r \rho_w S_w}{2h_w}$. Densities and specific heats were taken from Wright (1961). The assumed physical

constants were as follows :

Lead Wire

Type	Platinum-Iridium	1 mil diameter.
Radius	$r = 1.27 \times 10^{-3}$	cm
Conductivity	$k = 0.31$	watt $^{\circ}\text{C}^{-1}$ cm $^{-1}$
Density	$\rho_w = 21.45$	gm cm $^{-3}$
Specific heat	$S_w = 0.130$	joule $^{\circ}\text{C}^{-1}$ gm $^{-1}$

Beads

Density	$\rho_T = 3.9$	gm cm $^{-3}$
Specific heat	$S_T = 0.50$	joule gm $^{-1}$ $^{\circ}\text{C}^{-1}$
Volume	(a) "5 mil"	0.17×10^{-5} cm 3
	(b) "10 mil"	1.50×10^{-5} cm 3
Surface Area	(a) "5 mil"	0.75×10^{-3} cm 2
	(b) "10 mil"	3.00×10^{-3} cm 2 .

Values of the heat transfer coefficients h_w and h_T were chosen with the aid of Figs.34 and 35 to represent conditions at sea level and at 55 km under "still air" conditions.

Figs.A4-1 and A4-2 show semi-log plots of the thermistor temperature $T_T = T_{w0}$ for the "cooling" parts of the two types of tests. It is seen that the electrical method results in a more rapid drop in thermistor temperature

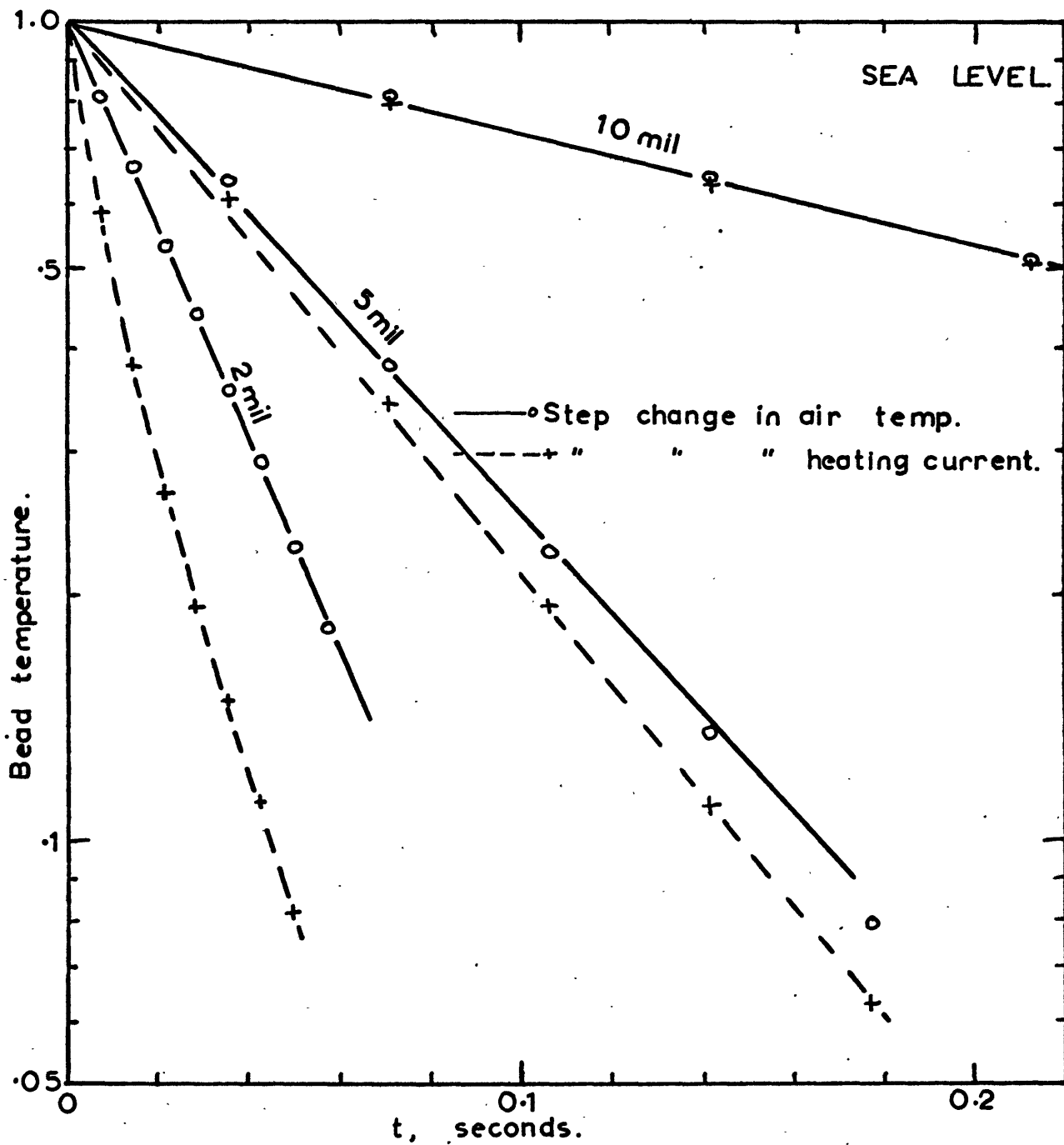


FIG A4-1, COMPUTED RESPONSE OF THERMISTORS.

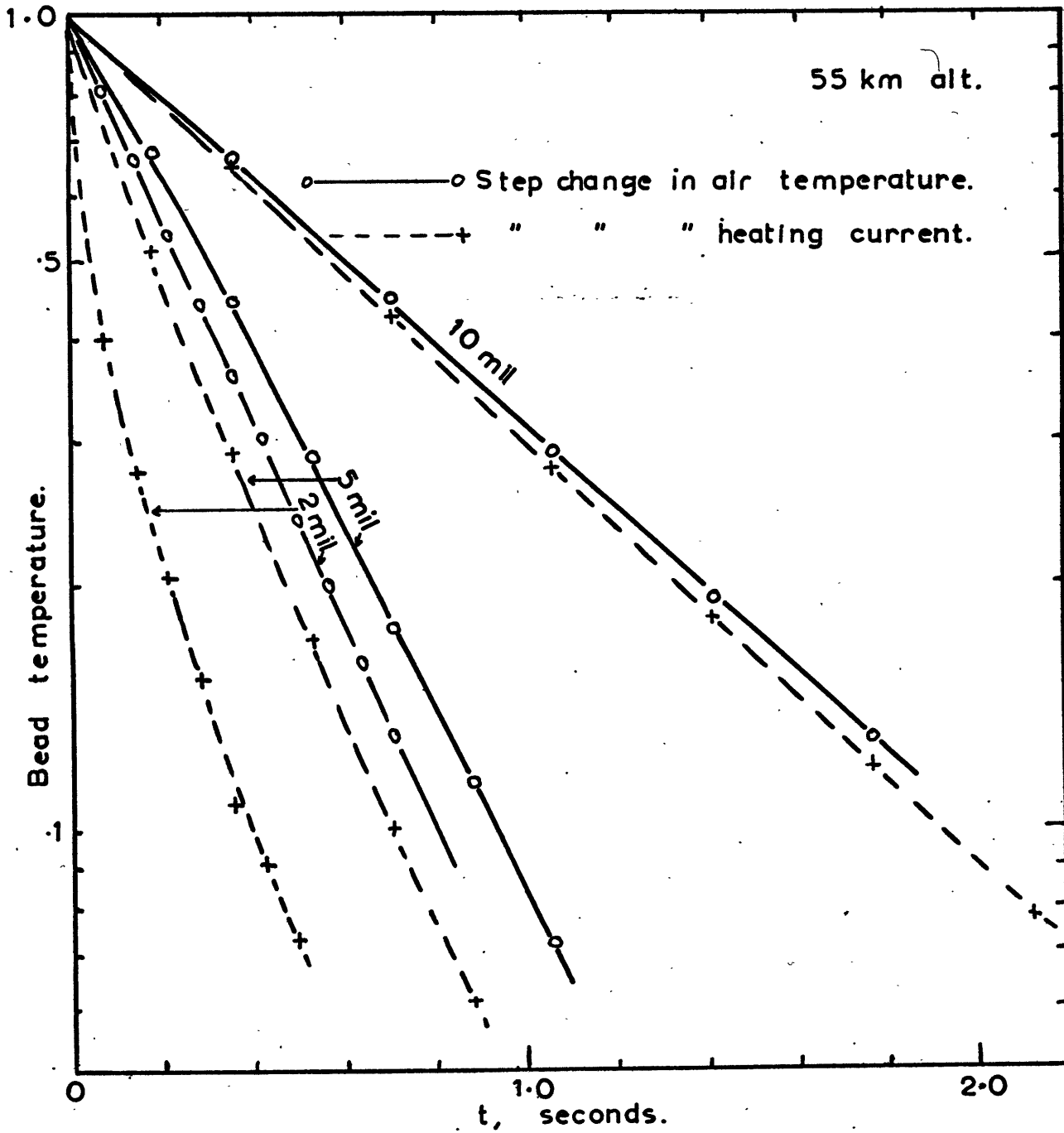


FIG. A4-2, COMPUTED RESPONSE OF THERMISTORS.

(and therefore a smaller measured time constant) than does a sudden drop in air temperature, but the difference is insignificant for the 10 mil bead and quite small for the 5 mil bead, especially at the lower altitude. For smaller thermistors, however the differences become appreciable, and also the effects would appear to be greater at higher altitudes. It was not possible to extend the computations to higher altitudes with the computation scheme used because of the small time-step required to maintain an adequate margin of computational stability.

BIOGRAPHICAL NOTE

The author was born in Wellington New Zealand on 8 May 1933. He was educated at Marlborough College, Blenheim and later at Victoria University of Wellington, from which he received his BSc degree in Physics and Radiophysics in 1955 and his MSc with 2nd class Honours in Physics in 1958.

After a short period of time in the Instrument Section of the N.Z. Meteorological Service he was seconded to the Geophysics Division, N.Z. D.S.I.R. to spend one year as senior scientific officer, N.Z. Antarctic Expedition at Scott Base during the latter part of the I.G.Y. While in Antarctica he was responsible for a wide range of geophysical observations.

Late in 1959 he returned to the N.Z. Meteorological Service where he served as a forecaster until 1963, mainly engaged in aviation forecasting. Early in 1963 he was transferred to the Research Section of the N.Z. Meteorological Service, where his duties included studies of air pollution problems.

Publications

Some Observations of Natural Atmospheric Radioactivity.

Thesis, Victoria University of Wellington N.Z. 1957.

Radiation Balance at Scott Base. Nature 184(4685)

pp.541-2. 1959. (With W.J.P. MacDonald)

Radiation Measurements at Scott base. N.Z.J.Geol. and

Geophysics Vol 5 No.5 pp.874-908. 1962. (With W.J.P. MacDonald)

The Accuracy of Thermistors in the Measurement of Upper Air Temperature. A.M.S./A.I.A.A. Paper No.66-386 presented at the A.M.S./A.I.A.A. Conference on Aerospace Meteorology, Los Angeles, March 1966. (With D.P. Keily).